



PERFORMANCE EVALUATION OF IOWA BRIDGE DECKS CONSTRUCTED WITH EPOXY-COATED REINFORCING BARS



Final Report

August 19, 2011

WJE No. 2010.0868

Prepared for:

Iowa Department of Transportation

Office of Bridges and Structures

800 Lincoln Way

Ames, Iowa 50010

Prepared by:

Wiss, Janney, Elstner Associates, Inc.

330 Pfingsten Road

Northbrook, Illinois 60062

847.272.7400 tel | 847.291.4813 fax



PERFORMANCE EVALUATION OF IOWA BRIDGE DECKS CONSTRUCTED WITH EPOXY-COATED REINFORCING BARS

A handwritten signature in black ink, reading 'James P. Donnelly'.

James P. Donnelly, P.E., S.E.

A handwritten signature in black ink, reading 'Paul D. Krauss'.

Paul D. Krauss, P.E.

A handwritten signature in black ink, reading 'John S. Lawler'.

John S. Lawler, P.E., Ph.D.

Final Report

August 19, 2011

WJE No. 2010.0868

Prepared for:

Iowa Department of Transportation

Office of Bridges and Structures

800 Lincoln Way

Ames, Iowa 50010

Prepared by:

Wiss, Janney, Elstner Associates, Inc.

330 Pfingsten Road

Northbrook, Illinois 60062

847.272.7400 tel | 847.291.4813 fax

TABLE OF CONTENTS

1.0 Introduction.....	1
1.1 Description of Structures.....	1
1.1.1 IA 17 over US Route 20.....	2
1.1.2 US 218 Southbound over Cedar River.....	2
1.1.3 IA 150 over Cedar River.....	3
1.1.4 IA 13 Southbound over Indian Creek.....	3
1.1.5 US 30 over Missouri River.....	3
1.1.6 US 18 over Floyd River.....	4
1.1.7 US 65 Southbound over the Union Pacific Railroad.....	4
1.1.8 US 65 Northbound over the Union Pacific Railroad.....	4
2.0 Methods.....	5
2.1 Bridge Condition Assessment - Field Investigation.....	5
2.1.1 Physical Condition Survey.....	5
2.1.2 Cover Measurement.....	5
2.1.3 Core Sampling.....	5
2.1.4 Half-Cell Potential Survey.....	5
2.1.5 Corrosion Rate Testing.....	6
2.1.6 Connectivity Measurements by AC Resistance.....	6
2.2 Bridge Condition Assessment - Laboratory Analysis.....	7
2.2.1 Petrographic Examination.....	7
2.2.2 Examination of Extracted Bars.....	7
2.2.3 Chloride Concentration Profiles.....	8
2.2.4 Chloride Concentration Analysis.....	9
3.0 Results.....	11
3.1 IA 17 over US Route 20.....	12
3.1.1 Visual and Delamination Surveys.....	12
3.1.2 Cover Measurements.....	12
3.1.3 AC Resistance, Half-Cell Potential, and Corrosion Rate Testing.....	12
3.1.4 Petrographic Analysis.....	12
3.1.5 Chloride Testing and Diffusion Analysis.....	13
3.1.6 Examination of Bar Conditions.....	13
3.2 US 218 Southbound over Cedar River.....	13
3.2.1 Visual and Delamination Surveys.....	13
3.2.2 Cover Measurements.....	13
3.2.3 AC Resistance, Half-Cell Potential, and Corrosion Rate Testing.....	14
3.2.4 Petrographic Analysis.....	14
3.2.5 Chloride Testing and Diffusion Analysis.....	14
3.2.6 Examination of Bar Conditions.....	14
3.3 IA 150 over Cedar River.....	15
3.3.1 Visual and Delamination Surveys.....	15
3.3.2 Cover Measurements.....	15
3.3.3 AC Resistance, Half-Cell Potential, and Corrosion Rate Testing.....	15
3.3.4 Petrographic Analysis.....	16
3.3.5 Chloride Testing and Diffusion Analysis.....	16
3.3.6 Examination of Bar Conditions.....	16

3.4 IA 13 Southbound over Indian Creek.....	16
3.4.1 Visual and Delamination Surveys.....	16
3.4.2 Cover Measurements	16
3.4.3 AC Resistance, Half-Cell Potential, and Corrosion Rate Testing.....	17
3.4.4 Petrographic Analysis	17
3.4.5 Chloride Testing and Diffusion Analysis.....	17
3.4.6 Examination of Bar Conditions.....	17
3.5 US 30 over Missouri River.....	17
3.5.1 Visual and Delamination Surveys.....	17
3.5.2 Cover Measurements	18
3.5.3 AC Resistance, Half-Cell Potential, and Corrosion Rate Testing.....	19
3.5.4 Petrographic Analysis	19
3.5.5 Chloride Testing and Diffusion Analysis.....	19
3.5.6 Examination of Bar Conditions.....	19
3.6 US 18 over Floyd River.....	19
3.6.1 Visual and Delamination Surveys.....	20
3.6.2 Cover Measurements	20
3.6.3 AC Resistance, Half-Cell Potential, and Corrosion Rate Testing.....	20
3.6.4 Petrographic Analysis	20
3.6.5 Chloride Testing and Diffusion Analysis.....	20
3.6.6 Examination of Bar Conditions.....	21
3.7 US 65 Southbound over the Union Pacific Railroad.....	21
3.7.1 Visual and Delamination Surveys.....	21
3.7.2 Cover Measurements	21
3.7.3 AC Resistance, Half-Cell Potential, and Corrosion Rate Testing.....	21
3.7.4 Petrographic Analysis	22
3.7.5 Chloride Testing and Diffusion Analysis.....	22
3.7.6 Examination of Bar Conditions.....	22
3.8 US 65 Northbound over the Union Pacific Railroad.....	22
3.8.1 Visual and Delamination Surveys.....	22
3.8.2 Cover Measurements	23
3.8.3 AC Resistance, Half-Cell Potential, and Corrosion Rate Testing.....	23
3.8.4 Petrographic Analysis	23
3.8.5 Chloride Testing and Diffusion Analysis.....	23
3.8.6 Examination of Bar Conditions.....	23
4.0 Analysis of Findings	25
4.1 Field Observations.....	25
4.1.1 Observed Deterioration	25
4.1.2 Corrosion Testing and AC Resistance	25
4.2 Bar Conditions.....	26
4.2.1 Bar Depth.....	26
4.2.2 Coating Adhesion.....	26
4.2.3 Backside Contamination	27
4.2.4 Chloride Concentration at Bar Depth.....	27
4.2.5 Time to Effective Coated Bar Threshold	27
4.2.6 Coating Thickness.....	28
4.2.7 Effect of Coating Top or Both Reinforcing Mats	28
4.2.8 Exposure Relative to Location on Deck	29

4.3 Service Life Analysis	29
4.3.1 Methods and Bases for Analysis.....	30
4.3.2 Findings	33
5.0 Discussion.....	35
6.0 Conclusions.....	38
7.0 Works Cited	39

Tables

Figures

Appendix A - Field Investigation Results

Appendix B - Report of Petrographic Studies

Appendix C - Laboratory Data

PERFORMANCE EVALUATION OF IOWA BRIDGE DECKS CONSTRUCTED WITH EPOXY-COATED REINFORCING BARS

1.0 INTRODUCTION

Epoxy coatings have been used on the embedded reinforcing bars of bridge decks since the mid-1970s to mitigate deterioration caused by chloride-induced corrosion. The use of chloride-based deicers became common in the early 1960s and caused corrosion of conventional uncoated bars in bridge decks within 5 to 10 years of commencement of deicer applications. In response to this rapid deterioration, the National Bureau of Standards researched coatings to protect the reinforcement (National Bureau of Standards, 1975), resulting in the development of epoxy-coated reinforcing bars, which were used in bridge decks beginning in 1973. While corrosion-related deterioration has been prevalent on bridge decks with uncoated reinforcing bars in northern climates where the use of deicing salts is common, bridge decks constructed after 1973 with epoxy-coated reinforcing have shown good corrosion resistance with only limited exceptions. On the whole, previous laboratory and field studies regarding the performance of epoxy-coated reinforcing bars are very promising; however, some laboratory and field studies have yielded differing results.

In recent years, maintenance personnel for the Iowa Department of Transportation (Iowa DOT) have reportedly performed patch repairs to some bridge decks reinforced with epoxy-coated bars. At one such bridge, the southbound US 65 bridge (Bridge No. 7788.5L065) over the Union Pacific Railroad near Bondurant in Polk County, Iowa, deck repairs were performed by Iowa DOT maintenance personnel in the Spring of 2010, based on our communications regarding this topic with Mr. Gordon Port of the Iowa DOT. These repairs were observed by engineers from the Iowa DOT Office of Bridges and Structures, who reported that significant corrosion was found at a number of epoxy-coated reinforcing bars uncovered during this patch work. These repairs were reportedly performed at spalls and delaminated areas corresponding to cracks over transverse reinforcing bars, and involved careful removal of the concrete from over the bars. Figures 1 through 4 contain photographs provided by Iowa DOT personnel showing the removal process (Figure 1), the conditions encountered (Figures 2 and 3), and close-up views of the corroded reinforcing (Figure 4).

As a result of these observations, the Iowa Department of Transportation has requested this study to gain further understanding of the long-term performance of bridge decks reinforced with epoxy-coated bars. The two main objectives of this study are to determine the long-term effectiveness of the epoxy coatings and to determine the potential causes for the deterioration at locations where corrosion has occurred. Wiss, Janney, Elstner Associates, Inc. (WJE) and the Iowa DOT identified eight different bridge decks across Iowa for this study that were constructed using epoxy-coated reinforcing bars. A field investigation consisting of visual inspections, a delamination survey, a concrete cover survey, electrical testing for susceptibility to corrosion, and concrete sampling was conducted within a survey area deemed to be representative of the condition of each bridge deck. Laboratory testing, including chloride ion content testing, characterization of the extracted bars, petrographic examination of the concrete, and carbonation testing, was conducted on the core samples taken from each bridge deck.

1.1 Description of Structures

The eight bridge decks selected for this study were built between 1978 and 1993 and were generally found to be in good to excellent condition. However, two of the bridge decks had recently been patched extensively. Four of the bridge decks had epoxy-coated reinforcing bars only in the top mat of

reinforcement, with uncoated bar as the lower mat of reinforcement. The other four bridge decks studied had epoxy-coated reinforcing bars as both the top and bottom mats of deck slab reinforcement. Seven of the eight bridges had a typical deck slab design thickness of 7 to 8 inches and one bridge was a reinforced concrete slab bridge with a slab design thickness of 17.5 inches. Table 1 provides general information on each of the eight bridges surveyed.

Three of the bridge decks selected had been previously evaluated in 1998 and 2002 during similar studies of the condition of the epoxy-coated reinforcing bars (Fanous, Wu, & Pape, 2000) (Lee & Krauss, 2003). Those bridge decks previously evaluated include Southbound US 218 over the Cedar River in Bremer County, Southbound IA 13 over Indian Creek in Linn County, and US 18 over the Floyd River in Sioux County.

1.1.1 IA 17 over US Route 20

This bridge is a four span structure that carries one lane each of northbound and southbound traffic over US 20. As-built drawings are dated February 2, 1980, and Iowa DOT inspection records indicate that the bridge was constructed in 1978. The Iowa DOT Structure number is 4054.3S017. Figure 5 is an aerial view of the structure, while Figure 6 shows a view of the east elevation. The superstructure consists of five longitudinal, precast, prestressed, I-shaped, Type D concrete beams which were made continuous over the three concrete piers by composite action with the cast-in-place concrete deck. The overall length of the structure is 254 feet-6 inches, which includes two 35 feet-9 inch end spans and two 91 feet-6 inch interior spans over the US 20 roadway. The overall roadway width is 32 feet-0 inches. The deck slab has a design thickness of 7-1/2 inches, including a 1/2 inch integral wearing course, and is reinforced in both directions with two mats of reinforcing bars. Epoxy-coated reinforcing bars were specified for only the top layer of transverse and longitudinal bars. Two inches of cover is specified for the top reinforcing bars, and 1 inch of cover is specified for the lower layer of longitudinal bars at the slab bottom. The bridge is located in Hamilton County approximately 5 miles west of Webster City, Iowa.

1.1.2 US 218 Southbound over Cedar River

This bridge consists of seven approximately equal length spans, each of which is constructed of a reinforced concrete deck cast on a set of six longitudinal precast prestressed I-shaped Type D concrete beams. As-built drawings are dated February 20, 1995, and the Iowa DOT inspection report indicates that the bridge was built in 1993. It is identified as Iowa DOT Structure number 0996.0L218. The bridge carries southbound traffic on US Route 218 over the Cedar River approximately one-half mile north of Janesville, Iowa in Bremer County. Figure 7 is an aerial view of the structure. Figure 8 shows a view of the west elevation. The overall length of the structure is approximately 673 feet-9 inches between end bearings, with each of the seven spans measuring approximately 96 feet. Roadway width is 40 ft-0 inches and is divided into two traffic lanes and left and right shoulders. Two expansion joints are present in the deck, which occur over the second and fifth piers from the abutment at the south end of the bridge, located on the east side of the river. These joints divide the deck into three sections, including the center spans which are mainly over the river (Section 2, Spans 3, 4 and 5) and the two approach spans on each end of the bridge (Sections 1 and 3, Spans 1, 2, 6 and 7). For the purpose of this report, Section 1 and Span 1 are located at the south end of the bridge adjacent to the abutment on the east side of the river. The design thickness of the deck is 8 inches, including a 1/2 inch integral wearing course, and both the top and bottom layers of reinforcing bars are epoxy-coated. The cover is specified as 2-1/2 inches for the top reinforcing bars and 1 inch at the bottom of the deck slab for the lower layer of transverse bars.

1.1.3 IA 150 over Cedar River

This bridge is identified as Iowa DOT Structure number 0601.5S150. Design drawings for this bridge are dated May 1979, while the most recent Iowa DOT inspection report indicates that the bridge was constructed in 1980. The bridge superstructure consists of six longitudinal, precast, prestressed, I-shaped Type D concrete beams for each of nine spans, which were made continuous over the non-expansion joint piers by composite action with the 8 inch thick reinforced concrete deck. Figure 9 is an aerial view of the structure, while Figure 10 shows a view of the east elevation. The bridge carries one lane each of northbound and southbound traffic over the Cedar River just north of downtown Vinton, Iowa in Benton County. The bridge has nine spans for an overall length of 807 feet-0 inches, with seven interior spans each 96 feet-6 inches long and two end spans that are somewhat shorter at 65 feet-9 inches in length. The roadway width is 32 feet-0 inches, not including the parapet walls or the 5 feet wide sidewalk along the east side of the deck. The 8 inch thick deck includes a 1/2 inch integral concrete wearing course and is conventionally reinforced, but with epoxy-coated reinforcing bars only in the top layer of transverse and longitudinal bars. The cover is specified as 2-1/2 inches for the top reinforcing bars and 1 inch at the bottom of the deck slab for the lower layer of transverse bars. The two expansion joints in the deck are located at the third and sixth piers as numbered from the south abutment toward the north, thereby dividing the deck into three sections. For the purpose of this report, Section 1 is the southernmost section and Section 3 the northernmost.

1.1.4 IA 13 Southbound over Indian Creek

This bridge is located in Linn County approximately six miles north of Marion, Iowa, and carries two lanes of southbound traffic on Iowa 13 over Indian Creek. It is identified as Iowa DOT Structure number 5713.7L013. As-built drawings are dated March 24, 1989, while the most recent Iowa DOT bridge inspection report indicates that the bridge was constructed in 1987. This bridge consists of a continuous reinforced concrete slab with integral pier caps at the two piers and the two abutments. Figure 11 is an aerial view of the structure, and Figure 12 shows a view of the east elevation. The concrete bridge deck is specified as 17-1/2 inches thick, including a 1/2 inch integral wearing course, and is oriented at a 20 degree skew to the direction of traffic. Both the top and bottom layers of slab reinforcing bars are epoxy-coated, with 2 1/2 inches of cover specified for the top reinforcing bars, and 1-1/2 inches specified at the bottom of the deck slab for the bottom layer of longitudinal bars. The overall length of the bridge is 100 ft between abutment piers, which is divided into two 30 feet-6 inches end approach spans and a 39 feet-0 inches center span over Indian Creek. The overall width of the roadway is 40 feet-0 inches.

1.1.5 US 30 over Missouri River

The structure carrying US Route 30 over the Missouri River is a seventeen span bridge with an overall length of 1,983 feet, measured to the outside faces of the abutment back walls. It is identified as Iowa DOT Structure number 4300.0S030. As-built drawings are dated January 27, 1993, and Iowa DOT inspection reports indicate that the bridge was built in 1991. Figure 13 is an aerial view of the structure, and Figure 14 shows a view of the south elevation of the bridge section over the river. The bridge is located in Harrison County, Iowa, and straddles the border between Iowa and Nebraska. It is situated approximately 11 miles west of Missouri Valley, Iowa, and just east of Blair, Nebraska. The roadway is 40 feet-0 inches wide and carries one lane each of eastbound and westbound traffic. The two main spans over the river are constructed of a set of four welded steel plate girders, while the approach spans on the east and west are supported by a series of six precast, prestressed concrete, I-shaped, Iowa Type D beams. The two main spans over the river (Spans 10 and 11, Section 3) total 666 feet in length. The nine approach spans on the west side of the bridge (Spans 1 through 9, Sections 1 and 2) total 773 feet-6

inches, with most spans totaling 86 feet-0 inches each. The six east approach spans (Spans 12 through 17, Section 4) total 538 feet-0 inches in length, with all but Spans 12 and 17 measuring 90 feet-0 inches in length. The bridge is linear except for a slight curvature of the two westernmost approach spans. Expansion joints divide the deck into four sections and are located over the top of the fourth, ninth, and eleventh piers as counted from the west end of the bridge. The slab has a design thickness of 8 inches in the east and west approach spans, but a design thickness of 8-1/2 inches in the two main spans. These thicknesses include a 1/2 inch thick integral wearing course. Both the top and bottom layers of reinforcing bars are epoxy-coated. The cover is specified as 2-1/2 inches for the top reinforcing bars and 1 inch at the bottom of the slab for the lower layer of transverse bars in all spans.

1.1.6 US 18 over Floyd River

This bridge is located in Sioux County approximately one mile west of Sheldon, Iowa. As-built drawings are dated June 8, 1993, with Iowa DOT inspection reports indicating the bridge was constructed in 1992. The bridge carries traffic on US Route 18 over the Floyd River and is identified as Iowa DOT Structure number 8441.3S018. Figure 15 is an aerial view of the structure, while Figure 16 shows a view of the north elevation. The superstructure consists of seven longitudinal, precast, prestressed concrete beams which are made continuous over the two concrete piers by the cast-in-place concrete deck. The bridge has an overall length of 205 feet-6 inches and is oriented at a 15 degree skew to the direction of traffic. The roadway is 44 feet-0 inches wide and carries one lane each of eastbound and westbound traffic. End spans are 68 feet-3 inches in length and the center span is 69 feet-0 inches long. The deck has a typical design thickness of 8 inches including a 1/2 inch integral wearing course. Both the top and bottom layers of reinforcing bars are epoxy-coated. The cover is specified as 2-1/2 inches for the top reinforcing bars and 1 inch at the bottom of the slab for the lower layer of transverse bars.

1.1.7 US 65 Southbound over the Union Pacific Railroad

This bridge is one of a pair of two identical bridges that carry US 65 over the Union Pacific rail lines on the northeast side of Bondurant, Iowa in Polk County. Design drawings are dated January 1977, but Iowa DOT inspection reports indicate the bridge was constructed in 1979. This bridge is identified as Iowa DOT Structure number 7788.5L065. Figure 17 is an aerial view of both the northbound and southbound structures. The bridge consists of three spans with an overall length of 332 feet. The end spans are each 101 feet long and the center span is 130 feet. Two lanes of southbound traffic are carried by the bridge, which is oriented at a 45 degree skew to the direction of traffic. The roadway width is 40 feet-0 inches. The superstructure consists of five longitudinal welded steel girders that are continuous over the three spans. The typical design deck thickness is 7.875 inches including a 1/2 inch integral wearing surface. Reinforcing bars are epoxy-coated only in the top layer of reinforcing. The cover is specified as 2-1/2 inches for the top reinforcing bars, and 1 inch at the bottom of the deck slab for the lower layer of transverse bars.

1.1.8 US 65 Northbound over the Union Pacific Railroad

The northbound bridge is identical to the southbound bridge in dimensions and construction. It carries two lanes of northbound traffic of US 65 over the Union Pacific rail lines on the northeast side of Bondurant, Iowa in Polk County. The Iowa DOT Structure number is 7788.5R065. Design drawings are dated January 1977 and indicate that the northbound bridge was to be constructed prior to the southbound structure. The most recent Iowa DOT inspection report indicates that the bridge was built in 1979. Figure 18 shows a view of the southeast elevation.

2.0 METHODS

The program for characterizing the performance of epoxy-coated bars in the eight bridge decks selected for study consisted of two main parts: field investigation and laboratory studies. After the field and laboratory data had been collected, the data was analyzed and a projection of service life was made for each bridge deck. The field investigation consisted of a visual survey, crack mapping, delamination survey, half-cell potential testing, corrosion rate testing, continuity testing, depth of cover measurements, and removal of core samples. In the laboratory, the following tests were performed on the core samples obtained: visual examination of the extracted bar samples, petrographic studies, chloride analysis, and determination of concrete chloride surface concentration and chloride diffusion coefficient.

2.1 Bridge Condition Assessment - Field Investigation

2.1.1 Physical Condition Survey

A detailed visual examination of the selected deck area was conducted on each bridge deck. The area examined typically consisted of one traffic lane and associated shoulder for the entire length of the bridge. The region of each bridge deck that was surveyed is provided in Table 1. In conjunction with the visual survey, a delamination survey was conducted using conventional chain dragging and hammer sounding methods (Figure 19). The location and estimated area or length of observed distress, including delaminations, spalls, cracks, and patches, were documented. Typical crack widths were measured, and the crack density (ft/ft²) was calculated for each bridge deck by dividing the total length of the cracks identified by the total surface area of the deck area that was surveyed.

2.1.2 Cover Measurement

Ground Penetrating Radar (GPR) was used to locate and determine the concrete cover over the reinforcing bars (Figure 20). Two scans parallel to the deck centerline were taken on each deck for the full length of each lane closure, typically with one scan along the right shoulder and one just inside the left wheel path of the travel lane. A number of scans perpendicular to the centerline were taken to assess cover depths of the longitudinal reinforcing bars. Indicated depths of the top reinforcing bars on the GPR scans were calibrated for each bridge to actual depth measurements of the top reinforcing bars taken at core locations.

2.1.3 Core Sampling

Seven to ten 4-inch diameter core samples were cut from each deck survey area (Figure 21). Cores were generally taken from the shoulder, the right wheel path, and the left wheel path of the travel lane within each survey area. All core samples were located to intersect one or more reinforcing bars. Approximately one third of the cores taken on each bridge deck were taken from areas of the deck that contained cracks and delaminations, if present. The locations of the cores for each bridge are shown in the deck plan views contained in Appendix A. Each core hole was patched with a rapid setting repair material.

2.1.4 Half-Cell Potential Survey

A copper-copper sulfate half-cell potential (HCP) survey was conducted to obtain an indication of corrosion risk for the reinforcing steel. HCP testing was performed in general accordance with ASTM C876, *Standard Test Method for Half-Cell Potentials of Uncoated Reinforcing Steel in Concrete* over the full survey area of each bridge using a rolling test frame on which five copper-copper sulfate reference cells were mounted 3 to 4 feet apart (Figure 22). Half-cell measurements were collected at 2.5-foot intervals along the length of the bridge using a data logger with a 10 M-ohm internal impedance.

Connections to the reinforcing steel were made at two to four locations no more than 80 feet apart in each continuous section of deck by drilling down through the concrete to expose individual bars (Figure 23). Before commencing HCP measurements, electrical continuity testing was performed in each structure to assess the electrical continuity between two distant electrical connections to the reinforcing steel, as discussed further in Section 2.1.6 on AC resistance testing. To encourage connectivity during the HCP testing, multiple parallel connections to the steel were made on each deck section. Despite this precaution, some background level of resistance between the half-cell and reinforcing bars was found due to the epoxy coating.

2.1.5 Corrosion Rate Testing

Corrosion rate testing was performed to assess locations of active corrosion of reinforcing. The corrosion rate was evaluated by measuring polarization resistance using the galvanostatic pulse technique. In galvanostatic pulse measurements, an electric current pulse is applied between the instrument and a defined region of reinforcing steel. The disruption in the corrosion potential from the equilibrium potential is measured as a function of time; from this data, the polarization resistance is calculated. The corrosion current is inversely proportional to the polarization resistance. The corrosion rate is the ratio of this corrosion current to the surface area of the reinforcing steel where the test is performed.

The results of the corrosion rate testing were reported in terms of corrosion current (I), the corrosion potential (E) versus the silver-silver chloride (SSC) reference electrode at the measurement location, the resistance (R) of the concrete between the measurement site and the steel, and the estimated area (A) of reinforcing bar over which the measurement was taken.

The corrosion rate was measured at selected locations where the measured half-cell potentials indicated corrosion might be occurring (Figure 24). Testing was also performed at areas where corrosion was not suspected but a nearby connection to the steel was possible. The same electrical connection made to the reinforcing steel for the HCP surveys was commonly used during this testing. The corrosion rate measurements are instantaneous snap shots of the rate of corrosion at the time of testing, and do not necessarily represent average rates.

Corrosion is a dynamic process and the results obtained are instantaneous measurements; consequently, changes in the site conditions, particularly temperature and moisture content, will influence the readings. Furthermore, the presence of the epoxy coating greatly affects the resistance and the area of applied current. As a reference, previous studies on uncoated deformed reinforcing bars using this equipment showed that corrosion rates can be interpreted as follows:

- Corrosion rate $< 1 \mu\text{A}/\text{cm}^2$ indicates a passive condition (very low rate of corrosion)
- Corrosion rate ≥ 1 and $< 5 \mu\text{A}/\text{cm}^2$ indicates low to moderate corrosion
- Corrosion rate ≥ 5 and $< 10 \mu\text{A}/\text{cm}^2$ indicates moderate to high corrosion
- Corrosion rate $\geq 10 \mu\text{A}/\text{cm}^2$ indicates very high corrosion

2.1.6 Connectivity Measurements by AC Resistance

Electrical connectivity tests were performed to evaluate the condition of the epoxy coating in terms of its ability to electrically isolate sections of the reinforcing bar mat. Lower resistance indicates that coated bars are in near or direct contact through bare metal contact or through ties, and may indicate that defects or cuts are present in the coating. If the resistance is high, then the coating is likely generally intact and the tested bars are electrically isolated from each other (not continuous). The corrosion resistance of

epoxy-coated reinforcing bars is improved if bars are electrically isolated, since the formation of corrosion cells, which requires both cathodic and anodic reaction sites, between bars are inhibited. The measured resistance is also related to the distance separating measurement sites and the area of reinforcement to which the electrical connection is made, as well as the condition of the coating on individual bars.

Connectivity was tested by measuring the AC resistance between the reinforcing bars exposed at core and HCP ground locations using a null-balancing ohmmeter according to the procedure outlined by the Provincial Highway Management Division of Ontario (Ministry of Transportation of Ontario, 2007). As shown in Figure 25, the AC resistance was measured between each core or ground location and at least two other locations in each continuous section of the tested deck. Based on these measurements, the resistance at each location was calculated. A total of 5 to 17 resistance measurements were made on each bridge section.

Connection was made at core holes by wedging a stainless steel pin across the opening of the core hole between the two ends of the exposed reinforcing bar at each location. At some locations, only one exposed bar could be placed in contact with the pin. The AC resistance meter was then connected to the pins at each location (Figure 26).

2.2 Bridge Condition Assessment - Laboratory Analysis

All of the cores removed from the surveyed bridge decks and the segments of reinforcing bars they contained were transported to WJE's laboratory, photographed, and assessed. Most of the cores contained a segment of both a longitudinal and a transverse reinforcing bar from the top mat of reinforcing. Some samples also included a segment of a bar from the lower mat of reinforcement. The reinforcing steel segments were extracted from the cores and visually inspected and assigned a corrosion condition rating. The coating thickness was measured, and portion of the coating was then peeled back to obtain adhesion and backside contamination ratings. The cores were then sectioned for chloride analysis and to allow for the determination of chloride surface concentration and diffusion coefficient.

2.2.1 Petrographic Examination

One core sample from each bridge deck was selected for petrographic analysis to characterize the overall quality and nature of the concrete, as outlined in ASTM C856-04 *Standard Practice for Petrographic Examination of Hardened Concrete*. The petrographic analysis included microscopic evaluation to assess the characteristics of the air void system, the cement paste, the soundness of the aggregate, and the water-cement ratio. The depth of carbonation, a reaction between the cement paste and carbon dioxide in the air that lowers the high pH of the concrete paste and can disrupt the passive protective layer on the reinforcing steel, was also measured on each core sample selected for petrographic examination.

2.2.2 Examination of Extracted Bars

The coating thickness on each bar segment was measured with an electromagnetic coating thickness gauge. Where possible, three readings were taken from each side of each bar segment for a total of six readings per bar segment. The average of three readings taken between consecutive deformations was considered as one measurement. For some bar segments, where corrosion product had developed under the coating, the coating thickness was measured directly using a micrometer on portions of coating cut from the bar segment. All coating thickness measurements were made on the flat section of bar between deformations per ASTM A775-07B *Standard Specification for Epoxy-Coated Reinforcing Bars*.

A visual inspection of each epoxy-coated bar was conducted to categorize the extent of the corrosion-related deterioration on the bar as a percentage of the bar surface area. The categories used were in accordance with a previously developed 5-point rating system, where a rating of “1” refers to a bar with no corrosion and a rating of “5” means corrosion is present on more than 60% of the bar area (Sohanghpurwala & Scannell, 1998). The rating scale is shown in Figure 27. In addition to this corrosion condition rating, a judgment was made as to whether active corrosion was occurring at the bar surface. This corresponded to a corrosion condition rating of 2 or greater.

A knife adhesion test was performed on each side of every bar segment. The results were qualitatively evaluated as detailed in Report FHWA-RD-94-103 (McDonald, Sherman, & Pfiefer, 1995). To conduct this test, a utility knife is used to cut an “X” in the epoxy coating. Using the point of the knife, the coating is peeled back to the extent possible. The adhesion is evaluated through the use of a five point rating system. A rating of “1” corresponds to no peeling (excellent adhesion), while a rating of “5” correlates to easy peeling (poor adhesion). This rating scale is depicted in Figure 28. The highest of the two ratings measured on a particular bar segment is reported for that bar segment. To ensure that the coating was not permitted to dry out before adhesion testing, this test was performed in the field on bar surfaces that were exposed during the coring process and in the lab on bars immediately after they were broken out of the core samples.

The backside contamination of the sections of the peeled epoxy coating was assessed by comparing them with the backside contamination visual standards used by the Concrete Reinforcing Steel Institute Coating Applicator Plant Certification Program (Concrete Reinforcing Steel Institute, 2008). The rating is essentially the percentage of the backside surface of the peeled epoxy coating that exhibits contamination. The highest of the two ratings measured on a particular bar segment is reported for that bar segment.

2.2.3 Chloride Concentration Profiles

For corrosion to initiate on reinforcing steel that is embedded in sound concrete, chloride ions must accumulate to a sufficient concentration, known as the chloride threshold, to break down the naturally occurring protective film that develops on a steel surface in the highly alkaline environment within concrete. The onset of corrosion is governed by the time required for chloride to penetrate through the concrete cover over the steel and build up at the bar depth to the chloride threshold value.

To evaluate the current distribution of chloride ions within the decks and to permit estimates of chloride concentrations in the future, the chloride concentration profiles with depth were determined for at least four cores from each bridge. The top approximately 1/8-in. of each of the concrete cores was removed and the cores were sectioned to obtain 1/4-in. slices centered at approximately the following depths in inches from the original wearing surface: 3/8; 1-1/4; 2-1/2; and 4. These section depths were generally selected to obtain two slices above the level of the top mat of reinforcing, one slice at or slightly above the top surface of the top bar, and one slice below the top mat of reinforcing. The slices were pulverized for acid-soluble chloride content analysis essentially according to ASTM C114-09 *Standard Test Methods for Chemical Analysis of Hydraulic Cement* or ASTM C1152-04 *Standard Test Method for Acid-Soluble Chloride in Mortar and Concrete*. These chemical tests were performed by Exova Accutest, of Ottawa, Ontario and at WJE’s Northbrook laboratory. For each bridge, slices were cut from at least two uncracked cores at a depth of approximately 5 inches or more. The average chloride content of these samples was used to establish the baseline chloride concentration (C_0) for each bridge.

For those cores for which a profile was not determined, a single approximately 1/4-in. slice was cut from the core at a depth centered at the top of the reinforcing bar segment closest to the top concrete surface. The acid-soluble chloride contents of these slices were determined essentially according to ASTM C1152-04 *Standard Test Method for Acid-Soluble Chloride in Mortar and Concrete*.

Two of the bridges examined, US 218 and US 18, contained significant levels of background chloride (i.e., greater than 0.010 percent by weight of concrete), which is identified by uniformly high chloride levels at varying depths or by high chloride levels at depths into the concrete beyond where significant surface-applied chlorides would be expected to penetrate. In this report, chloride concentrations are given in terms of acid-soluble chloride, which represents nearly all chloride contained in the concrete sample, **including any chloride chemically bound within the aggregate**. Where present, background chlorides are often due to such chloride-containing aggregate, or to salts admixed in the deck concrete to accelerate hydration. To determine the source of the background chlorides, additional chloride content analyses were performed at WJE's Northbrook laboratory in two core slices from these two bridge decks at depths greater than 4 inches essentially according to ASTM C1218-99(2008) *Standard Test Method for Water-Soluble Chloride in Mortar and Concrete*. This test measures chloride ions that can be extracted with water and **are not chemically bound** in the aggregate. These tests found negligible water-soluble chloride concentrations, confirming that the background acid-soluble chloride levels result from bound chloride in the limestone coarse aggregates. Such chloride is generally unavailable to promote corrosion.

2.2.4 Chloride Concentration Analysis

Chloride ion transport in concrete is complex and may occur through diffusion (related to chloride ion concentration gradient), capillary absorption (wetting and drying), and permeation (driven by pressure gradients) (Stanish, Hooton, & Thomas, 1997). Chloride transport may also be slowed by chemical binding of the chlorides with aluminate phases in the cement, or by physical absorption or trapping of chloride ions in pores. Despite the potential complexity of the chloride penetration process, it is commonly assumed that diffusion plays the largest role. Therefore, describing chloride transport by using a mathematical representation of diffusion, quantified based on an "apparent" diffusion coefficient calculated from chloride concentration profiles measured in the actual structure, is judged to be a reasonable representation of this process accounting for other influences (Sohanghpurwala A. A., 2006).

Another controlling parameter in chloride transport in concrete is exposure, or the amount of chloride that a deck is exposed to. This is quantified in terms of effective surface chloride concentration, C_s , which is the chloride concentration at depth equal to zero.

Chloride diffusion in concrete, driven by a concentration gradient, can be described by Fick's Second Law of Diffusion:

$$\frac{dC}{dt} = D \times \frac{d^2C}{dx^2} \quad (1)$$

where C is the chloride concentration at a depth of x from the concrete surface at time t , and D is the chloride diffusion coefficient.

If the surface chloride concentration C_s and D are assumed to be constants, the concentration $C(x, t)$ at depth of x and time t is given by the following solution (Crank, 1956):

$$C(x,t) = C_s - (C_s - C_0) \times \operatorname{erf}\left(\frac{x}{2 \times \sqrt{D \times t}}\right) \quad (2)$$

where $\operatorname{erf}()$ is the Gaussian error function, and C_0 is the background or original chloride concentration.

Based on this relationship, the values of C_s and D_a (the apparent diffusion coefficient) that provided the best fit to the measured chloride concentration profiles were determined using a least squares fitting method. The term t was assigned as the age of the bridge. With these values and Equation 2 from above, the chloride concentration at the core location at any depth can be predicted for any given time. Figure 29 shows an example of a fitted diffusion curve.

The values of C_s are strongly influenced by the exposure conditions (i.e. severity of deicing salt application), and D_a is governed by the quality of the concrete. Based on studies of bridge decks in northern states conducted by WJE, the C_s can range from greater than 0.80 percent by weight of concrete in New York to 0.15 percent by weight of concrete in Virginia (Lee & Krauss, 2003). Exposure conditions may be considered mild, moderate and severe if C_s falls in the following ranges, respectively: up to 0.25 percent by weight of concrete; 0.25 to 0.55 percent by weight of concrete; and 0.55 percent by weight of concrete or higher (Krauss, Lawler, & Steiner, 2009).

3.0 RESULTS

Summaries of the findings of the field and laboratory investigation at each of the eight bridge decks examined in 2010 are given in this chapter. Additional detailed results of the field investigation are presented in Appendix A, and detailed results from the laboratory analyses are contained in Appendices B and C.

The percentage of the deck area with evidence of corrosion-related damage (spalled, delaminated, or patched) and the measured crack densities are given in Table 2 for each continuous section of each deck. The average and standard deviation of cover measured using GPR and of measured AC Resistance on each continuous deck section are given in Tables 3 and 4, respectively.

As quantified during AC resistance testing, a variable amount of additional electrical resistance was present in the half-cell test circuit because of the coating on the bars, and this resistance is expected to shift the measured potential values. **Therefore, interpretation of the half-cell test results based on the numeric values, such as those cited in ASTM C876, is not appropriate.** Instead, contour maps of the measured potentials have been created and examined to determine where large potential gradients, manifested by closely spaced equipotential lines, have developed. If areas of more negative potential are surrounded by areas of more positive potential, the areas of more negative potential are probably anodic and likely undergoing corrosion, while those of more positive potential are probably cathodic and not generating corrosion product. Other things being equal, maximum corrosion currents will flow between points of high and low potential that are close to each other. Contour maps generated based on the measured half-cell potentials are included in Appendix A.

The average and standard deviation of corrosion rate currents by continuous deck section are given in Table 5; the individual results from the corrosion rate testing are also tabulated for each bridge in Appendix A. The presence of epoxy coating on the bars may also have affected these results by confining the surface area of steel polarized during testing to those regions on the bar where the electrical insulation of the coating has been compromised. **Therefore, the reported results may underestimate the corrosion rate occurring at localized areas of coating damage.**

Table 6 to Table 14 present the data collected in the laboratory for each core and the associated bar segments. In these tables, the bar depth, coating thickness, adhesion rating, backside contamination, corrosion condition, and the presence of active corrosion are provided. In addition, the presence of a crack in the core is listed. The crack direction given was defined relative to the deck, so horizontal cracks at the bar represent horizontal delaminations at the bar mat, and vertical cracks represent vertical cracks in the bridge deck, such as those typical of early-age shrinkage. Finally, these tables give the chloride concentration at the bar depth for each bar, whether measured directly or calculated based on the Fick's Law solution for that core. These values are termed "effective" chloride concentration, since they have been corrected for the amount of background (non-water soluble) chloride present in the concrete. The chloride concentration measured in each slice of each core and the calculated surface concentration and diffusion coefficient are listed based on the fit of the analytical solution to Fick's Law to the measured chloride profiles given for each core in Appendix C.

The calculated surface concentrations and diffusion coefficients are summarized in Table 15. This shows the average and standard deviation of the effective surface concentrations considering all cores, corrected for background chloride levels, which are also listed in the table. **The apparent diffusion coefficients for samples with and without vertical cracks are reported separately, since the presence of cracks is**

expected to have a large impact on chloride movement through the concrete and the amount of time that the reinforcing bars are exposed to sufficient chlorides for corrosion.

3.1 IA 17 over US Route 20

The full length of the northbound lane and shoulder was surveyed on this bridge. Seven core samples were taken.

3.1.1 Visual and Delamination Surveys

The visual survey found this bridge deck to be in good condition in the area surveyed. Some cracking was identified in the bridge deck over the piers and near the abutments, but these cracks were generally limited in number and length. As a result, the density of identified cracks was quite low, 0.007 ft per sq ft, which is the second lowest crack density of the eight bridge decks surveyed.

A few delaminations and existing patches were identified on the top deck surface by the visual and delamination surveys. Most of these delaminations and patches were located over the piers or in the end spans, and totaled less than 150 square feet, or approximately 3 percent of the deck area surveyed. No delaminations, spalling or cracks with efflorescence were observed on the deck underside. A portion of the deck underside is shown in Figure 30.

3.1.2 Cover Measurements

Cover measurements varied between 1.6 inches and 2.9 inches, with an average value of approximately 2.3 inches. Approximately 15 percent of the cover measurements are less than the specified cover of 2.0 inches; these measurements of low cover come from the set of measurements taken from the left wheel path. All of the cover measurements taken at the right shoulder meet or exceed the minimum depth of cover. Based on this data, the bars at the right shoulder have 1/4 to 1/2 inch more cover on average than those at the left wheel path.

3.1.3 AC Resistance, Half-Cell Potential, and Corrosion Rate Testing

The average AC resistance measured in the deck of IA 17 was 32 ohms, which is considered very low and is the lowest of the eight decks included in this survey, possibly indicating damage to the epoxy coating or poor quality of coating, and potential susceptibility to corrosion. The uncoated bars in the bottom mat of reinforcing likely affect the overall resistance measured. The measured half-cell potentials ranged from approximately -500 to -180 mV vs. CSE. More negative readings were measured near the expansion joints and were likely influenced by the presence of the uncoated steel armored joint at these locations. A localized zone of more negative potentials was identified over the first pier from the north. Corrosion rates over 2 $\mu\text{A}/\text{cm}^2$ were measured at 3 of 5 tested locations on this deck, indicating localized active corrosion has likely developed.

3.1.4 Petrographic Analysis

Core No. 1 was examined petrographically. The concrete was determined to be sound and of good quality, with a moderately low water-to-cementitious material ratio of 0.4 to 0.45. Carbonation of the concrete was generally limited, but varied up to a depth of 0.4 inches, which is the maximum depth of carbonation encountered during this study. The coarse aggregate was found to be sound. Alkali-silica reactive particles are present in the fine aggregate, although this does not appear to have affected the surrounding cement matrix. The entrained air content (6.4 percent) is sufficient to provide freeze-thaw

protection, although the air void spacing parameters are slightly above preferred levels. No damage or distress to the concrete was evident.

3.1.5 Chloride Testing and Diffusion Analysis

The average effective surface concentration measured in the cores from IA 17 was 0.777 percent by weight of concrete. This is the second highest surface concentration measured during this survey, and is considered to be a very severe exposure. The average apparent diffusion coefficient for uncracked concrete as represented by the core samples was 0.057 in.²/yr, which is a moderate to low value compared to the other seven decks.

3.1.6 Examination of Bar Conditions

The conditions of the fifteen reinforcing bar segments that were extracted from seven cores obtained from the deck of IA 17 are summarized in Table 6. Four bar segments, representing two cores, were found to be actively corroding. Both these cores were taken through delaminations in the deck, and the chloride concentration at bar depth ranged from 0.194 to 0.351 percent by weight of concrete. These values are 6 to 10 times above the accepted corrosion threshold for uncoated bars, which is approximately 0.035 percent by weight of concrete.

3.2 US 218 Southbound over Cedar River

The full length of the southbound right lane and shoulder was surveyed on this bridge. Nine core samples were taken.

3.2.1 Visual and Delamination Surveys

The current condition of this bridge deck is excellent, based on the findings from the visual and delamination survey in the area surveyed. The top deck surface did not have a single delamination or patch. The deck underside also did not exhibit any delamination or spalling, although the deck underside could not be observed for the three spans directly over the river.

Some cracking was observed on the top deck surface, generally consisting of longitudinal cracks in the wheel paths (see Figure 31), particularly in the two approach spans at the bridge ends (Sections 1 and 3), and randomly located transverse cracks. A few generally transverse cracks were concentrated over the first pier from each bridge end in the approach spans (Piers 1 and 6). All cracking observed was generally in the range of 0.010 inches wide. On the deck underside, some of the transverse cracks were visible, and generally were highlighted by efflorescence, indicating that these are through-thickness cracks, although the spans over the Cedar River were not inspected from below.

3.2.2 Cover Measurements

Cover measurements varied between 1.7 inches and 3.4 inches, with an average value of approximately 2.5 inches. Given that the specified minimum depth of cover is 2.5 inches, many bars do not have the specified cover. In fact, none of the cover measurements made in the left wheel path in Section 1 of the deck meet the specified cover. Sections 2 and 3 of the deck are clearly better, but still have approximately 40 percent of the readings below 2.5 inches. As noted at the IA 17 bridge deck, the bars typically have 1/4 to 1/2 in. more cover at the right shoulder than in the left wheel path.

3.2.3 AC Resistance, Half-Cell Potential, and Corrosion Rate Testing

The test locations in the three sections of the deck of Southbound US 218 separated by expansion joints exhibited average AC resistances of 798, 862, and 583 ohms, values near the middle of the range measured during this survey. The half-cell potentials ranged from approximately -790 to -290 mV vs. CSE. Significant differences in the range of HCP values were observed between the three sections, reflecting the variable level of reinforcing bar continuity. More negative potential readings were measured near the expansion joints and were likely influenced by the presence of the uncoated steel of the armored joint at these locations. The most negative measurements were observed on deck Section 3, but few areas of high potential gradient were observed throughout this deck. Corrosion rates over $2 \mu\text{A}/\text{cm}^2$ were measured at only 2 of 16 tested locations on this deck, indicating localized active corrosion is likely limited.

3.2.4 Petrographic Analysis

Core No. 3 from this deck was examined petrographically, and was found to contain sound concrete of good quality. This concrete has sound coarse aggregate, minimal carbonation, and a moderate water-to-cementitious material ratio of 0.45 to 0.5. The entrained air content was adequate, estimated at 5 to 6 percent, for this concrete, and no evidence of freeze-thaw damage was noted. The fine aggregate was found to contain alkali-silica reactive particles, but no disruption of the surrounding cement matrix was noted.

3.2.5 Chloride Testing and Diffusion Analysis

In addition to the chlorides entering the concrete from the deck top surface, a background chloride concentration of 0.048 percent by weight of concrete was measured in the cores from Southbound US 218. It is likely that the limestone aggregates used in the concrete for the Southbound US 218 deck contained bound chloride that is not available to help initiate the corrosion reaction. Additional water-soluble chloride content testing was able to extract a chloride content of only 0.011 percent by weight of concrete from this concrete, indicating that 75 percent of the background chlorides are not available to participate in the corrosion reaction.

The average effective surface concentration measured in the cores from Southbound US 218 was 0.557 percent by weight of concrete. This is considered to be a severe exposure, but was among the lowest for the eight bridges surveyed. It is also somewhat higher than the uncorrected average surface concentration of 0.425 percent by weight of concrete measured by WJE for this bridge in 2002. The average apparent diffusion coefficient for the uncracked concrete represented by the cores was $0.124 \text{ in.}^2/\text{yr}$, which was among the highest measured in this survey. In 2002, the average apparent diffusion coefficient measured for all tested cores (including cracked cores) was found to be $0.220 \text{ in.}^2/\text{yr}$.

3.2.6 Examination of Bar Conditions

The conditions of the sixteen reinforcing bar segments that were extracted from nine cores obtained from the deck of Southbound US 218 are summarized in Table 7. No sampled bar segments in this deck were judged to be actively corroding, despite the fact that the chloride concentrations at bar depth were greater than or equal to 0.250 percent by weight of concrete in two cores.

3.3 IA 150 over Cedar River

The full length of the northbound lane and shoulder was surveyed on this bridge. Nine core samples were taken.

3.3.1 Visual and Delamination Surveys

Overall, the bridge deck is in good condition in the area surveyed, with limited transverse cracking or corrosion-related deterioration noted on the top deck surface. In fact, this bridge deck had the least amount of cracking and the lowest crack density (avg. 0.003 ft/sq ft) of the eight bridge decks surveyed. In the approximately 13,000 sq ft of the top deck surveyed, the amount of delaminated concrete and existing patches was only about 150 sq ft, or approximately 1.2 percent of the deck top surface. Approximately 80 percent of this deterioration occurs in Sections 1 and 3 of the deck, generally occurring near the piers where the deck is continuous over the pier, and to a lesser degree, along the right edge of the northbound lane. Often, the areas of patching and delaminated concrete over the piers corresponded with the few transverse cracks noted in the deck, including the location shown in Figure 32. In one location, the deck had been patched with asphalt (see Figure 33), but the area had continued to deteriorate with additional delamination of the concrete outside of and adjacent to the patch. On the deck underside, no noticeable deterioration was observed, but the underside of most spans was not accessible due to the Cedar River. A view of the deck underside at the north abutment is provided in Figure 34. It should be noted that the most recent Iowa DOT inspection report noted a couple of hairline cracks with “light leaching, and one small hollow area,” as well as a few locations of spalls and delaminations on the beam ends.

3.3.2 Cover Measurements

Cover measurements ranged from approximately 1.9 inches to over 3.2 inches, averaging slightly under 2.5 inches. As a result, approximately 57 percent of the cover measurements are below the specified cover of 2.5 inches. Deck Section 2 is the best of the three deck sections, with only 35 percent of the cover measurements below 2.5 inches, whereas 85 percent of the cover measurements in Deck Section 3 are below 2.5 inches. It should also be noted that the cover measurements for the right shoulder and left wheel path are quite similar in this deck.

3.3.3 AC Resistance, Half-Cell Potential, and Corrosion Rate Testing

The test locations in the three sections of the deck of IA 150 separated by expansion joints exhibited average AC resistances of 203, 168, and 569 ohms. This is lower than most of the decks surveyed in this study, indicating possible susceptibility to corrosion, and possibly indicting that the uncoated bars in the bottom mat of reinforcement may reduce the effective resistance measured. The half-cell potentials ranged from approximately -770 to -340 mV vs. CSE. As with the other decks with multiple sections separated by expansion joints, significant differences in the typical HCP were observed between the three sections, reflecting the variable level of reinforcing bar continuity measured in each section. More negative readings were measured near the expansion joints and were likely influenced by the presence of the uncoated steel armored joint at these locations. Locally high potential gradients were measured over a number of piers and in local areas close to the centerline in the northern half of the deck. Corrosion rates over 4 $\mu\text{A}/\text{cm}^2$ were measured at 4 of 12 tested locations on this deck, with three of these occurring over piers, indicating localized active corrosion has likely developed. The concentration of gradients and the measured corrosion rates over the piers may reflect corrosion facilitated by cracking in the negative moment regions of the deck, and which is evidenced by the delaminations and patches there.

3.3.4 Petrographic Analysis

A petrographic examination was performed on Core No. 5 from the IA 150 deck. This core contained concrete of good quality, with a moderately low estimated water-to-cementitious material ratio of 0.4 to 0.45, and with an adequate entrained air content, estimated at 5 to 6 percent. Additionally, the crushed limestone coarse aggregate was sound, although not uniformly distributed. The depth of carbonation was 0.4 inches, which is the greatest depth of penetration encountered during this study, but is still far from the level of the top reinforcing. As with most other cores examined in this study, the fine aggregate contains some particles susceptible to alkali-silica reaction (ASR), but because of the small size of these particles, no disruption of the surrounding cement matrix had occurred.

3.3.5 Chloride Testing and Diffusion Analysis

The average effective surface concentration measured in the cores from the IA 150 bridge deck was 0.760 percent by weight of concrete. This is considered to be a very severe exposure. The average apparent diffusion coefficient for uncracked concrete was 0.067 in.²/yr.

3.3.6 Examination of Bar Conditions

The conditions of the seventeen reinforcing bar segments that were extracted from nine cores obtained from the deck of IA 150 are summarized in Table 8. Four sampled bar segments from three cores in this deck were judged to be actively corroding. All of these came from cores taken at vertical shrinkage-type cracks in delaminated areas of the deck. The chloride concentration at the depth of these actively corroding bars ranged from 0.184 to 0.434 percent by weight of concrete.

3.4 IA 13 Southbound over Indian Creek

The full length of the southbound right lane and shoulder was surveyed on this bridge. Seven core samples were taken.

3.4.1 Visual and Delamination Surveys

The visual and delamination surveys found this bridge deck to be in excellent condition. No delaminations or spalls were identified on the top or bottom surfaces of the deck in the area surveyed. Some cracking was noted in the deck slab, which resulted in a calculated crack density of 0.161 ft per square foot, which is the third highest crack density of the eight bridges surveyed. On the top deck surface, these cracks were almost entirely longitudinal in orientation, and occurred mostly in the traffic lane, not in the 10 ft wide shoulder. Most of the cracking on the deck underside was also longitudinal, although a few transverse cracks were noted in the vicinity of the piers. None of the cracks on the deck underside exhibited any efflorescence, and all were very narrow. Typical views of the top and bottom surfaces of the bridge deck are shown in Figures 35 and 36. At the southwest corner of the bridge deck, the deck slab and the adjacent barrier rail exhibited random hairline cracking (see Figure 37). Cracking of this nature is often associated with freeze-thaw damage or material-related degradation such as alkali-silica reaction.

3.4.2 Cover Measurements

This bridge deck has the highest average cover measurement, 3.1 inches, of any of the eight decks surveyed. As a result, only approximately 10 percent of the readings obtained are below the specified cover of 2.5 inches. Overall, the cover measurements ranged from 2.3 inches to 3.7 inches.

3.4.3 AC Resistance, Half-Cell Potential, and Corrosion Rate Testing

The average measured AC resistance in the deck of Southbound IA 13 was 408 ohms, which is moderately low compared to the other bridge decks studied. The half-cell potentials ranged from approximately -640 to -480 mV vs. CSE. While highly negative, these results reflect a relatively narrow range compared to the other decks, and locally high potential gradients were not identified. However, corrosion rates over 2 $\mu\text{A}/\text{cm}^2$ were measured at 5 of 9 tested locations on this deck, indicating localized active corrosion may have developed.

3.4.4 Petrographic Analysis

Core No. 5 from this bridge deck was examined petrographically. The concrete was determined to be sound and of good quality, with a moderate water-to-cementitious material ratio of 0.45 to 0.5, sound crushed limestone coarse aggregate, and a depth of carbonation of less than 0.2 inches. Fly ash is present in the concrete mix as a supplementary cementitious material. The entrained air content of this concrete is good, estimated at 6.0 percent, but the air void system parameters are a little above levels ideal for excellent protection from freeze-thaw damage. The fine aggregate contains alkali-silica reactive particles, and secondary deposits were noted in some air voids, but no disruption of the surrounding cement matrix was noted, presumably because of the small size of the reactive particles. No damage due to ASR or freeze-thaw was noted in the core.

3.4.5 Chloride Testing and Diffusion Analysis

The average effective surface concentration measured in the cores from the Southbound IA 13 bridge deck was 0.563 percent by weight of concrete. This is considered to be a severe exposure, but was the lowest for the bridges surveyed. It is also an increase from the uncorrected average surface concentration measured by WJE in 2002 of 0.464 percent by weight of concrete. The average apparent diffusion coefficient for the uncracked concrete cores was 0.242 $\text{in.}^2/\text{yr}$, which was the highest measured during this survey. It is also an increase from the average apparent diffusion coefficient determined for all cores in 2002, which was 0.172 $\text{in.}^2/\text{yr}$.

3.4.6 Examination of Bar Conditions

The conditions of the ten reinforcing bar segments that were extracted from seven cores obtained from the deck of Southbound IA 13 are summarized in Table 9. No sampled bar segments were actively corroding. The chloride concentrations at bar depth were higher than 0.200 percent by weight of concrete at two of the sampled bars where chloride contents were determined.

3.5 US 30 over Missouri River

The westbound right lane and shoulder were surveyed from the east abutment to a distance of 830 feet from the east end of the bridge. The eastbound right lane and shoulder were surveyed from the west abutment to a location approximately 873 feet from the east end of the bridge. Nineteen core samples were taken, nine in the westbound lane survey area and ten in the eastbound lane survey area.

3.5.1 Visual and Delamination Surveys

The condition of the deck slab varies along the length of the bridge as determined by the visual and delamination surveys. Of the four deck sections between expansion joints, Section 3, the section corresponding to the main spans over the river, was in very good condition, with minimal concrete deterioration. At the time of our survey, less than 10 sq ft of delaminations, spalls, and patches were

identified on the portion of the deck top surface surveyed in Section 3, or approximately 0.1 percent. Some shrinkage-type cracking was noted in the deck top surface, which resulted in a moderate calculated crack density of 0.093 ft/sq ft where surveyed. Much of the observed cracks were transverse cracks, particularly in the middle portion of this deck section, with typical crack widths in the range of 0.010 to 0.020 inches. Toward the east and west ends of this deck section, longitudinal cracks in the traffic lanes were the predominant type of cracking observed. Because this deck section is located over the river, the deck underside was not observed.

Section 4 of the bridge deck, which corresponds to the east approach spans, is generally in good to very good condition, although not quite as good as Section 3. A typical view of this deck section is provided in Figure 38. A total of 181 sq ft of delaminations were identified in this deck section, or approximately 1.7 percent of the area surveyed. Most of these delaminations occur along the transverse cracks which are quite common for most of the length of this deck section. One such location is shown in Figure 39. In the 60 ft of this deck section closest to the expansion joints at the east and west ends of this section, most of the cracks observed are longitudinal. Overall, the crack density in this section is moderate, totaling 0.130 ft/sq ft in this area. On the deck underside, many of the transverse cracks were visible, and were highlighted with efflorescence (see Figure 40). No spalls or delaminations were noted on the deck underside. This deck has epoxy-coated bars for the bottom mat of reinforcing.

At the west approach spans, which correspond to Sections 1 and 2 of the bridge deck, the overall condition of the deck is good, although the level of deterioration is greater than in the other two deck sections of this bridge. The delamination survey identified approximately 280 sq ft of delaminations, spalls, and existing patches in Section 2, or approximately 3.2 percent of the area surveyed, while over 400 sq ft of concrete deterioration and existing patches was noted in Section 1, or 6.1 percent of the area surveyed. An area of incipient spalling is shown in Figure 41. Some of the delaminations occurred around a previous repair, such as that shown in Figure 42, which is indicative of the “halo” or “ring anode” effect, where corrosion occurs on the reinforcing bar immediately outside of a patch after the patch is completed. Many of these areas of delamination correspond with cracks or construction joints in the deck. These two deck sections had two of the four highest calculated crack densities of any of the bridge deck sections surveyed, totaling 0.140 ft/sq ft in Section 1 and 0.173 ft/sq ft in Section 2. Most of the observed cracking was transverse to the span direction, although some longitudinal cracking was noted, particularly near expansion joints and construction joints. A typical transverse crack is shown in Figure 43. Like the east approach spans, many of the transverse cracks are readily apparent on the deck underside with efflorescence at most (see Figure 44). Such cracking was not observed in those spans adjacent to the expansion joints.

3.5.2 Cover Measurements

Cover measurements in this bridge ranged significantly, from 1.8 inches to 3.8 inches. Given the overall length of the bridge, a wider range of measurements is not unexpected. However, in all four sections of the bridge deck, the average cover measurement exceeded the 2.5 inch specified cover. The approximate percentage of cover measurements below 2.5 inches was 25 percent for Section 1, 40 percent for Section 2, 10 percent for Section 3, and 15 percent for Section 4. It should be noted that the two deck sections with the most low cover readings correspond to the two deck sections exhibiting the most corrosion-related damage. The cover measurements obtained were generally less in the left wheel path than in the right shoulder by approximately 1/4 inch, except in Deck Section 3, where the opposite is true. This may be due to the location where the readings were taken, since the transverse locations of the steel

girders supporting Section 3 are different than that of the prestressed concrete beams in the other three deck sections.

3.5.3 AC Resistance, Half-Cell Potential, and Corrosion Rate Testing

The test locations of the four sections of the deck between expansion joints in the US 30 bridge had average measured AC resistances of 670, 1,187, 406 and 751 ohms (for deck Sections 1 through 4, respectively). All these values are close to the middle of the range observed during this survey. The half-cell potentials ranged from approximately -590 to -190 mV vs. CSE. More negative readings were measured near the expansion joints and were likely influenced by the presence of the uncoated steel armored joint at these locations. Locally high potential gradients were measured across the width of the surveyed lane in some locations, suggesting that corrosion may be occurring along a top reinforcing bar, possibly influenced by a transverse crack. Corrosion rates over 4 $\mu\text{A}/\text{cm}^2$ were measured at relatively few (3 of 22) tested locations on this deck, indicating that localized active corrosion may have developed at a limited number of places.

3.5.4 Petrographic Analysis

A petrographic examination of Core No. 18 from this bridge deck found the concrete to be sound and of good quality, with a sound natural gravel coarse aggregate, sound fine aggregate, minimal carbonation, and a moderately low water-to-cementitious materials ratio estimated at 0.4 to 0.45. The entrained air content was estimated at 4 to 5 percent, which is slightly low, but no evidence of freeze-thaw damage was noted.

3.5.5 Chloride Testing and Diffusion Analysis

The average effective surface concentration measured in the cores from US 30 was 0.635 percent by weight of concrete. This is considered to be a severe exposure. The average apparent diffusion coefficient for the uncracked concrete cores was 0.029 $\text{in.}^2/\text{yr}$, which was the lowest measured during this survey.

3.5.6 Examination of Bar Conditions

The conditions of the thirty-nine reinforcing bar segments that were extracted from the nineteen cores obtained from the deck of US 30 are summarized in Table 10 and Table 11. Six bar segments were actively corroding, though one of these segments (Core No. 19) was located in a patch repair area. Because of the patch in Core No. 19, diffusion curve fitting was not performed for this core. The chloride concentration at the depth of the actively corroding bar segment in Core No. 2 was 0.063 percent by weight of concrete. The observed corrosion surrounded damage to the coating that likely occurred during construction as shown in Figure 45 and was not typical of the corrosion observed elsewhere on the structure. The chloride concentrations at bar depth for the remaining actively corroding bars ranged from 0.286 to 0.506 percent by weight of concrete, values which are approximately 8 to 15 times the corrosion threshold for uncoated bars.

3.6 US 18 over Floyd River

The full length of the westbound lane and shoulder was surveyed on this bridge. Eight core samples were taken.

3.6.1 Visual and Delamination Surveys

This bridge deck is in excellent condition in the study area, as determined by the visual and delamination surveys. No delaminations, spalls or existing patches were identified on the top or bottom surfaces of the bridge deck. The top deck surface does exhibit some cracking, particularly longitudinal cracking in both wheel paths that extend for most of the length of the bridge. One such crack is shown in Figure 42. In addition to the longitudinal cracking, transverse cracks were noted in the center span and in the east span near the east pier, with diagonal cracks also noted near the east pier and at the northeast corner of the deck. The density of cracking observed, 0.165 ft per sq ft, is the second highest of the eight bridge decks surveyed. Most of the transverse cracks appear to be visible on the deck underside, with light efflorescence highlighting the cracks. Some of these cracks can be seen in the view of the underside of the center span provided in Figure 47.

3.6.2 Cover Measurements

The cover measurements varied from approximately 2.1 inches to 3.4 inches, with an average value of 2.56 inches. Therefore, about 40 percent of the cover readings are below the specified cover of 2.5 inches. The difference between readings taken in the left wheel path and those taken at the right shoulder is minimal.

3.6.3 AC Resistance, Half-Cell Potential, and Corrosion Rate Testing

The average measured AC resistance of the deck of US 18 was 1592 ohms, the highest in any of the surveyed decks. The half-cell potentials ranged from approximately -850 to -560 mV vs. CSE. More negative readings were measured near the expansion joints and were likely influenced by the presence of the uncoated steel armored joint at these locations. Other large gradients were not observed. Corrosion rates were universally low (less than 1 $\mu\text{A}/\text{cm}^2$) throughout this deck. These results suggest active corrosion has not developed.

3.6.4 Petrographic Analysis

A petrographic examination was performed on Core No. 8 from this bridge deck. This concrete was found to be sound and of good quality, with a moderately low water-to-cementitious materials ratio estimated at 0.4 to 0.45, and minimal carbonation. The entrained air content was estimated at 4 to 5 percent, which is slightly low, but no evidence of freeze-thaw distress was noted in the cementitious matrix. In general, the coarse aggregate is a sound natural gravel, but one non-durable shale particle was noted which appears to be associated with shallow incipient surface scaling. Additionally, the fine aggregate includes some particles that are potentially susceptible to alkali-silica reaction, but because these particles are small, no disruption of the surrounding cementitious matrix was noted.

3.6.5 Chloride Testing and Diffusion Analysis

In addition to the chlorides entering the concrete from the deck top surface, an acid-soluble background chloride concentration of 0.027 percent by weight of concrete was measured in all cores from US 18. It is likely that the limestone aggregates used in the concrete for the US 18 deck contains bound chloride. Additional water-soluble chloride testing confirmed that little of the background chloride is available for participation in the corrosion reaction.

The average effective surface concentration measured in the cores from US 18 was 0.559 percent by weight of concrete, which is among the lowest observed. Nevertheless, this is still considered to be a

severe exposure. The average apparent diffusion coefficient for uncracked concrete cores was 0.059 in.²/yr. In 2002, the average uncorrected surface concentration was 0.556 percent by weight of concrete, while the apparent diffusion coefficient for all concrete cores was 0.130 in.²/yr. While the effective surface concentration determined in this study matches the one determined in the 2002 study, the apparent diffusion coefficient is less than one-half that determined in 2002. This difference is most likely due to the inclusion of cores with cracking in the 2002 data.

3.6.6 Examination of Bar Conditions

The conditions of the fifteen reinforcing bar segments that were extracted from eight cores obtained from the deck of US 18 are summarized in Table 12. No bar segments were actively corroding. The chloride concentrations at the bar depth in this deck were generally lower than in the other surveyed decks, with the maximum being 0.138 percent by weight of concrete, approximately four times the chloride threshold for uncoated reinforcement.

3.7 US 65 Southbound over the Union Pacific Railroad

The full length of the southbound right lane and shoulder was surveyed on this bridge. Ten core samples were taken.

3.7.1 Visual and Delamination Surveys

In general where surveyed, the visual and delamination surveys found this bridge deck to be in good condition, with no areas of spalling on the deck top surface. However, extensive patching of this deck had been performed by Iowa DOT maintenance personnel during the spring of 2010 and previously, presumably due to spalls and delaminations that had formed at cracks over transverse reinforcing bars. Some areas of delamination were found on the top deck surface, often along transverse cracks or immediately adjacent to existing patches, as is shown in Figures 48 and 49. Overall, approximately 80 sq ft of delaminations and 200 sq ft of existing patches were identified, which are a combined 3.8 percent of the area surveyed. Most of the cracking on the deck is transverse to the direction of traffic, although a few short, isolated longitudinal cracks were also noted. In general, the observed cracking was somewhat limited, with a calculated crack density of 0.021 ft per sq ft in the area surveyed, although some deck cracking was eliminated by the patching. This does not include the plastic shrinkage cracking noted in a couple areas of the deck top surface, which correspond with several patches and delaminations. A close-up view of the plastic shrinkage cracking is shown in Figure 50. On the deck underside, a number of areas of delaminated and spalled concrete below the uncoated reinforcing bars in the bottom mat were identified over the entire bridge deck, totaling approximately 250 sq ft, or about 1.8 percent of the entire deck area. One such area of spalling is shown in Figure 51.

3.7.2 Cover Measurements

The cover measurements at this bridge deck averaged 2.56 inches, and ranged from 2.1 inches to 3.2 inches, approximately. As a result, approximately 45 percent of the readings are below the specified cover of 2.5 inches. The differences between the readings taken in the left wheel path and those taken in the right shoulder were generally less than 1/4 inch.

3.7.3 AC Resistance, Half-Cell Potential, and Corrosion Rate Testing

The average measured AC resistance in the deck of the Southbound US 65 bridge was 1462 ohms, close to the highest of the bridges surveyed. The half-cell potentials ranged from approximately -370 to -130

mV vs. CSE. Moderately large gradients were observed over the southern pier and at mid-span of the center span in strip-like regions oriented transversely to the deck where cracking, patching, and delamination are evident. Corrosion rates were high throughout the deck, with only 2 of 19 measurements less than $4 \mu\text{A}/\text{cm}^2$. These results suggest active corrosion has developed over much of the deck, despite the high resistance.

3.7.4 Petrographic Analysis

Core No. 9 was examined petrographically and was found to contain sound concrete that is of good quality. This concrete contains a sound crushed limestone coarse aggregate, minimal depth of carbonation, a moderately low water-to-cementitious ratio estimated at 0.4 to 0.45, and a sufficient estimated entrained air content of 6 to 7 percent. Fly ash is present in the concrete mix as a supplementary cementitious material. As for most of the other bridge decks studied, the fine aggregate contains some particles that are potentially susceptible to alkali-silica reaction, but no disruption of the surrounding cementitious matrix had yet occurred.

3.7.5 Chloride Testing and Diffusion Analysis

Core No. 6, which contained a corroded bar, was taken at the edge of a patch, and half of the top approximately 2 in. of core consisted of a repair material. Because the chloride ingress was disrupted at this location by the patching, diffusion curve fitting was not performed for this core.

The average effective surface concentration measured in the cores from Southbound US 65 was 0.823 percent by weight of concrete. This was the highest measured in this study and represents a very severe exposure. The average apparent diffusion coefficient for the uncracked concrete represented by these cores was $0.083 \text{ in.}^2/\text{yr}$. This is the third highest average diffusion coefficient calculated in this study.

3.7.6 Examination of Bar Conditions

The conditions of the eighteen reinforcing bar segments that were extracted from eight cores obtained from the deck of the Southbound US 65 bridge are summarized in Table 13. Core No. 9 contained one uncoated bar segment with a cover of over 5 in. that represents the bottom mat of reinforcing steel. Seven bar segments from five cores were actively corroding. Core No. 6 from the edge of a patch contained a corroded bar. The corrosion conditions of these bar segments in Core No. 6 may have been influenced by the “halo” or “ring anode” effect, a process by which corrosion in bars adjacent to concrete repairs is accelerated by locally large differences in the internal concrete environment at the perimeter of patch repairs. The chloride concentrations at the depth of the actively corroding coated bars in this deck were high and ranged from 0.176 to 0.398 percent by weight of concrete. These values are 5 to 11 times the estimated corrosion threshold for uncoated bars.

3.8 US 65 Northbound over the Union Pacific Railroad

The full length of the northbound right lane and shoulder was surveyed on this bridge. Eight core samples were taken.

3.8.1 Visual and Delamination Surveys

The condition of the Northbound US 65 bridge deck in Bondurant is similar to that of the southbound deck with delaminations and extensive patching, except that the extent of deterioration is greater. The quantities of delaminations and patches on the top deck surface are higher, totaling approximately 500 sq

ft and 330 sq ft, respectively. This indicates that approximately 11.2 percent of the deck top surface has experienced corrosion-related damage. This is the highest level of deterioration encountered during this survey. As for the Southbound US 65 deck, most of the delaminations and patches seem to correspond with transverse deck cracks, although the patching obscured the cracks in some locations. Many of the new delaminations are located immediately adjacent to existing patches. Figures 52 and 53 show areas of extensive deck patching where some new delaminations were identified. The observed deck cracks were almost entirely transverse, and with twice the crack density (0.047 ft per sq ft) found in the Southbound US 65 deck. Short hairline randomly-oriented cracking similar to plastic-shrinkage cracking (see Figure 54) was noted throughout the area surveyed. Some delamination and spalling was also noted on the deck underside below uncoated bars in the bottom mat of reinforcing, although somewhat less (approximately 180 sq ft) than that found on the Southbound US 65 deck. Examples of deck underside deterioration are provided in Figures 55 and 56.

3.8.2 Cover Measurements

The average cover measurement at this bridge deck was 2.50 inches, which is equal to the specified cover. As a result, approximately 50 percent of the cover measurements are less than the specified amount. In general, the cover measurements varied from 1.8 inches to 3.0 inches, approximately, with minimal difference between the readings from the left wheel path and those from the right shoulder.

3.8.3 AC Resistance, Half-Cell Potential, and Corrosion Rate Testing

The average measured AC resistance of the deck of Northbound US 65 was 784 ohms. The half-cell potentials ranged from approximately -470 to -180 mV vs. CSE. Moderately large gradients were observed throughout the deck, especially in the center span. Corrosion rates were universally high, with only 4 of 16 measurements less than $4 \mu\text{A}/\text{cm}^2$. These results suggest active corrosion has developed over much of the deck.

3.8.4 Petrographic Analysis

It was expected that the concrete from this bridge deck would be the same as that found in the Southbound US 65 bridge deck. The petrographic examination of Core No. 6 from the Northbound US 65 bridge deck did find many similarities, including a sound, good quality concrete with the same coarse and fine aggregates, minimal carbonation, and a moderately low water-to-cementitious materials ratio estimated at 0.4 to 0.45. However, no fly ash was found in the concrete mix, and the entrained air was lower, estimated at 4 to 5 percent. Although the entrained air content is slightly low, no evidence of freeze-thaw damage was noted in the concrete.

3.8.5 Chloride Testing and Diffusion Analysis

The average effective surface concentration measured in the cores from Northbound US 65 was 0.705 percent by weight of concrete. This is considered to be a very severe exposure. The average apparent diffusion coefficient for the uncracked concrete cores was $0.040 \text{ in.}^2/\text{yr}$, which is the second lowest of the bridge decks surveyed.

3.8.6 Examination of Bar Conditions

The conditions of the eighteen reinforcing bar segments that were extracted from ten cores obtained from the deck of Northbound US 65 are summarized in Table 14. Eight bar segments from six cores were

actively corroding. The chloride concentrations at the depth of the actively corroding coated bars in this deck were generally high and ranged from 0.232 to 0.388 percent by weight of concrete.

4.0 ANALYSIS OF FINDINGS

4.1 Field Observations

4.1.1 Observed Deterioration

The eight bridge decks surveyed were generally in good to excellent condition, with most exhibiting evidence of corrosion-related deterioration, such as delaminations or existing patches, over less than 4 percent of the top deck surface. Three of the eight bridge decks exhibited no such deterioration. The westernmost deck section of the US 30 bridge and the Northbound US 65 bridge deck were the only two decks with more than 4 percent deterioration, having 6.1 percent and 11.2 percent, respectively. Additionally, the US 30 and both US 65 bridge decks exhibited the “halo” or “ring anode” effect, where concrete immediately adjacent to an existing patch has delaminated, although this effect was limited adjacent to newer repairs. Many areas of concrete deterioration on the top deck surfaces correspond to transverse shrinkage cracks in the deck such as those found over piers where the deck is continuous. Such cracks usually occur within the first 6 months after the deck is cast, penetrate full depth, and occur along the length of the transverse bars, providing a direct path for moisture and chlorides from deicing salts to reach the reinforcing.

Regarding the underside of these bridge decks, many exhibit full depth cracking with efflorescence along the cracks, but none of the decks with epoxy-coated bars in the bottom mat exhibit spalling or delamination on the deck underside. However, two of the four decks with black, uncoated bars in the bottom mat of reinforcing (the two US 65 bridge decks) have 150 to 250 square feet of deterioration on the deck underside, almost exclusively at through-thickness cracks in the deck. It should be noted that the deck underside could not be accessed for inspection at those spans of the bridges over the Cedar and Missouri Rivers.

All eight of the bridge decks exhibited some cracking on the top deck surface. Most commonly, this cracking was transverse to the bridge span, and appeared to be associated with early-age shrinkage of the deck concrete. Such cracking usually was not noted in those spans immediately adjacent to expansion joints. Several of these bridge decks also had longitudinal cracking, although this was most commonly limited to areas immediately adjacent to expansion joints or, in one case, construction joints. Interestingly, the amount of cracking identified did not directly correspond with the amount of concrete deterioration noted, considering that two of the three decks with the highest calculated cracking densities did not exhibit any concrete deterioration. It should be noted that the calculated cracking densities do not include the fine, short, closely-spaced cracking, which appears to be plastic shrinkage cracking, that was noted on the surfaces of the two US 65 bridge decks, in addition to the transverse cracking noted there. Those two bridge decks have the highest and the third highest percentages of corrosion-related deck deterioration of the sections of bridge decks studied.

4.1.2 Corrosion Testing and AC Resistance

Despite the fact that the reinforcing bars in the decks surveyed were coated, the half-cell potential and corrosion rate testing was generally useful in identifying the locations of corroding bars on the bridge decks. **However, it is important to be aware of the potential effect of the coating in interpreting these results**, namely that: 1) gradients in the corrosion potentials are more useful than the actual potential magnitudes for identifying areas of active corrosion, and 2) the magnitude of the corrosion rate measurements may underestimate actual corrosion rates at localized areas on the reinforcing bars where the coating has been compromised.

The average instantaneous corrosion rate versus damage for each deck section is shown in Figure 57. In general, the corrosion rates were positively correlated to the surveyed damage. Corrosion rate test sites were not randomly distributed on the deck surface, but were chosen based on where half-cell potential data and other conditions suggested corrosion was likely. The higher instantaneous corrosion rates measured on some of the deck sections with zero damage may indicate that corrosion is occurring, but has not yet resulted in detectable damage.

The average AC resistance is shown in Figure 58 versus damage noted in each continuous deck section between expansion joints for all bridges surveyed. Lower resistance was correlated to higher deck damage for decks where only the top mat of reinforcing was coated. This is expected since corrosion on the reinforcing bars likely results in additional damage to the coating, which would help facilitate an electrical path between the test locations on the deck. For decks in which both the top and bottom mats were coated, higher average AC resistances were measured, possibly because the bottom mat of steel is less likely to contribute to the continuity between different top reinforcing bars. However, for the decks with both mats coated, higher AC resistance was measured in the decks with the highest levels of deck damage. This result is somewhat unexpected, but suggests that corrosion-related damage in these types of decks is a relatively localized process that may occur with limited influence from the surrounding bars.

4.2 Bar Conditions

To further explore the performance of the epoxy-coated reinforcing bars in these decks, the data reported in Table 6 to Table 14 for each of the individual bridge decks has been combined, and an analysis of the properties and exposure conditions of the bars relative to the presence of corrosion has been performed. The findings from the analysis of the combined data are presented in this section of the report and in Figures 59 through 69. In the figures created to present this analysis, the data representing bars exhibiting active corrosion are shown as filled markers, while bars not currently exhibiting corrosion are shown as unfilled markers.

4.2.1 Bar Depth

Figure 59 shows the cumulative distribution of bar depth (concrete cover) measured for each epoxy-coated bar segment extracted from the top mat. The measured bar depth of corroding bars ranged from 1.8 to 3.7 in. Greater corrosion severity was generally associated with lower cover, since such bars likely were exposed to higher levels of chloride sooner than bars lower in the deck. However, bar depth did not control whether corrosion was present on the bar segments, and the other factors discussed below are likely more significant.

4.2.2 Coating Adhesion

The distribution of the coating adhesion ratings obtained during laboratory examination of the extracted bar segments is shown in Figure 60 for bars with and without evidence of active corrosion. Adhesion ratings varied widely, and active corrosion was observed on bars with adhesion ratings from 2 to 5, with most bars with active corrosion receiving an adhesion rating of 4 or 5, indicating poor adhesion. Therefore, active corrosion appears more likely where adhesion is poor. However, corrosion may occur even on bars with a relatively well-bonded coating (adhesion rating of 2) and corrosion may result in a loss of coating adhesion with time.

4.2.3 Backside Contamination

The distribution of backside contamination measured for all extracted bar segments is shown in Figure 61. The percentage of the coating backside that was contaminated on non-corroding bar segments was generally low, with the majority having a backside contamination of 2 percent. The backside contamination of actively corroding bars was generally higher, indicating that the contamination buildup adhered to the backside of the coating may include corrosion by-products. A backside contamination of 2 percent was measured on one actively corroding bar, but this bar had a corrosion condition rating of 2, reflecting the presence of only limited corrosion at areas of coating damage that had not spread to the portion of the bar where the backside contamination was measured.

4.2.4 Chloride Concentration at Bar Depth

Figure 62 shows the cumulative distribution of chloride concentrations at the depth of each extracted bar segment. Also shown on this plot is the chloride threshold for uncoated bar, i.e. the concentration of chloride ions above which corrosion is typically expected, which is approximately 0.035 percent by weight of concrete. Fifty-one of 70 coated bar segments had a chloride concentration of greater than 0.035 percent by weight of concrete without active corrosion. Only a single coated bar segment was identified as undergoing active corrosion where the chloride concentration is less than 0.179 percent by weight of concrete. The coating on this single segment exhibited pre-existing damage to the coating that apparently occurred during construction as discussed in Section 3.5.6, and the limited and minor corrosion observed on this bar (Figure 45) is considered atypical of the performance of the coated bars sampled during this study. Nine bar segments that did not exhibit corrosion were exposed to chloride concentrations higher than 0.179 percent by weight of concrete, while the highest chloride concentration at a coated bar that was not actively corroding was 0.304 percent by weight of concrete. The most actively corroding bars, with a rating of 5, all exceeded 0.335 percent chloride by weight. This clearly shows that the epoxy coating provided a significant level of protection against chloride-induced corrosion of the reinforcing steel.

Based on this data, a chloride concentration of 0.180 percent by weight of concrete represents a reasonable, conservative estimate of the effective chloride threshold for the coated bars sampled during this study. This is more than five times the corrosion-threshold for uncoated bars and is discussed further in Section 4.3. It should be noted that this level of chloride will be exceeded at most transverse cracks relatively soon in the life of the deck.

4.2.5 Time to Effective Coated Bar Threshold

Using the Fick's Law solution at each core location to project the rate of chloride ingress, the age of the bridge at which the chloride concentration at each extracted bar segment exceeded the effective coated bar threshold of 0.180 percent by weight of concrete was determined. This age was subtracted from the current ages of each bridge to give the time elapsed since the chloride concentration at the bar reached this effective coated bar corrosion threshold of 0.180 percent by weight of concrete for each extracted bar segment. The distribution of these times is given in Figure 63. Also indicated on this plot are the corrosion ratings of the bar segments and the presence of delaminations at the core locations.

In the data shown in Figure 63, more severe corrosion was observed in those bars exposed to high chloride concentrations for longer periods of time. Concrete delamination was observed only at bars that exceeded the effective threshold of 0.180 percent by weight of concrete more than 12 years ago. This suggests that it may take at least 10 years for corrosion to propagate on coated bars before sufficient stresses are generated to crack and delaminate the concrete. The data shown in Figure 63 includes

samples where the bars are in line with early-age deck cracks, but the testing and modeling process employed here underestimates the chloride content at such bars, which likely have been exposed to large amounts of chloride over much of the deck life of 17 to 32 years.

Active corrosion was not observed on some bar segments that have been exposed to chloride concentrations higher than the effective coated bar threshold for more than 10 years. Analysis of the data did not readily explain this delay in the initiation of corrosion. However, it could indicate that the quality of the epoxy coating may affect the effective corrosion threshold, with those coatings having less damage, fewer holidays, or perhaps a greater coating thickness providing protection beyond a chloride concentration of 0.180 percent by weight of concrete. It may also be due to electrochemical changes in the deck as bar mat corrosion initiates.

4.2.6 Coating Thickness

In Figure 64, the distribution of measured coating thickness is shown. The coating thickness on the extracted bar segments ranged from 6 to 14 mils. An increased frequency of coating holidays or other defects is known to be associated with thinner coatings, and such defects would be expected to produce a more rapid onset of corrosion (Pfeifer, Landgren, & Krauss, 1992). However, for this sample set, this property was not strongly correlated to corrosion, with bar segments judged to be experiencing active corrosion having coating thicknesses ranging from 6.5 to 12.5 mils.

The Iowa Department of Transportation Standard Specifications for Highway and Bridge Construction from 1984, which governed the construction of the IA 13, US 218, US 30 and US 18 bridges, cited AASHTO M-284 (which required a coating thickness of 5 to 12 mils), but modified the stated thickness criteria to require the coating thickness to be within 5 to 11 mils. The Iowa DOT Standard Specifications from 1977, which governed the construction of the older bridges in this study (IA 17, IA 150, and both US 65 bridges), required a coating thickness of 6 to 10 mils. Regarding holidays, the Iowa DOT Standard Specifications from both 1977 and 1984 limit the number of holidays to 2 per foot of bar using an in-line detector, whereas AASHTO M-284 had the same amount of holidays but did not require the use of an in-line detector. Since the 1984 Standard Specifications, the required thickness has increased, and the current Iowa Department of Transportation standard (Materials IM 451.03B) requires that the coating thickness be between 7 to 12 mils for bar sizes No. 3 to 5 and between 7 to 16 mils for bar sizes No. 6 to 18. While some bar segments sampled from the tested bridges had coating thicknesses less than 7 mils, all measured thicknesses were greater than 5 mils and would have met the applicable requirements at the time of construction.

To evaluate whether a combined effect of chloride concentration and coating thickness influenced corrosion, the corrosion condition as indicated by the corrosion rating was plotted versus chloride at bar depth and coating thickness in Figure 65. With the one exception previously discussed (Core No. 2 of US 30), active corrosion did not occur where the chloride concentration at bar depth is less than 0.179 percent by weight of concrete. Above this chloride concentration where corrosion was observed, there was little correlation between corrosion condition and coating thickness. However, the bars with most active corrosion tended to have the highest chloride content and thinner coatings (7 to 9 mils).

4.2.7 Effect of Coating Top or Both Reinforcing Mats

To examine the consequences of constructing bridges with only coated reinforcing bars in the top mat compared to coated bars in both top and bottom mats, the data shown in Figure 62 has been reproduced in Figure 66, with cores from these two groups of bridges separated by color. Relatively few bars from the

decks constructed with coated reinforcing bars in both top and bottom mats exhibited active corrosion. With the one exception where minor corrosion occurred at construction-related damage to the epoxy coating (Core No. 2 of US 30), active corrosion was not observed at chloride concentrations below 0.286 percent by weight of concrete in the decks with coated top and bottom mats. This is more than 0.100 percent by weight of concrete greater than the 0.179 percent by weight of concrete measured for the decks with only the top mat coated, and eight times the corrosion threshold for uncoated reinforcing. While only a limited number of corroding bars from decks with coated top and bottom mats were found, the presence of a coating on both top and bottom deck mats may have helped to delay the initiation of corrosion.

4.2.8 Exposure Relative to Location on Deck

Variations in exposure conditions on the deck surface were evaluated based on the location relative to the marked shoulder by plotting effective surface concentrations, apparent diffusion coefficients for uncracked cores, and chloride at the bar depth in relation to the core location (Figure 67 through 69). In these figures, the effective surface concentrations and apparent diffusion coefficients have been normalized to the values measured for that bridge (by subtracting the average from each value and dividing by the standard deviation).

The effective surface concentration (surface chloride concentration minus background chloride) conceptually represents the severity of chloride exposure. As shown in Figure 67, the surface concentration is mostly scattered, but appears to decrease slightly moving toward the center of the deck. This may reflect the tendency for snow to be plowed to the shoulder and for deicing runoff and rainwater to drain away from the crown of the deck.

The apparent diffusion coefficient represents the resistance of the concrete to chloride ingress. In the plot of apparent diffusion coefficient versus location from the edge of the traffic lane shown in Figure 68, the apparent diffusion coefficients vary widely in relation to their relative location, but those in the travel lane appear to be slightly higher than those from the shoulder. The mechanism responsible for this is unclear, but may be due to more frequent wetting and drying cycles or increased pressure gradients caused by vehicular traffic.

The effective chloride concentration at the bar depth, which is a function of both effective surface concentration and apparent diffusion coefficient, was relatively independent of location, as shown in Figure 69. Chloride at the bar depth is also dependent on concrete cover, and a clear influence of location on the deck to concrete cover was not observed.

4.3 Service Life Analysis

Based on the findings of the field survey and laboratory assessments, the primary distress mechanism for the surveyed decks is chloride-induced corrosion of reinforcement. The long-term performance of these decks was projected using a service model to estimate the rate of deterioration that can be expected in the future due to reinforcing bar corrosion. The applied model predicts the quantity of bridge deck area to exhibit damage (delamination, spalls or repair) over time, considering the inherent variability in exposure conditions, concrete quality, cover depth, and cracking across the bridge deck.

As discussed previously, for corrosion to initiate in reinforcing steel that is embedded in sound concrete, chloride ions must accumulate to a sufficient concentration, known as the chloride threshold, to break down the naturally occurring passive film protecting the steel. For uncoated reinforcing, the magnitude of the chloride threshold is influenced by many factors, including concrete moisture content and the

corrosion condition of adjacent reinforcing, but is often assumed to be approximately 0.035 percent by weight of concrete. Corrosion initiation for epoxy-coated reinforcing bars is subject to the same influences as uncoated bars, but is also governed by the properties of the coating (thickness, holidays, level of damage occurring during construction, etc.) that may vary from site to site. Therefore, any corrosion threshold for epoxy-coated bars is most appropriately considered as an effective chloride threshold selected for the specific conditions examined. Despite the broad assumptions inherent in the concept of chloride threshold, chloride thresholds are a useful and necessary component of service life modeling.

The time required for corrosion-related damage to occur at any point on the deck can be conceptually separated into two time periods: the corrosion initiation time (t_i) and the corrosion propagation time (t_p). Figure 70 illustrates this corrosion sequence (Tuutti, 1982). The initiation time is the time required for chloride to penetrate through the concrete and accumulate up to the chloride threshold value. The propagation time is the time during which corrosion products build up to a sufficient volume to create tensile stress in the surrounding concrete capable of cracking or delaminating the concrete. These two periods can be considered individually and then combined to predict the time before deterioration becomes apparent at a given location.

The properties of the bridge deck will vary across the deck surface. Corrosion can be expected to start first where cover is low, the ability of the concrete to resist chloride ingress is low, and the chloride exposure is high, and then advance over time to areas where the deck is progressively less susceptible to corrosion. As a result, bars located in line with cracks are particularly susceptible to corrosion, since resistance to chloride ingress is locally reduced. The service life of a bridge deck is the time until the amount of damaged area (i.e., the number of locations where the sum of the corrosion initiation time and the propagation time has passed) exceeds some level of acceptability. This level or limit can be based on the maximum amount of damage that may be permitted before structural capacity is diminished or based on concerns regarding serviceability or appearance. A limit of 10 to 12 percent is often considered the maximum allowable damaged area for bridge decks before rehabilitation, such as the installation of an overlay, is performed (Koch, Brongers, Thompson, Virmani, & Payer, 2002) (Krauss, Lawler, & Steiner, 2009). A 10 percent threshold was adopted for this work, assuming that at this level of damage, some maintenance action is needed to address decreases in ride quality and considering the time necessary to plan, coordinate and implement a repair program.

An established statistical model developed by Sagüés (Sagüés, 2003) was adapted to estimate the service lives of the surveyed bridges. This model determines the amount of bridge deck area affected by corrosion initiated by chloride ingress based on the statistical distribution of the key parameters that govern the initiation of corrosion (exposure conditions, concrete quality, cover depth, and cracking). This recognizes the fact that corrosion in reinforced concrete structures is a local process that spreads across the deck over time.

4.3.1 Methods and Bases for Analysis

The rate of damage development for each of the deck sections examined in this survey has been projected using the service life model based on: 1) the existing performance with epoxy-coated bars, and 2) the expected performance of the bridge decks if they had been constructed with uncoated bars.

The initiation of corrosion is governed largely by: 1) the quality of the concrete and its ability to resist chloride ingress, 2) the exposure conditions (i.e. severity of deicing salt application), 3) the concrete

cover, 4) the existence of cracks over the bars, and 5) the chloride threshold. These factors, as well as the propagation time, were quantified for modeling purposes based on WJE's field observations as discussed below. It is assumed that the range for each parameter, except chloride threshold, can be represented as a normal distribution defined in terms of an average and standard deviation.

4.3.1.1 Chloride Transport and Exposure

As described in Section 2.2.4, the apparent diffusion coefficient (D_a) and the average surface concentration (C_s) represent the ability of the concrete to resist chloride penetration and the severity of the exposure conditions, respectively. Table 16 shows the average and standard deviation of C_s and D_a used to model each bridge section.

The values for apparent diffusion coefficient (D_a) were separated into uncracked and cracked regions, in recognition of the fact that chloride transport is likely to occur more rapidly through cracks. In cracked regions, the average and standard deviation of D_a were kept constant for all bridges at $0.300 \text{ in.}^2/\text{yr.}$ and $0.180 \text{ in.}^2/\text{yr.}$, respectively. These values were chosen based on the average measured diffusion coefficient in cracked cores and included an approximately 50 percent increase to account for the fact that the chloride profiles based on a 4-inch diameter core will underestimate the concentration of chloride immediately adjacent to the crack, which will impact the performance of the reinforcing bars. Reinforcing bars at cracks are typically in line and in direct contact with the deicing-bearing runoff when it is penetrating through the crack.

Since the concentration of deicing salts on the deck surface is not influenced by the presence of cracks, the average and standard deviation of C_s was modeled similarly in cracked and uncracked regions. An effective C_s was calculated by subtracting the background chloride, C_0 , at each bridge in order to model the driving force behind chloride ingress. This was done to discount the effect of bound chlorides, which are not available to promote corrosion.

For the purposes of developing model inputs, similar chloride transport and exposure properties were assumed for Northbound US 65 and Southbound US 65, and the results for all cores from those bridges were averaged.

4.3.1.2. Concrete Cover over Reinforcing Bars

The reinforcing bar depth was measured using GPR as described in Section 2.1.2. The average and standard deviations of concrete cover for all top bars that were identified in each deck were determined. These averages and standard deviations are given in Tables 3 and 16. Note that it was assumed that the actual cover distribution is well-represented by a normal distribution, even though this was not always the case.

4.3.1.4. Chloride Threshold and Propagation Time

The selection of the chloride threshold and propagation times, which are the model inputs representing the corrosion resistance of reinforcing bar, has direct consequences for the predicted performance.

The epoxy coating applied to steel provides protection from the effects of chloride to the steel surface of the reinforcing bar. As described in Section 4.2.4, a chloride concentration of 0.180 percent by weight of concrete was selected as the effective chloride threshold for coated bars. This value was found to be appropriate for decks with epoxy-coated top bars and uncoated bottom bars, and overly conservative for

decks where both mats of reinforcing utilize epoxy-coated bars. For comparison, the chloride threshold for uncoated bar was assumed to be 0.035 percent acid-soluble chloride by weight of concrete.

The propagation time is governed by the rate of corrosion after corrosion initiates. Because the coating on epoxy-coated reinforcing bars can electrically isolate individual reinforcing bars from the surrounding bars, the electrochemical corrosion reaction is slowed and a greater propagation time is required before damage to the concrete becomes apparent. The propagation time used for each bridge was adjusted to calibrate the model to the actual damage measured during the field investigation. These calibrated propagation times ranged from 12 to 23 years.

4.3.1.5 Damage Model

The model as applied here can be interpreted as follows: The bridge deck is virtually divided into finite elements of equal size. Each element is randomly assigned a unique value of surface chloride concentration (C_s), concrete cover, and apparent diffusion coefficient (D_a), based on normal distribution functions for these three parameters. Using the solution to Fick's Second Law of Diffusion (Equation 2 from Page 10), the model is based on evaluating t_i , the time for the chloride concentration at the steel depth to exceed the chloride threshold at which corrosion initiates, for each element. The propagation time, t_p , is estimated as a fixed value. A damage function (percentage of area deteriorated versus time) is generated based on the percentage of elements where the combined t_i and t_p is exceeded.

The transverse deck cracking observed in these bridge decks is most likely early-age cracks that occurred due to normal drying shrinkage of the deck concrete and thermally-induced stresses. Because early-age shrinkage cracks usually occur within the first six months after construction, transverse deck cracking was assumed to be present immediately after construction. The effect of this cracking was accounted for in the model by setting the apparent diffusion coefficient of an area of concrete affected by cracks equal to the diffusion coefficient assumed for cracked concrete, but limiting the concrete area affected by the crack to a width of 4 in. (2 in. on either side of the crack). It was also assumed that the damage that develops in cracked concrete is twice the concrete area where the diffusion is increased, thereby allowing each individual crack to cause damage over an overall width of 8 in. The area affected by cracks in each bridge section was determined based on the crack density measured during the field surveys.

Based on these assumptions, damage was calculated based on the following function:

$$Damage(t) = \int_{D_{a-min}}^{D_{a-max}} \int_{C_{s-min}}^{C_{s-max}} PCs(C_s) \cdot PD(D_a) \cdot Nc(2 \cdot \sqrt{tt(t) \cdot D_a} \cdot \text{inverf}(\frac{C_s - C_T}{C_s - C_o})) dC_s dD_a \quad (3)$$

Where:

- D_{a-min} and D_{a-max} represent the lowest and highest considered values of D_a ;
- C_{s-min} and C_{s-max} represent the lowest and highest considered values of C_s ;
- $PCs()$ is the probability density function of chloride surface concentration (C_s);
- $PD()$ is the probability density function of apparent chloride diffusion coefficient (D_a);
- $Nc(x)$ is the cumulative distribution function of elements with cover less than x ;
- $\text{inverf}()$ is the inverse Gaussian error function; and
- $tt(t)=t-t_p$ when $t>t_p$, otherwise, $tt(t)=0$.

4.3.2 Findings

To compare bridge deck performance, the service life model was used to project expected service life before rehabilitation. For this discussion, the limit of damage allowed before rehabilitation was defined as 10 percent of the deck area. The current bridge age, projected rehabilitation age, and measured damage for each section is provided in Table 17. The predicted damage given in terms of percent of delaminated deck area versus time for all bridge sections is also shown in Figure 71 through 78. These figures also show the amount of damage observed on the individual bridges during this survey and during previous surveys by WJE (Lee & Krauss, 2003) and Iowa State University (Fanous, Wu, & Pape, 2000), where available.

On average, the bridges are projected to provide 39 years of service life before requiring rehabilitation. The performance of the epoxy-coated bars greatly exceeds the projected service life for uncoated bars, which averages only 13 years before rehabilitation is required. This suggests that the average service life extension achieved through the use of epoxy-coated reinforcing bars in the decks is 26 years.

The progression of damage on two sections of bridge deck, specifically the Northbound US 65 bridge deck and deck Section 1 of US 30, was underestimated by approximately 3 and 9 years, respectively, using this methodology. Both deck sections had previously been repaired by concrete patches, which may influence the results for two reasons. First, a patched area is generally larger than the delaminated area, due to the typical practice of squaring-off patch areas, and this leads to a quantity of damage greater than would have been observed if no repairs had been performed. Second, concrete repairs in chloride-contaminated concrete can accelerate corrosion adjacent to the patch if protective measures are not used. Furthermore, these models are based on the assumption that the input parameters are normally distributed. In the deck of Northbound US 65, a region was identified in the center of the deck where cover is lower than the surrounding deck, so the assumed normal distribution would underestimate the number of bars with low cover.

The statistical approach taken for this modeling is intended to give a general understanding of predicted performance, but not an “exact” prediction. The accuracy of the predictions made with the model will vary, and the output of the model should be considered to be accurate to no more than 5 years. The modeling parameters used were mainly based on very early vintage decks that contained uncoated bars for the bottom mat of reinforcing. Accelerated laboratory testing has consistently shown that decks with epoxy-coated reinforcing for both mats have less corrosion than when only the top mat is coated. Further, improved quality of the bar coatings through the plant certification program introduced by the Concrete Reinforcing Steel Institute (CRSI) in the early 1990’s (CRSI, 2008), and tighter specifications for epoxy-coated reinforcing should result in improvements in the performance of bridge decks built after the mid-1990s. It should be noted that Iowa Department of Transportation specifications for epoxy-coated reinforcing met or exceeded the national standard (AASHTO M-284) at the time of construction for the eight bridge decks studied. Finally, this model is not intended to predict the development of initial, isolated instances of corrosion, such as may occur on aberrant bars close to the concrete surface, but is intended to predict broader scale deterioration.

It should be noted that the estimates of deterioration rate are highly dependent on the assumptions made regarding chloride exposure and concrete performance. The accuracy of the estimates made regarding the factors involving chloride penetration will strongly influence the predicted performance. Due to the limitations of site access and in the interest of minimizing the number of core and bar samples extracted from the decks, the number of measurements made on each bridge deck were somewhat limited. Because

these measurements were used to estimate the diffusion coefficient and surface chloride concentration for each bridge deck, a higher degree of precision in the projections of the service life modeling would require more sampling, measurements, and testing to be performed.

5.0 DISCUSSION

Corrosion-related damage was observed on five of the eight bridge decks containing epoxy-coated reinforcing that were investigated during this study. Of the five bridge decks exhibiting damage, four exhibited such damage over an average of less than 4 percent of the deck top surface, and no damage on the deck underside. The eight bridges ranged in age from 17 to 32 years at the time of the inspection, though the three decks that were undamaged were among the younger decks examined, being no more than 23 years old. If the epoxy coatings placed on reinforcing bars were completely impervious to moisture and chlorides, were completely effective as an electrical isolator, and had no damage or imperfections, it could be expected that epoxy-coated reinforcing bars would not corrode regardless of exposure, in which case the damage observed on these decks would be premature. **However, epoxy coatings are not free of defects and are not 100 percent effective at stopping moisture, chlorides, and electrical current**, so such a perception is unrealistic. In this study, bridge decks using epoxy-coated reinforcement were shown to have significant improvements in service life as compared to if the bridge decks had been constructed with uncoated reinforcing bars, averaging an additional 25 years of service life prior to repair. Additionally, it is important to note that the observed chloride exposure conditions at these decks, as quantified in terms of the chloride surface concentrations, **are very severe**.

Because of the severe exposure of these decks to chlorides, many of the epoxy-coated reinforcing bars encountered during this study have been exposed to chloride levels higher than the corrosion threshold for uncoated bars (0.035 percent by weight of concrete) for an extended period of time. The lowest chloride concentration at which active corrosion of an undamaged epoxy-coated bar segment was observed in this study was 0.179 percent by weight of concrete (five times the uncoated bar threshold), although chloride concentrations as high as 0.304 percent by weight of concrete were observed at the level of the epoxy-coated reinforcing bar without apparent corrosion. Additionally, where both mats of deck reinforcing were epoxy-coated, no corrosion-related damage was found for chloride levels up to 0.286 percent by weight of concrete, or 8 times the corrosion threshold for uncoated bars. **Therefore, the epoxy coating has provided a significant level of protection to the reinforcing steel from the corrosion-promoting effects of chloride contamination.**

Of the eight bridge decks included in this study, the US 65 bridge decks developed the most widespread damage. These bridges are two of the four oldest included in this survey, but it appears that more than just age contributed to the observed damage. For one, these bridge decks experience a higher level of traffic than do the two other bridges surveyed of a similar age. Additionally, the US 65 decks have a significant amount of full depth transverse cracking, and the top surfaces of both these decks have significant areas with what appear to be plastic shrinkage cracking. The full depth cracking clearly increases the penetration of chlorides into the deck locally, and the plastic shrinkage cracking could also enhance early-age penetration of chlorides. Also, in a region near the middle of Northbound US 65 where much of the damage was concentrated, the concrete cover over the bars was as much 1/2 inch less than in the rest of the bridge deck.

Past studies of epoxy-coated bar performance have suggested that decks constructed with both top and bottom mats of epoxy-coated bar may be expected to be more durable than those with epoxy-coated bars only in the top mat (Lee & Krauss, 2003). In this study, damage in portions of the deck of US 30 was found to have developed in 17 years, even though both mats of steel are coated. However, a higher level of chloride was necessary to initiate corrosion of bars in decks where both mats are coated compared to when only the top mat is coated. It is clear that the use of epoxy coating on the bottom mat of reinforcing of the examined decks has helped delay the development of distress on the top and bottom surfaces of

these bridge decks. As much as 11.2 percent of the top deck surface and 250 sq ft of the deck soffit exhibited corrosion-related damage on decks in which only the top bar mat was coated, whereas no soffit deterioration, and no more than 6.1 percent of damage on the deck top surface was found on any of the decks studied with epoxy-coated bars in both the top and bottom reinforcing mats.

The service life projections, based on the observed properties of the decks and the performance of the epoxy-coated bars, suggest that the ages at which these deck sections may reach 10 percent damage ranges from 29 to 60 years. By comparison, projections of damage based on the same conditions suggest that these same bridges would have developed 10 percent damage in 9 to 23 years if they had been constructed with uncoated reinforcing steel.

Where corrosion-related deterioration such as delaminations, spalls, and existing patches were identified in the eight bridge decks studied, the observed deterioration was often concentrated along transverse cracks located above top bars. These cracks have provided a path for rapid ingress of chloride and moisture, and have had an obvious influence on the evolution of corrosion-related damage. Information provided by the Iowa Department of Transportation indicates that full depth transverse cracks are present in many Iowa bridge decks, and can be found in numerous bridge decks nationwide.

Based on the observed cracking and corrosion-related damage, it was necessary that the service life modeling effort performed for these decks consider the effect of the cracks. This was done by assuming an accelerated rate of chloride diffusion over an area defined based on the observed crack density, **but such projections only roughly approximate the actual mechanisms of chloride ingress and damage propagation at cracks.** Even corrosion-resistant reinforcing, such as epoxy-coated reinforcing bars, will develop corrosion at high chloride concentrations, and cracks provide ready access for chlorides to reach the bar and to accumulate rapidly to such levels.

Past studies of epoxy-coated reinforcing bar performance in bridge decks in Iowa, including the investigation by WJE in 2002, saw little deterioration on the examined bridges. All of the 39 bar segments extracted from core samples in 2002 showed no active corrosion. Service life modeling was performed in that study based on an effective chloride threshold of 0.375 percent by weight of concrete and a propagation time of 15 years. Following from these inputs, it was suggested that the surveyed epoxy coated bridges in Iowa may last for 90 years or more. Based on current findings for effective chloride threshold and surface concentration, these estimates have been revised. While the 2002 study did not sample any corroding bars, the current study had the benefit of observable surface damage such as delaminations and existing repairs to help guide the selection of core sample locations containing corroded bars. This allowed a more accurate estimate of the amount of chloride needed to initiate corrosion. In addition, chloride surface concentrations have increased slightly at US 18, and by 20 to 30 percent on IA 13 and US 218. **This rapid increase in chloride surface concentration may relate to more aggressive deicing practices being used by the Iowa DOT.** However, it should be noted that the current service life model assumes a constant surface concentration throughout the period modeled, and **so may underestimate the service life of the decks.**

Significant concentrations of chloride have accumulated at or near bar level on all bridges examined. Despite the high levels of chloride, corrosion-related damage in some decks is not yet widespread. **However, such damage is expected within the next 10 to 15 years.** While it may be appealing to postpone action until damage becomes more widespread, rehabilitation of the deck in the near term may be more cost-effective. At present, there is an opportunity to remove the chloride-contaminated concrete down to within approximately 1/2 inch of the bar and to replace the concrete wearing surface with an

overlay. If initiated within the next few years, removal of this concrete by milling methods is a viable option. This approach will not address chlorides in the concrete below this level, such as the higher levels of chlorides in the concrete immediately adjacent to cracks, but will remove most of the chlorides in the deck concrete.

If chloride concentrations at and below the bar depth reach sufficiently high levels to make excavation of the concrete at those depths necessary, as may have already occurred at cracks, more expensive and more complex concrete removal operations may be needed, and other techniques for reducing future corrosion-related damage may be required. Because some of the greatest chloride penetration has occurred at cracks, significant additional service life extension can be gained if cracking can be minimized or sealed to prevent moisture and chloride infiltration in bridge decks reinforced with epoxy-coated bars. At existing bridge decks, it is recommended that efforts be made to seal cracks soon after they develop in order to postpone the onset of damage. Such techniques may include crack filling with a high molecular weight methacrylate, injection with epoxy, or covering with a cementitious or polymer overlay. For new structures, efforts should be made in design or concrete mix selection to help minimize cracking to the extent possible.

6.0 CONCLUSIONS

This investigation was initiated to assess the corrosion protection provided by epoxy-coated bars to the decks of eight concrete bridges built in Iowa between 1978 and 1993. This investigation consisted of a field investigation, which included evaluation of existing condition of the decks and material sampling, an extensive laboratory evaluation of the concrete and bar samples obtained, and service life modeling to project the level of protection provided.

The conclusions made based on this investigation are summarized as follows:

- Three of the eight bridge decks built with epoxy-coated bars inspected during this study exhibited no corrosion-related damage. The remaining five decks had damage (sum of delaminations, spalls, and patches) of between 0.1 to 11.2 percent of the deck area, with four of those decks having damage averaging less than 4 percent of the deck area.
- Approximately 73 percent (51 of 70) of the extracted epoxy-coated bar segments that were exposed to chloride concentrations in excess of the level expected to corrode uncoated reinforcement did not exhibit corrosion. With one exception, corrosion was not observed on epoxy-coated bar in concrete containing less than 0.179 percent chloride by weight of concrete in decks with epoxy-coated top bars and uncoated bottom bars, and 0.286 percent chloride by weight of concrete in decks with epoxy-coated bars in both reinforcing mats.
- Service life projections of the time required to reach 10 percent damage in the decks surveyed ranged from 29 to 60 years with epoxy-coated reinforcing using the 0.180 percent chloride threshold by weight of concrete and from 9 to 23 years for uncoated reinforcing steel. The average service life extension provided by the use of epoxy-coated reinforcing bars versus uncoated bars, determined as the time until significant repair is required, is estimated to be approximately 26 years for the eight decks studied.
- Transverse cracks located directly over reinforcing bars, as commonly occur in many bridge decks, provide a pathway for moisture, chlorides, and oxygen to penetrate to the reinforcing. As a result, the potential for corrosion of the reinforcing bars at these locations is significant, and deck deterioration is likely to initiate and be concentrated along such cracks.

7.0 WORKS CITED

- Concrete Reinforcing Steel Institute. (2008). *Voluntary Certification Program for Fusion-Bonded Epoxy Coating Applicator Plants, 10th Edition*, Schaumburg, IL.
- Crank, J. (1956). *The Mathematics of Diffusion*: Clarendon Press, Oxford.
- Fanous, F., Wu, H., & Pape, J. (2000). *Impact of Deck Cracking on Durability*; Center for Research and Education Iowa State University, Ames, IA.
- Koch, G. H., Brongers, M. P., Thompson, N. G., Virmani, Y. P., & Payer, J. H. (2002). *Corrosion Costs and Preventative Strategies in the United States, Publication No. FHWA-RD-01-156*. Federal Highway Administration.
- Krauss, P. D., Lawler, J. S., & Steiner, K. A. (2009). *Guidelines for Selection of Bridge Deck Overlays, Sealers and Treatments, NCHRP Project 20-07, Task 234*; National Cooperative Highway Research Program, Washington, D.C.
- Lee, S. K., & Krauss, P. (2003). *Service Life Extension of Northern Bridge Decks Containing Epoxy-Coated Reinforcing Bars*; Wiss, Janney, Elstner Associates, Inc., Northbrook, IL
- McDonald, D. B., Sherman, M. R., & Pfeifer, D. W. (1995). *The Performance of Bendable and Nonbendable Organic Coatings for Reinforcing Bars in Solution and Cathodic Debonding Tests, FHWA-RD-94-103*; FHWA, Mclean, VA.
- Ministry of Transportation of Ontario. (2007). *Structure Rehabilitation Manual*; Publications Ontario, St. Catharines, Ontario, Canada.
- National Bureau of Standards (1975), *Nonmetallic Coatings for Concrete Reinforcing Bars*, Washington, D.C.
- Pfeifer, D. W., Landgren, J. R., & Krauss, P. D. (1992). *Investigation for CRSI on CRSI-Sponsored Corrosion Studies at Kenneth C. Clear Inc.*; Wiss, Janney, Elstner Associates, Inc., Northbrook, IL
- Sagüés, A. (2003, October). Modeling the Effects of Corrosion on the Lifetime of Extended Reinforced Concrete Structures. *Corrosion*, 854-866.
- Sohanghpurwala, A. A. (2006). *NCHRP Report 558: Manual on Service Life of Corrosion-Damaged Reinforced Concrete Bridge Superstructure Elements*; Transportation Research Board., Washington, D.C.
- Sohanghpurwala, A. A., & Scannell, W. T. (1998). *Verification of Effectiveness of Epoxy-Coated Rebar-Project No. 94-05, Final Report Submitted to Pennsylvania Department of Transportation*, Concorr Inc., Virginia
- Stanish, K. D., Hooton, R. D., & Thomas, M. D. (1997). *Testing the Chloride Penetration Resistance of Concrete: A Literature Review, FHWA Contract DTFH61-97-R-00022*; University of Toronto, Toronto, Ontario, Canada.
- Tuutti, K. (1982). *Corrosion of Steel in Concrete*; Swedish Cement and Concrete Research Institute, Stockholm, Sweden.

TABLES

Table 1. Summary of Surveyed Bridges

Facility Carried	IA 17	US 218 SB	IA 150	IA 13 SB	US 30	US 18	US 65 SB	US 65 NB
Feature Crossed	US 20	Cedar River	Cedar River	Indian Creek	Missouri River	Floyd River	Union Pacific Railroad	Union Pacific Railroad
Location	5 miles west of Webster City, IA	Janesville, IA	Vinton, IA	Marion, IA	Blair, NE	Sheldon, IA	Bondurant, IA	Bondurant, IA
County	Hamilton	Bremer	Benton	Linn	Harrison	Sioux	Polk	Polk
Bridge ID	4054.3S017	0996.0L218	0601.5S150	5713.7L013	4300.0S030	8441.3S018	7788.5L065	7788.5R065
Year Constructed (Age)	1978 (32 years)	1993 (17 years)	1980 (30 years)	1987 (23 years)	1991 (19 years)	1992 (18 years)	1979 (31 years)	1979 (31 years)
Previous Condition Surveys	--	1998, 2002	--	1998, 2002	--	1998, 2002	--	--
Studied Area	right lane, NB	right lane, SB	right lane, NB	right lane, SB	partial length right lane, WB and EB	right lane WB	right lane, SB	right lane, NB
Epoxy Bar Location	Top mat only	Top and bottom mats	Top mat only	Top and bottom mats	Top and bottom mats	Top and bottom mats	Top mat only	Top mat
Overall Length	254'-6"	673'-8.875"	807'-0"	100'-0"	1,983'-0"	205'-6"	332'-0"	332'-0"
Overall Width of Roadway	32'-0"	40'-0"	32'-0"	40'-0"	40'-0"	44'-0"	40'-0"	40'-0"
No. of Spans	Four	Seven	Nine	Three	Seventeen	Three	Three	Three
Orientation	0 degree skew	0 degree skew	0 degree skew	20 degree skew	0 degree skew, slight curve of two westernmost approach spans	15 degree skew	45 degree skew	45 degree skew
Bridge Type	Precast Prestressed Concrete Beam Bridge	Precast Prestressed Concrete Beam Bridge	Precast Prestressed Concrete Beam Bridge	Continuous Concrete Slab Bridge	Steel girder main spans, Prestressed Concrete Girder approach spans	Precast Prestressed Concrete Beam Bridge	Continuous Welded Girder Bridge	Continuous Welded Girder Bridge
Approach Length	two 35'-9" end spans	95'-9" east, 95'-6.25" west end spans	two 65'-9" end spans	two 30'-6" end spans	773'-6" west = 9 spans, 538'-0" east = 6 spans	two 68'-3" end spans	two 101'-0" end spans	two 101'-0" end spans
Main Span Length	two 91'-6" interior spans	4 @ 96'-6", 1 @ 96'-5.625"	7 @ 96'-6"	39'-0" center span	666'-0" (2 spans)	69'-0" center span	130'-0" center span	130'-0" center span
Lanes	one NB lane, one SB lane	two SB lanes	one NB lane, one SB lane	two SB lanes	one EB lane, one WB lane	one EB lane, one WB lane	two SB lanes	two NB lanes
Live Load	HS20-44 + 20psf for future wearing surface	HS20-44 + 20psf for future wearing surface	HS20-44 + 20psf for future wearing surface	HS20-44 + 20psf for future wearing surface (0.5" orig)	HS20-44 + alternate military loading + 20psf for future wearing surface	HS20-44 + 20psf for future wearing surface	HS20-44 + 20psf for future wearing surface	HS20-44 + 20psf for future wearing surface
Other Loads	--	--	--	--	Barge Impact - 1000 kips normal/500 kips parallel to centerline	--	--	--
Deck Slab Design Thickness	7 1/2"	8"	8"	17.5"	8" (approach spans), 8-1/2" (main spans)	8"	7.875"	7.875"
Specified Slab Concrete	3,500 psi	3,500 psi	3,500 psi	3,500 psi	3,500 psi	3,500 psi	3,500 psi	3,500 psi
Specified Minimum Cover	2" top transverse, 1" bottom of slab longitudinal	2.5" top transverse, 1" bottom of slab transverse	2.5" top transverse, 1" bottom of slab transverse	2-1/2" top longitudinal bars, 1 1/2" bottom longitudinal	2.5" top transverse, 1" bottom of slab transverse	2.5" top transverse, 1" bottom of slab transverse	2-1/2" top transverse, 1" bottom of slab transverse	2-1/2" top transverse, 1" bottom of slab transverse

Table 2. Observed Bridge Conditions

Facility Carried	Age at Survey (yr)	Section	Area Surveyed (sq ft)	Delaminations & Spalls (Top) (sq ft)	Patches (sq ft)	Damage ^[1] (%)	Crack Density (ft/sq ft)
IA 17	32	1	4369	51	95	3.3	0.007
US 218 SB	17	1	4246	0	0	0.0	0.055
		2	6358	0	0	0.0	0.020
		3	4202	0	0	0.0	0.057
IA 150	30	1	4144	54	0	1.3	0.003
		2	4624	13	15	0.6	0.004
		3	4160	70	0	1.7	0.002
IA 13 SB	23	1	2266	0	0	0.0	0.161
US 30	19	1	6840	390	25	6.1	0.140
		2	8600	246	31	3.2	0.173
		3	10700	5	4	0.1	0.093
		4	10820	181	0	1.7	0.130
US 18	18	1	4554	0	0	0.0	0.165
US 65 SB	31	1	7348	79	199	3.8	0.021
US 65 NB	31	1	7348	496	328	11.2	0.047

[1] Sum of delaminations, spalls and patched areas.

Table 3. Cover Measured in Inspected Decks Using GPR

Facility Carried	Section	Cover (in.)	
		Average	Standard Deviation
IA 17	1	2.29	0.29
US 218	1	2.15	0.26
	2	2.69	0.35
	3	2.63	0.36
IA 150	1	2.50	0.24
	2	2.59	0.28
	3	2.31	0.19
IA 13	1	3.09	0.34
US 30	1	2.72	0.32
	2	2.58	0.24
	3	3.03	0.38
	4	2.85	0.25
US 18	1	2.56	0.29
US 65 SB	1	2.56	0.22
US 65 NB	1	2.50	0.25

Table 4. Measured AC Resistance in Inspected Decks

Facility Carried	Section	AC Resistance (ohms)	
		Average	Standard Deviation
IA 17	1	32	33
US 218	1	798	803
	2	862	665
	3	583	546
IA 150	1	203	209
	2	168	278
	3	569	499
IA 13	1	408	299
US 30	1	670	786
	2	1187	1768
	3	406	176
	4	751	198
US 18	1	1592	1537
US 65 SB	1	1462	1936
US 65 NB	1	784	667

Table 5. Corrosion Rate of More Active Locations in Inspected Decks

Facility Carried	Section	I_{corr} ($\mu\text{A}/\text{cm}^2$)	
		Average	Standard Deviation
IA 17	1	2.19	1.10
US 218 SB	1	3.49	4.56
	2	0.83	0.26
	3	0.48	0.28
IA 150	1	7.50	2.57
	2	0.27	0.06
	3	1.08	0.52
IA 13 SB	1	2.25	0.85
US 30	1	3.28	5.84
	2	1.10	1.72
	3	2.40	2.15
	4	0.23	0.08
US 18	1	0.23	0.02
US 65 SB	1	6.28	1.70
US 65 NB	1	5.78	2.49

Table 6. Iowa 17 over US Route 20 - Extracted Cores and Bars

Age of deck	32 years														
Background chloride, C ₀	0.008% by wt. conc.														
Cores															
Core ID	1			2		3	4		5			6		7	
Vertical crack (depth, in.)	-			-		-	-		-			-		1.5	
Horizontal crack (depth, in.)	-			0.8 - not at bar		-	-		-			2.0 - at bar		1.3 - at bar	
Bars															
Bar size	6	8	5	6	5	6	6	5	6	5	5	6	7	6	5
Depth (in.)	2.54	3.28	3.33	2.19	2.90	2.56	1.83	2.59	2.48	3.43	3.43	2.11	2.88	2.20	3.03
Epoxy coated?	Y	Y	Y	Y	Y	Y	Y	Y	Y	Y	Y	Y	Y	Y	Y
Coating Thickness (mils) ^[1]	6.9	8.1	13.5	7.5	10.2	7.1	10.4	7.6	8.5	13.9	12.6	10.4	7.7	7.0	9.8
Adhesion Rating ^[2]	3	4	3	4	4	4	4	5	4	3	3	5	5	4	5
Backside Contamination ^[3]	50	20	50	50	50	30	75	15	20	10	50	100	100	100	100
Corrosion Condition ^[2]	1	1	1	1	1	1	1	1	1	1	1	4	3	5	3
Active Corrosion?	N	N	N	N	N	N	N	N	N	N	N	Y	Y	Y	Y
Effective chloride concentration at bar depth (% by wt. conc.) ^[4]	N/A	N/A	N/A	0.053	0.010	0.094	N/A	0.172	0.167	0.073	0.073	0.290	0.194	0.351	0.253

NOTES:

^[1] Specified 8 mils ± 2 mils per 1977 Iowa DOT Standard Specifications

^[2] See Section 2.2.2 and Figures 27 and 28 for explanation of rating scale. “1” indicates no corrosion/ excellent adhesion; “5” indicates over 60% corroded/poor adhesion.

^[3] Backside contamination rating equals percentage of backside surface of peeled epoxy coating exhibiting contamination

^[4] As shown in Section 4.2.4, the effective corrosion thresholds are assumed as 0.035 (uncoated) and 0.180 (epoxy-coated), percent by weight of concrete.

Table 7. US 218 Southbound over Cedar River - Extracted Cores and Bars

Age of deck	17 years															
Background chloride, C ₀	0.048% by wt. conc.															
Cores																
Core ID	1	2	3	4	5	6	7	8	9							
Vertical crack (depth, in.)	-	-	-	-	-	3.7	-	Full	-							
Horizontal crack (depth, in.)	-	-	-	-	-	-	-	-	-							
Bars																
Bar size	6	5	6	5	5	6	5	6	5	6	8	6	5	5	6	7
Depth (in.)	2.07	2.92	1.76	4.76	5.02	3.43	4.17	3.04	3.95	2.90	3.67	2.50	3.32	3.17	2.36	3.22
Epoxy coated?	Y	Y	Y	Y	Y	Y	Y	Y	Y	Y	Y	Y	Y	Y	Y	Y
Coating Thickness (mils) ^[1]	11.2	12.5	13.8	10.4	13.4	12.7	12.9	13.0	7.6	13.0	9.2	11.4	9.2	7.1	11.1	11.0
Adhesion Rating ^[2]	5	1	1	1	1	1	1	5	5	1	4	1	1	2	1	1
Backside Contamination ^[3]	10	2	2	2	2	2	2	50	20	2	30	2	2	2	2	2
Corrosion Condition ^[2]	1	1	1	1	1	1	1	1	1	1	1	1	1	1	1	1
Active Corrosion?	N	N	N	N	N	N	N	N	N	N	N	N	N	N	N	N
Effective chloride concentration at bar depth (% by wt. conc.) ^[4]	0.162	N/A	0.265	0.010	N/A	0.045	0.022	0.252	N/A	0.139	0.086	0.081	N/A	0.103	0.157	0.075

NOTES:

^[1] Specified 8 mils ± 3 mils per 1984 Iowa DOT Standard Specifications

^[2] See Section 2.2.2 and Figures 27 and 28 for explanation of rating scale. “1” indicates no corrosion/ excellent adhesion; “5” indicates over 60% corroded/poor adhesion.

^[3] Backside contamination rating equals percentage of backside surface of peeled epoxy coating exhibiting contamination

^[4] As shown in Section 4.2.4, the effective corrosion thresholds are assumed as 0.035 (uncoated) and 0.180 (epoxy-coated), percent by weight of concrete.

Table 8. Iowa 150 over Cedar River - Extracted Cores and Bars

Age of deck	30 years																	
Background chloride, C ₀	0.006% by wt. conc.																	
Cores																		
Core ID	1	2	3	4	5	6	7	8	9									
Vertical crack (depth, in.)	-	-	-	Full	1.9	-	1.8	-	-									
Horizontal crack (depth, in.)	-	-	-	1.9 - at bar	1.9 - at bar	-	1.8 - at bar	-	-									
Bars																		
Bar size	6	6	5	6	5	6	8	6	5	6	5	6	5	6	5	6	5	
Depth (in.)	3.03	2.69	3.44	3.11	3.88	1.91	2.87	1.90	2.75	2.38	3.20	1.87	2.73	2.80	3.56	2.33	3.11	
Epoxy coated?	Y	Y	Y	Y	Y	Y	Y	Y	Y	Y	Y	Y	Y	Y	Y	Y	Y	
Coating Thickness (mils) ^[1]	11.9	6.6	7.8	7.4	7.8	8.9	9.2	11.5	10.2	8.3	11.3	7.6	11.4	7.1	10.6	9.1	6.4	
Adhesion Rating ^[2]	1	2	1	2	1	4	4	4	4	2	1	4	1	1	1	5	2	
Backside Contamination ^[3]	2	2	2	2	2	100	30	100	2	2	2	100	10	2	2	2	2	
Corrosion Condition ^[2]	1	1	1	1	1	4	2	4	1	1	1	5	1	1	1	1	1	
Active Corrosion?	N	N	N	N	N	Y	Y	Y	N	N	N	Y	N	N	N	N	N	
Effective chloride concentration at bar depth (% by wt. conc.) ^[4]	0.016	0.104	N/A	0.075	0.030	0.269	N/A	0.184	N/A	0.278	0.172	0.434	0.247	0.012	N/A	0.114	0.046	

NOTES:

^[1] Specified 8 mils ± 2 mils per 1977 Iowa DOT Standard Specifications

^[2] See Section 2.2.2 and Figures 27 and 28 for explanation of rating scale. “1” indicates no corrosion/ excellent adhesion; “5” indicates over 60% corroded/poor adhesion.

^[3] Backside contamination rating equals percentage of backside surface of peeled epoxy coating exhibiting contamination

^[4] As shown in Section 4.2.4, the effective corrosion thresholds are assumed as 0.035 (uncoated) and 0.180 (epoxy-coated), percent by weight of concrete.

Table 9. Iowa 13 Southbound over Indian Creek - Extracted Cores and Bars

Age of deck	23 years									
Background chloride, C ₀	0.007% by wt. conc.									
Cores										
Core ID	1	2	3	4	5	6	7			
Vertical crack (depth, in.)	-	-	-	-	3.0	3.1	-			
Horizontal crack (depth, in.)	-	-	-	-	-	2.0 - not at bar	-			
Bars										
Bar size	10	10	6	5	5	10	5	10	5	10
Depth (in.)	2.98	3.32	3.32	4.16	4.45	3.12	4.48	3.12	4.50	3.50
Epoxy coated?	Y	Y	Y	Y	Y	Y	Y	Y	Y	Y
Coating Thickness (mils) ^[1]	9.3	9.8	6.7	11.7	8.9	11.1	7.0	8.0	7.8	10.0
Adhesion Rating ^[2]	3	3	3	1	3	3	4	4	4	3
Backside Contamination ^[3]	20	10	20	10	2	2	15	20	10	10
Corrosion Condition ^[2]	1	1	1	1	1	1	1	1	1	1
Active Corrosion?	N	N	N	N	N	N	N	N	N	N
Effective chloride concentration at bar depth (% by wt. conc.) ^[4]	0.248	0.134	0.135	N/A	0.061	0.163	N/A	0.211	0.090	0.122

NOTES:

^[1] Specified 8 mils ± 3 mils per 1984 Iowa DOT Standard Specifications

^[2] See Section 2.2.2 and Figures 27 and 28 for explanation of rating scale. “1” indicates no corrosion/ excellent adhesion; “5” indicates over 60% corroded/poor adhesion.

^[3] Backside contamination rating equals percentage of backside surface of peeled epoxy coating exhibiting contamination

^[4] As shown in Section 4.2.4, the effective corrosion thresholds are assumed as 0.035 (uncoated) and 0.180 (epoxy-coated), percent by weight of concrete.

Table 10. US 30 over Missouri River Westbound Lanes- Extracted Cores and Bars

Age of deck	19 years																		
Background chloride, C ₀	0.011% by wt. conc.																		
Cores																			
Core ID	1		2		3		4		5		6		7		8		9		
Vertical crack (depth, in.)	-		1.3		Full		-		3.0		-		-		-		-		
Horizontal crack (depth, in.)	-		-		2.7 - at bar		-		-		-		-		-		-		
Bars																			
Bar size	5	5	5	5	5	5	5	6	6	6	6	6	5	6	6	6	6	6	6
Depth (in.)	2.75	3.52	3.52	2.62	3.34	2.70	3.36	2.53	3.43	3.88	3.42	4.21	4.50	2.90	3.70	3.00	3.88	3.66	4.48
Epoxy coated?	Y	Y	Y	Y	Y	Y	Y	Y	Y	Y	Y	Y	Y	Y	Y	Y	Y	Y	Y
Coating Thickness (mils) ^[1]	9.3	10.4	10.6	9.1	6.7	7.8	11.7	9.0	10.1	9.7	8.8	9.1	9.5	12.7	6.7	11.6	11.4	12.3	13.3
Adhesion Rating ^[2]	3	1	1	3	2	5	2	2	3	1	1	1	1	3	4	1	2	1	1
Backside Contamination ^[3]	10	2	2	50	2	50	2	2	10	2	2	2	2	10	10	2	2	2	2
Corrosion Condition ^[2]	1	1	1	2	1	5	2	1	1	1	1	1	1	1	1	1	1	1	1
Active Corrosion?	N	N	N	Y	N	Y	Y	N	N	N	N	N	N	N	N	N	N	N	N
Effective chloride concentration at bar depth (% by wt. conc.) ^[4]	0.000	0.000	0.000	0.063	0.024	0.506	N/A	0.021	N/A	0.071	0.000	N/A	N/A	0.010	0.001	0.007	0.001	0.000	N/A

NOTES:

^[1] Specified 8 mils ± 3 mils per 1984 Iowa DOT Standard Specifications

^[2] See Section 2.2.2 and Figures 27 and 28 for explanation of rating scale. “1” indicates no corrosion/ excellent adhesion; “5” indicates over 60% corroded/poor adhesion.

^[3] Backside contamination rating equals percentage of backside surface of peeled epoxy coating exhibiting contamination

^[4] As shown in Section 4.2.4, the effective corrosion thresholds are assumed as 0.035 (uncoated) and 0.180 (epoxy-coated), percent by weight of concrete.

Table 11. US 30 over Missouri River Eastbound Lanes - Extracted Cores and Bars

Age of deck	19 years																			
Background chloride, C ₀	0.008% by wt. conc.																			
Cores																				
Core ID	10	11	12	13	14	15	16	17	18	19 ^[1]										
Vertical crack (depth, in.)	-	-	-	Full	3.0	2.0	-	Full	-	-										
Horizontal crack (depth, in.)	-	-	-	2.5 - at bar	-	-	-	-	-	-										
Bars																				
Bar size	6	6	6	6	5	5	5	5	5	5	5	5	5	5	6	6	6	5	5	5
Depth (in.)	3.58	4.40	2.73	3.49	2.83	3.53	2.48	3.10	3.26	3.85	2.92	3.55	2.50	3.30	3.52	4.26	4.26	2.43	3.12	2.15
Epoxy coated?	Y	Y	Y	Y	Y	Y	Y	Y	Y	Y	Y	Y	Y	Y	Y	Y	Y	Y	Y	Y
Coating Thickness (mils) ^[1]	12.0	9.6	10.5	9.0	7.9	8.0	8.9	6.6	8.8	7.8	8.7	6.5	6.4	7.2	12.7	8.6	12.7	7.3	6.0	7.9
Adhesion Rating ^[2]	2	1	2	2	2	3	4	4	3	3	2	3	2	2	3	2	1	2	2	5
Backside Contamination ^[3]	2	2	2	2	2	2	50	50	15	2	2	2	2	2	15	2	2	2	2	50
Corrosion Condition ^[2]	1	1	1	1	1	1	4	2	1	1	1	1	1	1	1	1	1	1	1	4
Active Corrosion?	N	N	N	N	N	N	Y	Y	N	N	N	N	N	N	N	N	N	N	N	Y
Effective chloride concentration at bar depth (% by wt. conc.) ^[4]	0.003	0.001	0.001	0.000	0.001	N/A	0.356	0.286	0.112	N/A	0.012	N/A	0.000	0.000	0.116	0.069	0.069	0.003	N/A	N/A

[1] Top approximately 3 inches of core was patch material.

NOTES:

[1] Specified 8 mils ± 3 mils per 1984 Iowa DOT Standard Specifications

[2] See Section 2.2.2 and Figures 27 and 28 for explanation of rating scale. “1” indicates no corrosion/ excellent adhesion; “5” indicates over 60% corroded/poor adhesion.

[3] Backside contamination rating equals percentage of backside surface of peeled epoxy coating exhibiting contamination

[4] As shown in Section 4.2.4, the effective corrosion thresholds are assumed as 0.035 (uncoated) and 0.180 (epoxy-coated), percent by weight of concrete.

Table 12. US 18 over Floyd River - Extracted Cores and Bars

Age of deck	18 years													
Background chloride, C ₀	0.027% by wt. conc.													
Cores														
Core ID	1	2	3	4	5	6	7	8						
Vertical crack (depth, in.)	Full	-	-	-	Full	-	-	-						
Horizontal crack (depth, in.)	-	-	-	-	-	-	-	-	3.3 - at bar					
Bars														
Bar size	6	5	6	5	6	5	6	6	5	6	5	6	5	5
Depth (in.)	2.53	5.13	N/A	N/A	1.95	2.69	2.74	2.38	5.14	2.78	3.61	2.39	3.29	3.29
Epoxy coated?	Y	Y	Y	Y	Y	Y	Y	Y	Y	Y	Y	Y	Y	Y
Coating Thickness (mils) ^[1]	12.4	11.1	11.4	9.0	14.0	10.2	10.8	12.9	11.8	9.3	10.4	13.8	7.0	11.1
Adhesion Rating ^[2]	1	1	1	1	3	1	3	1	1	1	1	1	1	1
Backside Contamination ^[3]	2	2	2	2	10	2	10	2	2	2	2	2	2	2
Corrosion Condition ^[2]	1	1	1	1	1	1	1	1	1	1	1	1	1	1
Active Corrosion?	N	N	N	N	N	N	N	N	N	N	N	N	N	N
Effective chloride concentration at bar depth (% by wt. conc.) ^[4]	0.138	0.012	N/A	N/A	0.125	0.064	0.053	0.198	0.022	0.005	0.000	0.046	0.009	0.000

NOTES:

^[1] Specified 8 mils ± 3 mils per 1984 Iowa DOT Standard Specifications

^[2] See Section 2.2.2 and Figures 27 and 28 for explanation of rating scale. “1” indicates no corrosion/ excellent adhesion; “5” indicates over 60% corroded/poor adhesion.

^[3] Backside contamination rating equals percentage of backside surface of peeled epoxy coating exhibiting contamination

^[4] As shown in Section 4.2.4, the effective corrosion thresholds are assumed as 0.035 (uncoated) and 0.180 (epoxy-coated), percent by weight of concrete.

Table 13. US 65 Southbound over the Union Pacific Railroad - Extracted Cores and Bars

Age of deck	31 years																	
Background chloride, C ₀	0.010% by wt. conc.																	
Cores																		
Core ID	1	2	3	4	5	6 ^[1]	7	8	9	10								
Vertical crack (depth, in.)	-	-	-	2.0	Full	Full	-	-	-	Full								
Horizontal crack (depth, in.)	-	1.0 - not at bar	-	-	2.7 - at bar 3.7 - at bar	2.4 - at bar	1.0 - not at bar	-	-	2.8 - at bar								
Bars																		
Bar size	7	6	7	6	7	6	7	6	7	6	7	7	6	7	6	7	7	6
Depth (in.)	2.12	3.00	2.21	3.12	3.03	3.89	2.74	3.72	2.69	3.65	2.41	2.69	3.65	2.72	3.59	5.01	2.81	3.61
Epoxy coated?	Y	Y	Y	Y	Y	Y	Y	Y	Y	Y	Y	Y	Y	Y	Y	N	Y	Y
Coating Thickness (mils) ^[1]	7.2	9.1	6.1	10.0	8.4	8.0	10.5	8.7	11.0	10.1	12.7	16.7	7.4	9.3	8.7	-	8.2	9.4
Adhesion Rating ^[2]	2	2	4	2	2	1	4	1	3	4	5	1	3	3	4	-	5	4
Backside Contamination ^[3]	10	2	10	2	20	2	50	2	50	50	50	2	15	30	50	-	50	50
Corrosion Condition ^[2]	1	1	1	1	1	1	2	1	4	4	5	1	1	1	2	1	4	3
Active Corrosion?	N	N	N	N	N	N	Y	N	Y	Y	Y	N	N	N	Y	N	Y	Y
Effective chloride concentration at bar depth (% by wt. conc.) ^[4]	0.042	N/A	0.125	0.037	0.003	N/A	0.179	0.078	0.398	N/A	N/A	0.040	0.006	0.221	N/A	0.001	0.310	0.206

[1] Top approximately 2 inches of core was half patch material.

NOTES:

[1] Specified 8 mils \pm 2 mils per 1977 Iowa DOT Standard Specifications

[2] See Section 2.2.2 and Figures 27 and 28 for explanation of rating scale. “1” indicates no corrosion/ excellent adhesion; “5” indicates over 60% corroded/poor adhesion.

[3] Backside contamination rating equals percentage of backside surface of peeled epoxy coating exhibiting contamination

[4] As shown in Section 4.2.4, the effective corrosion thresholds are assumed as 0.035 (uncoated) and 0.180 (epoxy-coated), percent by weight of concrete.

Table 14. US 65 Northbound over the Union Pacific Railroad - Extracted Cores and Bars

Age of deck	31 years																			
Background chloride, C ₀	0.010% by wt. conc.																			
Cores																				
Core ID	1	2			3			4			5			6			7			8
Vertical crack (depth, in.)	-	-			-			-			Full			2.4			Full			-
Horizontal crack (depth, in.)	-	-			-			-			2.9 - at bar			2.4 - at bar 3.4 - at bar			2.3 - at bar			-
Bars																				
Bar size	7	6	7	6	6	7	6	7	6	7	6	7	6	7	6	7	6	6		
Depth (in.)	2.41	3.41	2.67	3.47	4.09	1.54	2.44	3.12	3.92	2.90	3.70	2.37	3.39	2.29	3.25	2.40	5.06	5.89		
Epoxy coated?	Y	Y	Y	Y	Y	Y	Y	Y	Y	Y	Y	Y	Y	Y	Y	Y	N	N		
Coating Thickness (mils) ^[1]	11.9	9.3	8.6	7.8	10.8	6.9	8.6	6.0	9.0	12.8	12.5	9.0	10.8	12.3	11.7	7.8	-	-		
Adhesion Rating ^[2]	2	2	4	3	3	5	3	4	1	4	2	3	4	5	3	3	-	-		
Backside Contamination ^[3]	10	15	15	10	15	50	20	10	2	50	50	50	50	50	50	10	-	-		
Corrosion Condition ^[2]	1	1	1	1	1	1	1	1	1	4	3	5	4	4	2	1	1	1		
Active Corrosion?	N	N	N	N	N	N	N	N	N	Y	Y	Y	Y	Y	Y	N	N	N		
Effective chloride concentration at bar depth (% by wt. conc.) ^[4]	0.021	0.002	0.122	N/A	N/A	0.304	0.178	0.014	0.003	0.232	N/A	0.388	N/A	0.364	0.236	0.026	0.000	0.000		

NOTES:

^[1] Specified 8 mils ± 2 mils per 1977 Iowa DOT Standard Specifications

^[2] See Section 2.2.2 and Figures 27 and 28 for explanation of rating scale. “1” indicates no corrosion/ excellent adhesion; “5” indicates over 60% corroded/poor adhesion.

^[3] Backside contamination rating equals percentage of backside surface of peeled epoxy coating exhibiting contamination

^[4] As shown in Section 4.2.4, the effective corrosion thresholds are assumed as 0.035 (uncoated) and 0.180 (epoxy-coated), percent by weight of concrete.

Table 15. Summary of Background Chloride (C_0), Effective Surface Concentrations (C_s), and Diffusion Coefficients (D_a)

Bridge	C_0 (% by wt. conc.)	Effective C_s (% by wt. conc.) ^[1]			D_a (in. ² /yr.)					
					Uncracked Cores			Cores with Vertical Crack		
		Avg.	Std. dev.	Number	Avg.	Std. dev.	Number	Avg.	Std. dev.	Number
Iowa 17	0.006	0.777	0.150	5	0.057	0.024	2	N/A	N/A	0
US 218	0.048	0.557	0.130	5	0.124	0.014	3	0.189	0.048	2
Iowa 150	0.006	0.760	0.156	5	0.067	0.039	4	0.093	N/A	1
Iowa 13	0.007	0.563	0.121	5	0.242	0.109	4	0.175	N/A	1
US 30	0.011	0.635	0.184	10	0.029	0.019	6	0.237	0.115	3
US 18	0.027	0.559	0.094	5	0.059	0.037	3	0.157	0.023	2
US 65 SB	0.010	0.823	0.034	4	0.083	N/A	1	0.146	N/A	1
US 65 NB	0.010	0.705	0.100	5	0.040	0.031	4	0.158	N/A	1

[1] Corrected for background chloride.

Table 16. Summary of Inputs for Service Life Model

Bridge	Section	Effective C _s (% by wt. conc.) ^[1]		D _a (in. ² /yr.)				Cover (in.)		Crack Density (ft. / sq. ft.)	Epoxy- coated t _p (yrs)
				Uncracked		Cracked					
		Avg.	Std. dev.	Avg.	Std. dev.	Avg.	Std. dev.	Avg.	Std. dev.		
Iowa 17	1	0.777	0.150	0.057	0.024	0.300	0.180	2.29	0.29	0.007	18
US 218 SB	1	0.557	0.130	0.124	0.014	0.300	0.180	2.15	0.26	0.055	17 ^[2]
	2							2.69	0.35	0.020	
	3							2.63	0.36	0.057	
Iowa 150	1	0.760	0.156	0.067	0.039	0.300	0.180	2.50	0.24	0.003	20
	2							2.59	0.28	0.004	
	3							2.31	0.19	0.002	
Iowa 13 SB	1	0.563	0.121	0.242	0.109	0.300	0.180	3.09	0.34	0.161	23 ^[2]
US 30	1	0.635	0.184	0.029	0.019	0.300	0.180	2.72	0.32	0.140	13
	2							2.58	0.24	0.173	
	3							3.03	0.38	0.093	
	4							2.85	0.25	0.130	
US 18	1	0.559	0.094	0.059	0.037	0.300	0.180	2.56	0.29	0.165	18 ^[2]
US 65 SB ^[3]	1	0.757	0.096	0.048	0.033	0.300	0.180	2.56	0.22	0.021	12
US 65 NB ^[3]	1	0.757	0.096	0.048	0.033	0.300	0.180	2.50	0.25	0.047	12

[1] Corrected for background chloride.

[2] No damage area in deck was measured during field investigation, so t_p was set to the current age of the bridge.

[3] For both US 65 bridges, a combined average of measured effective C_s and D_a were used for modeling.

Table 17. Summary of Service Life Projections

Bridge	Epoxy-coated Bar Mats	Current Age (years)	Section	Measured Damage (% of area)	Projected Age ^[1] at 10% Damage		Service Life Extension (yrs.) Epoxy-coated vs. Uncoated
					Epoxy-coated	Uncoated	
Iowa 17	top only	32	1	3.3	36	12	24
US 218	top & bottom	17	1	0.0	29	9	20
			2	0.0	36	11	25
			3	0.0	35	11	24
Iowa 150	top only	30	1	1.3	37	12	25
			2	0.6	39	12	27
			3	1.7	36	11	25
Iowa 13	top & bottom	23	1	0.0	35	9	26
US 30	top & bottom	19	1	6.1	47	18	29
			2	3.2	39	14	25
			3	0.1	60	23	37
			4	1.7	56	21	35
US 18	top & bottom	18	1	0.0	37	11	26
US 65 SB	top only	31	1	3.8	36	13	23
US 65 NB	top only	31	1	11.2	33	13	20
Average					39	13	26

[1]. Projected ages should be considered approximate. Actual age at 10 percent damage may vary by 5 years or more.

FIGURES



Figure 1. Concrete removal process at deck patching performed by Iowa DOT maintenance personnel at Southbound US 65 Bridge over the Union Pacific Railroad in Bondurant, Iowa (photography courtesy of Iowa DOT).



Figure 2. Corroded reinforcing bar exposed during the deck patching performed by Iowa DOT maintenance personnel at Southbound US 65 bridge over the Union Pacific Railroad in Bondurant, Iowa (photograph courtesy of Iowa DOT).



Figure 3. Delaminated section of concrete at a corroded reinforcing bar exposed during the deck patching performed by Iowa DOT maintenance personnel at Southbound US 65 Bridge over the Union Pacific Railroad in Bondurant, Iowa (photograph courtesy of Iowa DOT).



Figure 4. Close-up views of corroded epoxy-coated reinforcing bars uncovered during deck patching performed by Iowa DOT maintenance personnel at Southbound US 65 Bridge over the Union Pacific Railroad in Bondurant, Iowa (photograph courtesy of Iowa DOT).



Figure 5. Aerial view of IA 17 Bridge over US 20 (Courtesy of Bing Maps).



Figure 6. East elevation of IA 17 Bridge over US 20.



Figure 7. Aerial view of Southbound US 218 over the Cedar River (Courtesy of Bing Maps). The southbound bridge is in the foreground, the northbound bridge in the background.



Figure 8. West elevation of Southbound US 218 over the Cedar River.



Figure 9. Aerial view of the IA 150 bridge over the Cedar River (Courtesy of Bing Maps).



Figure 10. East elevation of IA 150 over the Cedar River.

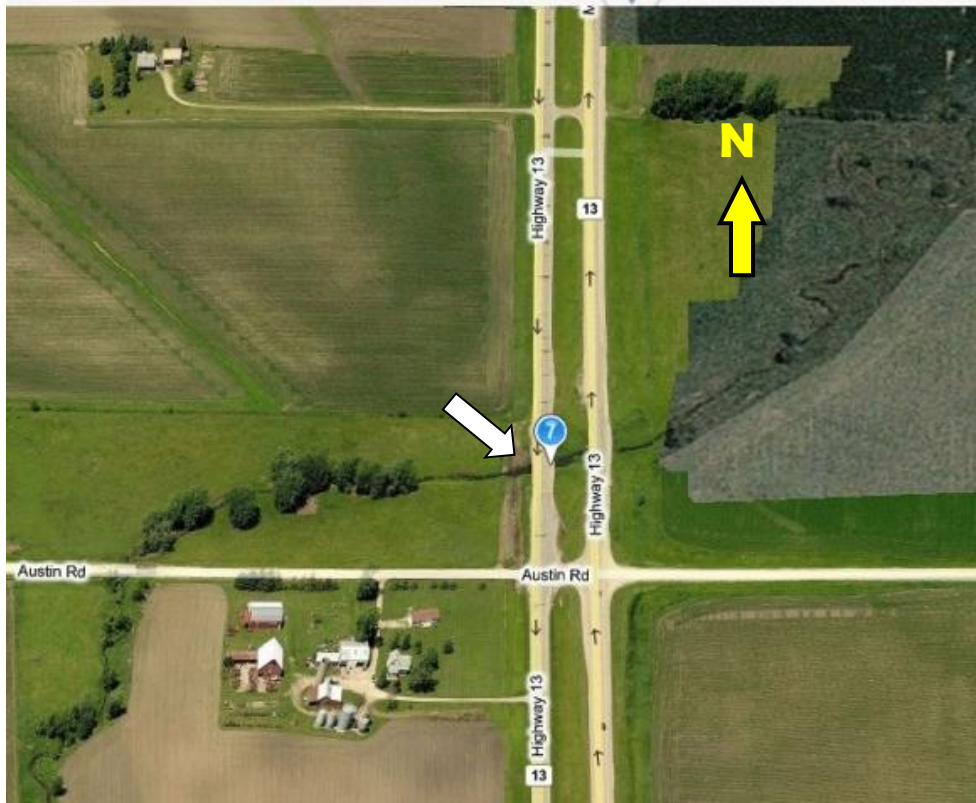


Figure 11. Aerial view of Southbound IA 13 bridge over Indian Creek (Courtesy of Bing Maps). The southbound bridge is on the left.



Figure 12. East elevation of Southbound IA 13 over Indian Creek.

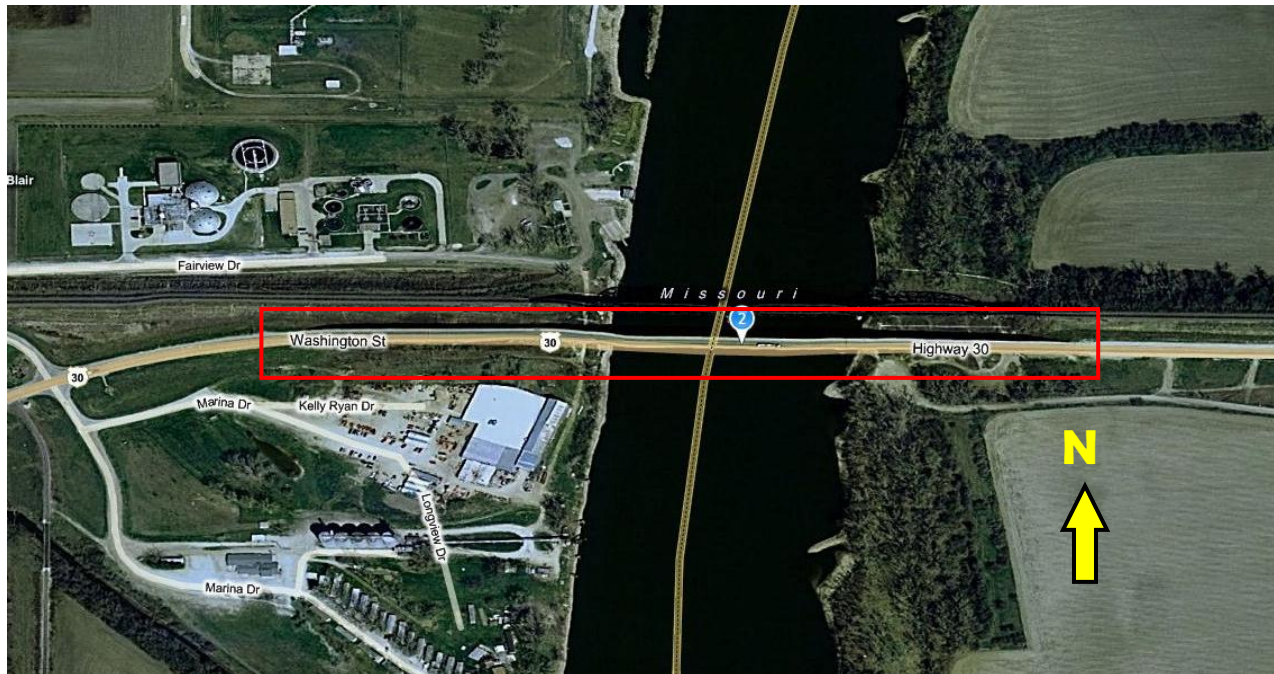


Figure 13. Aerial view of US 30 bridge over the Missouri River (Courtesy of Bing Maps).



Figure 14. South elevation of US 30 over the Missouri River, with adjacent railroad truss bridge in the background.

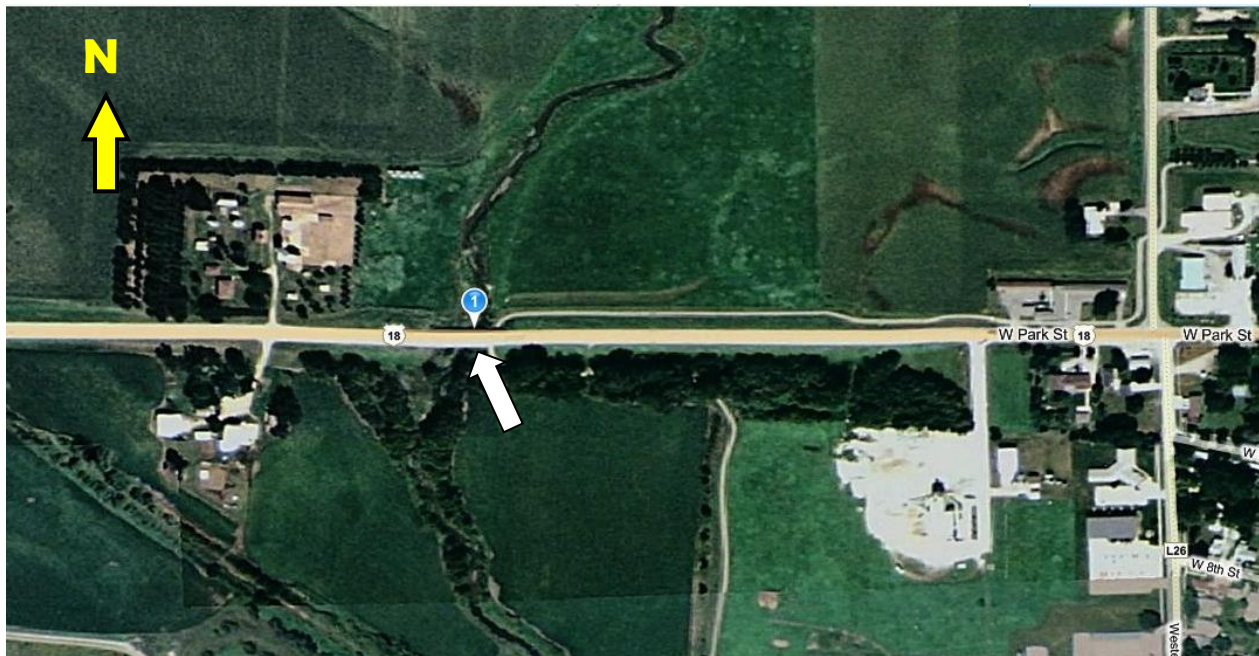


Figure 15. Aerial view of the US 18 bridge over the Floyd River (Courtesy of Bing Maps).



Figure 16. North elevation of the US 18 bridge over the Floyd River.



Figure 17. Aerial view of the US 65 northbound and southbound bridges over the Union Pacific Railroad (Courtesy of Bing Maps).



Figure 18. Southeast elevation of the Northbound US 65 bridge over the Union Pacific Railroad.



Figure 19. Conducting the delamination survey of a bridge deck by chain dragging to locate delaminations.



Figure 20. Using the GSSI StructureScan Mini Ground Penetrating Radar unit to identify locations of reinforcing bars.



Figure 21. Core sample extraction.



Figure 22. Half-cell survey test frame.



Figure 23. Drilling ground locations for the half-cell survey.



Figure 24. Instantaneous corrosion rate testing with the Galvapulse meter.

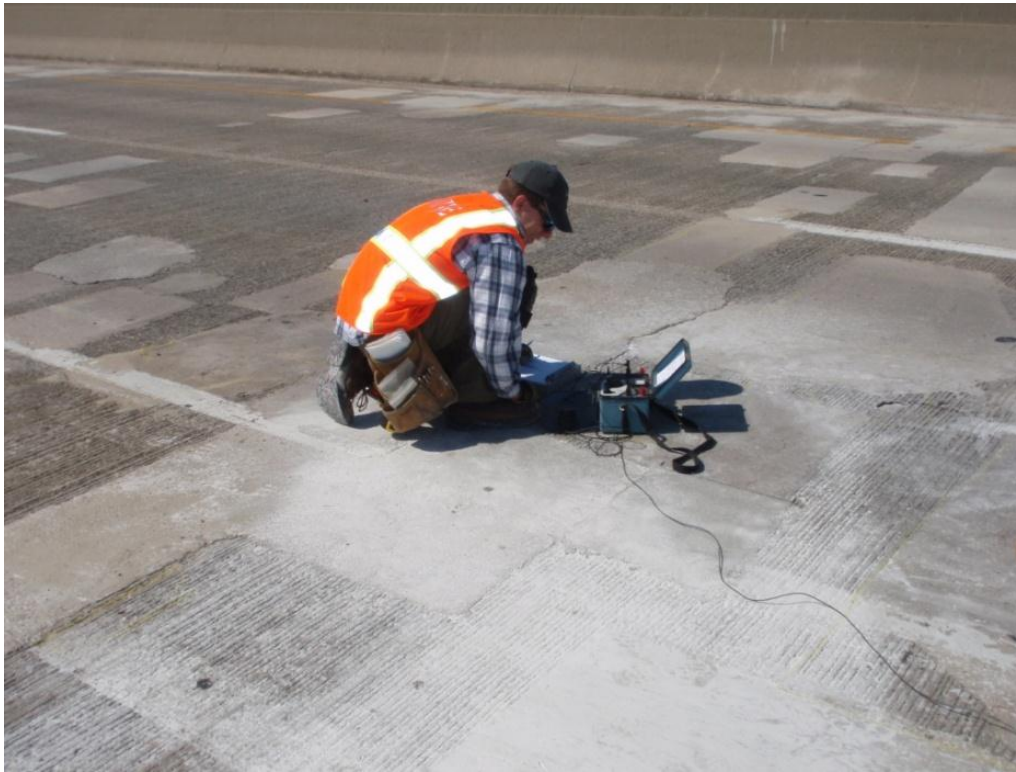


Figure 25. Measuring continuity (electrical resistance) of the reinforcing bar mat between core locations.



Figure 26. Pin affixed between the ends of the exposed reinforcing bars in the core holes for the purpose of continuity testing.



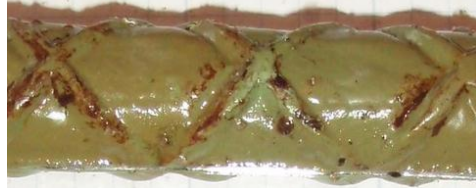


Value	Description	Representative photographs Epoxy-coated
1	No evidence of corrosion	
2	A number of small, countable corrosion spots	
3	Corrosion area less than 20% of total surface area	
4	Corrosion area between 20% to 60% of total surface area	
5	Corrosion area greater than 60% of total surface area	

Figure 27. Rating scale used to assess corrosion condition of bars taken from cores. All bars rated 2 or greater were considered to be actively corroding.










Value	Description	Representative photographs	
1	Excellent adhesion; epoxy does not peel from bar		
2	Epoxy peels from bar in 1/8-inch sections		
3	Moderate adhesion; epoxy peels from bar in 1/4-inch sections		
4	Epoxy peels from bar in 3/8-inch sections		
5	Poor adhesion; epoxy peels from bar in 1/2-inch sections		

Figure 28. Rating scale used to assess epoxy adhesion on bars taken from cores.

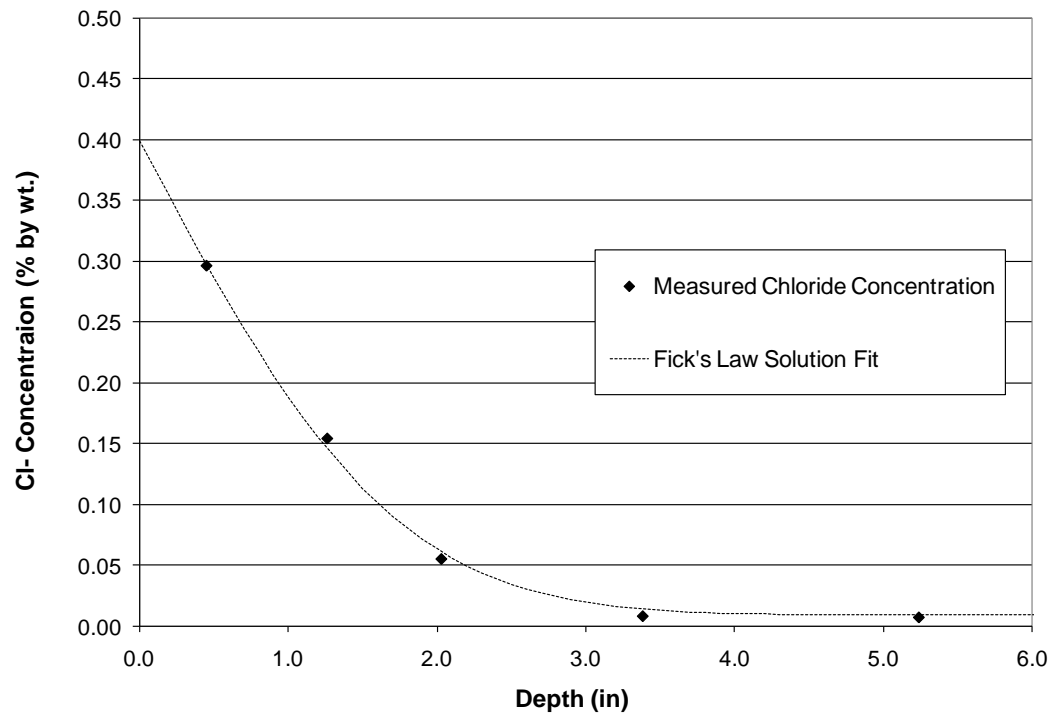


Figure 29. Measured chloride concentration and fitted solution to Fick's Law



Figure 30. Typical view of IA 17 deck underside



Figure 31. Typical longitudinal crack in wheel path of approach spans at Southbound US 218 bridge.

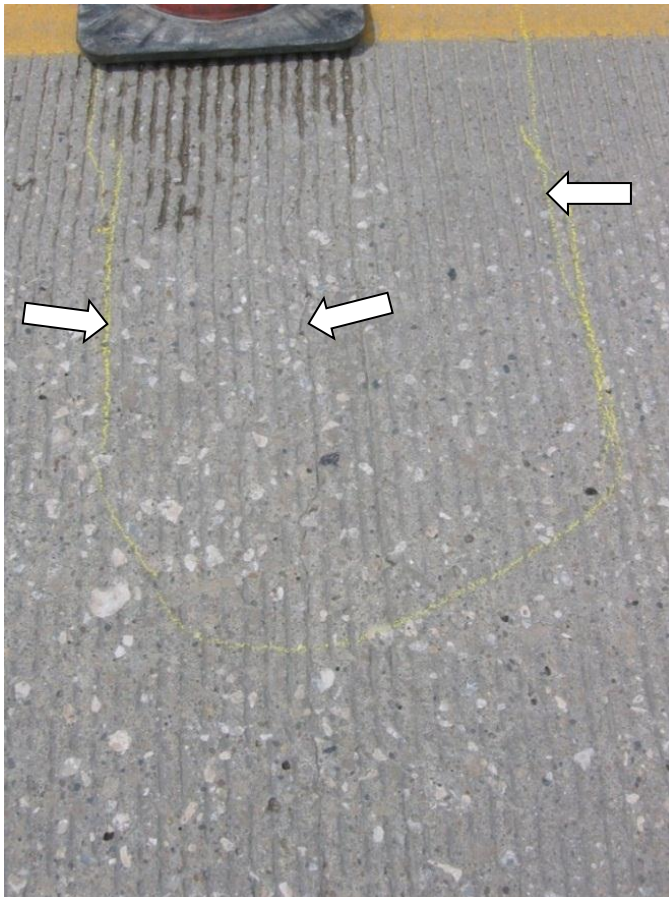


Figure 32. Area of delaminated concrete (outlined in yellow) at a transverse crack in the IA 150 bridge deck.

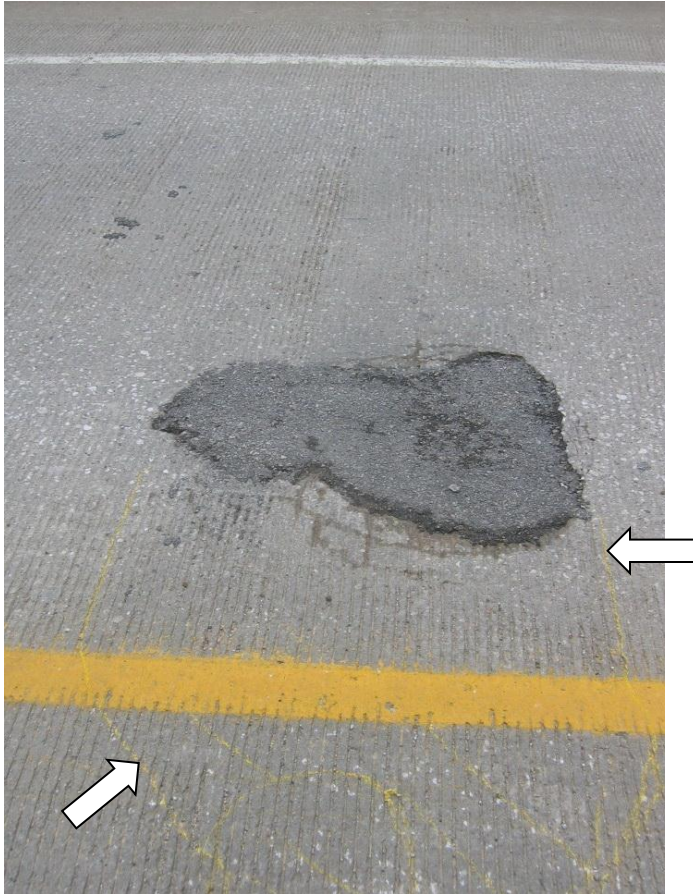


Figure 33. Asphalt patch on IA 150 bridge deck, with areas of continued delamination marked in yellow.



Figure 34. View of underside of IA 150 deck adjacent to the north abutment.



Figure 35. Typical view of top surface of the Southbound Iowa 13 bridge deck.



Figure 36. Typical view of the underside of the Southbound Iowa 13 bridge deck.



Figure 37. Hairline cracking in edge of deck slab and barrier rail at southwest corner of the Southbound Iowa 13 bridge deck.



Figure 38. Typical view of US 30 bridge deck in east approach spans.

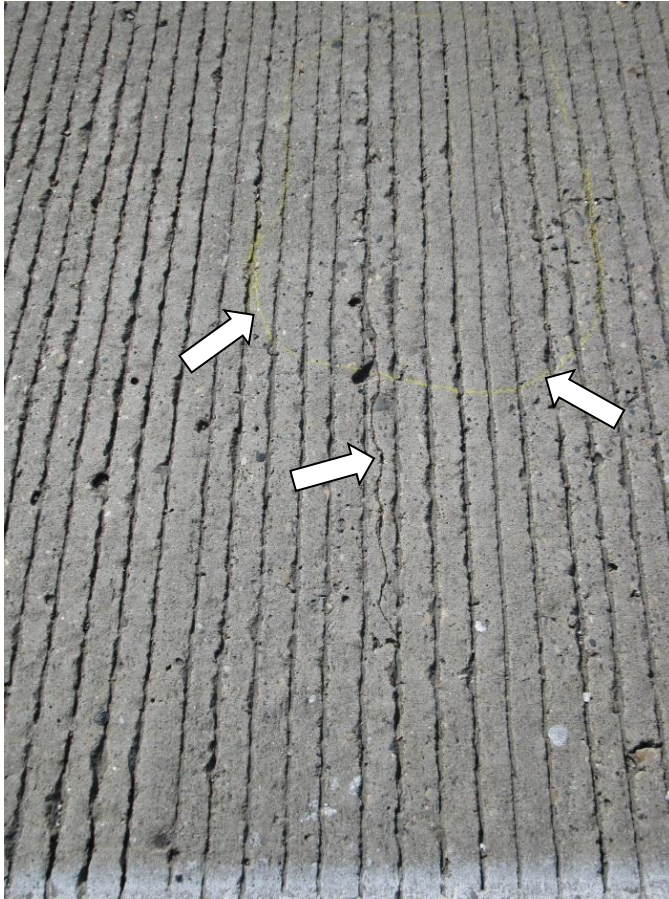


Figure 39. Typical transverse crack in east approach spans of US 30 bridge deck. Note delamination outlined in yellow (see arrows)



Figure 40. Regular through deck transverse cracks highlighted by efflorescence on the underside of east approach spans for the US 30 bridge deck



Figure 41. Incipient spalling at an area of delaminated concrete on the US 30 bridge deck.



Figure 42. Area of delaminated concrete (outlined in yellow) immediately adjacent to an existing patch on the west approach spans of the US 30 bridge



Figure 43. Typical transverse crack in US 30 bridge deck.



Figure 44. Area of typical transverse cracking with efflorescence at underside of west approach spans for the US 30 bridge.



Figure 45. Pre-existing damage to coating of actively corroding bar in Core #2 from US 30 bridge deck (location of damage indicated by red arrow).

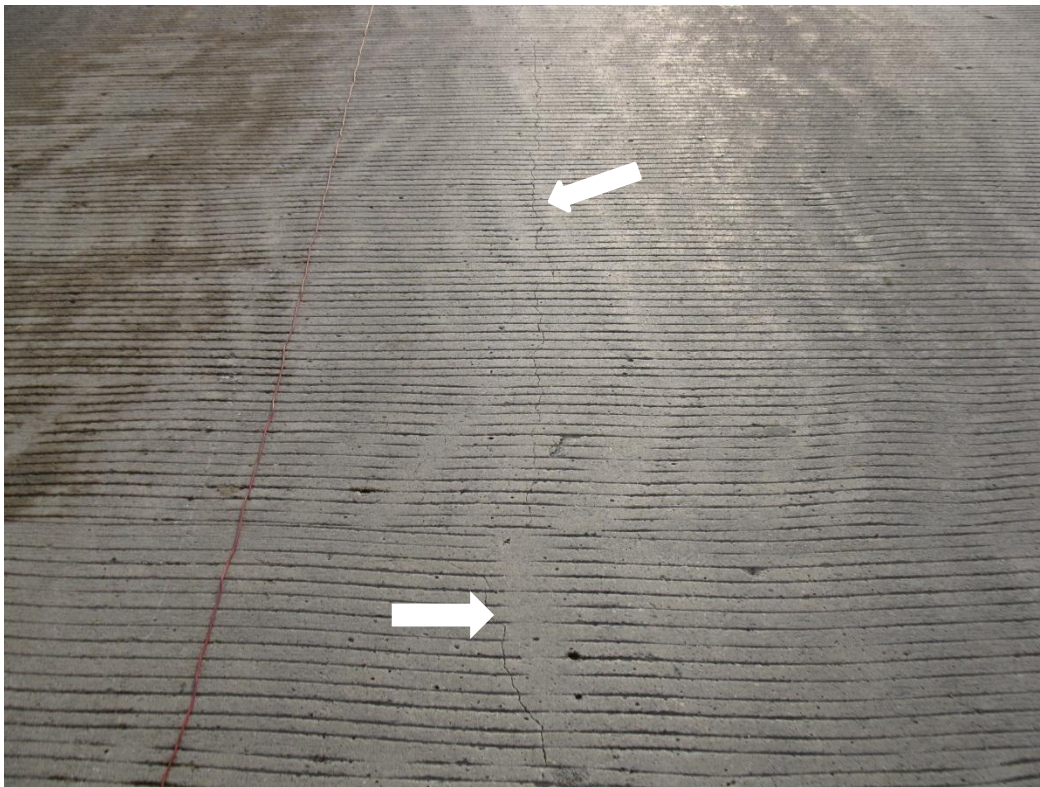


Figure 46. Typical view of longitudinal crack in US 18 bridge deck.



Figure 47. Typical view of underside of center span of US 18 bridge deck, with cracking indicated by arrows.



Figure 48. Area of patching on top surface of Southbound US 65 bridge deck, with adjacent area of delaminated concrete outlined in yellow.



Figure 49. Area of delaminated concrete outlined in yellow between two patches and along a transverse crack in the Southbound US 65 bridge deck.



Figure 50. Fine hairline cracking in deck top surface with the appearance of plastic shrinkage cracking.



Figure 51. Area of spalled concrete on underside of Southbound US 65 bridge deck



Figure 52. Area of extensive patching on the surface of Northbound US 65 bridge deck, with adjacent delaminations outlined in yellow.



Figure 53. Area of extensive patching on Northbound US 65 bridge deck.



Figure 54. Multiple short hairline cracks on deck top surface (Northbound US 65) similar to plastic shrinkage cracking.



Figure 55. Area of spalled concrete on underside of Northbound US 65 deck.



Figure 56. Marked areas of delamination on underside of Northbound US 65 bridge deck (marked by others).

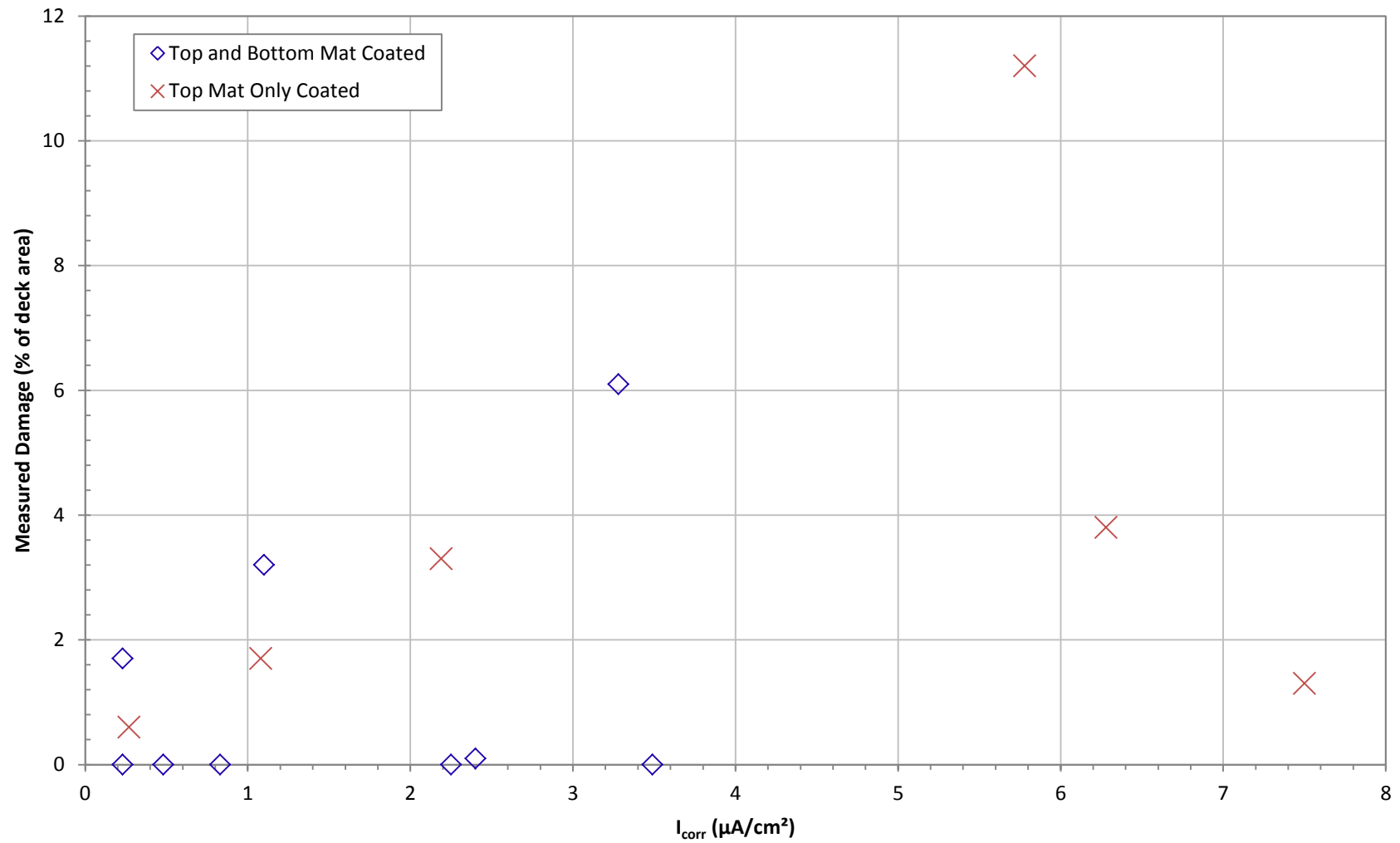


Figure 57. Measured damage to deck (delaminations, spalls, and repairs) compared to average instantaneous corrosion rate (I_{corr}) measured for all deck sections surveyed.

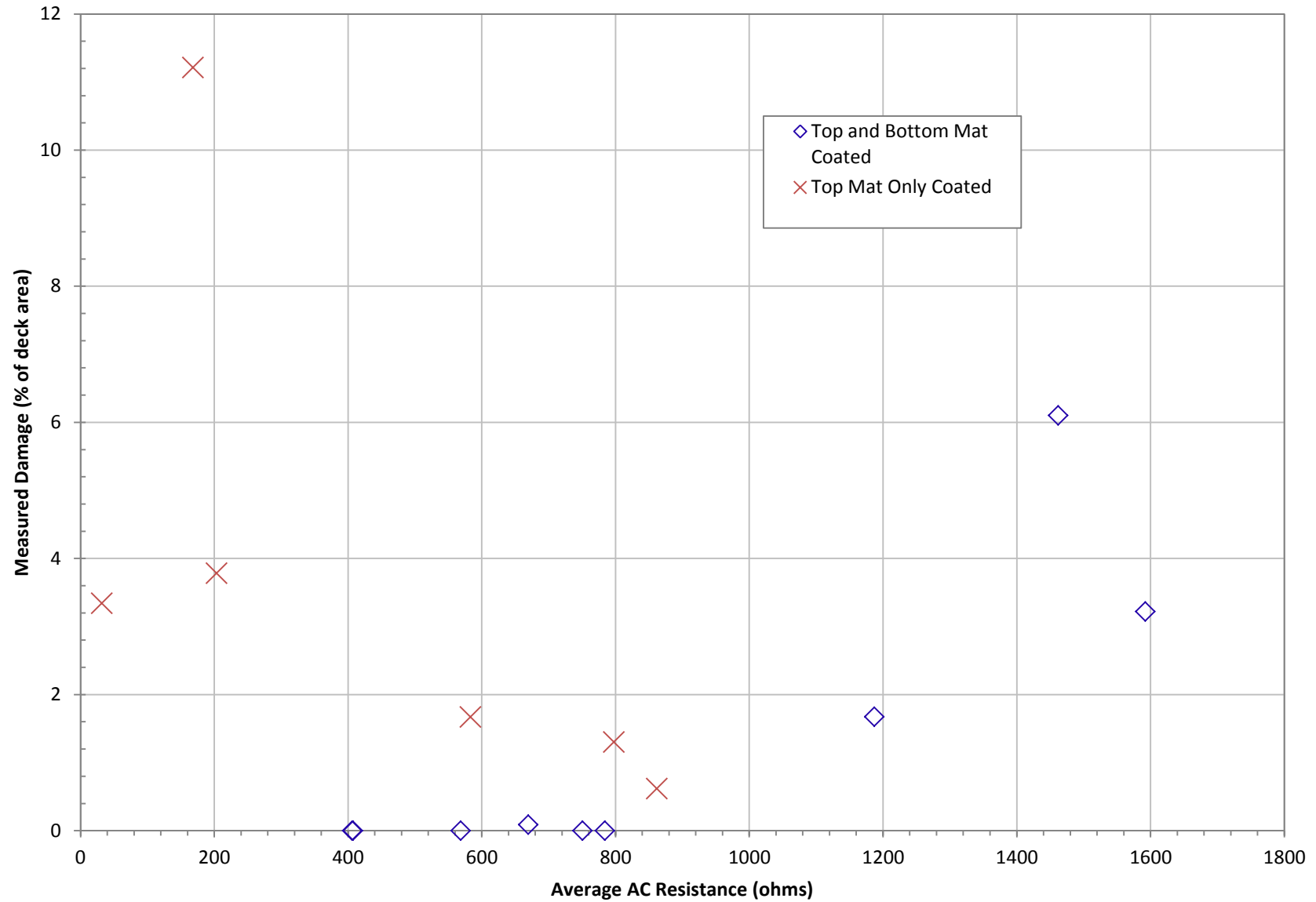


Figure 58. Measured damage to deck (delaminations, spalls and repairs) compared to average AC resistance for all deck sections surveyed.

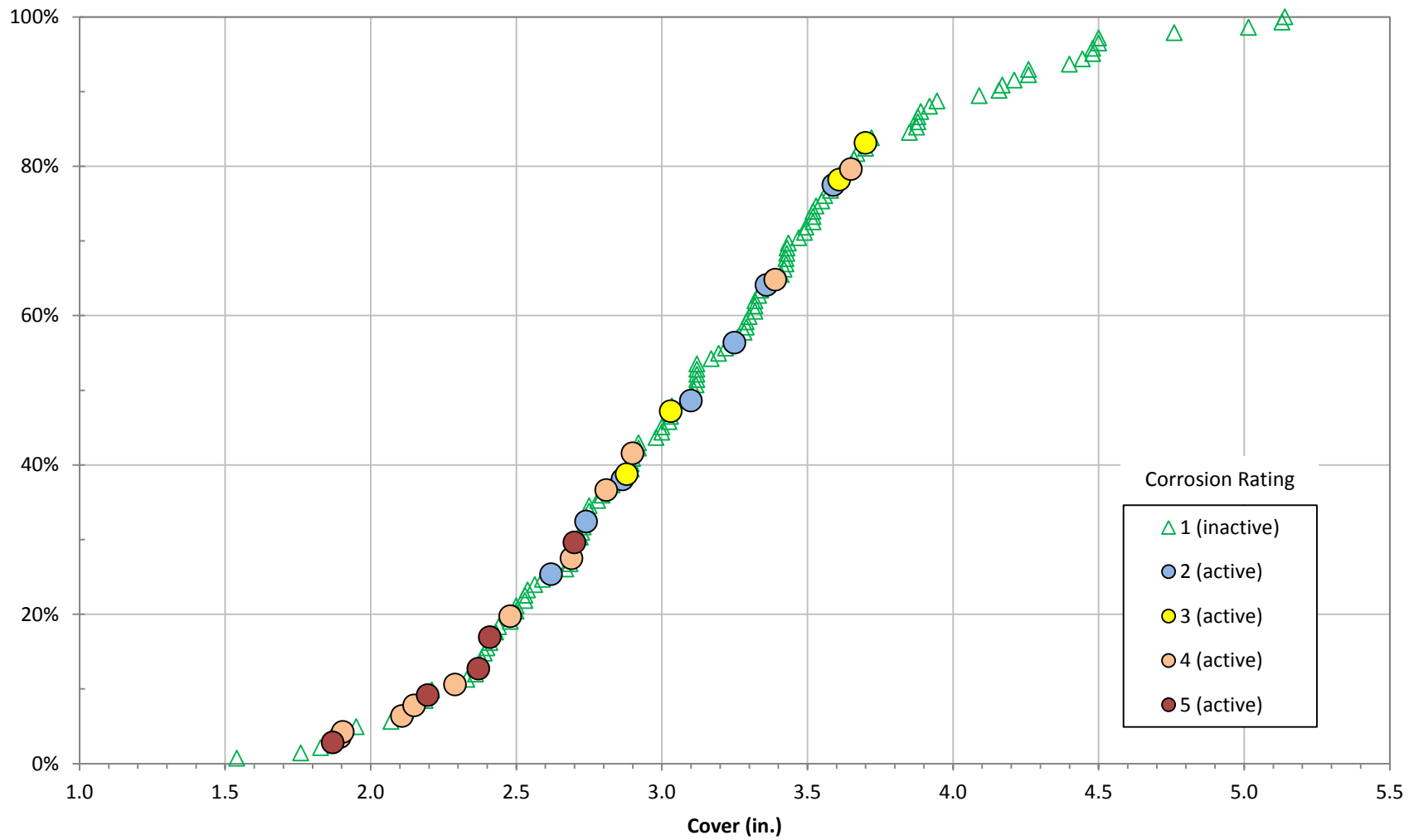


Figure 59. Cumulative distribution of concrete cover, categorized by corrosion activity.

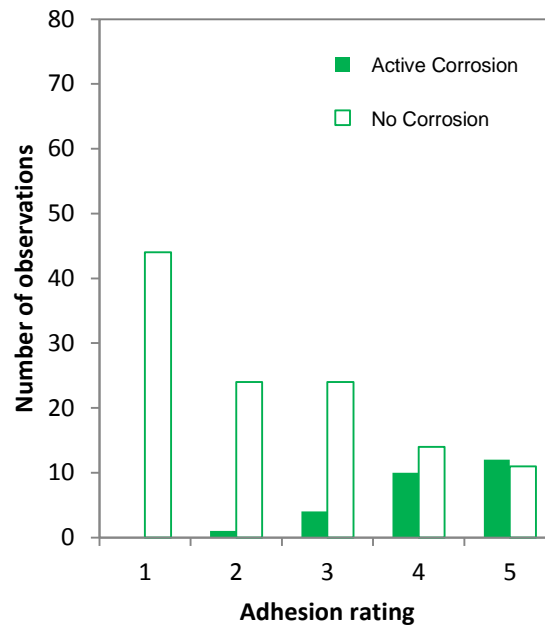


Figure 60. Histogram of adhesion of epoxy coating, categorized by corrosion activity.

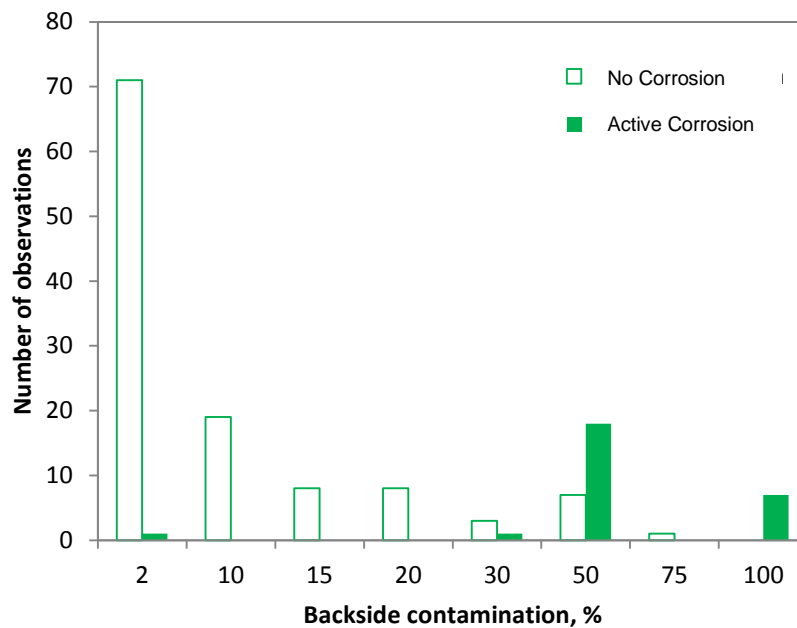


Figure 61. Histogram of backside contamination of epoxy coating, categorized by corrosion activity.

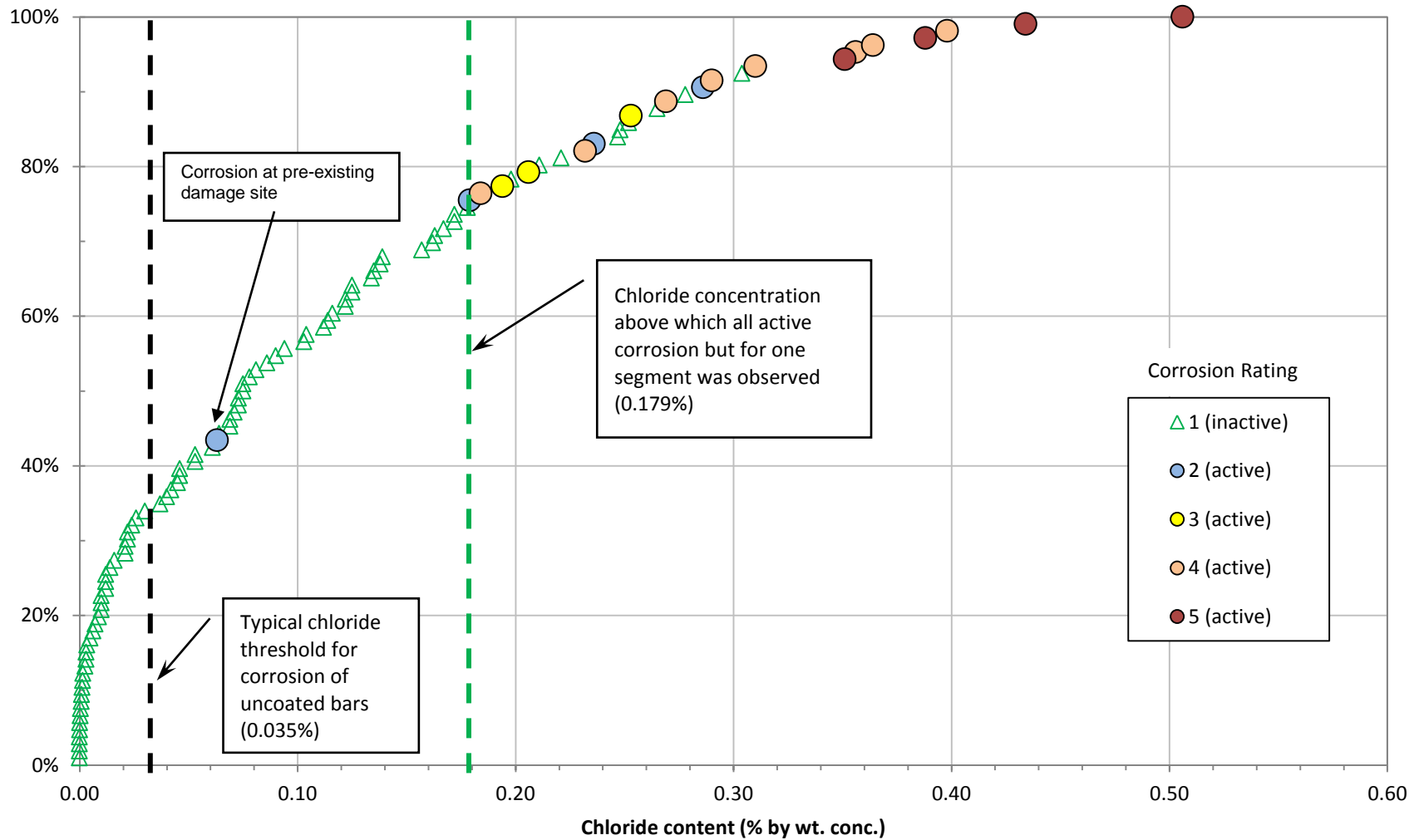


Figure 62. Cumulative distribution of chloride content at bar depth for epoxy-coated bars, categorized by corrosion rating.

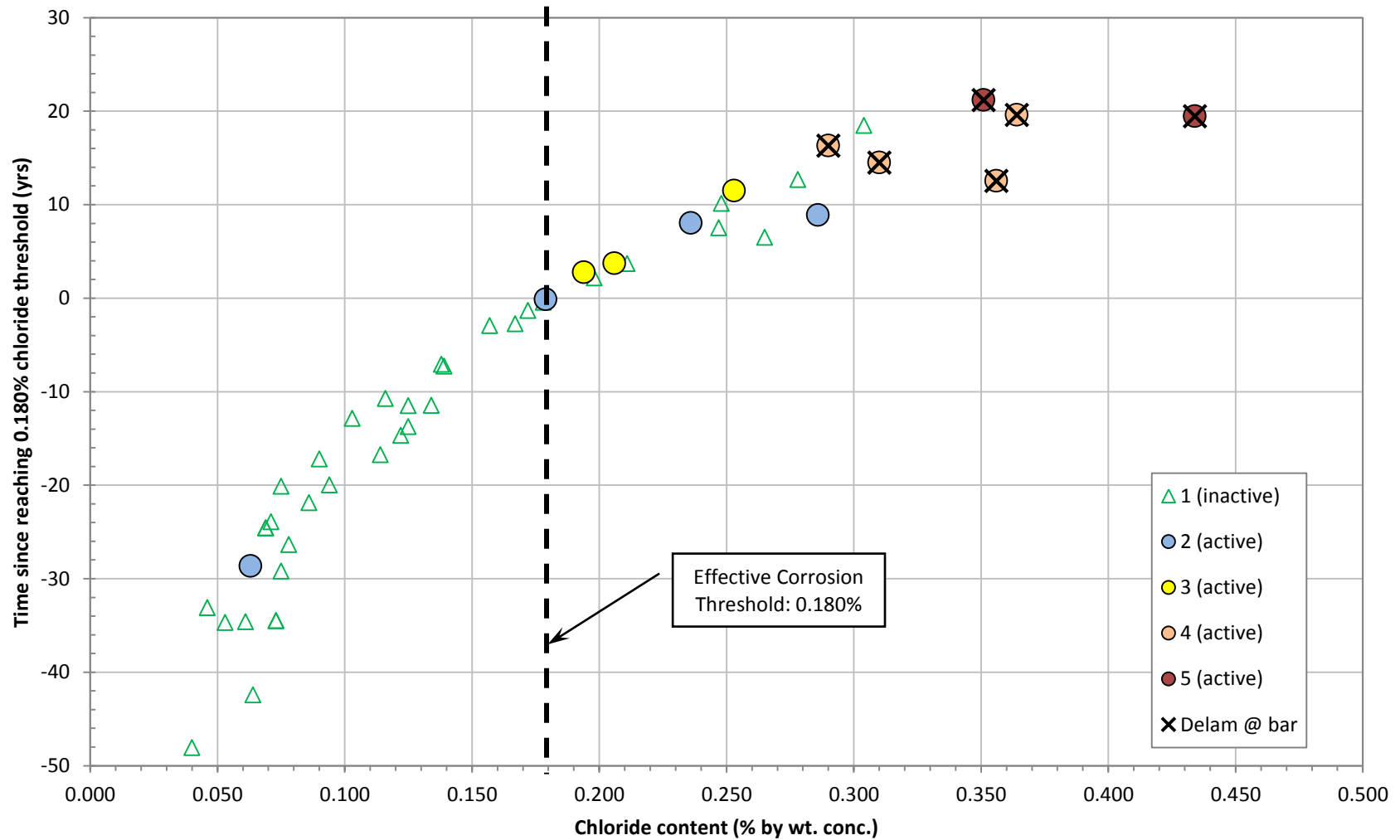


Figure 63. Time since reaching 0.180% by wt. chloride content at bar depth vs. chloride content at bar depth, categorized by corrosion rating. Positive numbers indicate the length of time since reaching the specified threshold. Negative numbers indicate that the chloride content at the bar has not yet reached 0.180 % by wt.

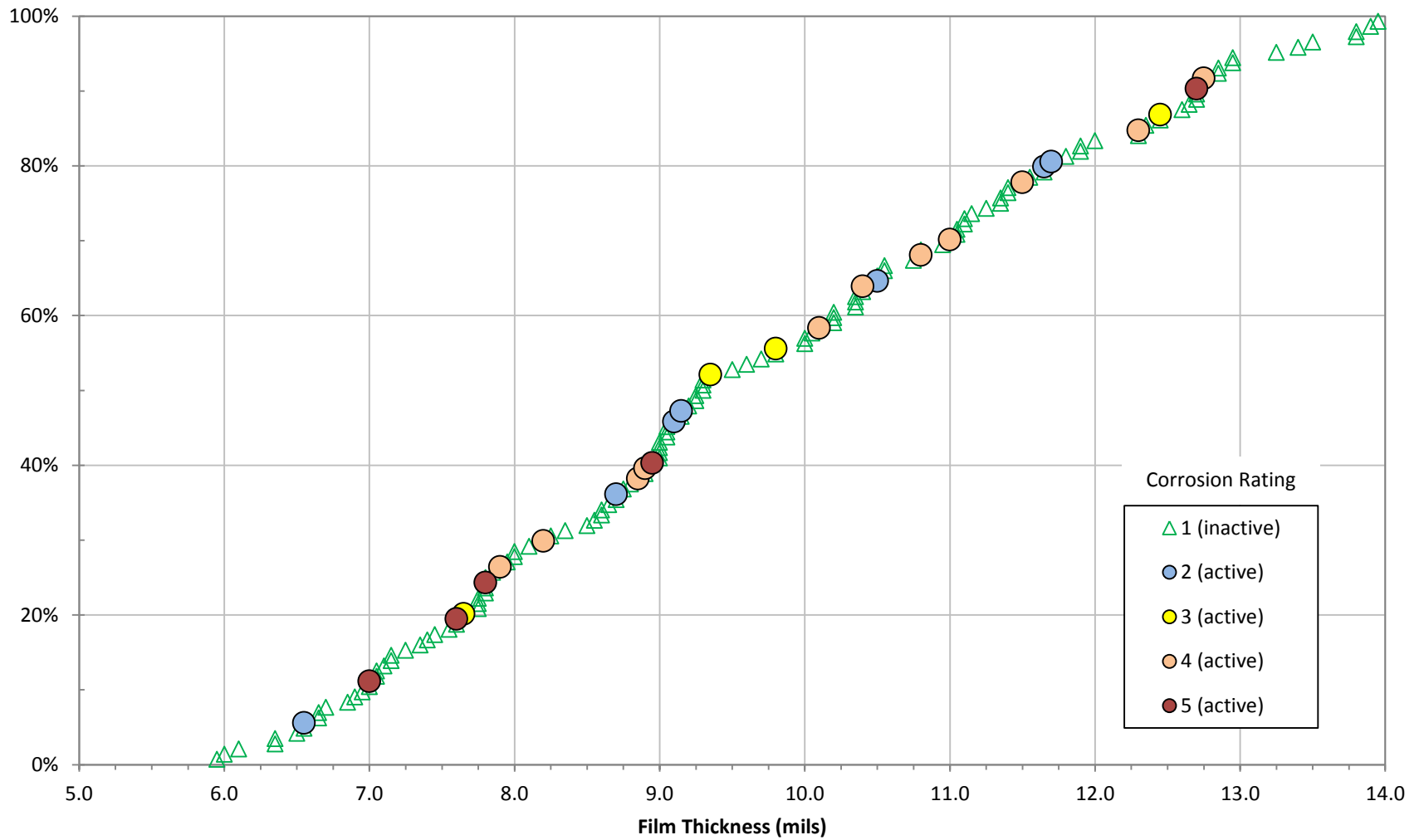


Figure 64. Cumulative distribution of epoxy film thickness, categorized by corrosion activity.

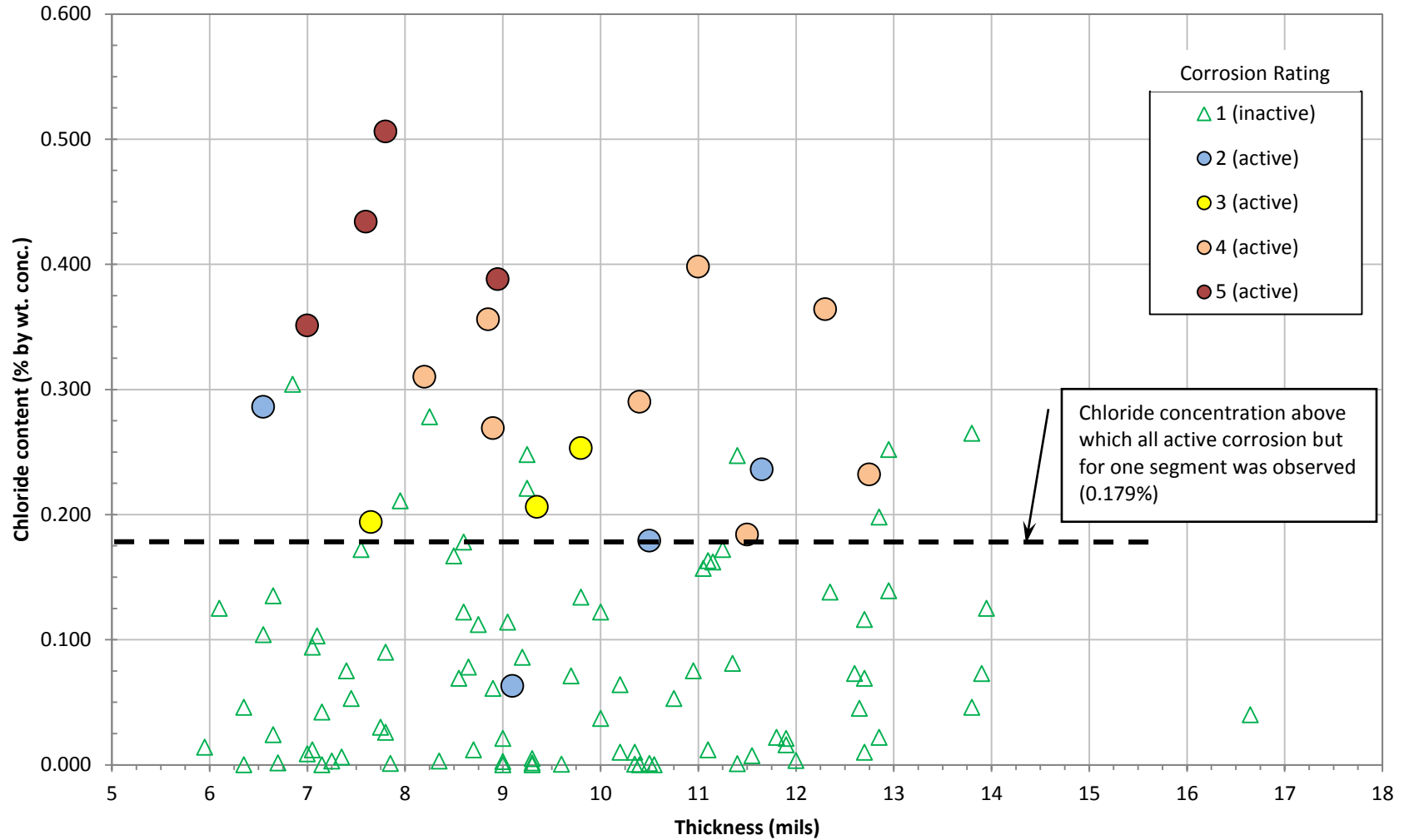


Figure 65. Net chloride content at bar depth versus epoxy film thickness, categorized by corrosion rating.

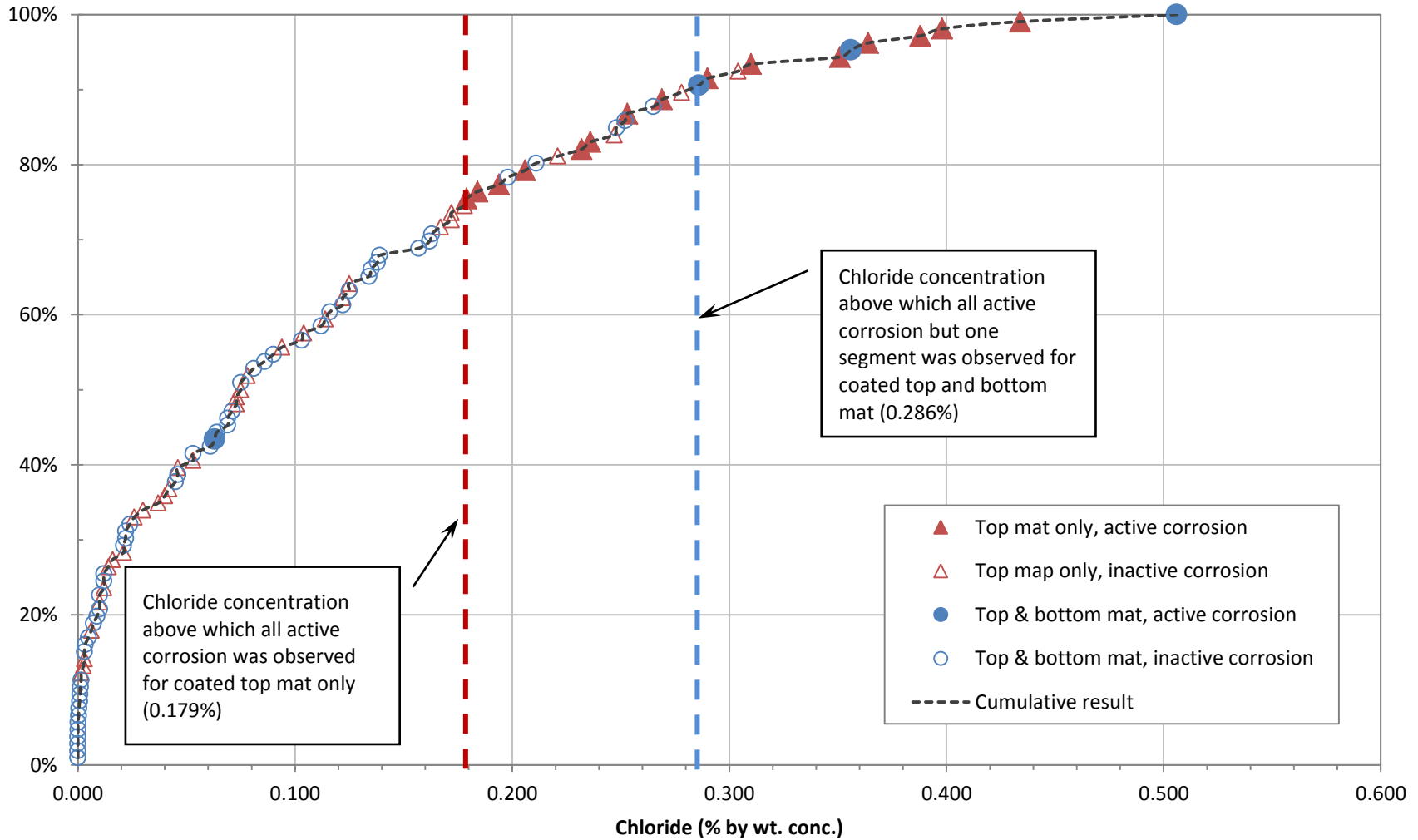


Figure 66. Cumulative distribution of net chloride content at bar depth, categorized by deck construction and corrosion activity.

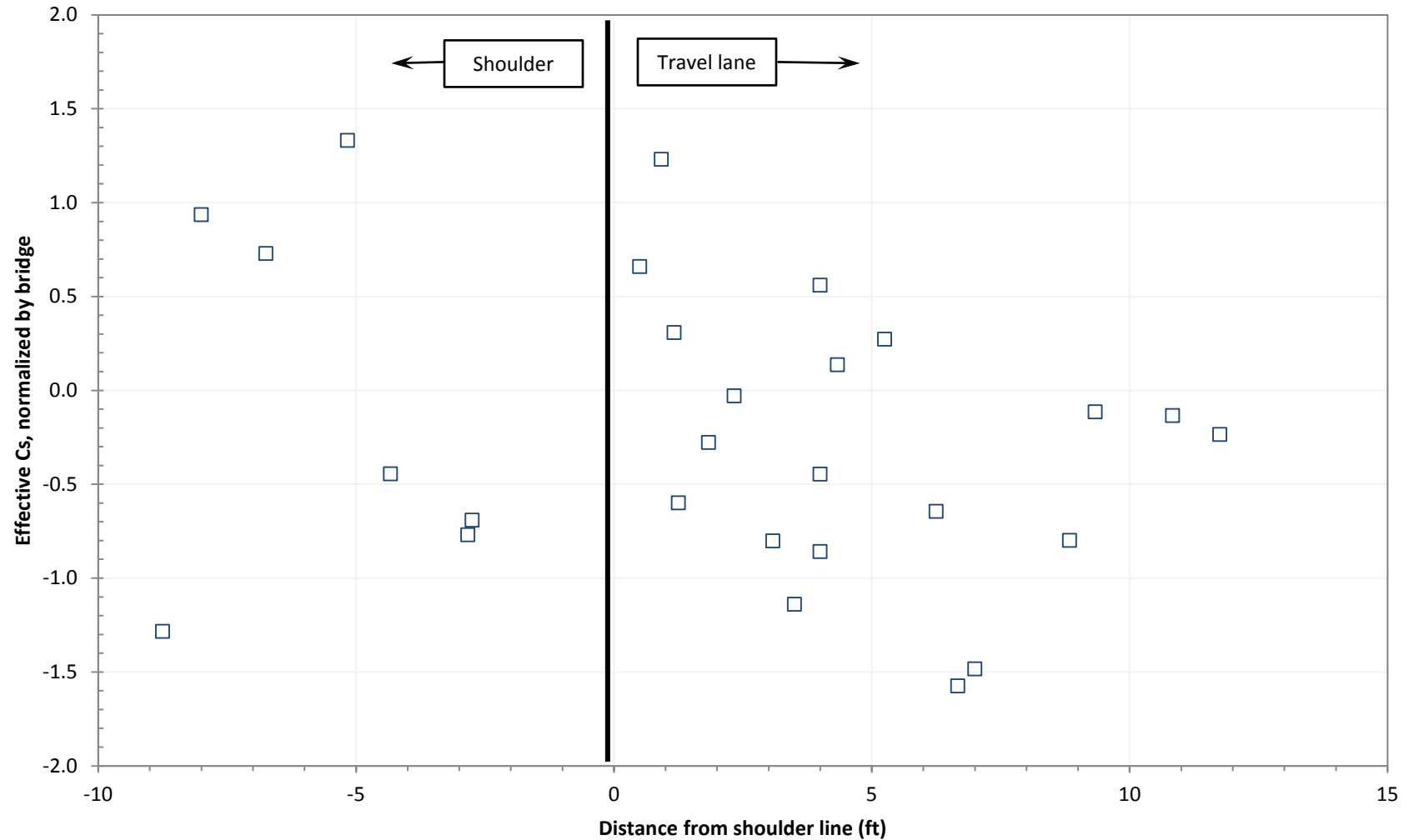


Figure 67. Effective surface chloride concentration versus distance from shoulder line. Positive values in distance indicate that the sample was obtained in the travel lane, and negative values indicate the sample was obtained from the shoulder.

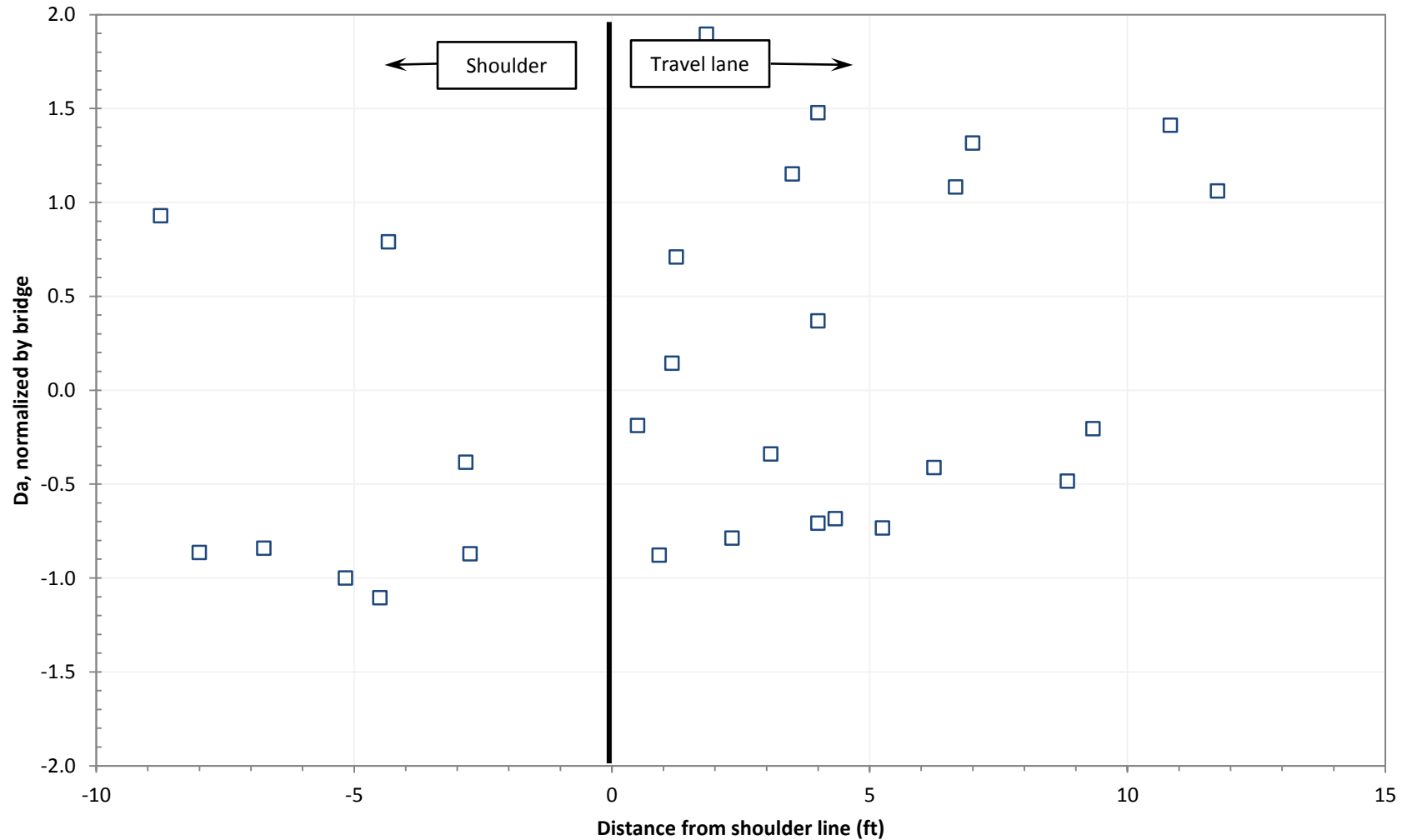


Figure 68. Apparent diffusion coefficient, D_a , versus distance from shoulder line. Positive values in distance indicate that the sample was obtained in the travel lane, and negative values indicate the sample was obtained from the shoulder.

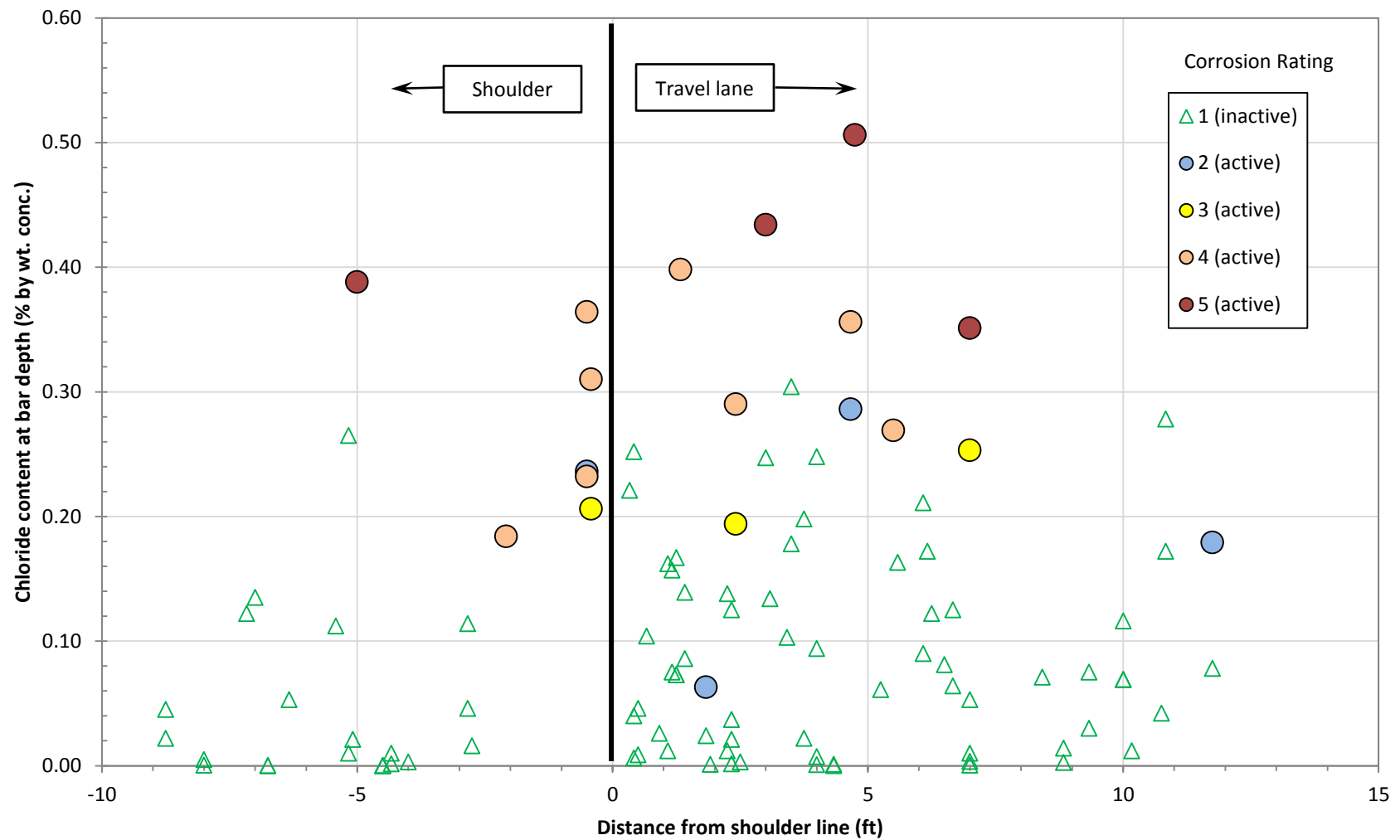


Figure 69. Effective chloride content at bar depth versus distance from shoulder line. Positive values in distance indicate that the sample was obtained in the travel lane, and negative values indicate the sample was obtained from the shoulder.

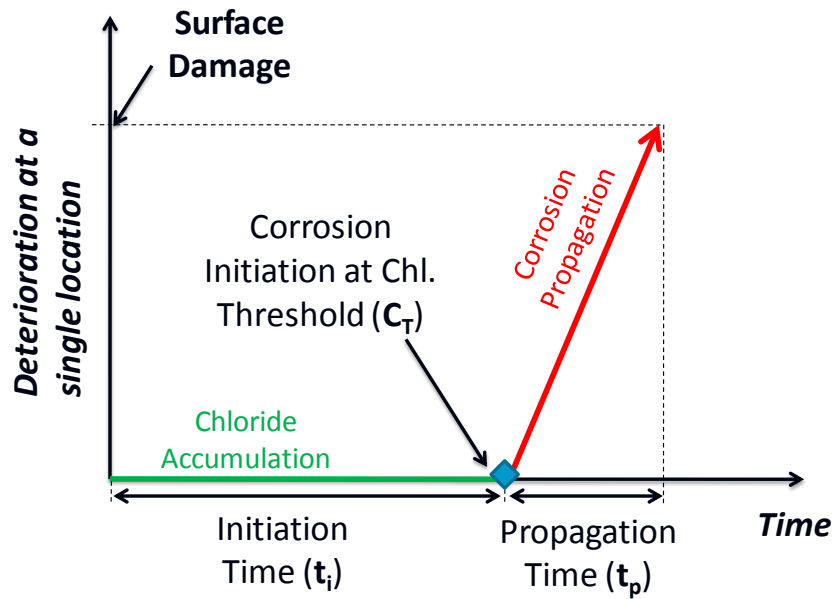


Figure 70. Corrosion sequence (adapted from Tuutti 1982).

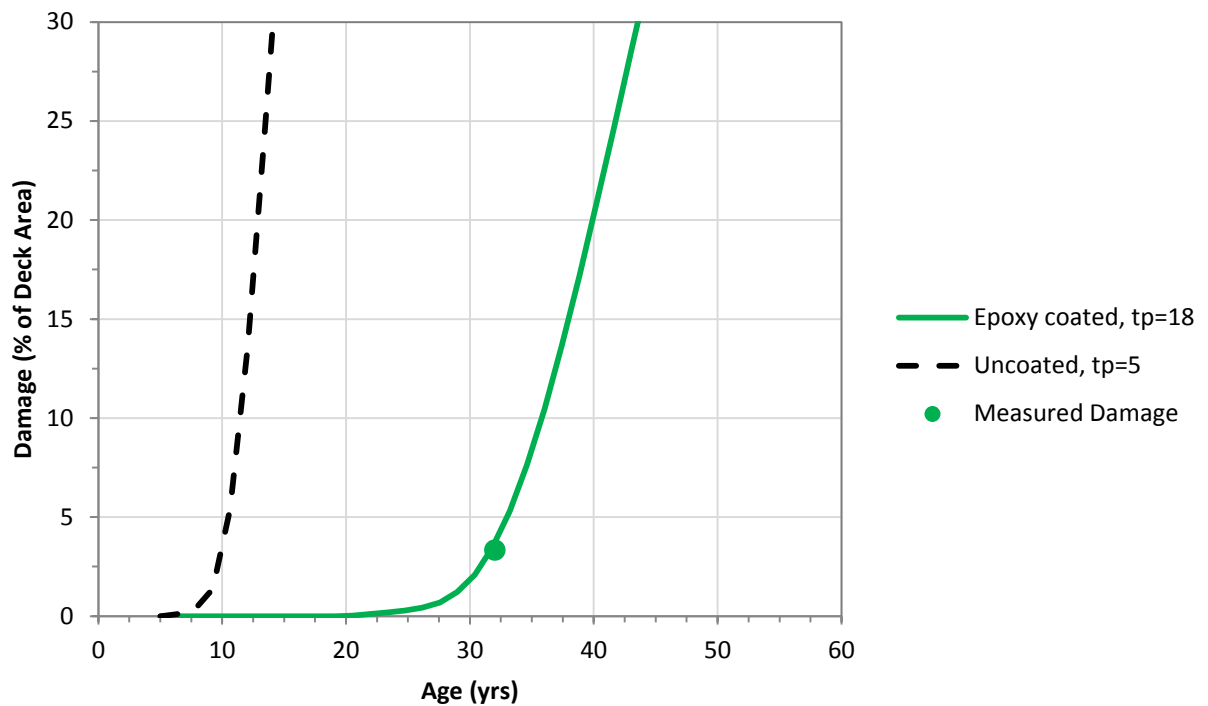


Figure 71. Projected damage development for Iowa 17.

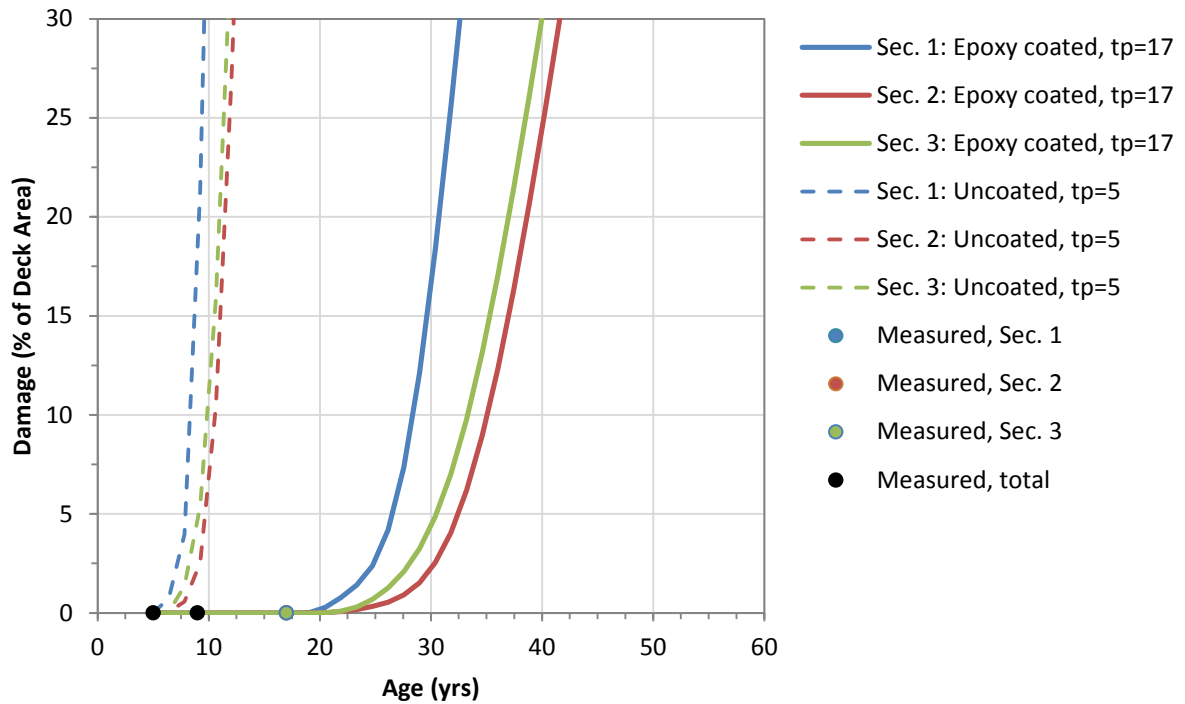


Figure 72. Projected damage development for US 218 (includes previous surveys by WJE and others).

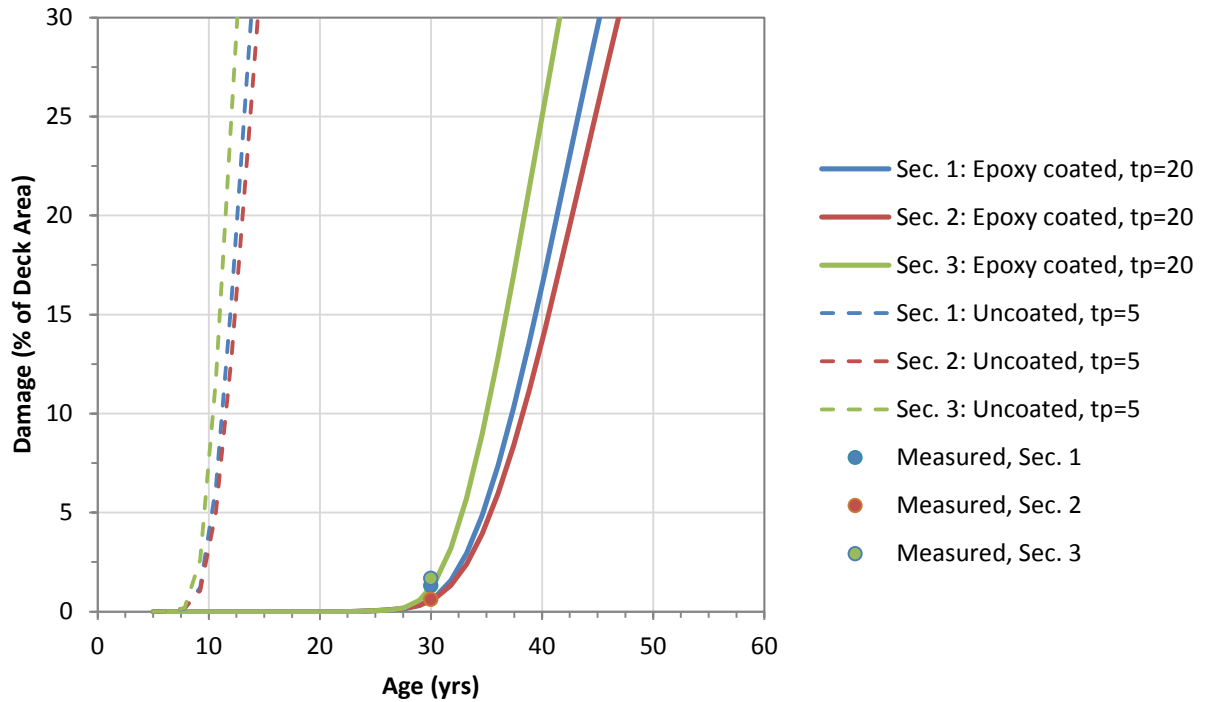


Figure 73. Projected damage development for Iowa 150.

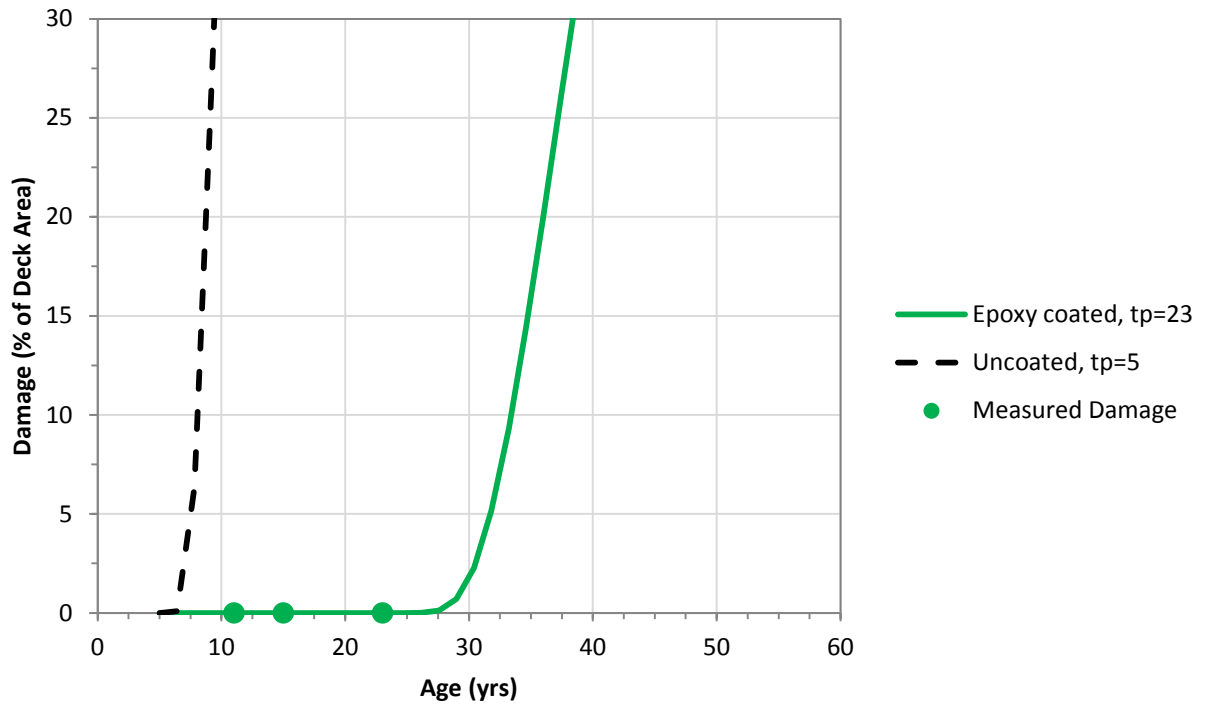


Figure 74. Projected damage development for Iowa 13 (includes previous surveys by WJE and others).

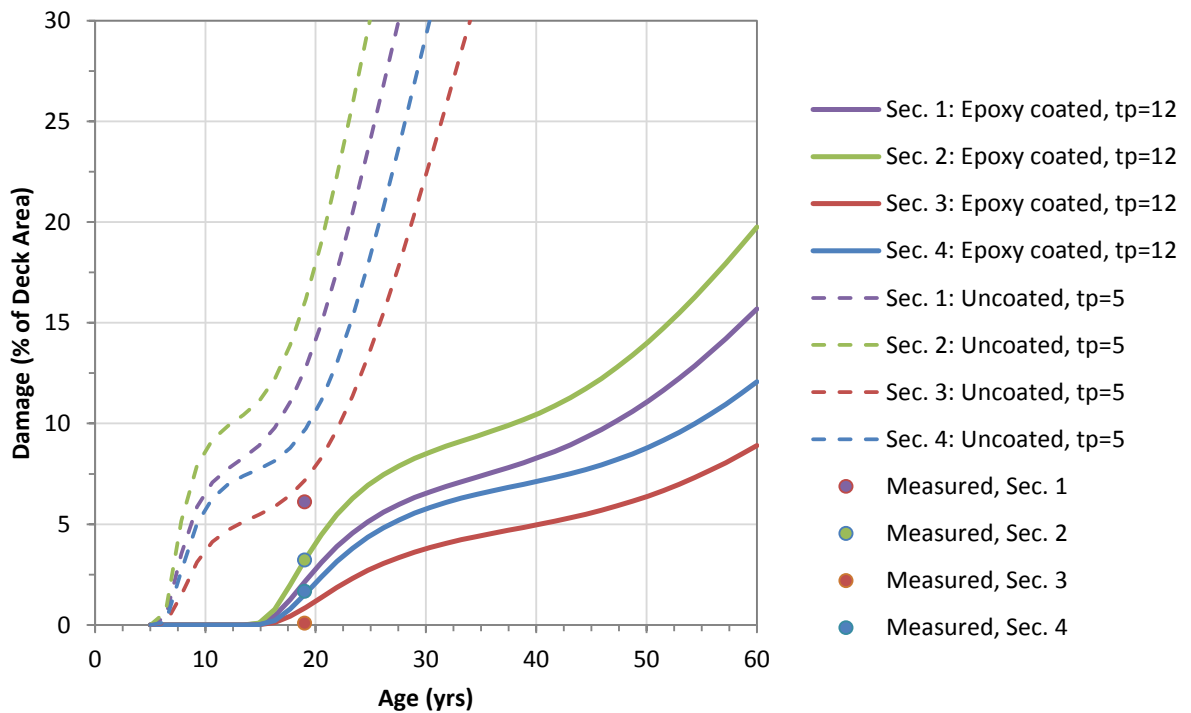


Figure 75. Projected damage development for US 30.

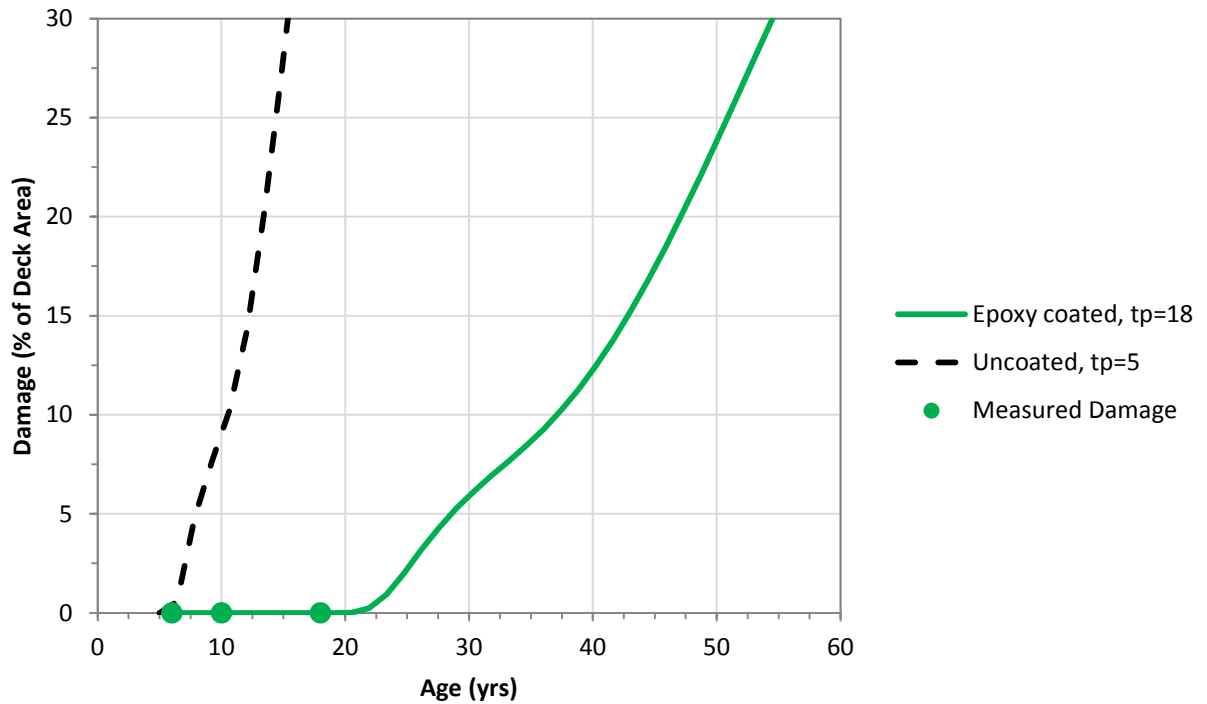


Figure 76. Projected damage development for US 18 (includes previous surveys by WJE and others).

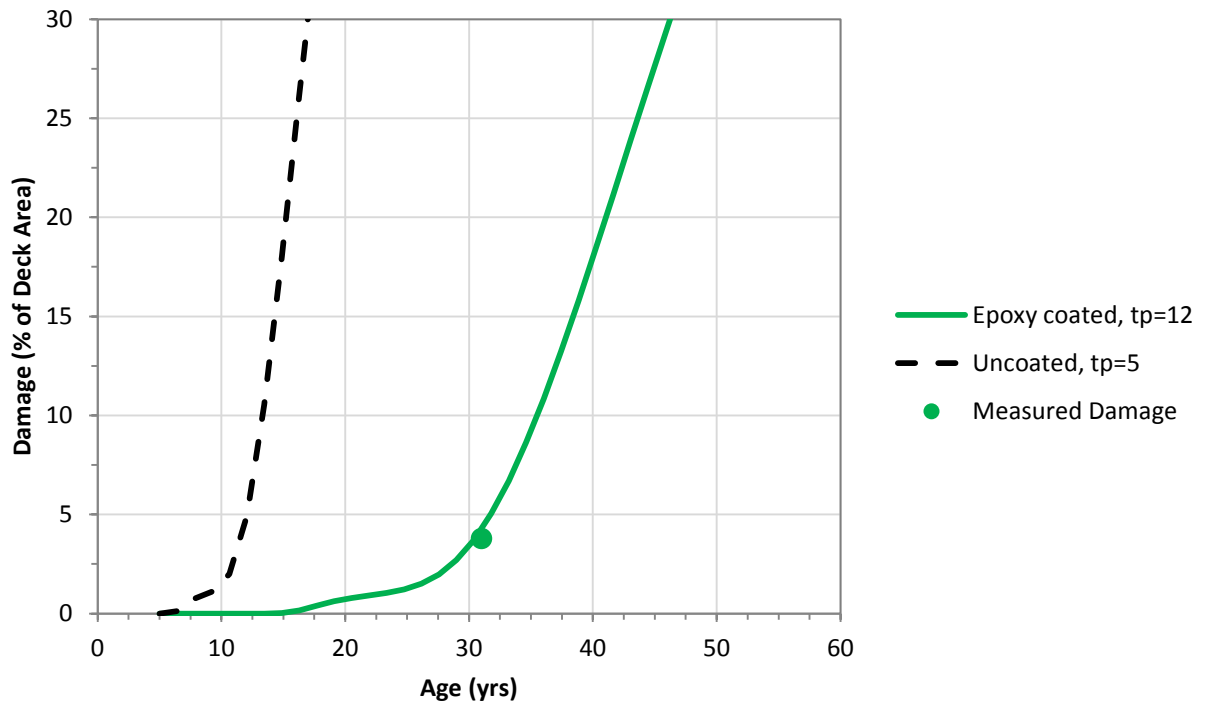


Figure 77. Projected damage development for Southbound US 65.

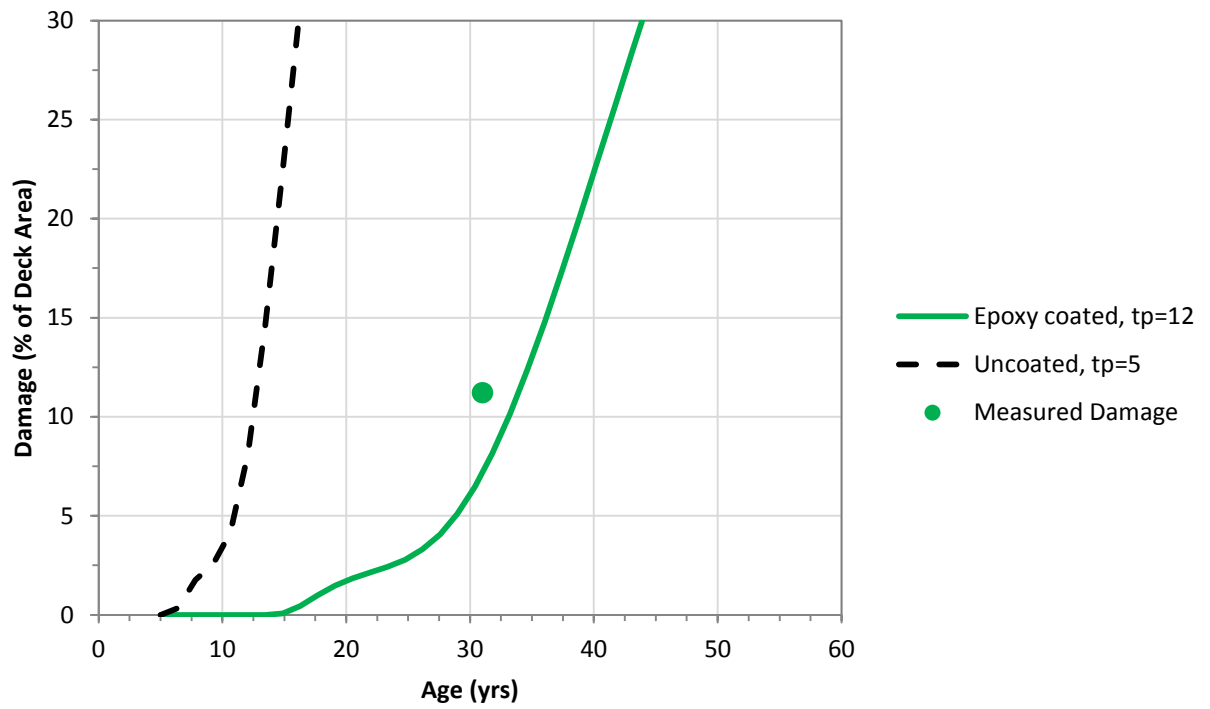


Figure 78. Projected damage development for Northbound US 65.

Appendix A

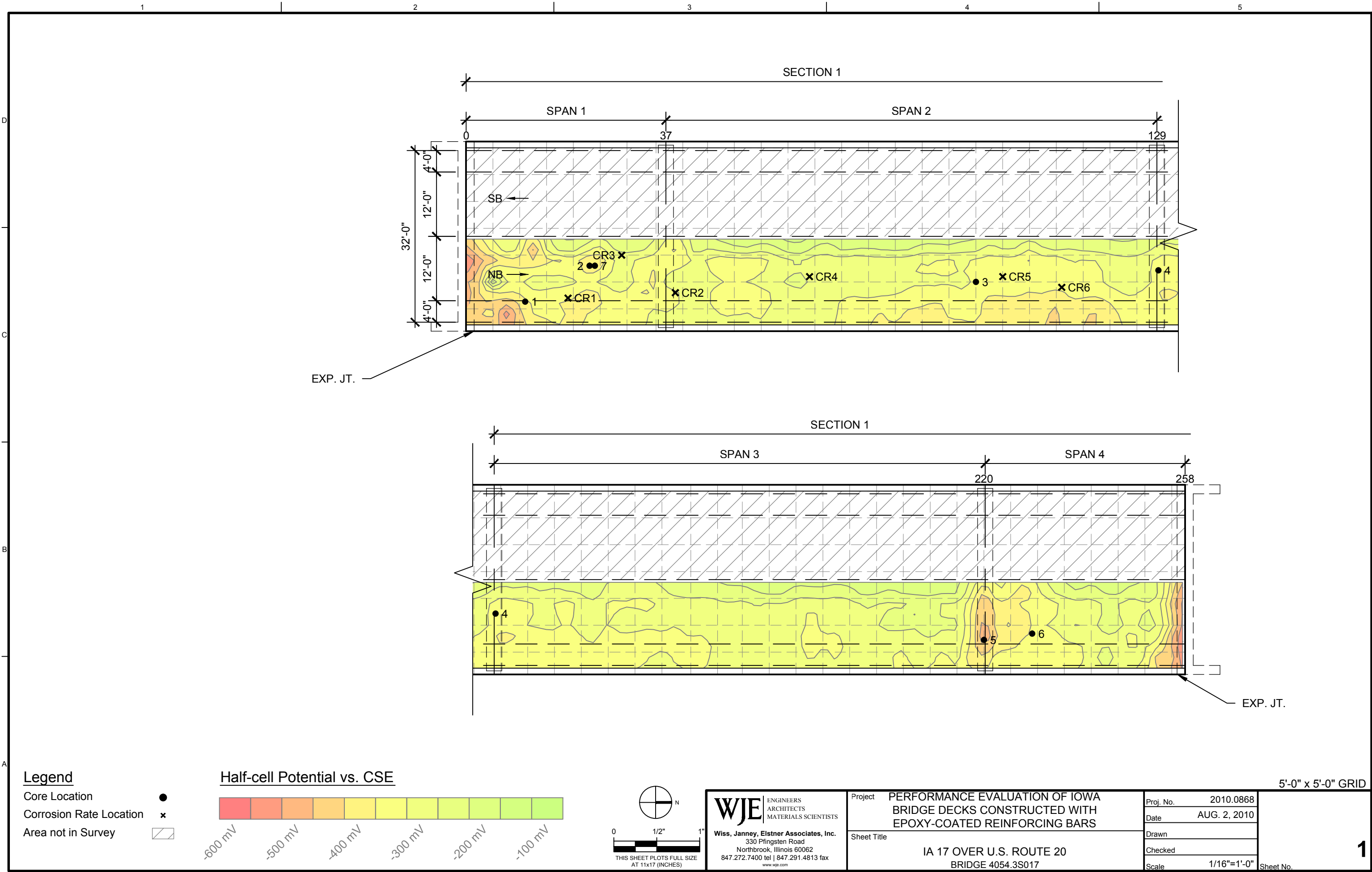
Field Investigation Results

Drawings - HCP Contours, Core and Ground Locations

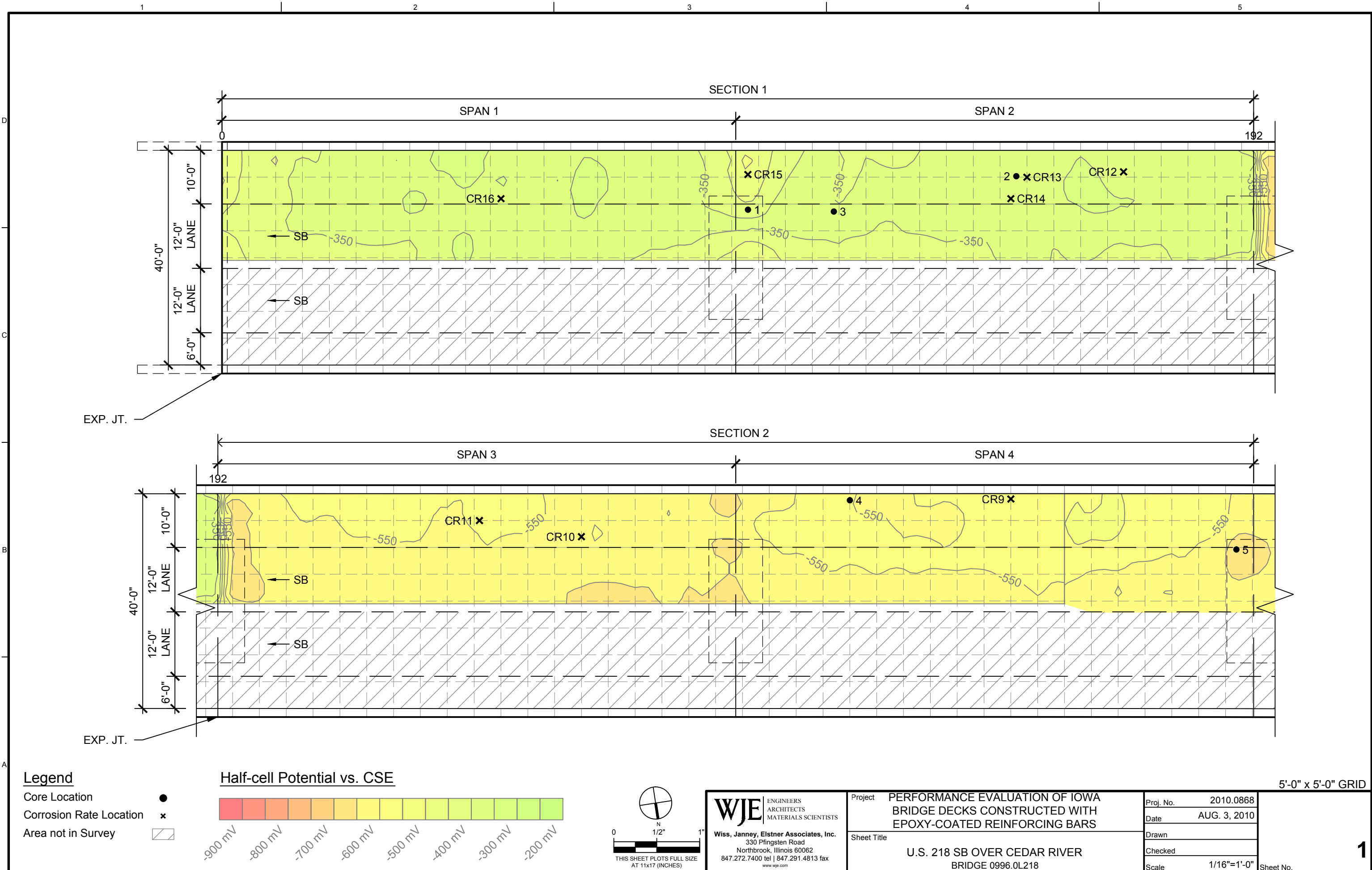
Tables - Corrosion Rate Measurements

Graphs - Cover Measurement (GPR) Distributions

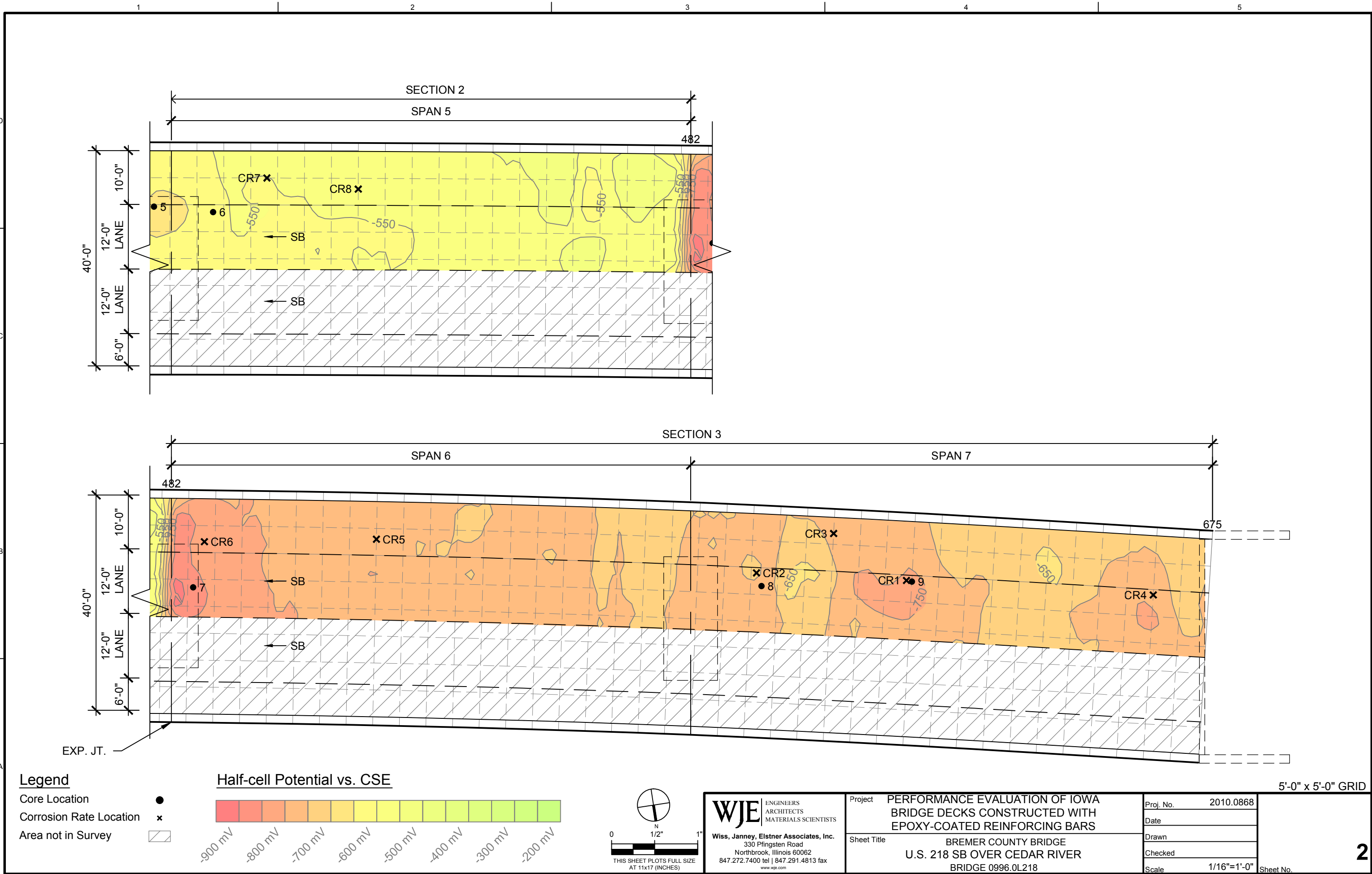
© Copyright 2011 All rights reserved. No part of this document may be reproduced in any form or by any means without permission from Wiss, Janney, Elstner Associates, Inc. (WJE). WJE disclaims any responsibility for its unauthorized use.



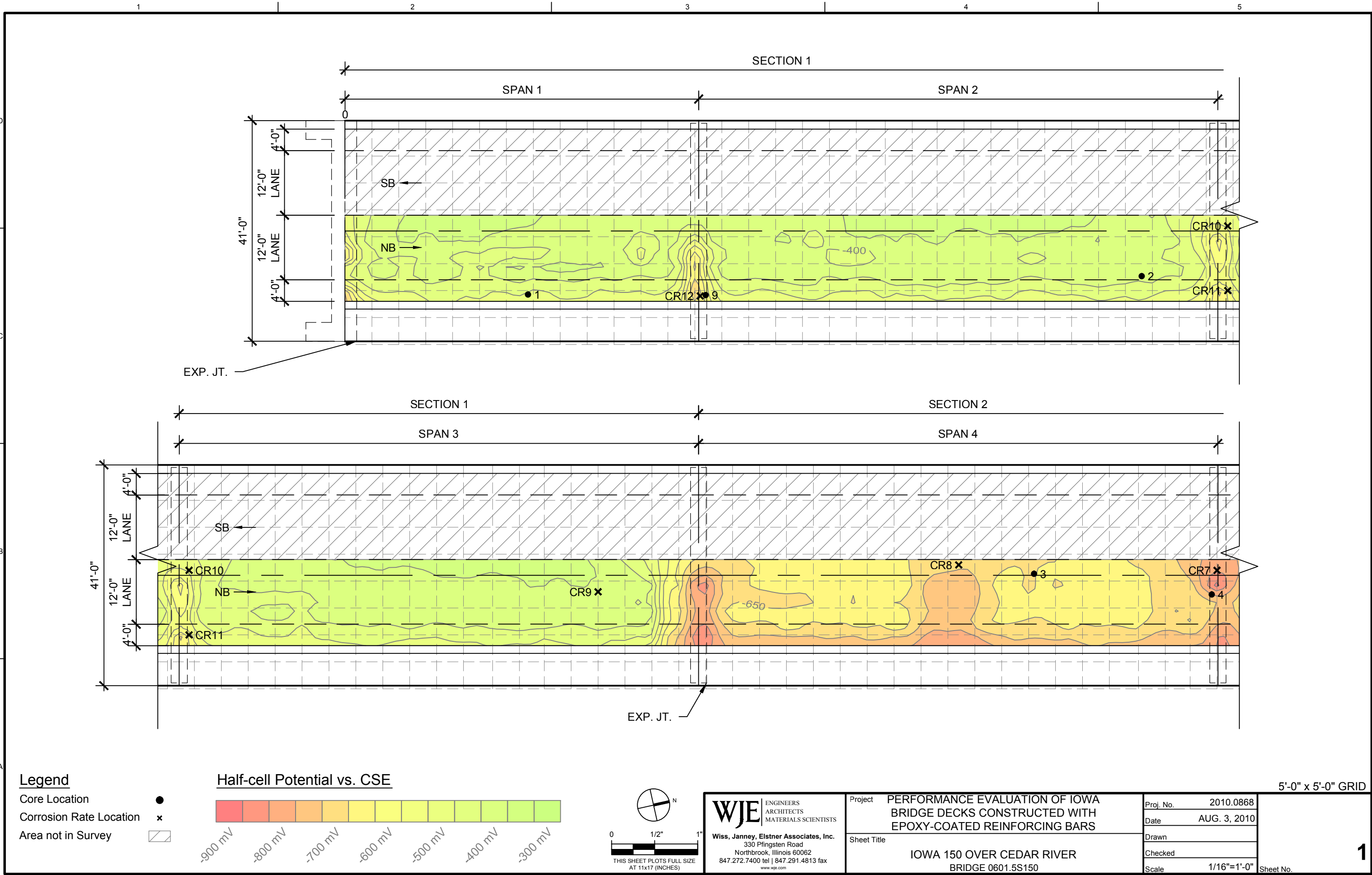
© Copyright 2011 All rights reserved. No part of this document may be reproduced in any form or by any means without permission from Wiss, Janney, Elstner Associates, Inc. (WJE). WJE disclaims any responsibility for its unauthorized use.



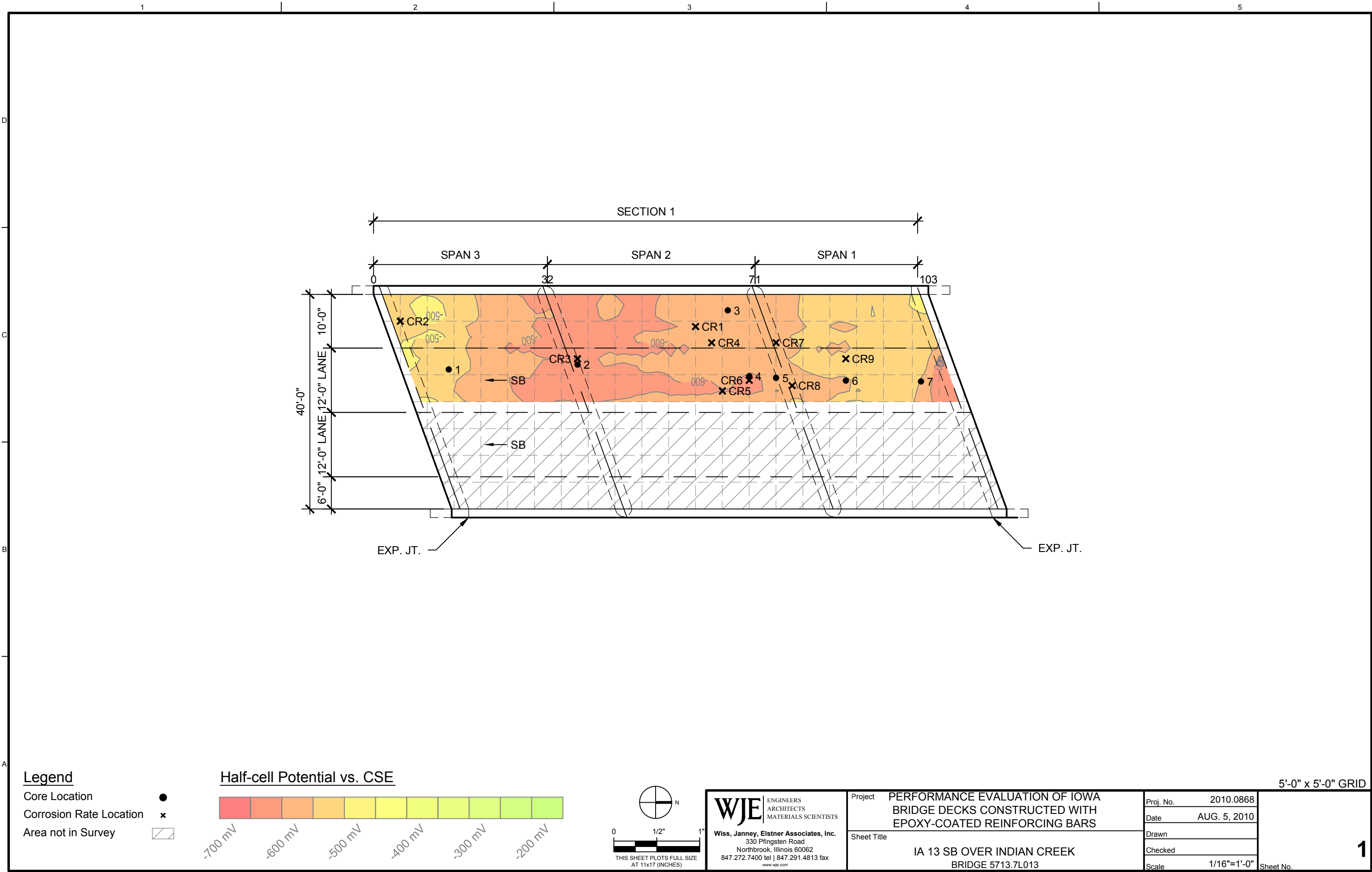
© Copyright 2011 All rights reserved. No part of this document may be reproduced in any form or by any means without permission from Wiss, Janney, Elstner Associates, Inc. (WJE). WJE disclaims any responsibility for its unauthorized use.



© Copyright 2011 All rights reserved. No part of this document may be reproduced in any form or by any means without permission from Wiss, Janney, Elstner Associates, Inc. (WJE). WJE disclaims any responsibility for its unauthorized use.



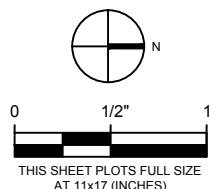
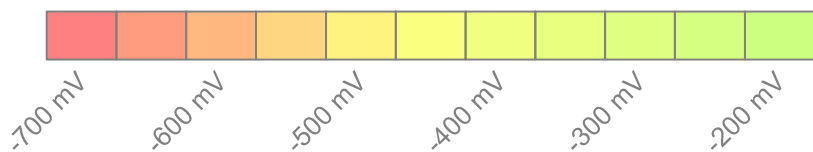
© Copyright 2011. All rights reserved. No part of this document may be reproduced in any form or by any means without permission from Wiss, Janney, Elstner Associates, Inc. (WJE). WJE disclaims any responsibility for its unauthorized use.



Legend

- Core Location ●
- Corrosion Rate Location x
- Area not in Survey ▨

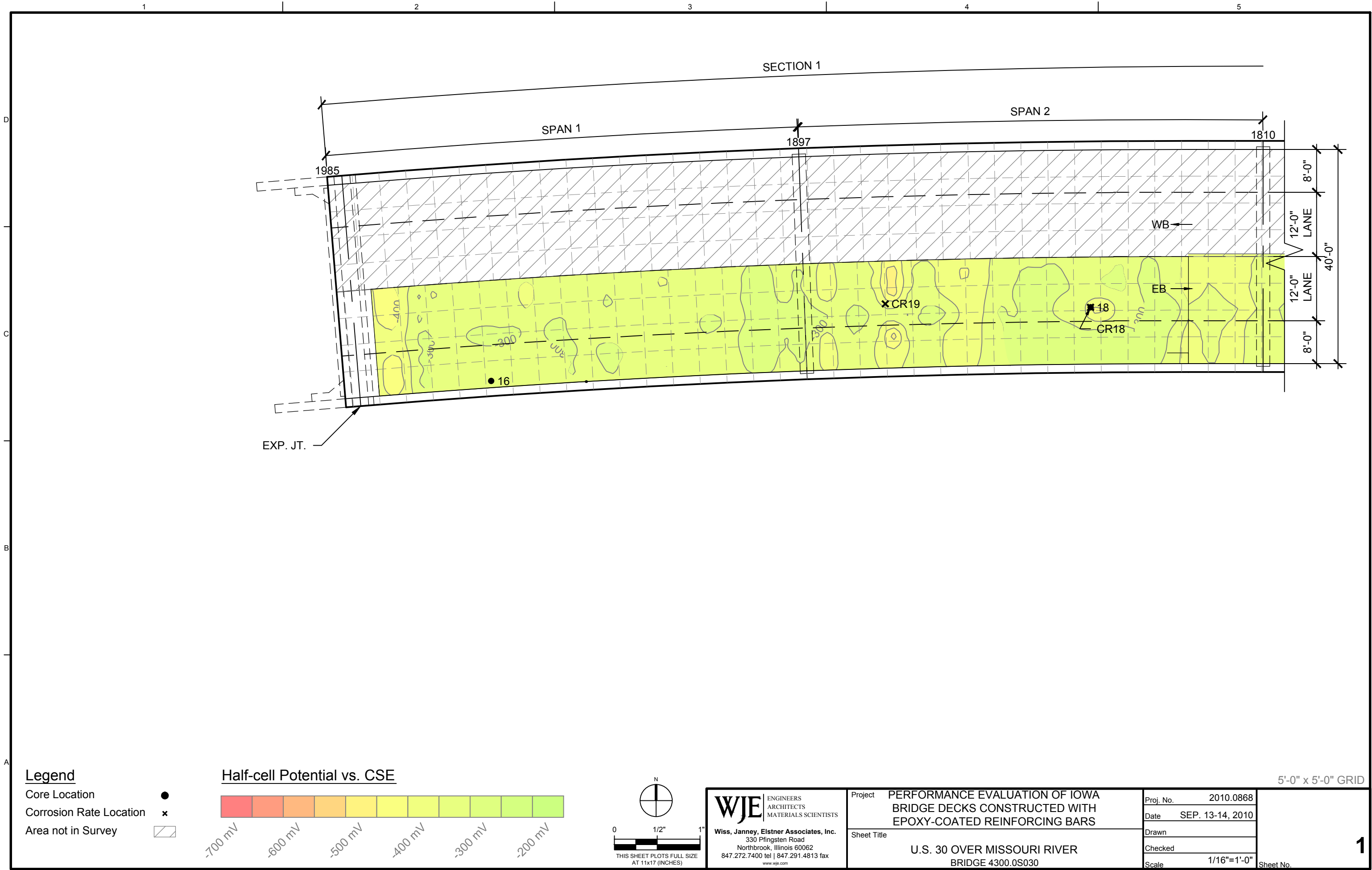
Half-cell Potential vs. CSE



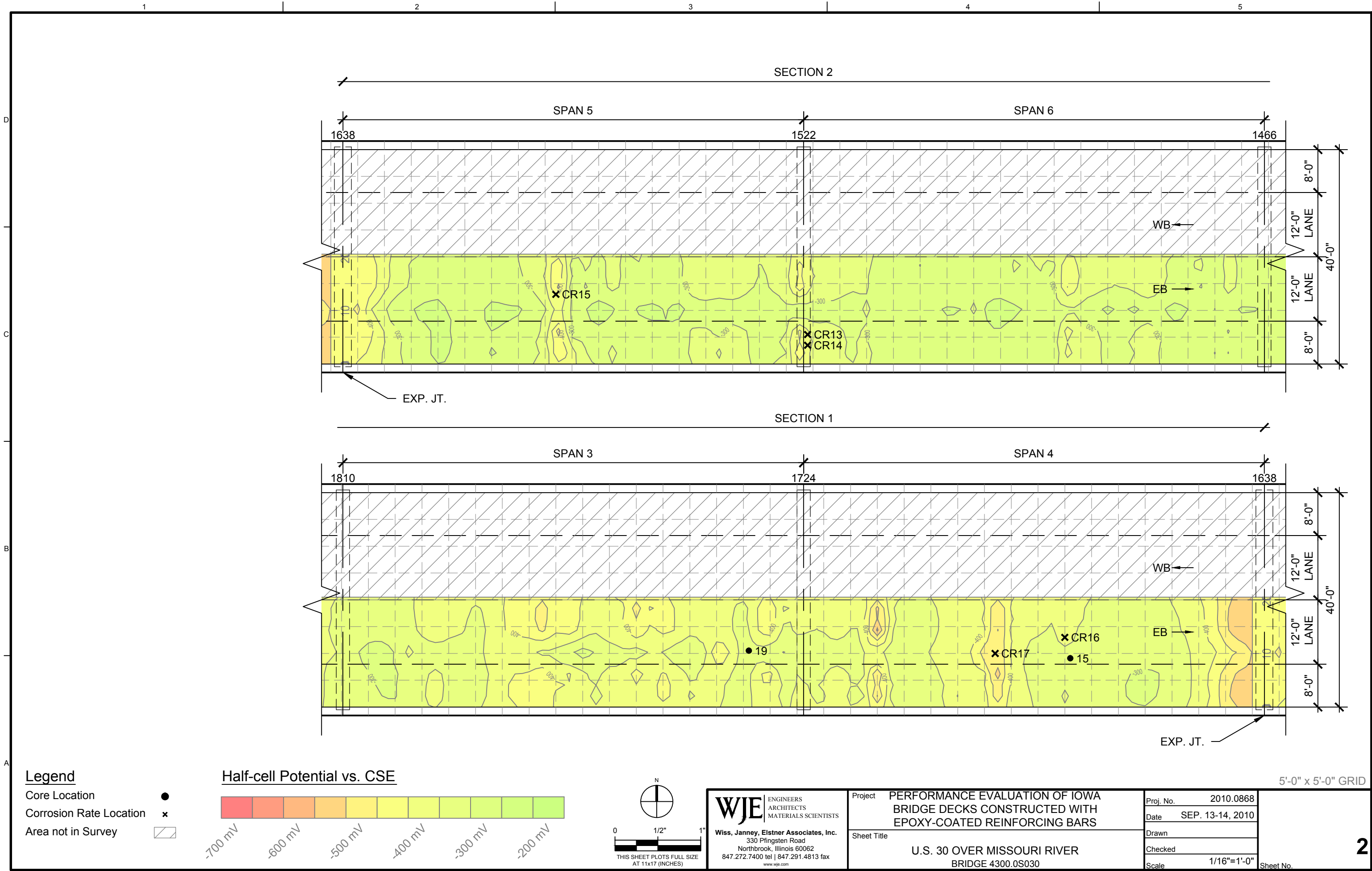
WJE ENGINEERS
ARCHITECTS
MATERIALS SCIENTISTS
Wiss, Janney, Elstner Associates, Inc.
330 Pfingsten Road
Northbrook, Illinois 60062
847.272.7400 tel | 847.291.4813 fax
www.wje.com

Project	PERFORMANCE EVALUATION OF IOWA BRIDGE DECKS CONSTRUCTED WITH EPOXY-COATED REINFORCING BARS		Proj. No.	2010.0868	Sheet No. 1
			Date	AUG. 5, 2010	
			Drawn		
			Checked		
Sheet Title		IA 13 SB OVER INDIAN CREEK BRIDGE 5713.7L013		Scale	1/16"=1'-0"

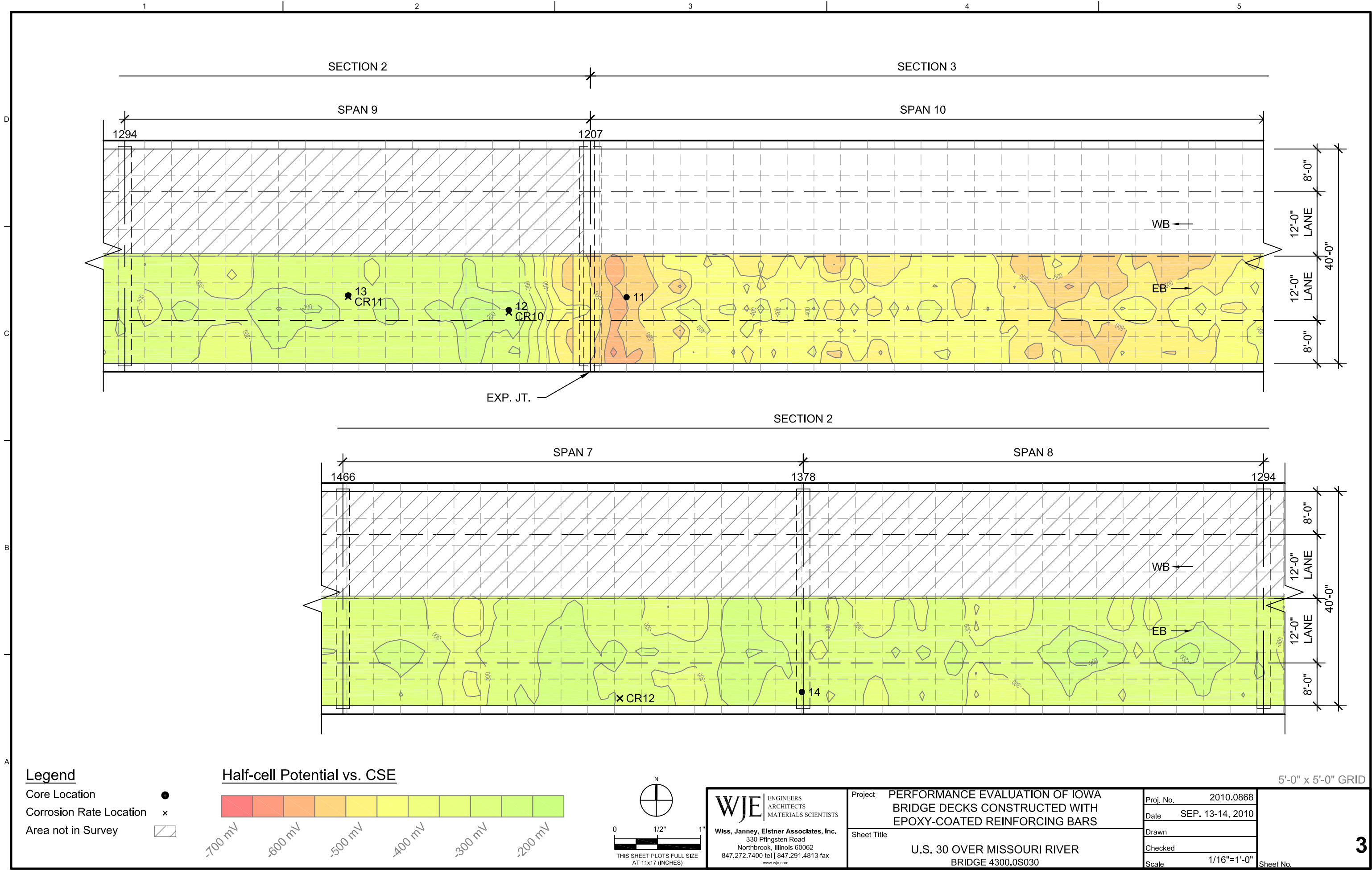
© Copyright 2011 All rights reserved. No part of this document may be reproduced in any form or by any means without permission from Wiss, Janney, Elstner Associates, Inc. (WJE). WJE disclaims any responsibility for its unauthorized use.



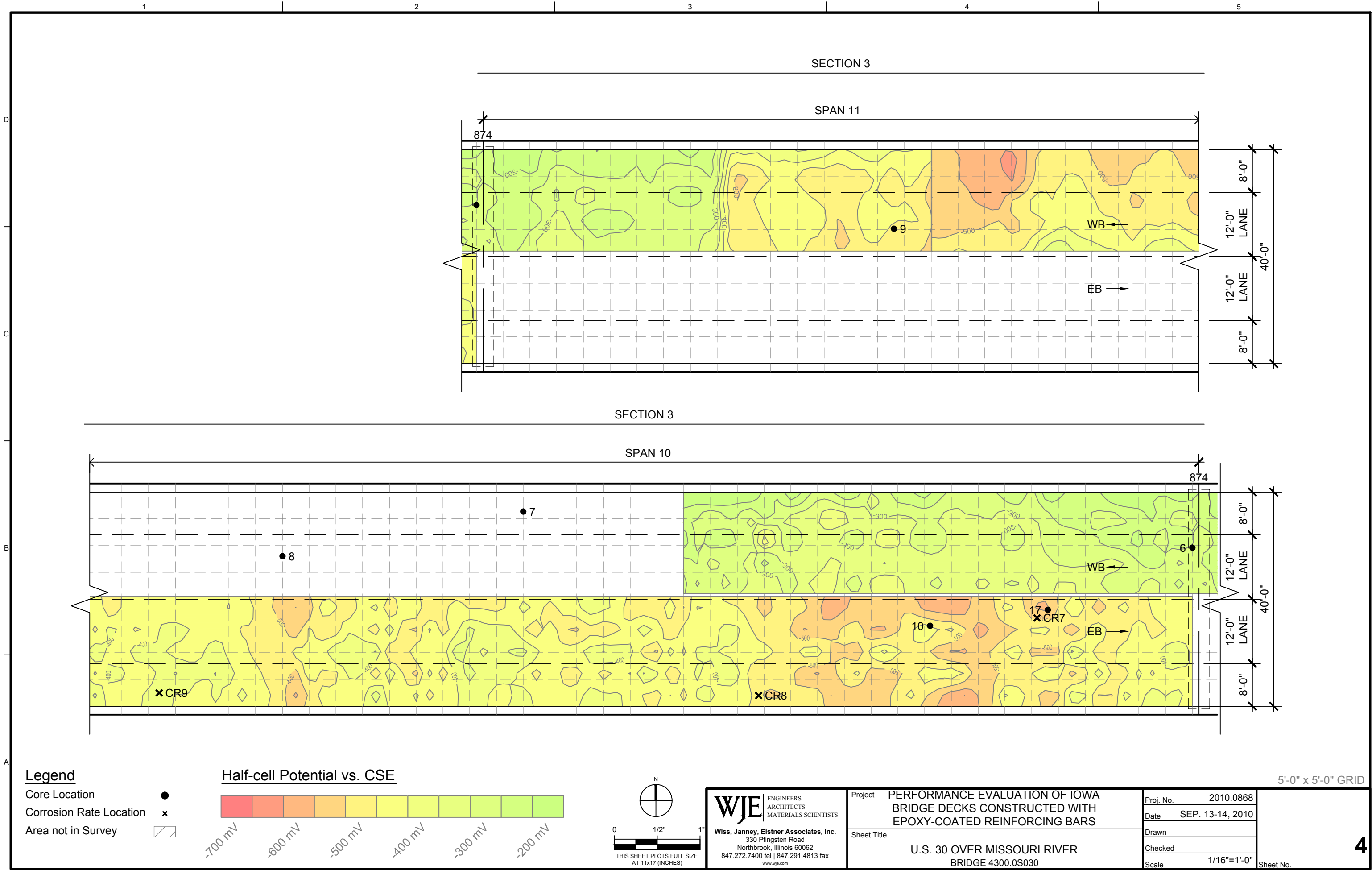
© Copyright 2011 All rights reserved. No part of this document may be reproduced in any form or by any means without permission from Wiss, Janney, Elstner Associates, Inc. (WJE). WJE disclaims any responsibility for its unauthorized use.



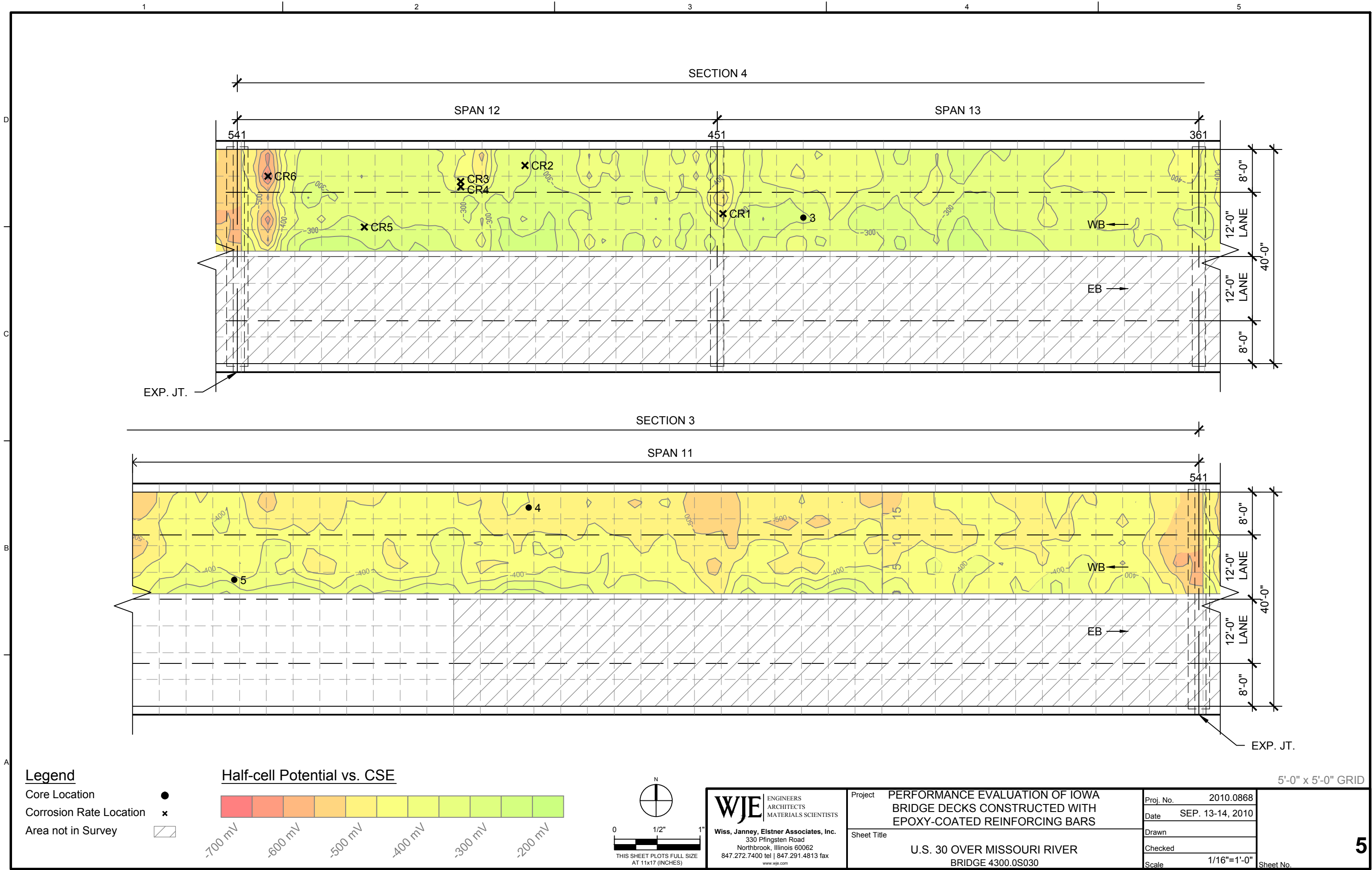
© Copyright 2011 All rights reserved. No part of this document may be reproduced in any form or by any means without permission from Wiss, Janney, Elstner Associates, Inc. (WJE). WJE disclaims any responsibility for its unauthorized use.



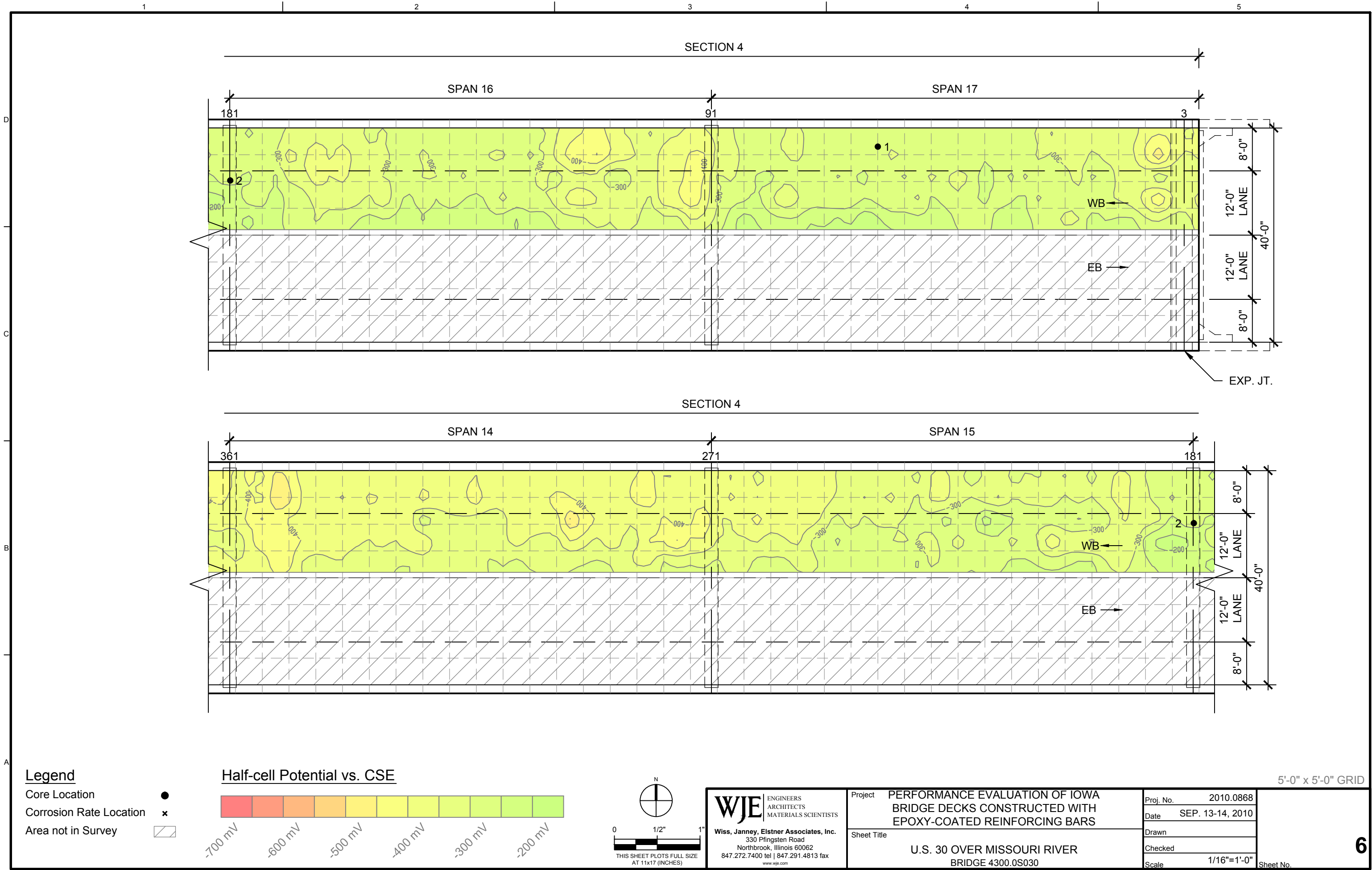
© Copyright 2011 All rights reserved. No part of this document may be reproduced in any form or by any means without permission from Wiss, Janney, Elstner Associates, Inc. (WJE). WJE disclaims any responsibility for its unauthorized use.



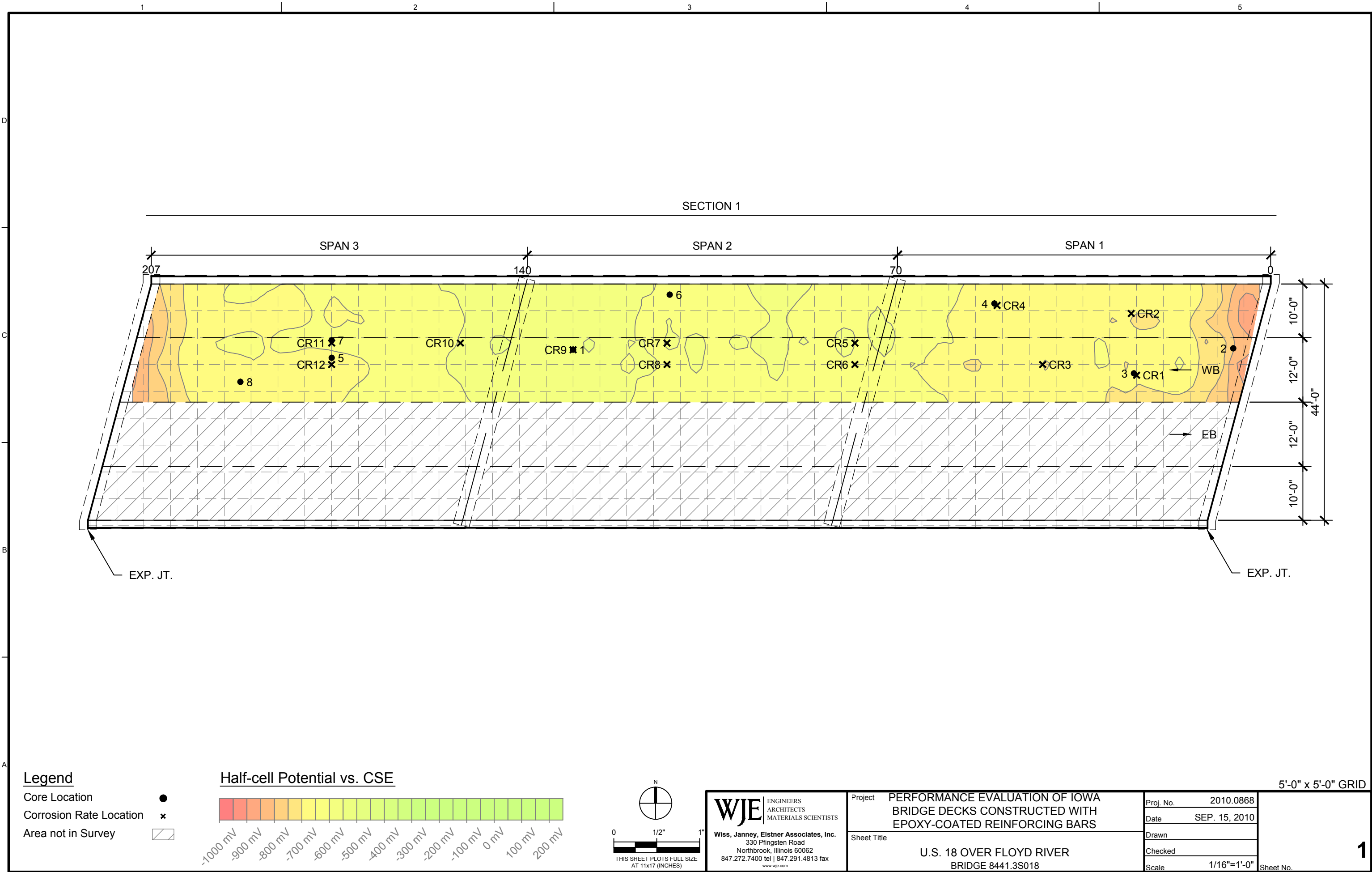
© Copyright 2011 All rights reserved. No part of this document may be reproduced in any form or by any means without permission from Wiss, Janney, Elstner Associates, Inc. (WJE). WJE disclaims any responsibility for its unauthorized use.



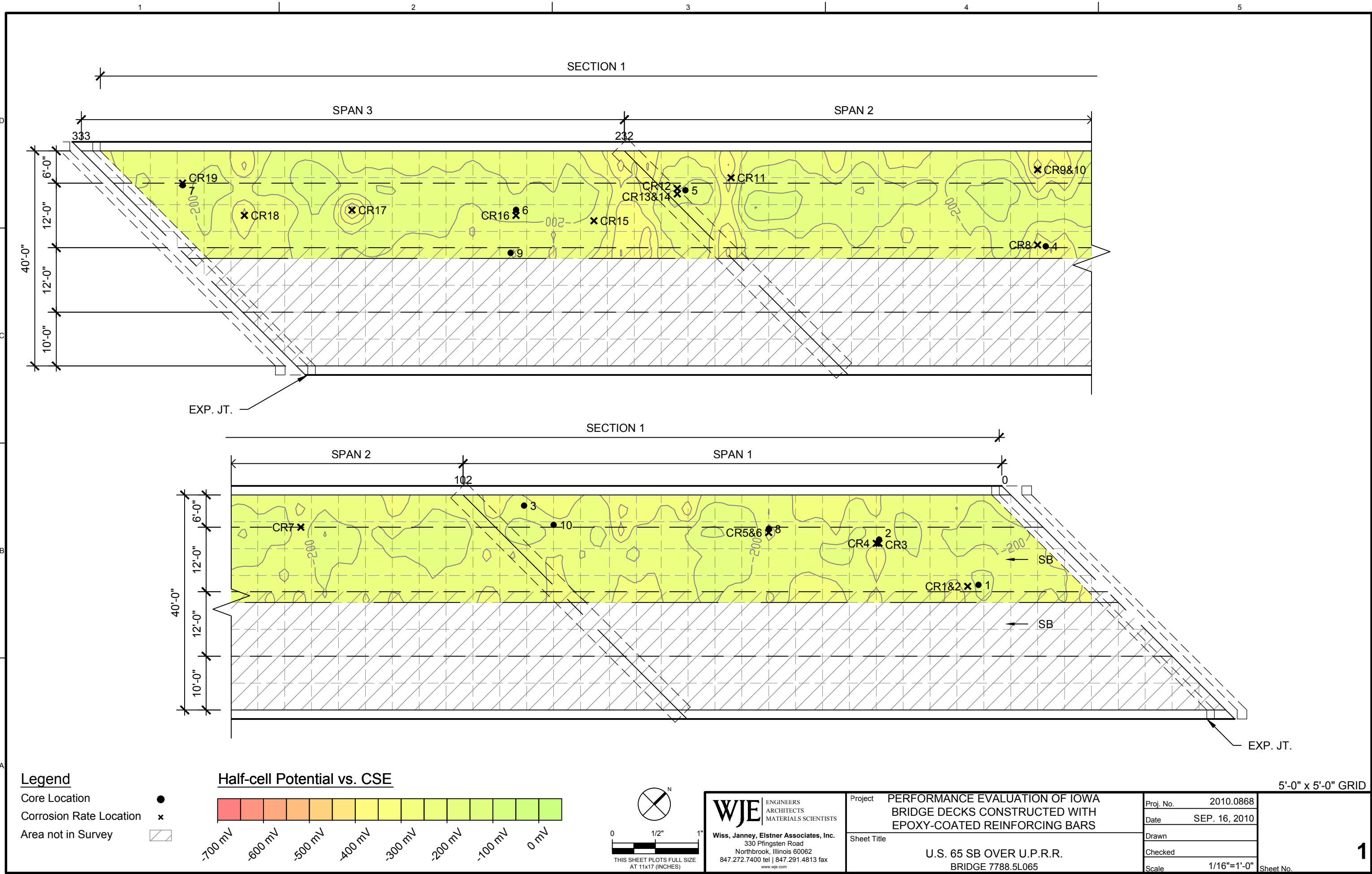
© Copyright 2011 All rights reserved. No part of this document may be reproduced in any form or by any means without permission from Wiss, Janney, Elstner Associates, Inc. (WJE). WJE disclaims any responsibility for its unauthorized use.



© Copyright 2010 All rights reserved. No part of this document may be reproduced in any form or by any means without permission from Wiss, Janney, Elstner Associates, Inc. (WJE). WJE disclaims any responsibility for its unauthorized use.



© Copyright 2010 All rights reserved. No part of this document may be reproduced in any form or by any means without permission from Wiss, Janney, Elstner Associates, Inc. (WJE). WJE disclaims any responsibility for its unauthorized use.



© Copyright 2010 All rights reserved. No part of this document may be reproduced in any form or by any means without permission from Wiss, Janney, Elstner Associates, Inc. (WJE). WJE disclaims any responsibility for its unauthorized use.

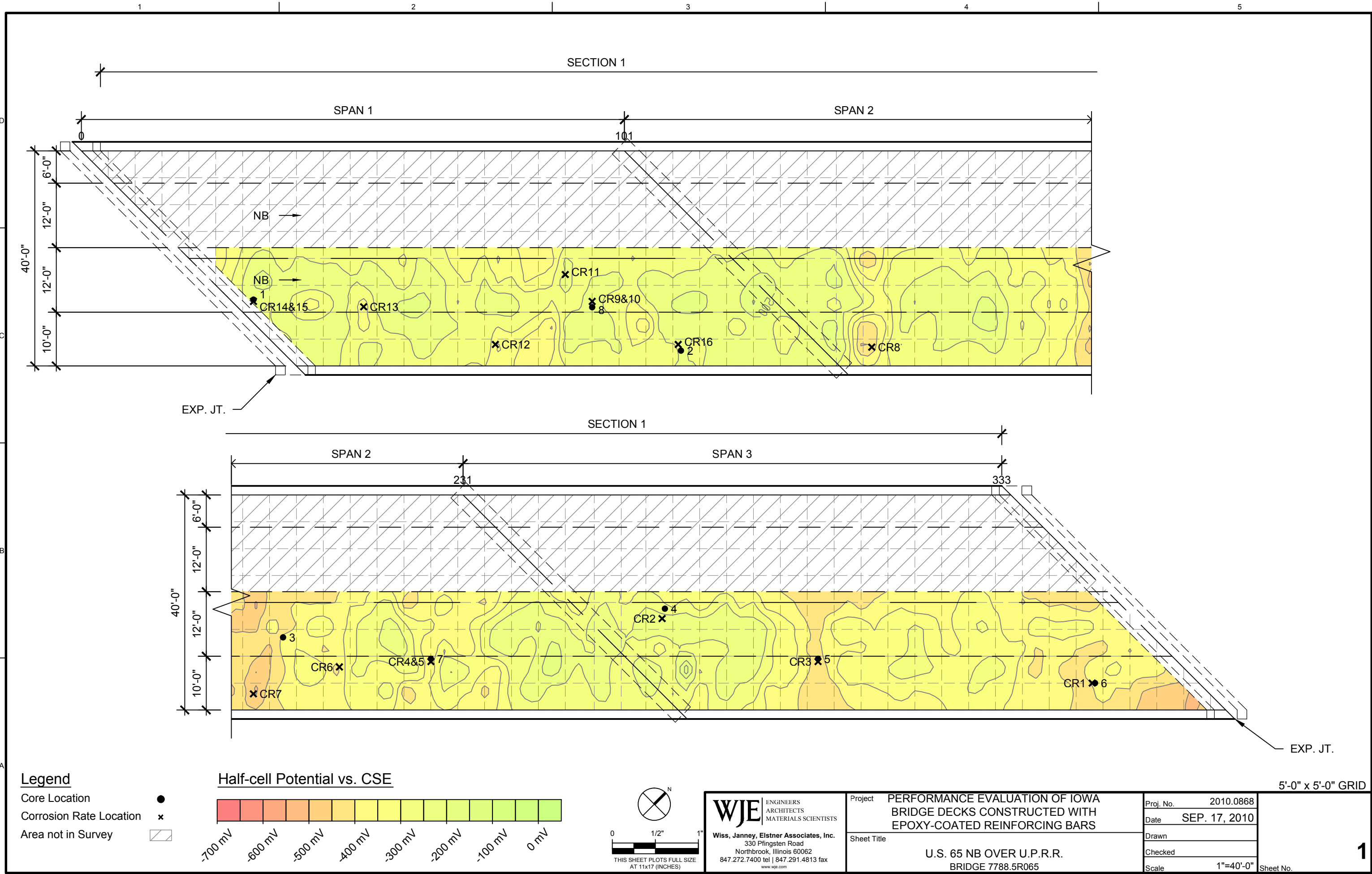


Table A.1. Corrosion Rate Measurements - IA 17

Location ID	E _{corr} (mV vs. SSC)	I _{corr} (μA/cm ²)	R (kΩ)	Applied Current (μA)
CR1	-369	3.25	2.7	100
CR2	-132	0.74	3.3	100
CR3	-137	3.02	3.8	100
CR4	-69	1.33	5.6	400
CR5	-165	2.59	4.1	400

Table A.2. Corrosion Rate Measurements - US 218 SB

Location ID	E _{corr} (mV vs. SSC)	I _{corr} (μA/cm ²)	R (kΩ)	Applied Current (μA)
CR1	-662	0.59	8.1	200
CR2	-656	0.88	5.3	100
CR3	-587	0.65	4.6	100
CR4	-638	0.40	4.9	100
CR5	-572	0.18	3.9	100
CR6	-662	0.17	3.5	100
CR7	-347	0.79	1.9	100
CR8	-308	1.14	2.2	100
CR9	-282	0.46	3.7	100
CR10	-422	0.76	2.5	100
CR11	-356	1.00	2.2	100
CR12	-353	1.43	4.7	400
CR13	-454	0.10	5.1	100
CR14	-481	0.09	5.0	100
CR15	-528	10.8	1.2	100
CR16	-363	5.03	3.2	100

Table A.3. Corrosion Rate Measurements - IA 150

Location ID	E _{corr} (mV vs. SSC)	I _{corr} (μA/cm ²)	R (kΩ)	Applied Current (μA)
CR1	-388	0.93	5.7	400
CR2	-183	0.65	6.1	400
CR3	-297	1.65	3.5	100
CR4	-443	0.34	3.3	100
CR5	-417	0.32	3.1	100
CR6	-420	0.21	3.2	100
CR7	-495	0.26	1.7	100
CR8	-529	0.22	3.5	100
CR9	-266	4.12	4.0	100
CR10	-364	10.2	0.9	400
CR11	-568	8.48	1.1	200
CR12	-428	7.18	3.0	200

Table A.4. Corrosion Rate Measurements - IA 13 SB

Location ID	E _{corr} (mV vs. SSC)	I _{corr} (μA/cm ²)	R (kΩ)	Applied Current (μA)
CR1	-370	2.66	2.0	100
CR2	-274	1.44	1.6	100
CR3	-407	1.92	1.5	100
CR4	-401	1.15	1.7	100
CR5	-427	2.34	2.0	100
CR6	-433	4.07	1.8	100
CR7	-430	1.81	1.7	100
CR8	-435	2.24	1.5	100
CR9	-400	2.61	1.9	100

Table A.5. Corrosion Rate Measurements - US 30

Location ID	E _{corr} (mV vs. SSC)	I _{corr} (μA/cm ²)	R (kΩ)	Applied Current (μA)
CR-1	-294	0.44	17	100
CR-2	-395	0.19	16	100
CR-3	-692	0.23	14	100
CR-4	-685	0.18	13	100
CR-5A	-403	0.18	15	100
CR-5B	-385	0.16	15	100
CR-6A	-722	0.20	13	100
CR-6B	-701	0.23	13	100
CR-6C	-712	0.22	13	100
CR-7	-293	1.79	4.6	100
CR-8	-382	4.79	2.8	150
CR-9	-333	0.63	8.4	300
CR-10	-59	1.82	11	300
CR-11	-245	4.33	3.0	300
CR-12	-481	0.14	11	100
CR-13	-390	0.11	10	100
CR-14	-392	0.12	12	100
CR-15	-300	0.11	11	100
CR-16	-134	0.55	13	100
CR-17	-385	12.0	0.8	300
CR-18	-363	0.31	2.0	100
CR-19	-148	0.24	10	100

Table A.6. Corrosion Rate Measurements - US 18

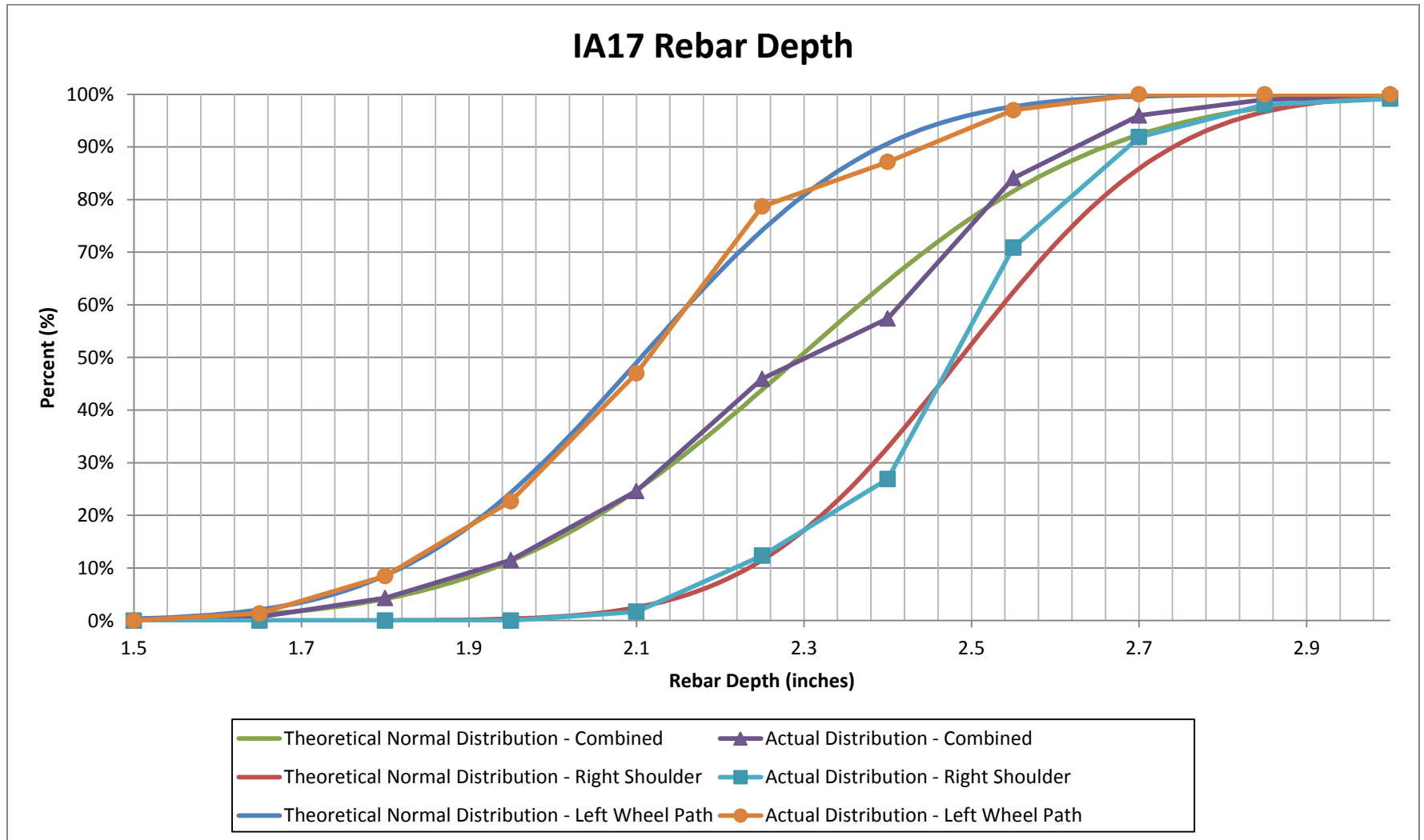
Location ID	E_{corr} (mV vs. SSC)	I_{corr} ($\mu\text{A}/\text{cm}^2$)	R (k Ω)	Applied Current (μA)
CR-1	-484	0.19	5.0	100
CR-2	-455	0.25	4.7	100
CR-3	-468	0.22	5.5	100
CR-4	-486	0.24	6.8	100
CR-5	-389	0.25	7.6	100
CR-6	-388	0.21	7.5	100
CR-7	-394	0.22	7.4	100
CR-8	-418	0.25	6.9	100
CR-9	-407	0.22	5.3	100
CR-10	-419	0.23	4.7	100
CR-11	-456	0.26	9.3	100
CR-12	-517	0.23	5.5	100

Table A.7. Corrosion Rate Measurements - US 65 SB

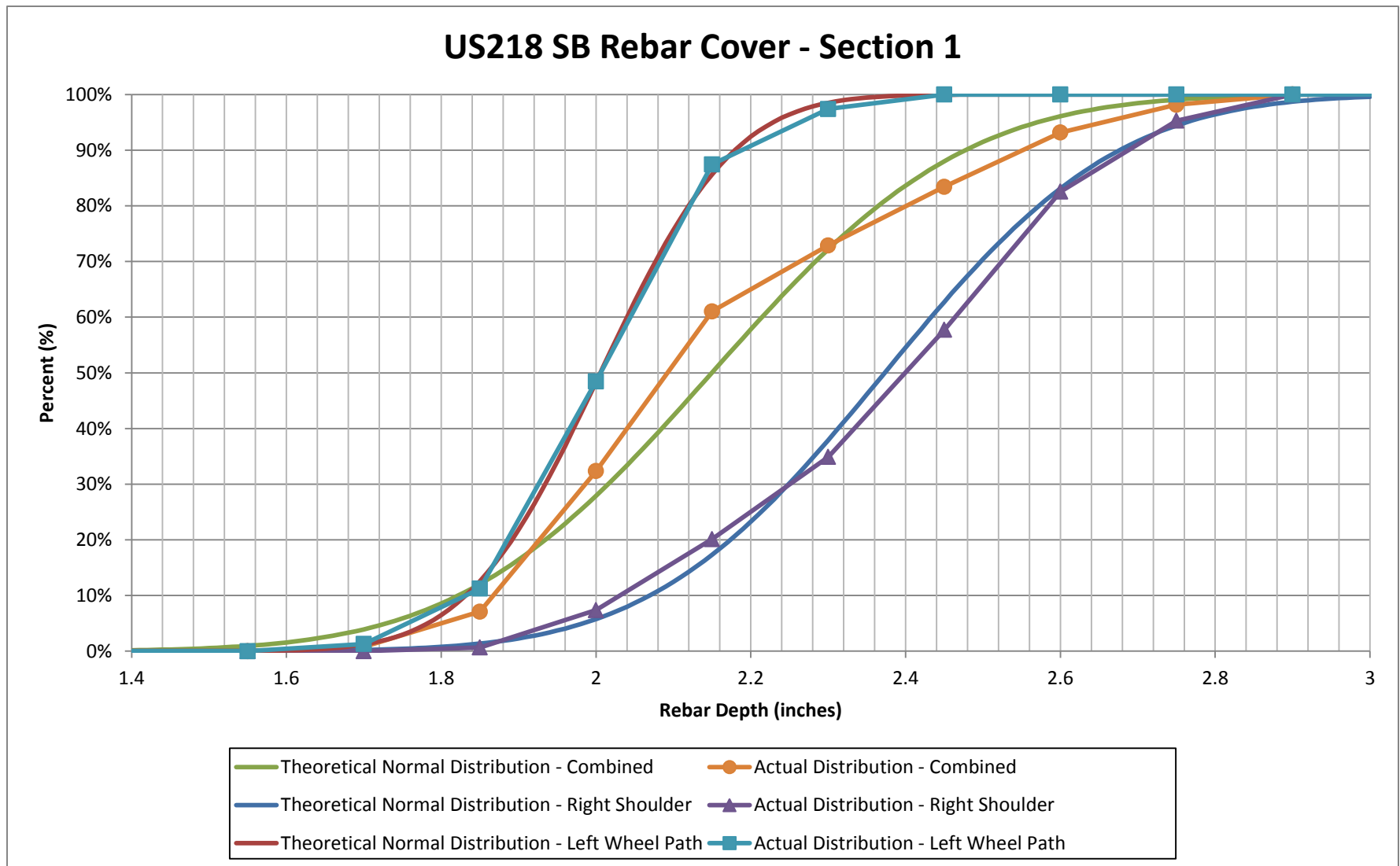
Location ID	E_{corr} (mV vs. SSC)	I_{corr} ($\mu\text{A}/\text{cm}^2$)	R (k Ω)	Applied Current (μA)
CR-1	-15	5.90	5.8	100
CR-2	-153	5.48	6.2	400
CR-3	-165	5.06	0.8	100
CR-4	-191	5.24	1.1	100
CR-5	-178	9.48	2.8	200
CR-6	-178	8.80	2.7	300
CR-7	-220	6.78	1.7	100
CR-8	-49	2.84	5.1	100
CR-9	-287	6.95	1.4	100
CR-10	-287	7.36	1.4	300
CR-11	-104	7.22	4.4	400
CR-12	-280	7.24	1.9	200
CR-13	-77	6.80	2.0	100
CR-14	-71	5.99	2.0	300
CR-15	-102	3.09	2.8	400
CR-16	-86	7.23	2.9	200
CR-17	-188	6.91	2.7	200
CR-18	-97	6.77	2.5	300
CR-19	-120	4.18	1.9	100

Table A.8. Corrosion Rate Measurements - US 65 NB

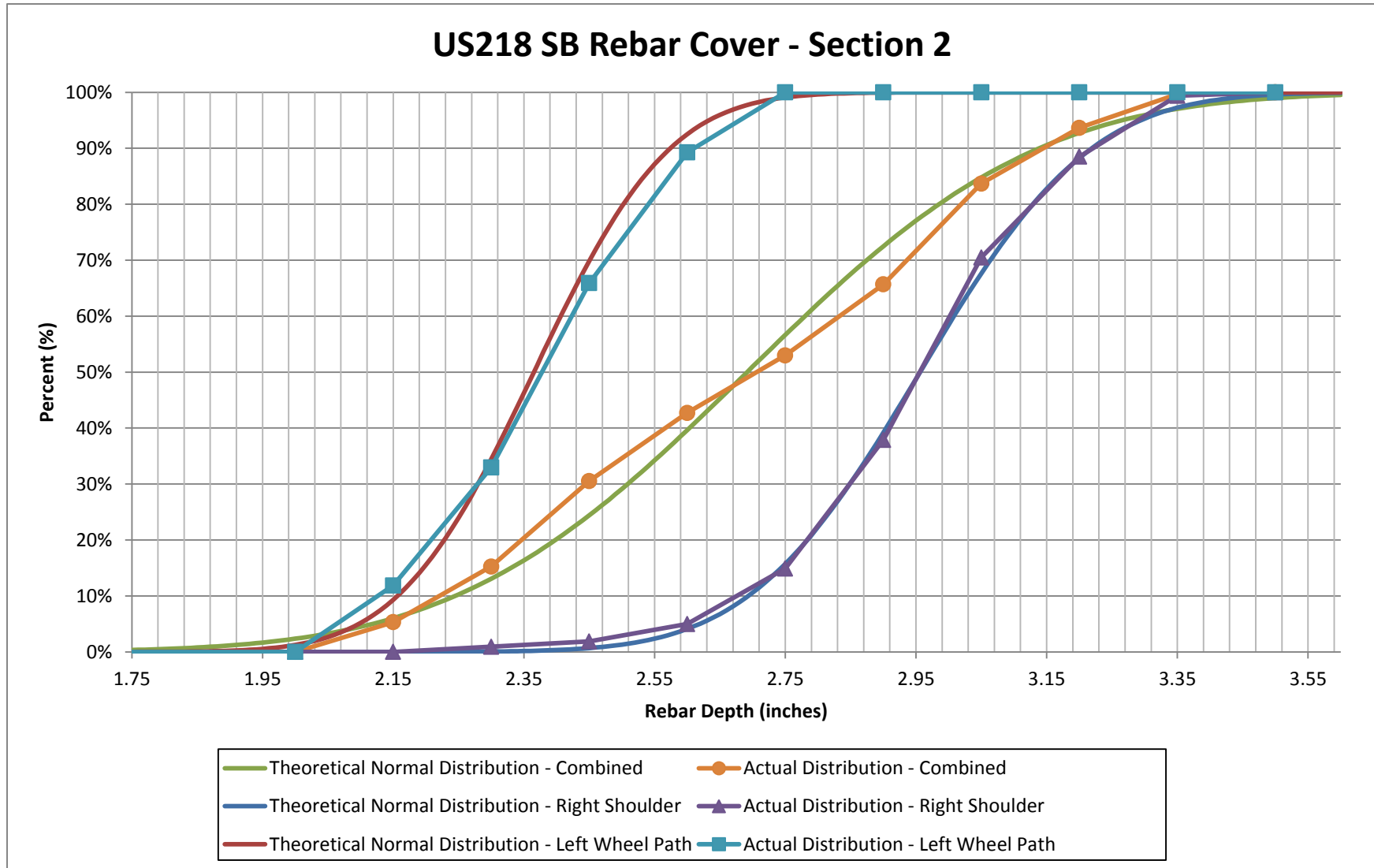
Location ID	E_{corr} (mV vs. SSC)	I_{corr} (μA/cm²)	R (kΩ)	Applied Current (μA)
CR-1	-320	7.05	1.7	100
CR-2	-213	0.54	7.4	400
CR-3	-280	2.11	2.8	400
CR-4	-362	4.97	1.6	100
CR-5	-362	9.55	1.6	300
CR-6	-454	5.46	3.0	100
CR-7	-469	9.12	1.9	100
CR-8	-424	7.91	0.8	100
CR-9	-103	3.55	4.2	100
CR-10	-100	5.03	4.9	300
CR-11	-123	3.42	5.6	300
CR-12	-285	6.66	2.0	100
CR-13	-218	7.84	1.9	100
CR-14	-122	7.55	4.6	100
CR-15	-119	5.59	4.5	300
CR-16	-129	6.14	3.9	300



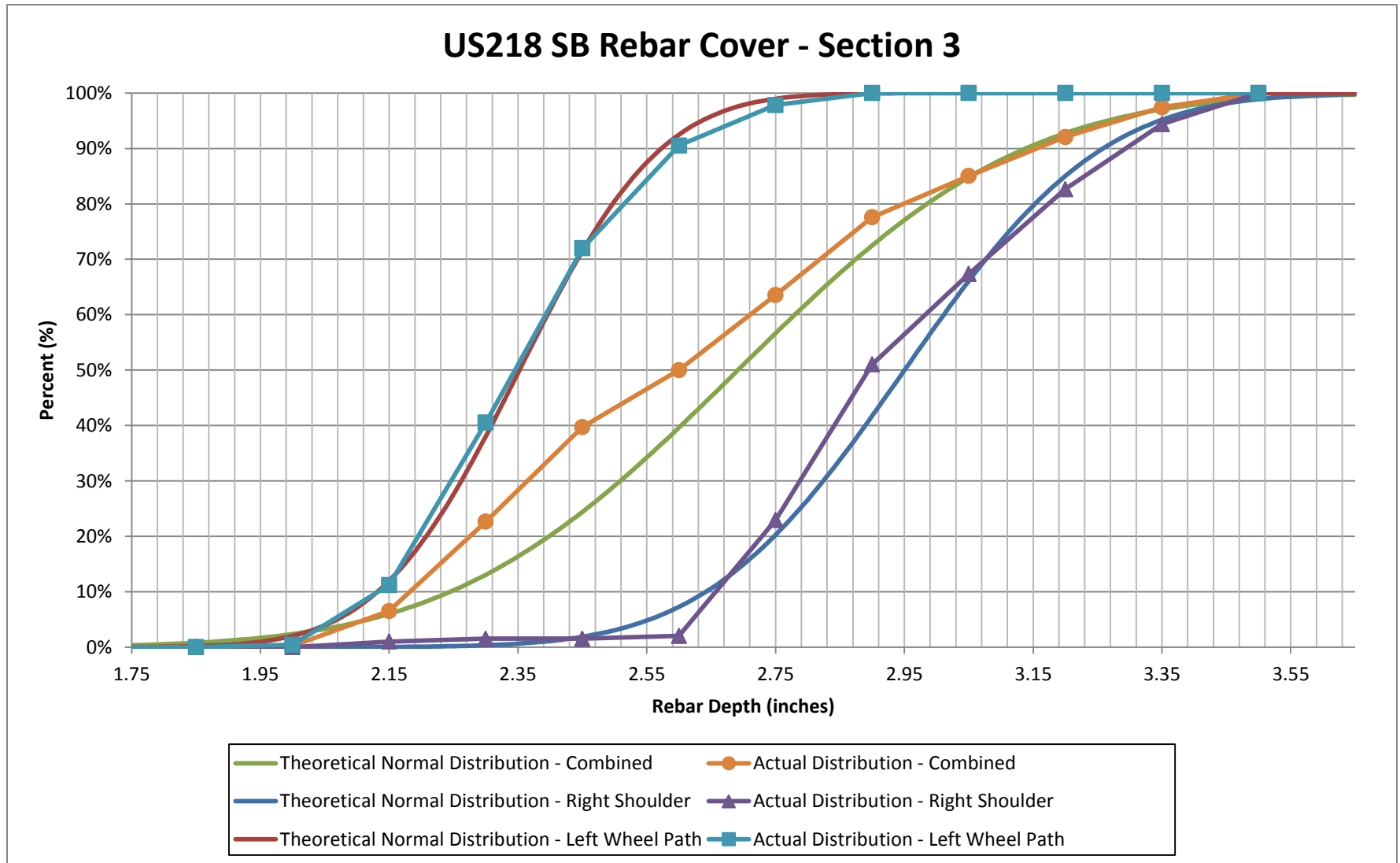
Graph 1. Cumulative distribution of reinforcing bar cover on IA 17.



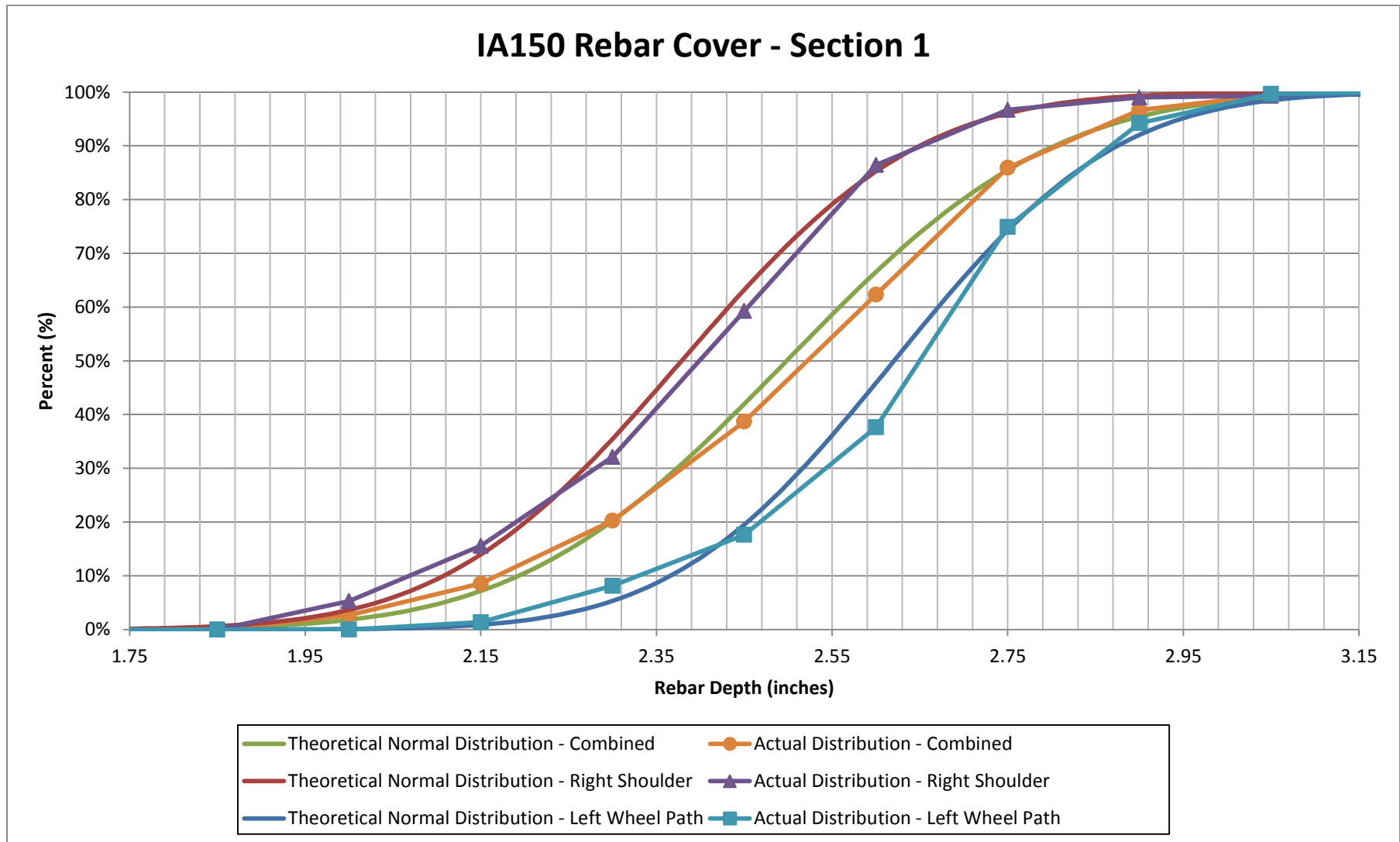
Graph 2. Cumulative distribution of reinforcing bar cover on US 218 SB Section 1.



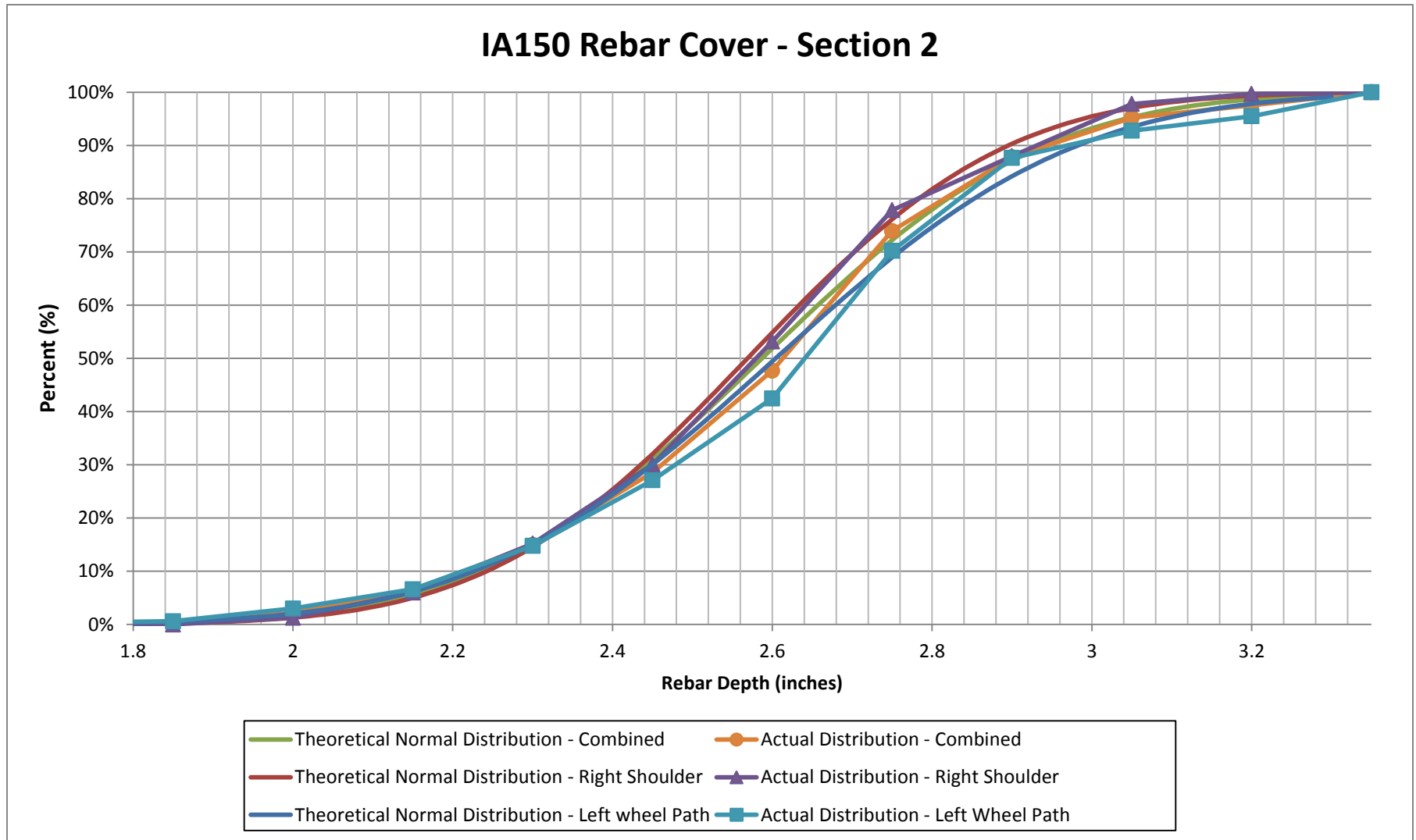
Graph 3. Cumulative distribution of reinforcing bar cover on US 218 SB Section 2.



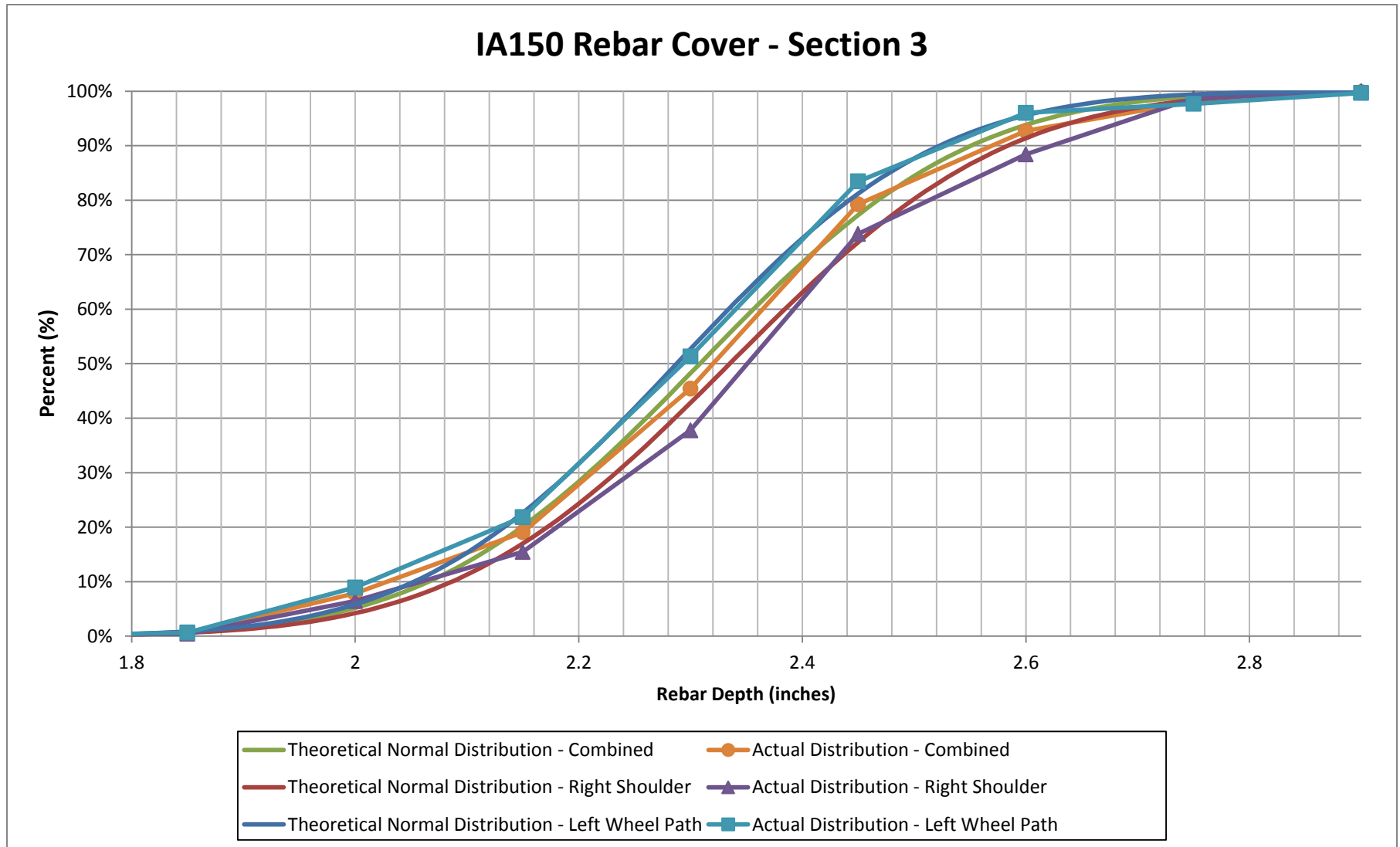
Graph 4. Cumulative distribution of reinforcing bar cover on US 218 SB Section 3.



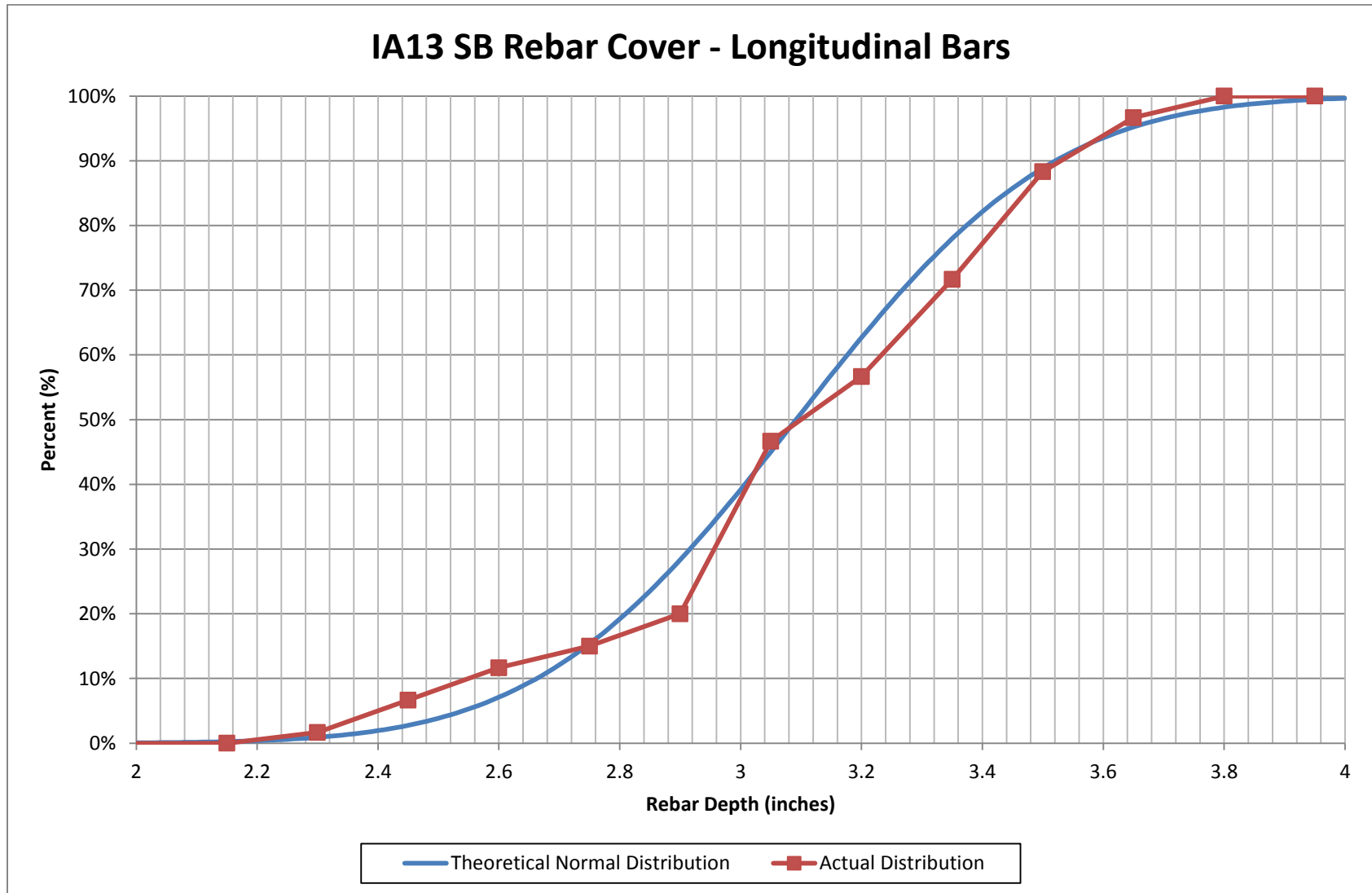
Graph 5. Cumulative distribution of reinforcing bar cover on IA 150 Section 1.



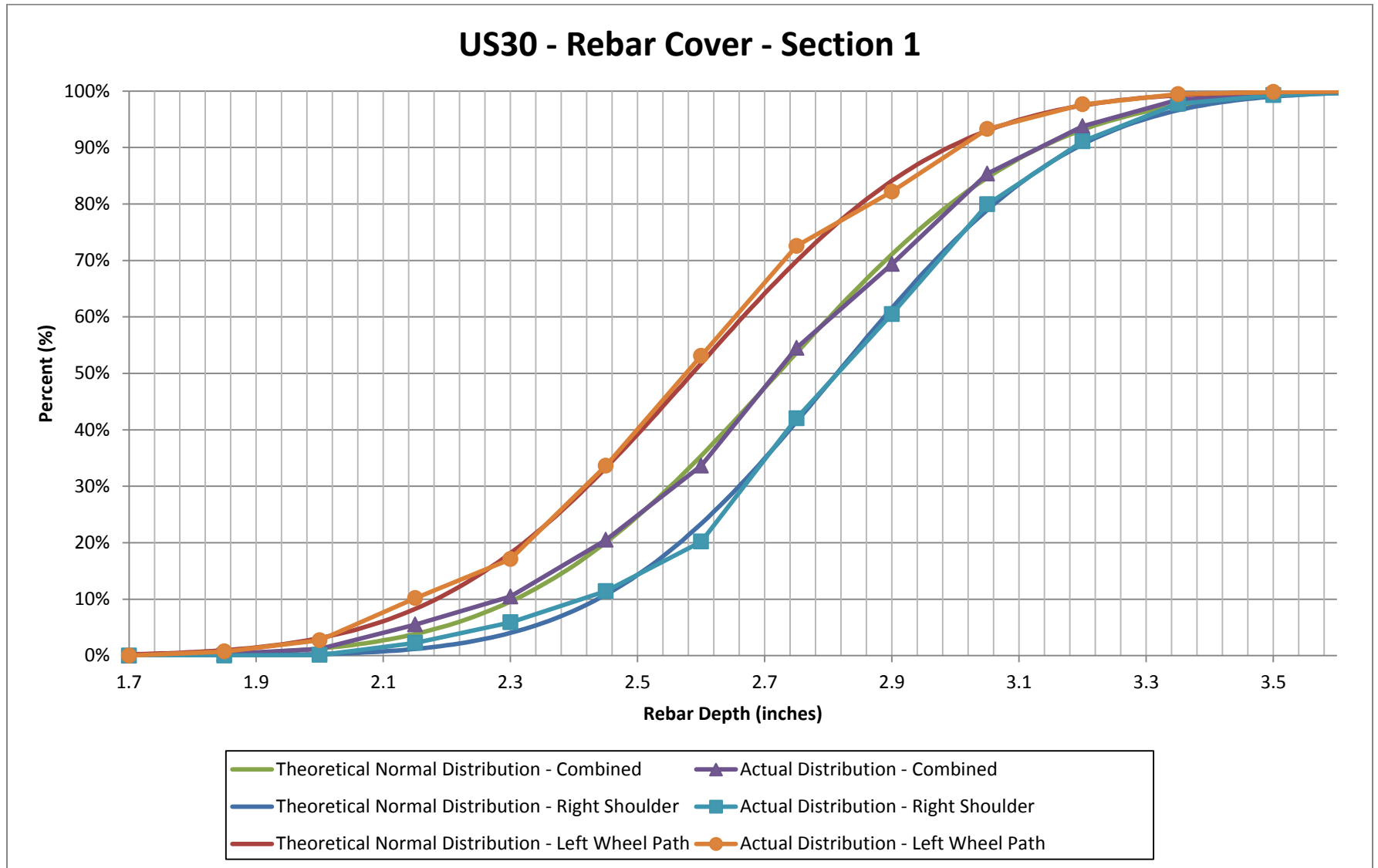
Graph 6. Cumulative distribution of reinforcing bar cover on IA 150 Section 2.



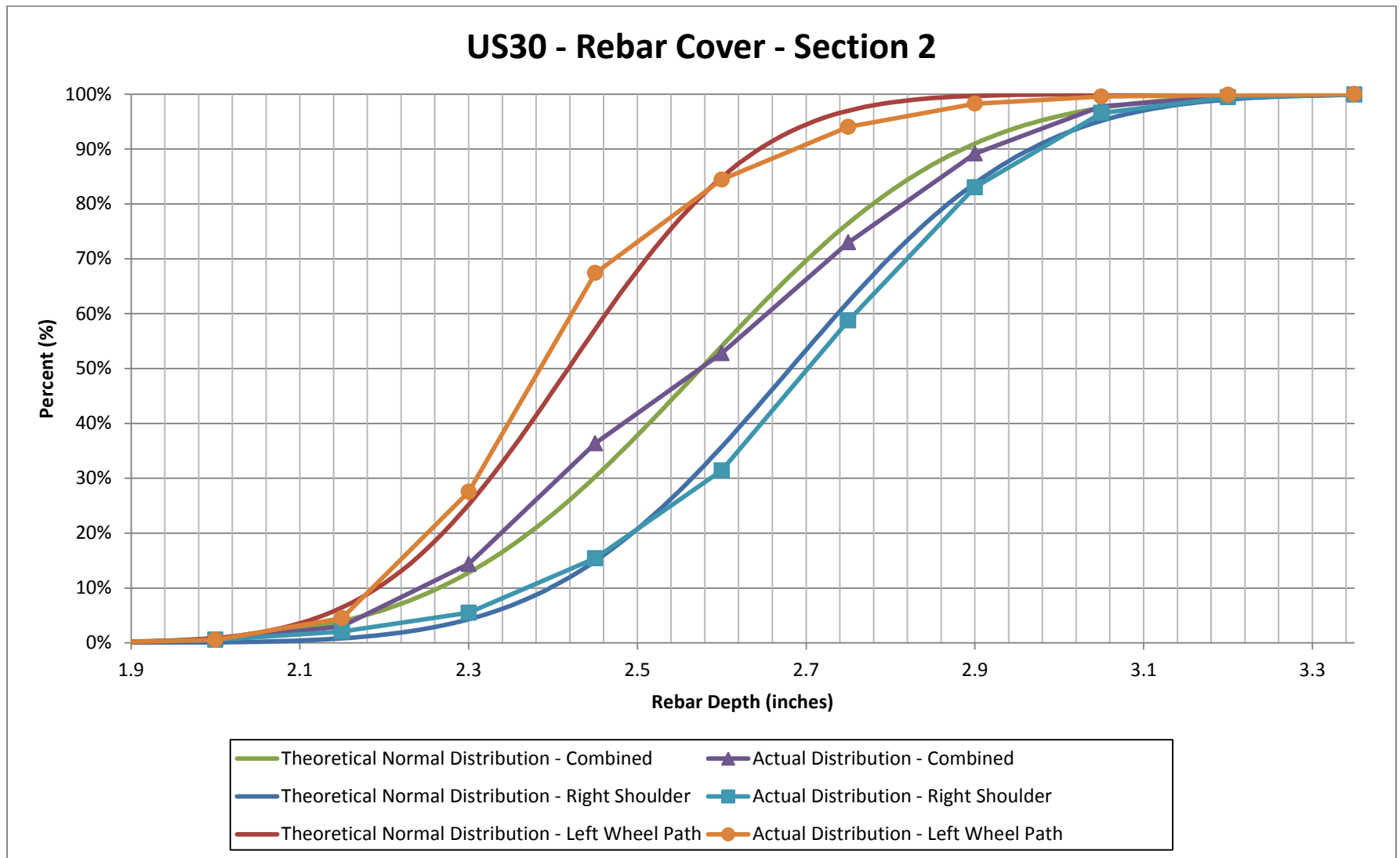
Graph 7. Cumulative distribution of reinforcing bar cover on IA 150 Section 3.



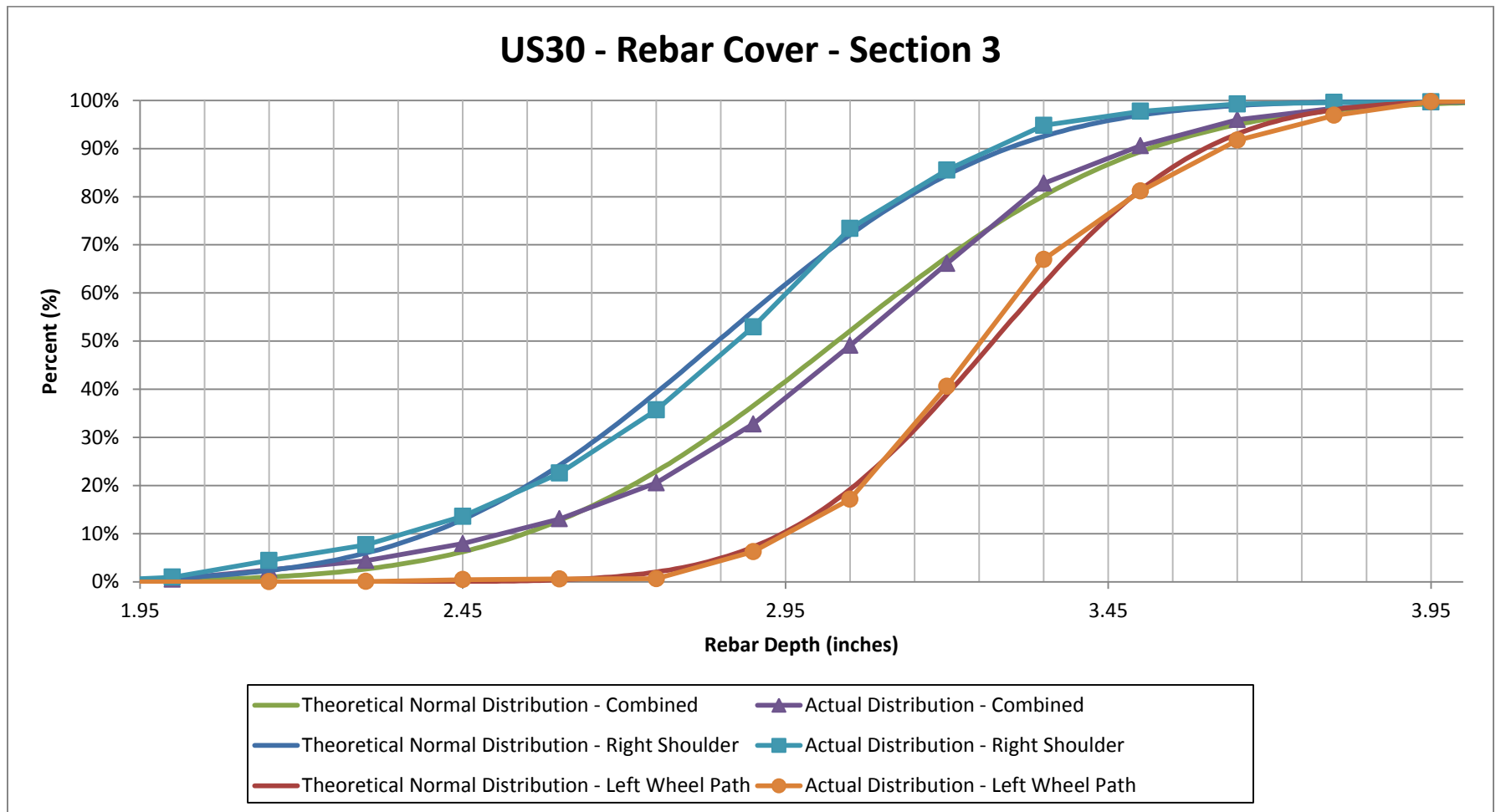
Graph 8. Cumulative distribution of reinforcing bar cover on IA 13.



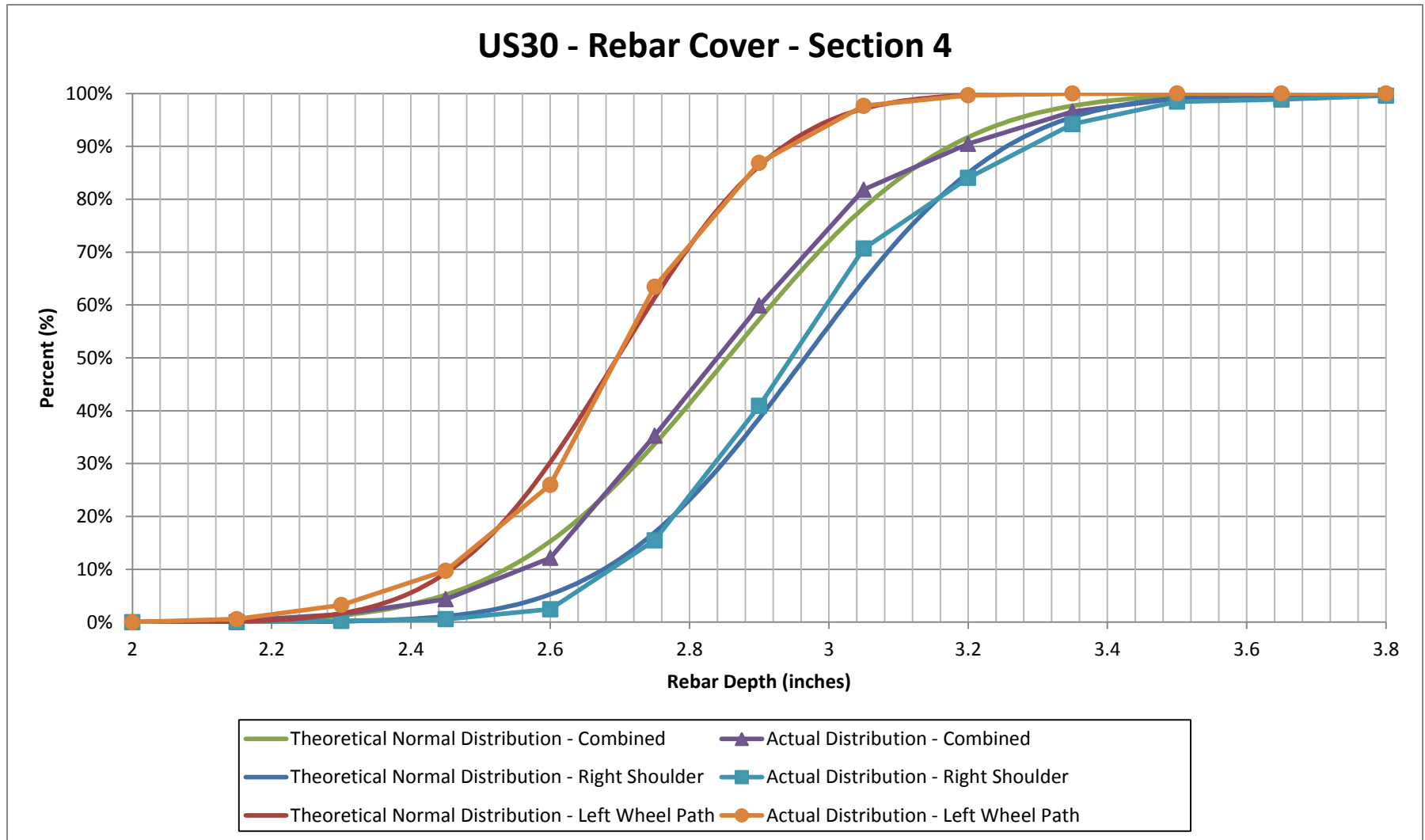
Graph 9. Cumulative distribution of reinforcing bar cover on US 30 Section 1.



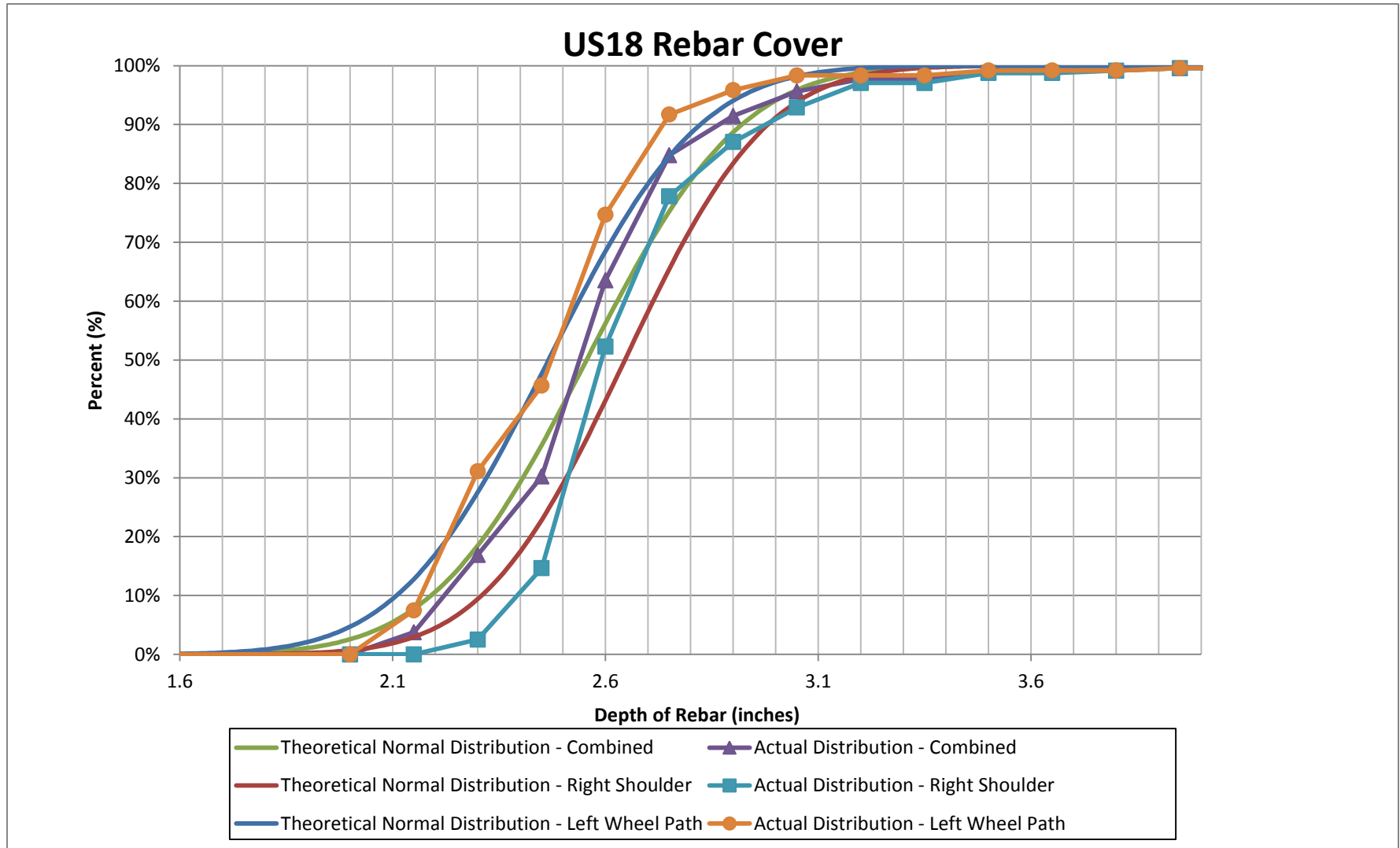
Graph 10. Cumulative distribution of reinforcing bar cover on US 30 Section 2.



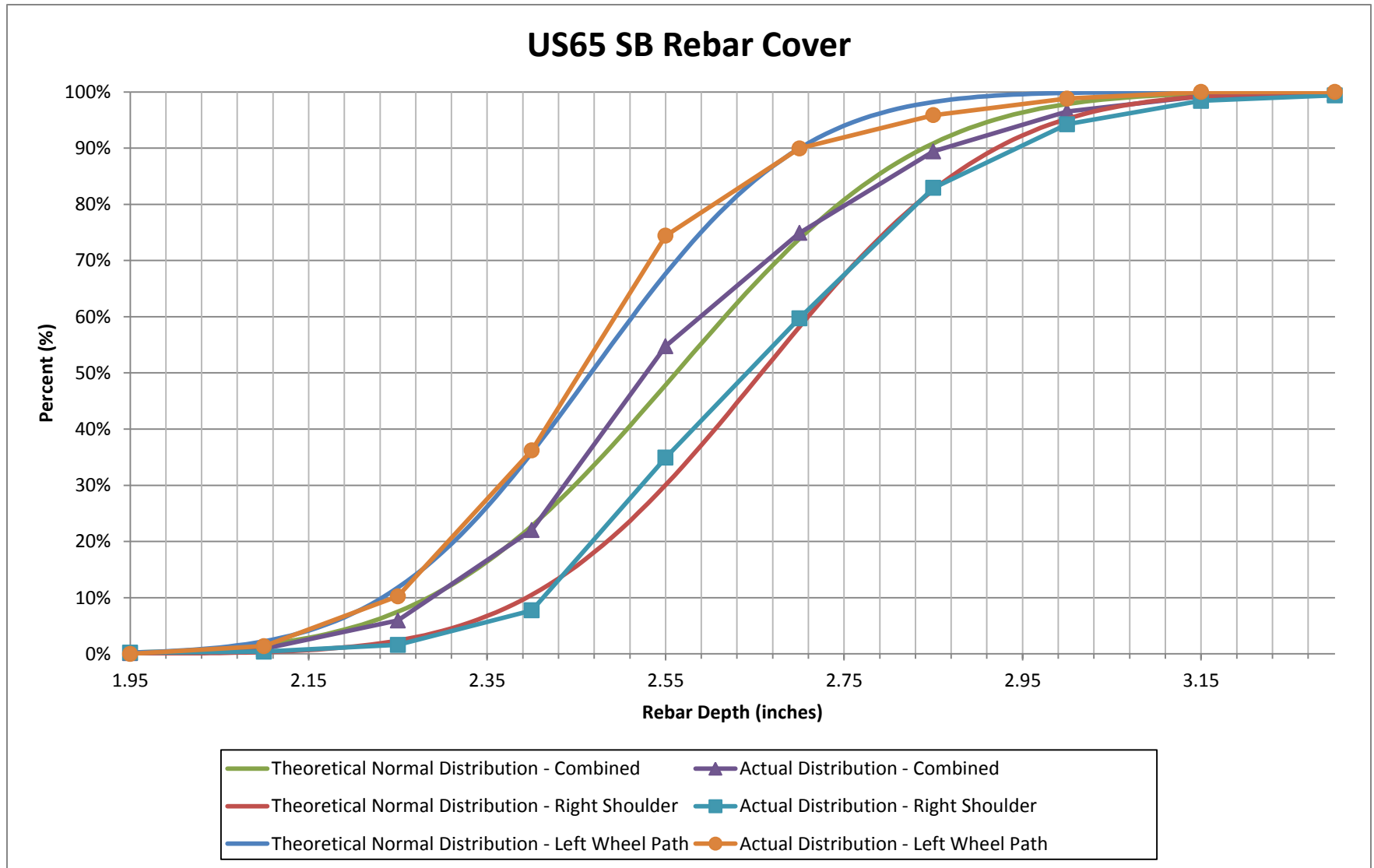
Graph 11. Cumulative distribution of reinforcing bar cover on US 30 Section 3.



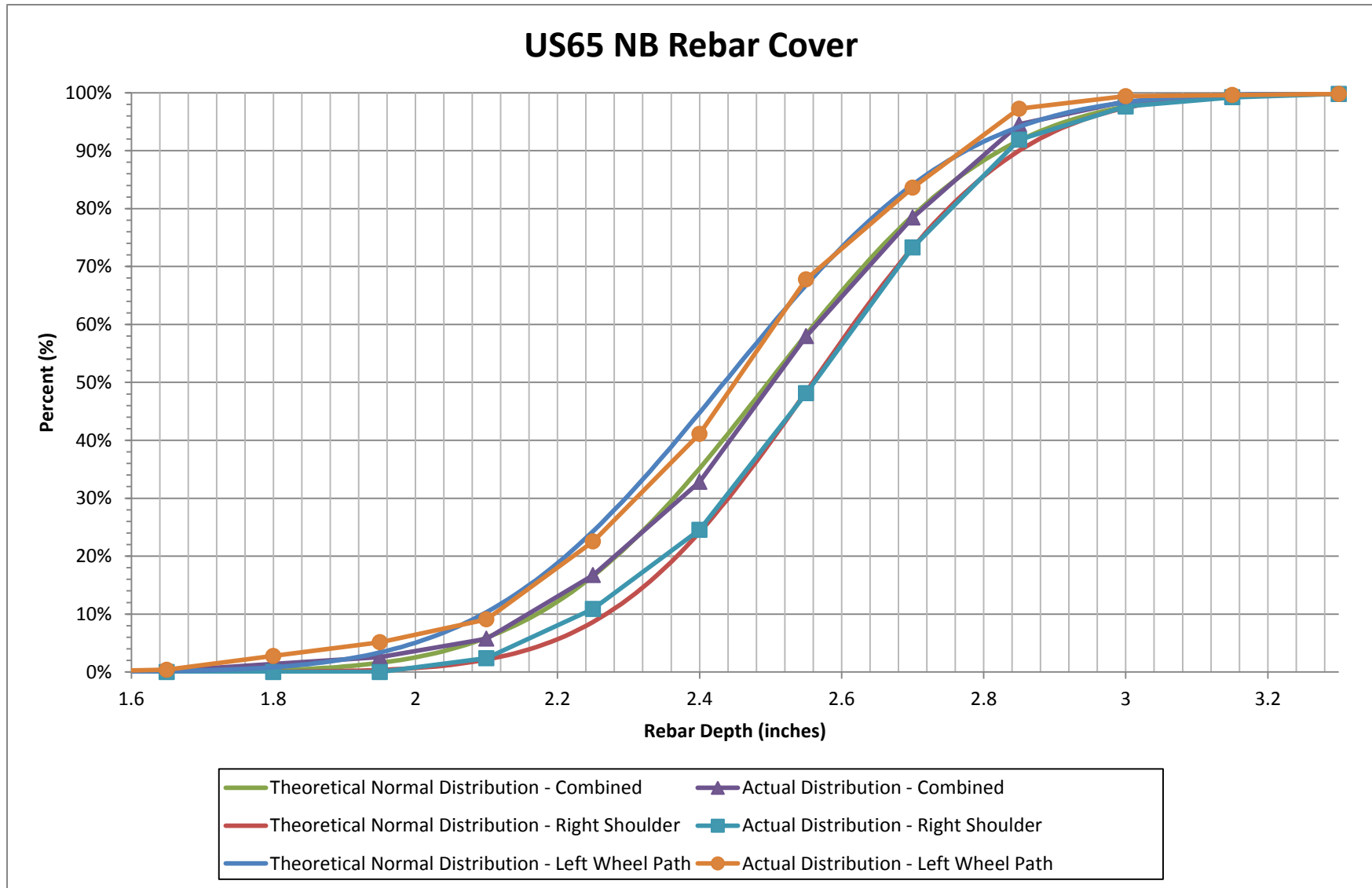
Graph 12. Cumulative distribution of reinforcing bar cover on US 30 Section 4.



Graph 13. Cumulative distribution of reinforcing bar cover on US 18.



Graph 14. Cumulative distribution of reinforcing bar cover on US 65 SB.



Graph 15. Cumulative distribution of reinforcing bar cover on US 65 NB.

Appendix B

Report of Petrographic Studies

Petrographic Studies

Eight Cores from Iowa Bridge Decks

2010.0868

Introduction

On behalf of the Iowa Department of Transportation - Office of Bridges and Structures, petrographic studies of eight partial depth concrete cores were conducted. These studies were performed to identify any conditions or characteristics of the concrete that could affect the performance of the epoxy-coated reinforcing bars in the eight bridge decks being evaluated.

Samples

The appearance of the cores examined in this study immediately after they were extracted from the eight bridge decks and as they were first examined in the laboratory prior to testing is shown in Figures 1 through 32. As can be seen in these figures, each core intersected steel reinforcement somewhere along its length. The steel reinforcement was removed from the cores prior to the petrographic studies. In addition to removal of steel reinforcement, portions of each core were removed for chemical studies. The results of the chemical studies are reported in Appendix C.

Petrographic Studies

A representative portion of each of the eight cores submitted for petrographic examination was prepared by cutting a thin (0.7 inch thick) slice lengthwise from the center of each core using a water-cooled continuous-rim diamond saw blade. This resulted in a planar surface on each half of each core, which did not necessarily extend the full length of the core due to the position of the cracks and reinforcing bars in the cores, but always included the upper portion of the core. The planar surfaces of the cores were then lapped using progressively finer silicon carbide abrasives, resulting in a smooth flat surface for examination. The lapped surfaces, the thin sections, and the remainders of the cores were then examined using methods outlined in ASTM C856 *Standard Practice for Petrographic Examination of Hardened Concrete* and ASTM C457 *Standard Test Method for Microscopical Determination of Parameters of the Air-Void System in Hardened Concrete*. The lapped surfaces prepared for each core are shown in Figures 33 through 40.

A summary of the petrographic findings is given in the Table 1. The approximate age of the bridge and the depth of the horizontal slices taken for chemical testing are also listed in Table 1. Based on the appearance of the concrete, the eight cores appear to represent eight distinct concrete mixes, as can be seen in Figures 33 through 40.

The maximum nominal size of the coarse aggregates contained in all cores was 1 inch. With the exception of Core IA150 #5, the coarse aggregate was uniformly distributed. As detailed in Table 1, the coarse aggregate in six of the cores was composed of crushed limestone, while the other two cores (Cores US 18 #8 and US 30 #18) contained a natural gravel coarse aggregate. Based on textural differences, the limestone coarse aggregates appeared to be from five distinctly different geologic sources, with Cores US 65 NB #6 and US 65 SB #9 containing coarse aggregate from the same geologic source. The limestone coarse aggregates were typically fine-grained and virtually free of physically unsound particles. However, in the case of Core US18 #8, the coarse aggregate contained a single particle of non-durable shale that was associated with shallow incipient surface scaling, as shown in Figure 41. Regarding the two cores with natural gravel as the coarse aggregate, the gravel consisted of siliceous rock types such as

granite, quartzite and basalt, as well as fine-grained limestone. No evidence of coarse aggregate deterioration was detected in these two cores.

The fine aggregate in all eight cores was composed of natural rounded sand that contained various siliceous rock and mineral types, as well as some minor amounts of rounded limestone particles. The fine aggregate in all but one of the cores contained very small numbers of internally fractured particles. In a few cases, some of these particles expanded and fractured after they became exposed on the lapped surfaces of the cores (see Figure 42). Silica gel was occasionally associated with these particles, as can be seen in Figure 43. These features are consistent with alkali-silica reaction (ASR). Due to the small size of these particles, no significant disruption of the surrounding cementitious matrix had occurred. However, the fractures seen in a few of the fine aggregate particles in Core IA 150 #5 likely formed due to corrosion-induced deposition of iron oxide, and were also seen to also contain silica gel (Figure 44).

The concrete represented by all of the cores was air entrained. The parameters of the air void system were determined per ASTM C457 for two of the cores, Cores IA 13 SB #5 and IA 17 #1. The results are given in Table 2. Although these results indicate that the air void spacing factors are slightly greater than the 0.008 inch value normally associated with excellent freeze-thaw durability, the long term performance of the concrete confirms that the air void systems are adequate for protection of the concrete in the environment(s) in which they have been exposed.

The cementitious matrices of the cores were all sound and intact. Freshly fractured surfaces made in the laboratory were seen to pass through coarse aggregate particles. This is consistent with a firm matrix-to-aggregate bond. Lapped surfaces could not be scratched with a copper probe, and fresh fracture surfaces prepared in the laboratory had a vitreous to sub vitreous luster. Examination of the thin sections revealed that residual (unhydrated) portland cement particles were common, and in many of the cores the cement particles were seen to be surrounded with clear rims of cement hydrates. Fly ash was detected in only two of the cores. The depth of complete cement paste carbonation was determined for the cores, and was generally found to be less than 0.2 inches, although carbonation depths of up to 0.4 inches were observed in Cores IA 17 #1 and IA 150 #5. The features described above are consistent with a moderate to moderately low water to cementitious material (w/cm) ratio. Information regarding the depth of carbonation and the estimated water to cementitious material ratio for each core is provided in Table 1.

Cracks in Cores IA 150 #5 and US 65 NB #6 appear to be associated with corrosion of embedded steel (see Figures 5 and 24). Also, in the case of Core IA 150 #5, additional opening of the crack may be associated with deposition of silica gel (Figure 44).

Summary and Discussion

The concrete represented by the eight cores was determined to be sound and of good quality. The air entrained nature of the concrete, relatively low estimated w/cm ratio, sound coarse aggregate, and the minimal depth of cement paste carbonation found in this study are consistent with this assessment. Although the parameters of the air void systems for the two cores where this was measured were slightly out of the range normally associated with excellent freeze-thaw durability, the overall condition of the air void systems, in combination with the relatively low w/cm ratio, has provided good freeze-thaw performance.

The pattern of cracking detected in Cores IA 150 #5 and US 65 NB #6 appeared to be due to corrosion of embedded steel reinforcement. Secondary opening of the cracks due to deposition of silica gel (a by-product of ASR) also occurred in Core IA 150 #5. The cause of the shallow near-surface cracks in Core US 18 #8 was due to the deterioration of a non-durable shale particle that was a trace component of the coarse aggregate used in this core. The fine aggregate in the concrete of all but one core included a very

small amount of particles with internally fracturing consistent with ASR, but the surrounding cement matrix had not yet been affected by this distress. The cause for other cracks and distress observed in the cores was not determined by the current studies.

Storage: Thirty days after completion of our studies, samples will be discarded unless the client submits a written request for their return. Shipping and handling fees will be assessed for any samples returned to the client. Any hazardous materials that may have been submitted for study will be returned to the client and shipping and handling fees will apply. The client may request that WJE retain samples in storage in our warehouse. In that case, a yearly storage fee will apply.

TABLE 1. Description of the Cores

Core Identification	Year Constructed	Perpendicular cracks present on surface	Depth of horizontal 0.25 inch thick slice removed for chemical studies	Depth to embedded steel reinforcement (inch)	Evidence of corrosion of embedded steel	Depth of complete cement paste carbonation	Thickness of carbonation zone adjacent to vertical cracks	Depth of fine-grained black debris on vertical fracture surface	Concrete air entrainment (percent)	Air voids coated with white secondary deposits	Coarse Aggregate Type	Evidence of Freeze-Thaw Distress	ASR reactive particles in sand	Estimated w/c ratio	Fly Ash Present
IA 17 #1	1978	No	2.2	3.4	No	0.15 to 0.4	n/a	n/a	6.4	No	Crushed Limestone	No	Yes	0.40 to 0.45	No
US 218 SB #3	1993	Yes	No test ²	5	No	0.05	<0.05 to 0.1	1.7 to 2.5	5 to 6	No	Crushed Limestone	No	Yes	0.45 to 0.5	No
IA 150 #5	1980	Yes	1.5	2 and 2.7	Yes	0.4	nil ³	n/a	5 to 6	No	Crushed Limestone	No	Yes	0.40 to 0.45	No
IA 13 SB #5	1987	Yes	2.75	2.75	No	0.1 to 0.2	nil	1.3	6.0	Yes	Crushed Limestone	No	Yes	0.45 to 0.50	Yes
US 30 #18	1991	No	n/a ⁶	2.75	No	nil	n/a	n/a	4 to 5	No	Siliceous and carbonate gravel	No	No	0.40 to 0.45	No
US 18 #8	1992	No ⁴	n/a ⁵	3	No	0.05	n/a	n/a	4 to 5	No	Siliceous and carbonate gravel	Yes ⁶	Yes	0.40 to 0.45	No
US 65 SB #9	1979	No	n/a ⁶	5	No	0.05 to 0.1	n/a	n/a	6 to 7	No	Crushed Limestone	No	Yes	0.40 to 0.45	Yes
US 65 NB #6	1979	Yes ⁷	n/a ⁶	3 ⁸	Yes ⁹	0.1	nil	1.1	4 to 5	No	Crushed Limestone	No	Yes	0.40 to 0.45	No

¹ Samples for chloride testing removed after cores submitted for petrographic studies listed. For other cores, samples for chloride testing removed before petrographic studies (Note 6).

² No upper layer of steel reinforcement was present.

³ Iron oxide detected on vertical fracture surface starting at a depth of 1 inch beneath the finished surface.

⁴ Fractures visible on the surface generally were oriented parallel to the surface and were associated at least in part with porous non-durable aggregate.

⁵ Representative portions of the cores were removed for chemical studies before the cores were received for petrographic studies.

⁶ Associated with porous shale in the coarse aggregate.

⁷ Multiple cracks associated with embedded steel reinforcement. See Figures 24 and 27.

⁸ Two reinforcing bars oriented perpendicular to each other.

⁹ Significant cracking associated with corrosion of steel reinforcement.

TABLE 2. Air Void System Parameters Determined by ASTM C457

	Observed Parameters		Usual Requirements
Core Sample Identification	IA 13 SB #5	IA 17 #1	--
Air Content (%)	6.0	6.4	5 to 8
Paste Content (%)	30.8	26.5	--
Sand Content (%)	40.7	33.6	--
Coarse Aggregate (%)	22.5	33.5	--
Number of Voids/inch	5.09	7.2	Greater than the percent of entrained air
Average Chord Intercept (inch)	0.0117	0.0089	--
Specific Surface (in ² / in ³)	342	448	Greater than 600
Spacing Factor (inch)	0.0138	0.0092	Less than 0.008



Figure 1. The site photo of the side of Core IA 13 SB #5.



Figure 2. The as-received appearance of the top of Core IA 13 SB #5 using low angle lighting to emphasize timing of deck top surface.



Figure 3. The as-received appearance of the bottom of Core IA 13 SB #5.



Figure 4. The site photo of the side of Core IA 17 #1 (reinforcing bar identified by arrow).



Figure 5. The as-received appearance of the top of Core IA 17 #1 using low angle lighting to emphasize tined top surface.



Figure 6. The as-received appearance of the bottom of Core IA 17 #1.



Figure 7. The site photo of the side of Core IA 150 #5. The rebar (arrow) was subsequently removed in the laboratory for examination.



Figure 8. The as-received appearance of the top of Core IA 150 #5.



Figure 9. The as-received appearance of the inner fracture surfaces of Core IA 150 #5.



Figure 10. The as-received appearance of the bottom of Core IA 150 #5.



Figure 11. The as-received appearance of the side of Core US 218 SB #3. Note imprint of reinforcing bar at bottom of core (arrow).



Figure 12. The as-received appearance of the top of Core US 218 SB #3 using low angle lighting to emphasize crack and tinting on top surface.



Figure 13. The as-received appearance of the bottom of Core US 218 SB #3.



Figure 14. The site photo of the side of Core US 18 #8. The rebar was subsequently removed in the laboratory for examination.



Figure 15. The as-received appearance of the top of Core US 18 #8.



Figure 16. The as-received appearance of the bottom of the top section of Core US 18 #8.

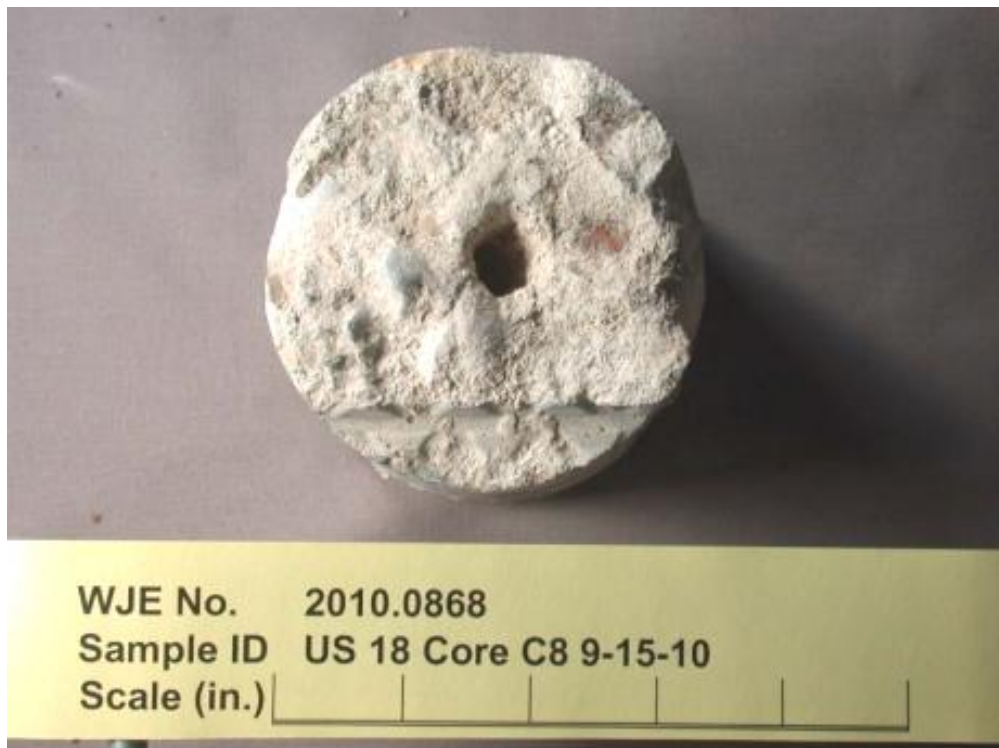


Figure 17. The as-received appearance of the top of the bottom section of Core US 18 #8 using low angle lighting.



Figure 18. The as-received appearance of the bottom of Core US 18 #8.



Figure 19. The site photo of the side of Core US 30 #18. The rebar was subsequently removed in the laboratory for examination.



Figure 20. The as-received appearance of the top of Core US 30 #18 using low angle lighting to emphasize tining of top surface.



Figure 21. The as-received appearance of the bottom of the top section of Core US 30 #18.



Figure 22. The as-received appearance of the top of the bottom section of Core US 30 #18 using low angle lighting.



Figure 23. The as-received appearance of the bottom of Core US 30 #18.



Figure 24. The site photo of the side of Core US 65 NB #6. The rebar was subsequently removed in the laboratory for examination.



Figure 25. The inner crack faces of the horizontal delamination plane in Core US 65 NB #6.



Figure 26. The as-received appearance of the top of Core US 65 NB #6 using low angle lighting to emphasize rake finish of top deck surface.



Figure 27. The as-received appearance of the bottom of the top section of Core US 65 NB #6 showing multiple cracks at the location of the removed reinforcing.



Figure 28. The as-received appearance of the top of the bottom section of Core US 65 NB #6.



Figure 29. The as-received appearance of the bottom of Core US 65 NB #6.

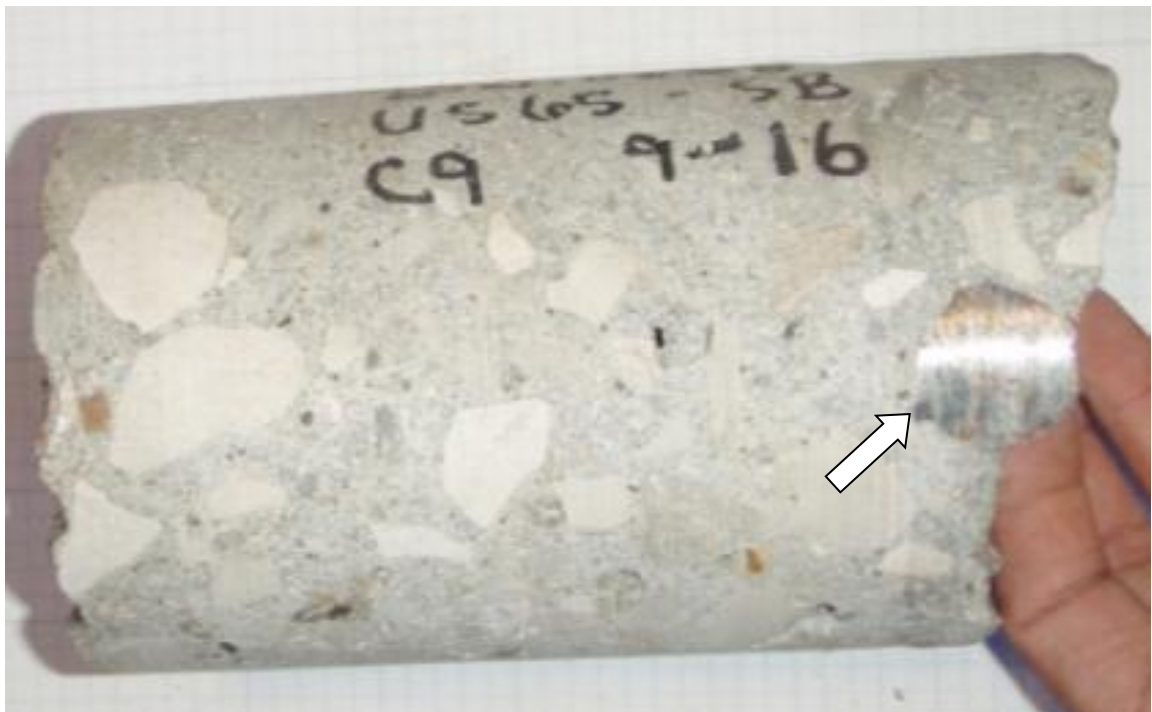


Figure 30. The site photo of the side of Core US 65 SB #9. The reinforcing bar (arrow) was subsequently removed in the laboratory for examination.



Figure 31. The as-received appearance of the top of Core US 65 SB #9 using low angle lighting to emphasize rake finish.



Figure 32. The as-received appearance of the bottom of Core US 65 SB #9.

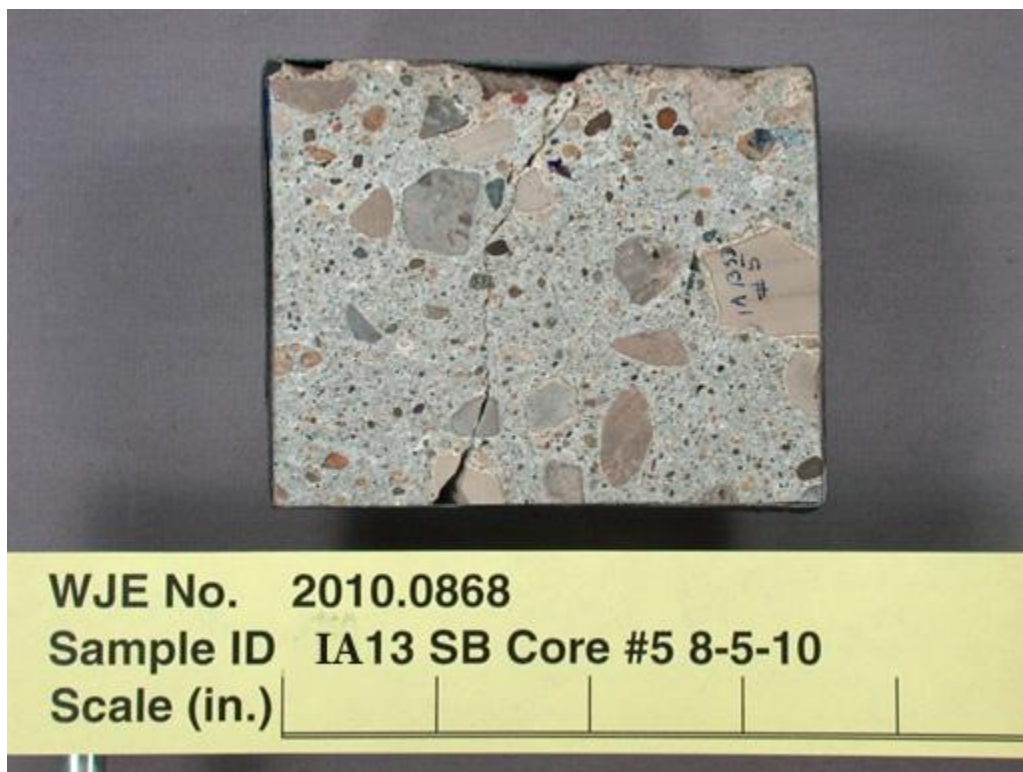
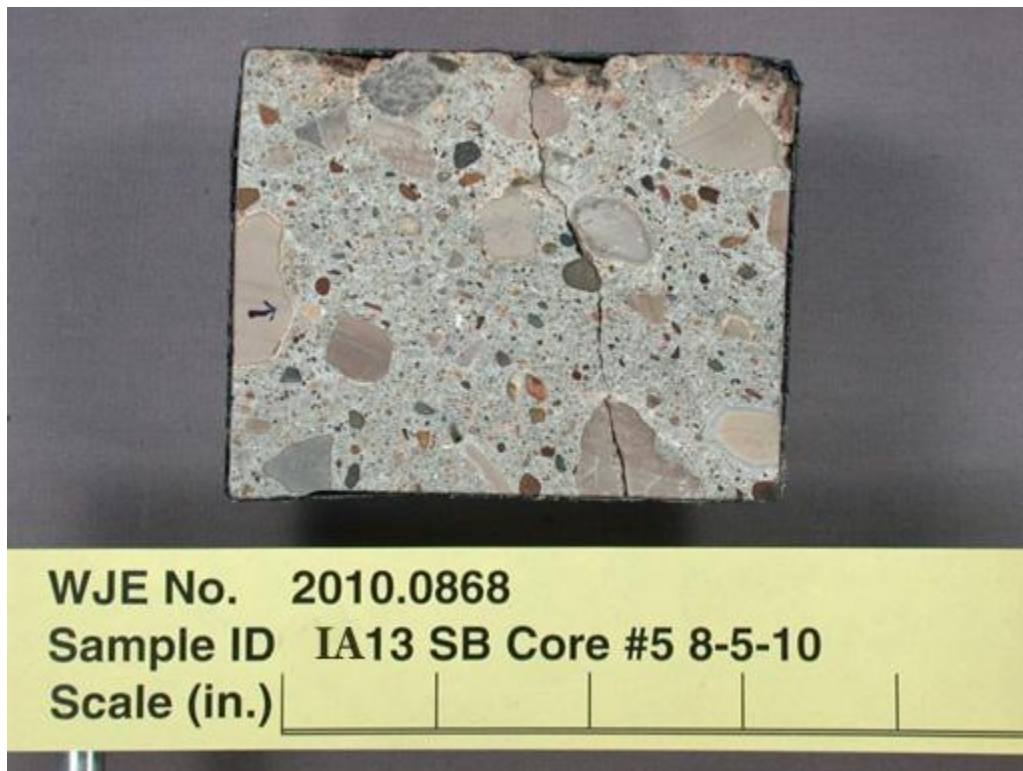


Figure 33. The lapped surfaces of Core IA 13 SB #5. The top of the core is to the top of the photos.

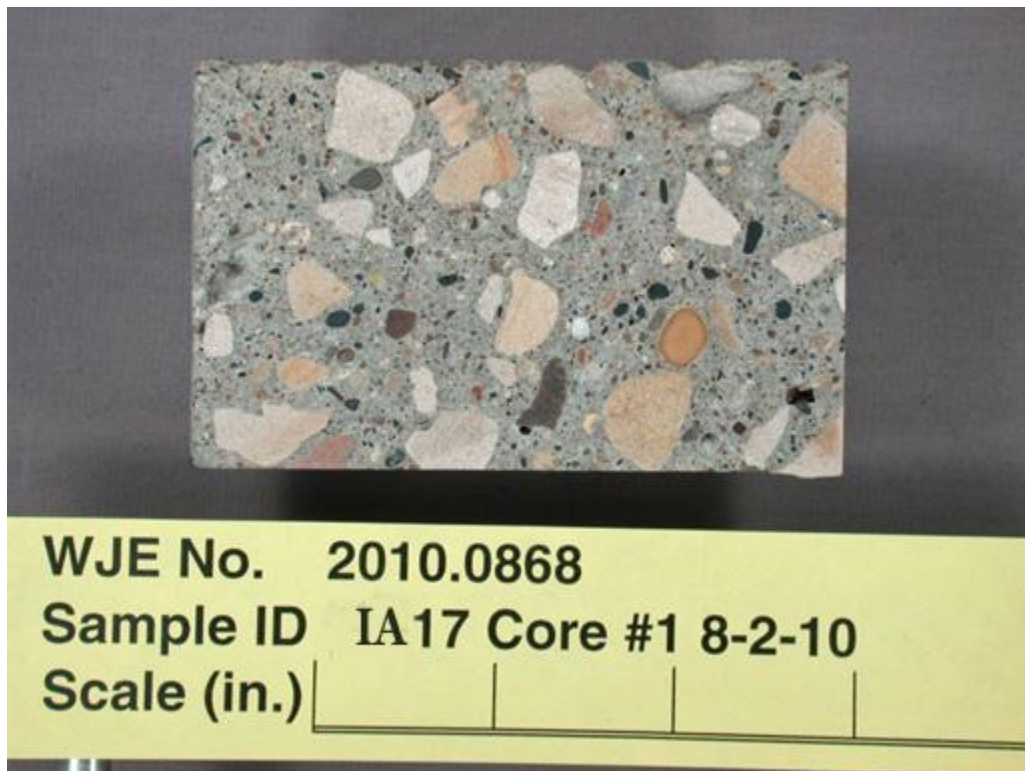


Figure 34. The lapped surfaces of Core IA 17 #1. The top of the core is to the top of the photos.

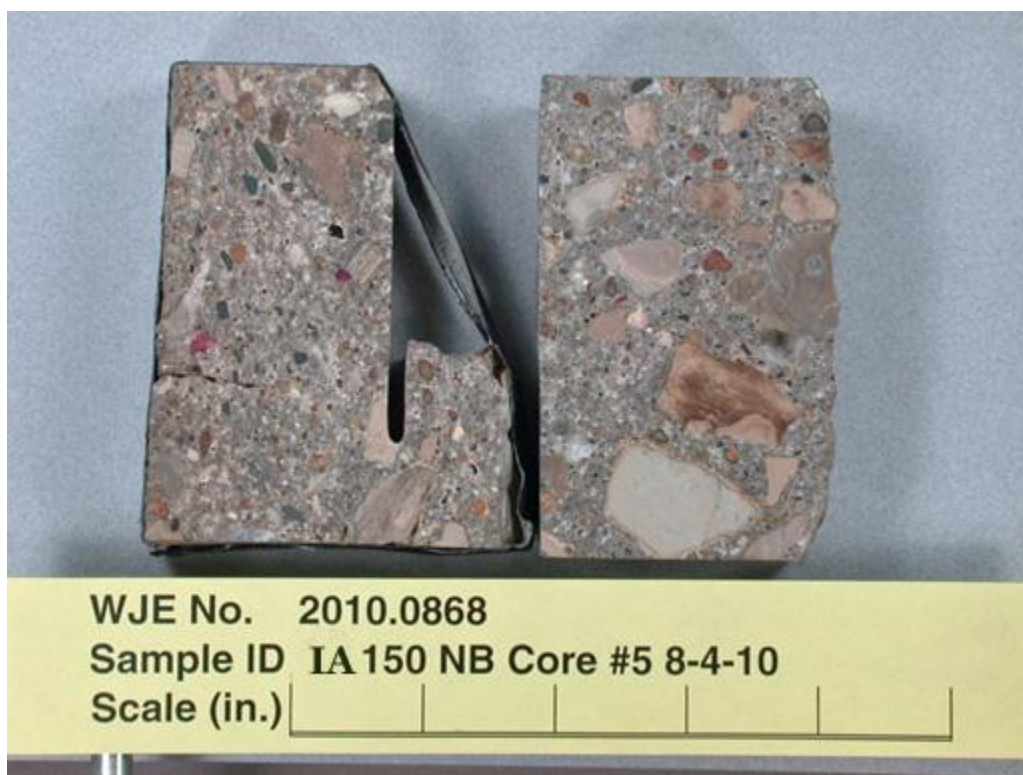


Figure 35. The lapped surfaces of Core IA 150 #5. The top of the core is to the left in the photos.

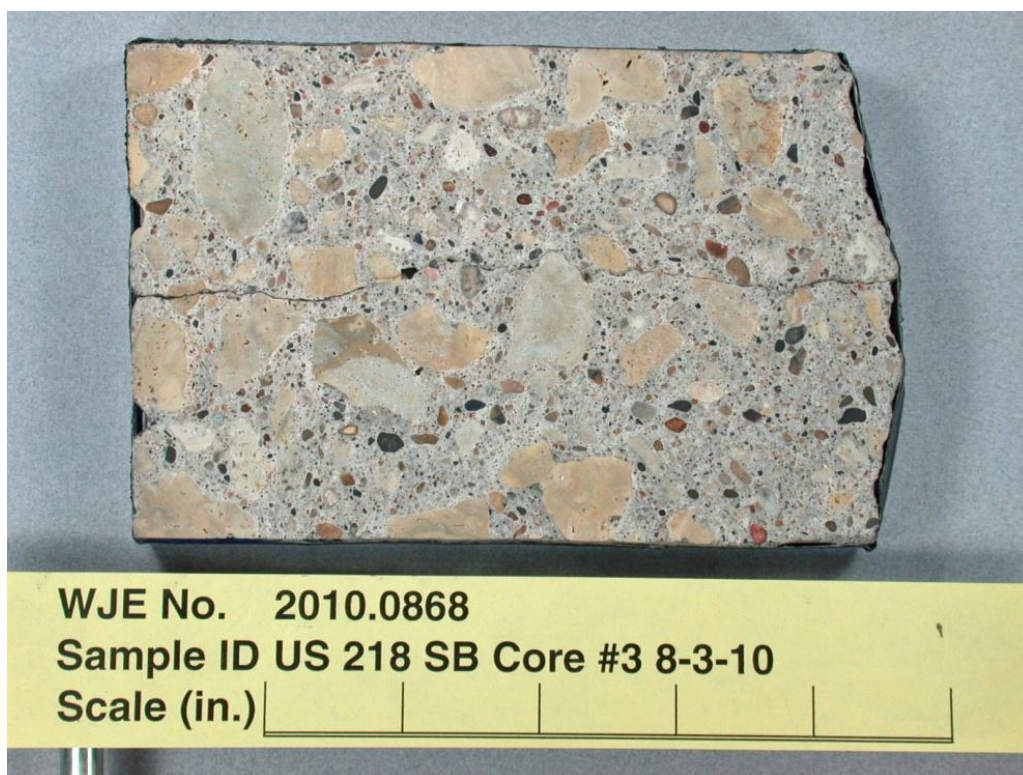
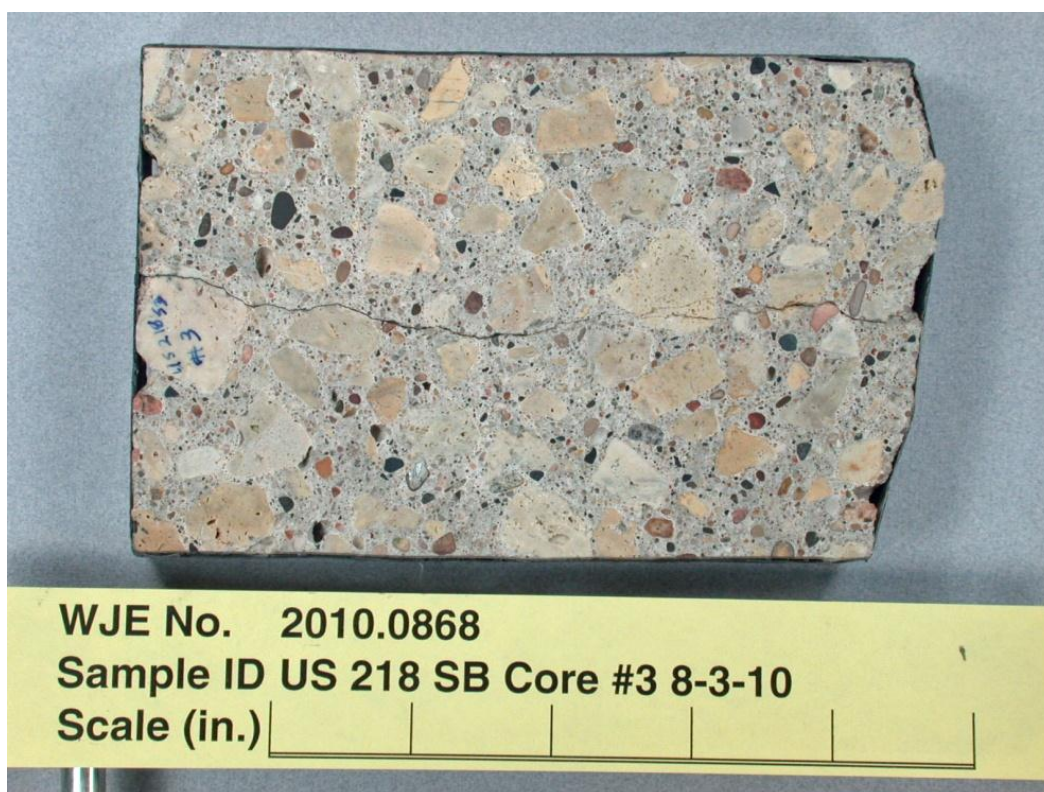


Figure 36. The lapped surfaces of Core US 218 SB #3. The top of the core is to the left in the photos.

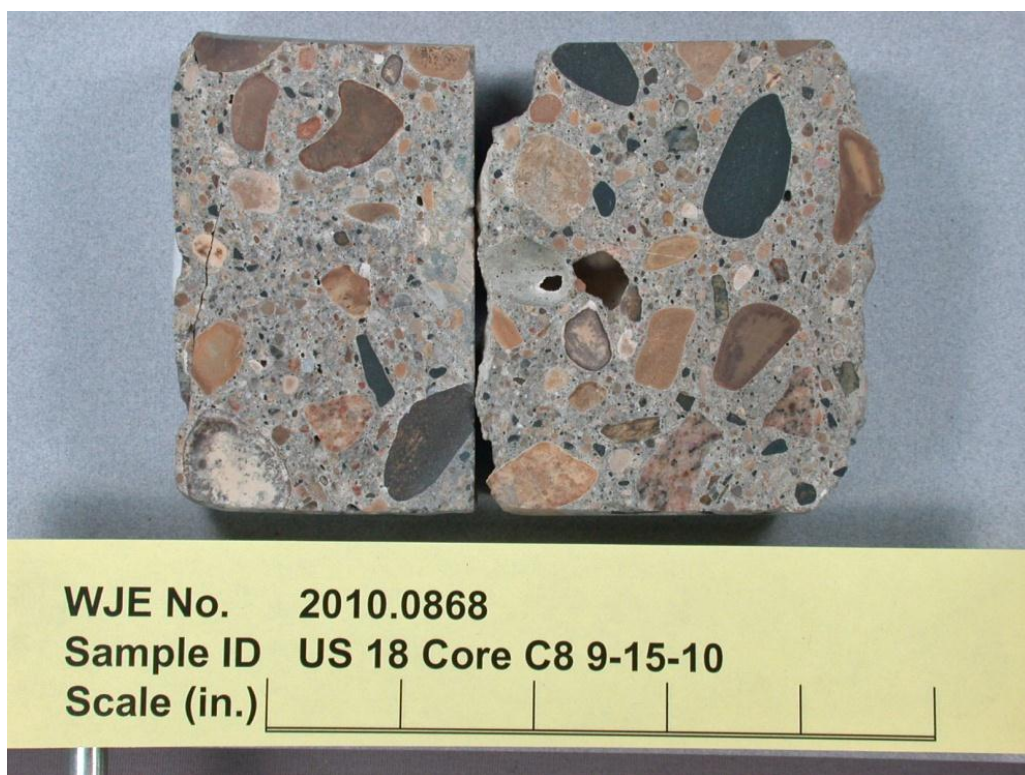


Figure 37. The lapped surfaces of Core US 18 #8. The top of the core is to the left in the photos.

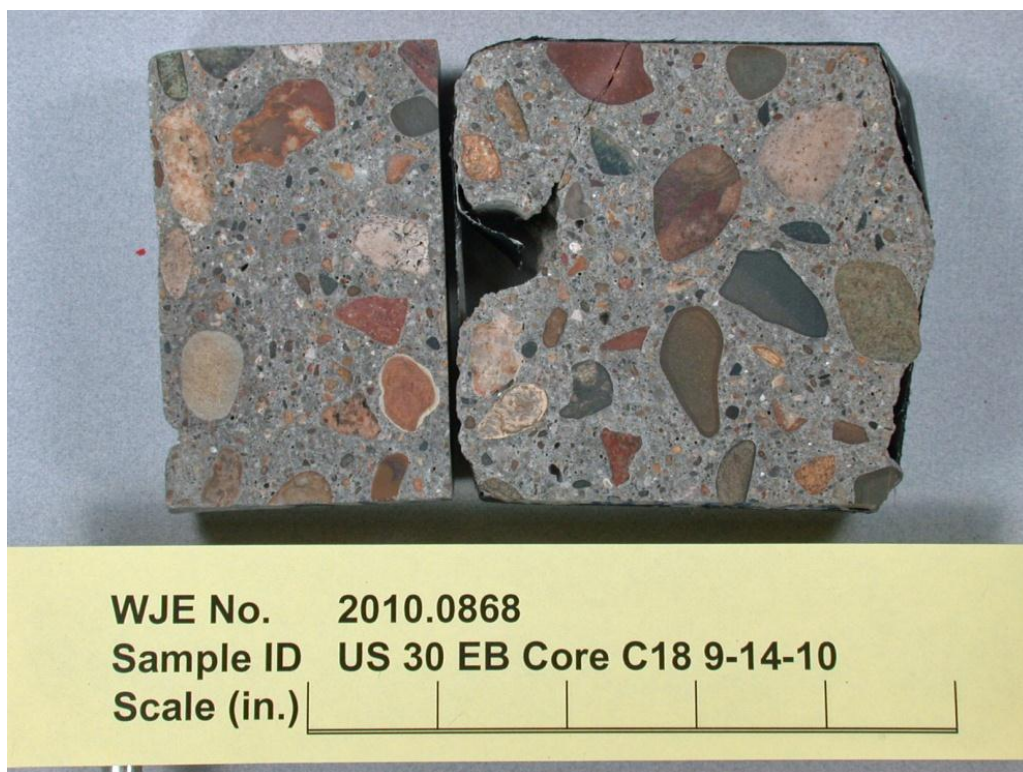


Figure 38. The lapped surfaces of Core US 30 #18. The top of the core is to the left in the photos.



Figure 39. The lapped surfaces of Core US 65 NB #6. The top of the core is to the left in the photos.



Figure 40. The lapped surfaces of Core US 65 SB #9. The top of the core is to the left in the photos.

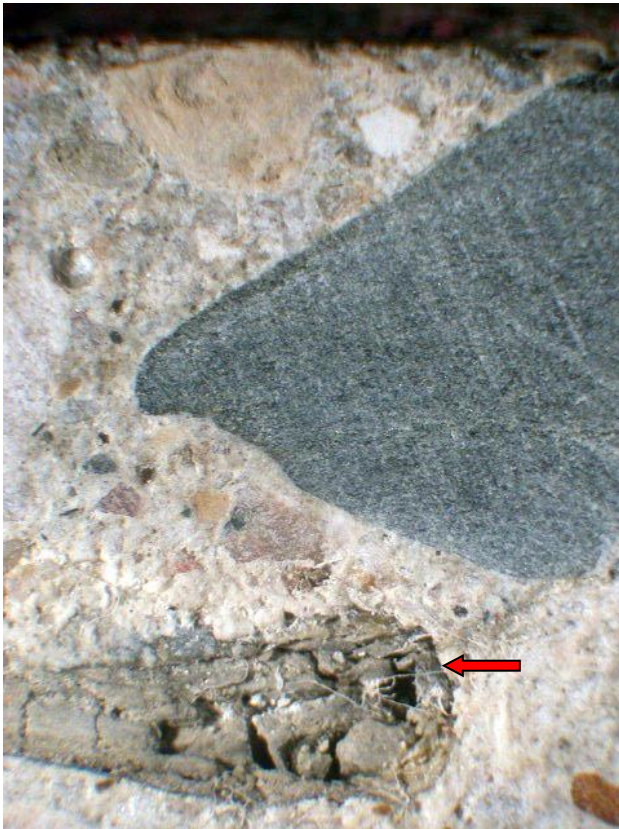


Figure 41. A non-durable shale particle that is embedded near the surface of Core US 18 #8 is marked with an arrow. The particle is intersected by a fracture that is oriented approximately horizontally. The height of the field of view is 0.5 inch in this photo.

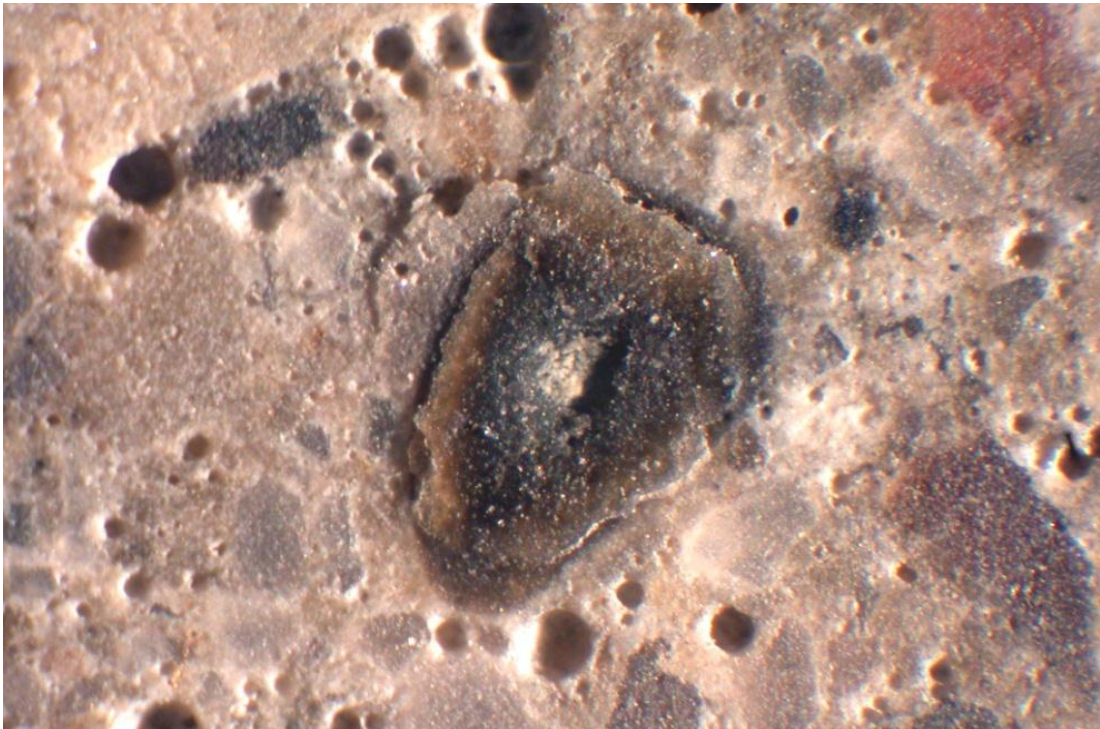


Figure 42. A sand particle that expanded after it was exposed on a lapped surface of Core IA 17 #1. The height of the field of view is 0.18 inch.



Figure 43. Two internally fractured sand particles contained in Core IA 17 #1 are marked with red arrows. The yellow arrow marks a void that is partially filled with silica gel, which is indicative of ASR. The width of the field of view is 0.15 inch.

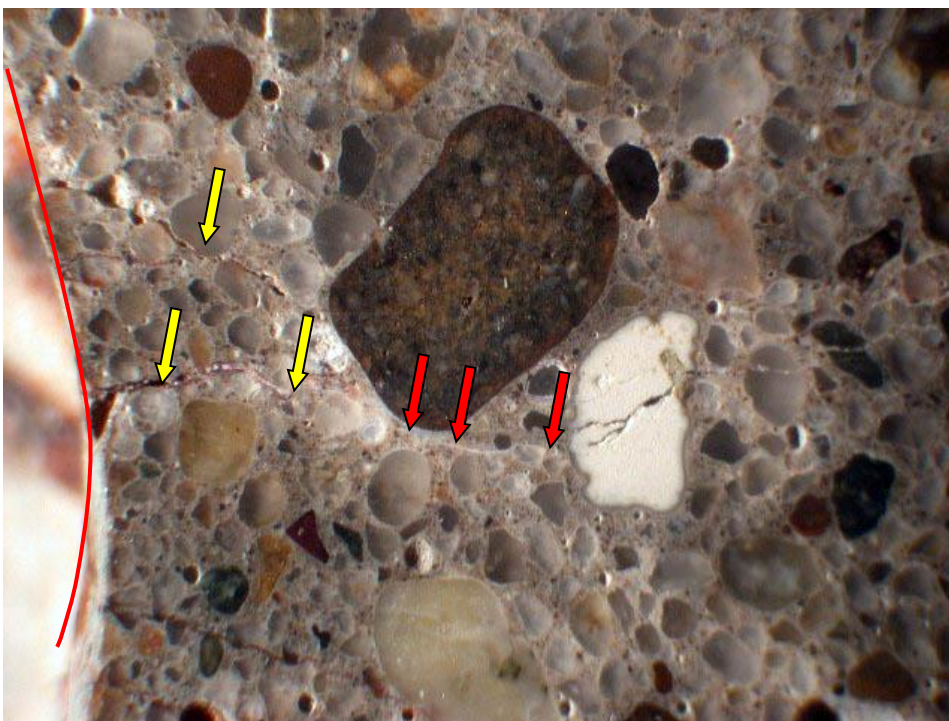


Figure 44. A cross-sectional view oriented perpendicular to the axis of an impression of an embedded steel reinforcing bar contained in Core IA 150 #5. The red curve marks the intersected surface of the steel reinforcing bar impression. Several cracks that were judged to have initially been induced by deposition of corrosion by-products from the embedded steel reinforcement are marked with yellow arrows. Iron oxide deposits are visible along these cracks. The red arrows mark the extension of the one of the corrosion-induced cracks. Silica gel has been deposited along the portion of the same crack in the region marked with red arrows. The width of the field of view is 0.5 inch.

Appendix C

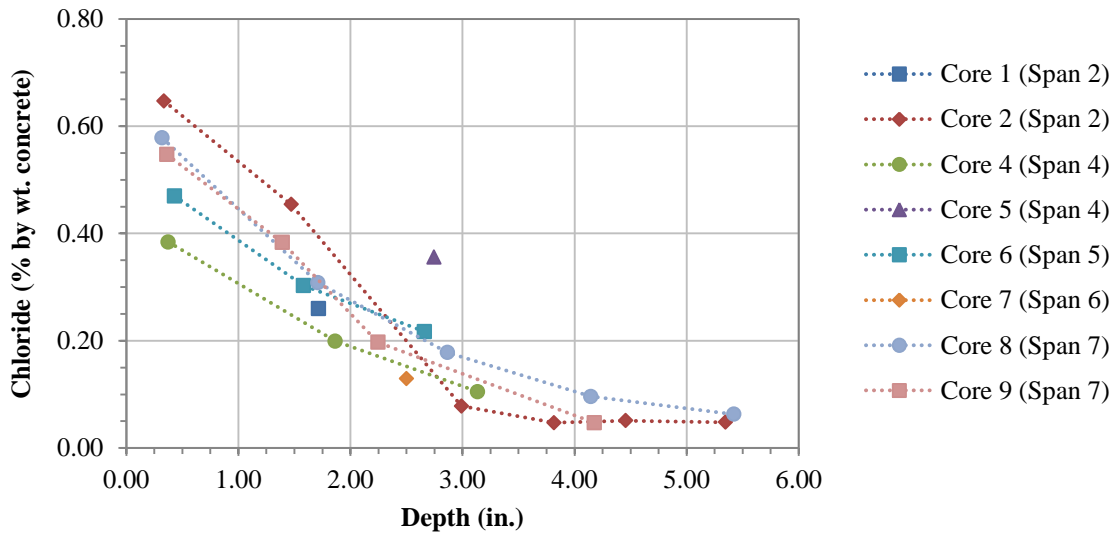
Laboratory Data

Core Number	Location	Cracking		Diffusion Coefficients		Acid-soluble Chloride Contents	
		Vertical (Depth, in.)	Horizontal (Depth, in.)	C _s (% by wt. conc.)	D (in. ² /yr.)	Average Depth (in.)	Chloride (% by wt. conc.)
1	Span 1	-	-			1.88	0.044
2	Span 1	-	0.8 - not at bar	1.006	0.024	0.75	0.555
						1.45	0.226
						1.77	0.182
						3.76	0.007
						5.36	0.007
3	Span 2	-	-	0.869	0.040	0.47	0.663
						1.46	0.357
						2.25	0.111
						3.75	0.022
						5.19	0.008
4	Span 3	-	-			1.33	0.270
5	Span 3	-	-	0.695	0.074	0.35	0.601
						1.26	0.408
						2.19	0.214
6	Span 4	-	2.0 - at bar	0.653	0.122	0.38	0.577
						0.68	0.537
						1.64	0.364
7	Span 1	1.5	1.3 - at bar	0.690	0.179	0.39	0.627
						0.68	0.584
						1.79	0.415

Bridge: US 218 Southbound

Age: 17 years

Background Chloride (% by wt. conc.): 0.048



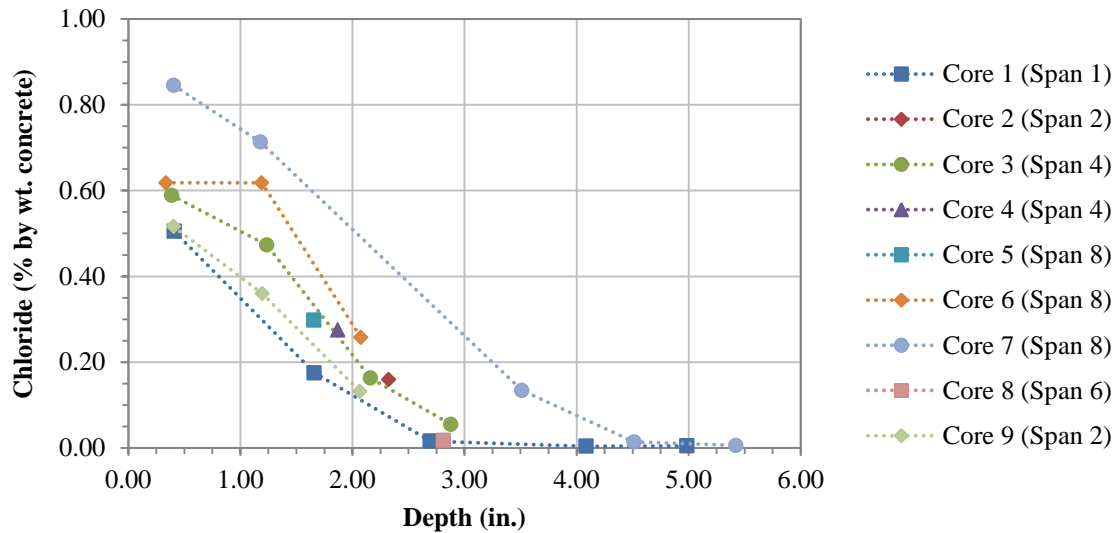
Core Number	Location	Cracking		Diffusion Coefficients		Acid-soluble Chloride Contents	
		Vertical (Depth, in.)	Horizontal (Depth, in.)	C _s (% by wt. conc.)	D (in. ² /yr.)	Average Depth (in.)	Chloride (% by wt. conc.)
1	Span 2	-	-			1.72	0.260
2	Span 2	-	-	0.778	0.110	0.34	0.647
						1.47	0.454
						2.99	0.078
						3.82	0.047
						4.46	0.051
						5.35	0.048 / 0.011 [1]
4	Span 4	-	-	0.438	0.137	0.37	0.384
						1.87	0.199
						3.14	0.105
5	Span 4	-	-			2.75	0.356
6	Span 5	3.7	-	0.524	0.223	0.43	0.470
						1.58	0.303
						2.66	0.217
7	Span 6	-	-			2.50	0.129
8	Span 7	Full	-	0.640	0.155	0.32	0.578
						1.71	0.308
						2.87	0.178
						4.15	0.096
						5.42	0.063
9	Span 7	-	-	0.645	0.126	0.36	0.547
						1.39	0.383
						2.25	0.197
						4.18	0.047

[1]. Water-soluble chloride measurement

Bridge: Iowa 150

Age: 30 years

Background Chloride (% by wt. conc.): 0.006



Core Number	Location	Cracking		Diffusion Coefficients		Acid-soluble Chloride Contents	
		Vertical (Depth, in.)	Horizontal (Depth, in.)	C _s (% by wt. conc.)	D (in. ² /yr.)	Average Depth (in.)	Chloride (% by wt. conc.)
1	Span 1	-	-	0.658	0.033	0.41	0.505
						1.66	0.175
						2.70	0.016
						4.09	0.004
						4.99	0.005
2	Span 2	-	-			2.33	0.159
3	Span 4	-	-	0.748	0.059	0.39	0.589
						1.24	0.473
						2.16	0.163
						2.88	0.055
4	Span 4	Full	1.9 - at bar			1.87	0.275
5	Span 8	1.9	1.9 - at bar			1.66	0.298
6	Span 8	-	-	0.745	0.122	0.34	0.618
						1.19	0.618
						2.08	0.258
7	Span 8	1.8	1.8 - at bar	1.032	0.093	0.40	0.845
						1.18	0.713
						3.51	0.134
						4.51	0.014
8	Span 6	-	-			5.42	0.006
9	Span 2	-	-	0.646	0.052	2.81	0.018
						0.40	0.516
						1.20	0.360
						2.07	0.132

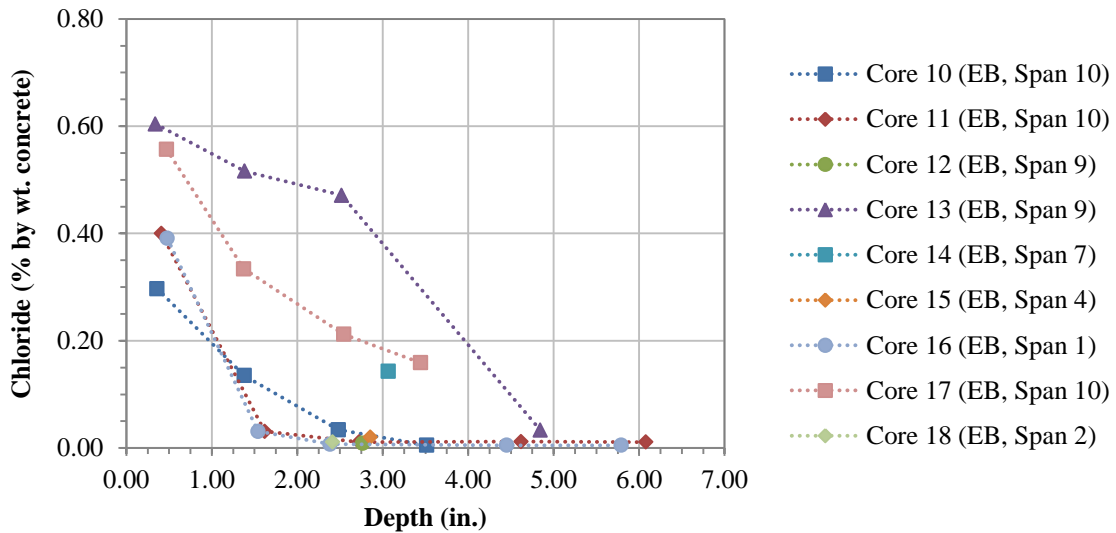
Core Number	Location	Cracking		Diffusion Coefficients		Acid-soluble Chloride Contents	
		Vertical (Depth, in.)	Horizontal (Depth, in.)	C _s (% by wt. conc.)	D (in. ² /yr.)	Average Depth (in.)	Chloride (% by wt. conc.)
1	Span 3	-	-	0.516	0.403	0.29	0.477
						1.44	0.408
						2.64	0.268
2	Span 2	-	-	0.473	0.205	0.29	0.420
						1.74	0.324
						3.06	0.118
3	Span 2	-	-			3.32	0.142
4	Span 2	-	-	0.603	0.162	0.28	0.525
						1.51	0.408
						2.81	0.202
						4.14	0.019
5	Span 2	3.0	-			2.85	0.216
6	Span 1	3.1	2.0 - not at bar	0.768	0.175	0.41	0.676
						1.75	0.416
						2.62	0.298
						5.28	0.022
7	Span 1	-	-	0.492	0.197	0.30	0.433
						1.81	0.322
						3.12	0.125
						6.02	0.006
						8.68	0.007

Core Number	Location	Cracking		Diffusion Coefficients		Acid-soluble Chloride Contents	
		Vertical (Depth, in.)	Horizontal (Depth, in.)	C _s (% by wt. conc.)	D (in. ² /yr.)	Average Depth (in.)	Chloride (% by wt. conc.)
1	Span 17, Westbound	-	-	1.060	0.008	0.42	0.471
						1.38	0.022
						2.03	0.023
						2.67	0.011
2	Span 15, Westbound	1.3	-	0.595	0.065	0.41	0.472
						1.44	0.233
						2.64	0.053
						4.44	0.011
						5.63	0.011
3	Span 13, Westbound	Full	2.7 - at bar			2.72	0.517
4	Span 11, Westbound	-	-			2.50	0.032
5	Span 11, Westbound	3.0	-	0.616	0.155	0.48	0.507
						1.45	0.373
						2.62	0.172
						3.91	0.061
6	Span 10, Westbound	-	-			3.35	0.008
7	Span 10, Westbound	-	-	0.564	0.044	0.41	0.424
						1.40	0.173
						2.74	0.016
						4.67	0.007
8	Span 10, Westbound	-	-	0.488	0.036	0.37	0.369
						1.62	0.090
						2.97	0.012
						4.56	0.008
						5.63	0.011
9	Span 11, Westbound	-	-			3.40	0.006

Bridge: US 30 (continued)

Age: 19 years

Background Chloride (% by wt. conc.): 0.008

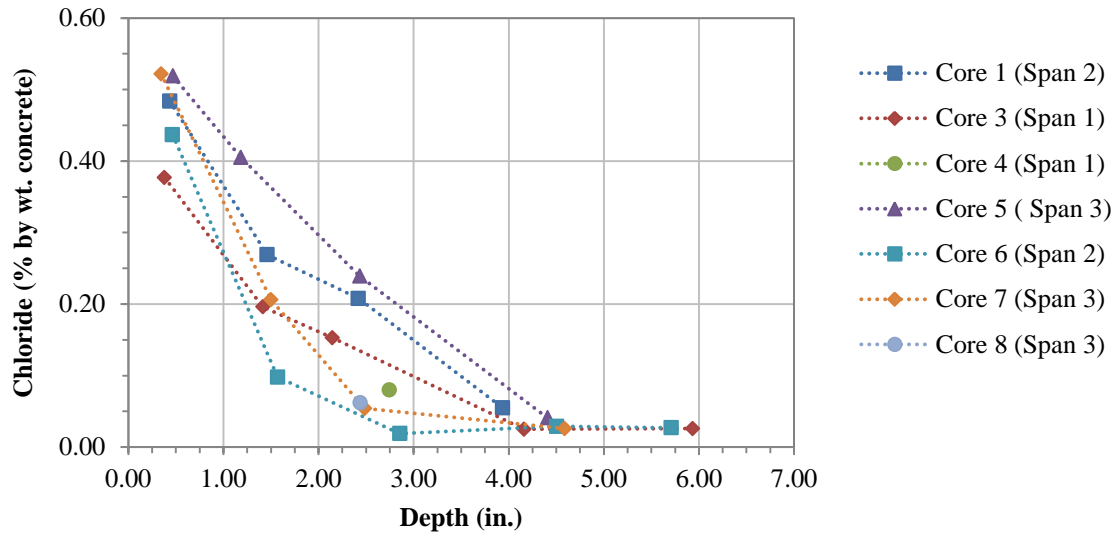


Core Number	Location	Cracking		Diffusion Coefficients		Acid-soluble Chloride Contents	
		Vertical (Depth, in.)	Horizontal (Depth, in.)	C _s (% by wt. conc.)	D (in. ² /yr.)	Average Depth (in.)	Chloride (% by wt. conc.)
10	Span 10, Eastbound	-	-	0.370	0.054	0.36	0.297
						1.38	0.135
						2.48	0.034
						3.52	0.005
11	Span 10, Eastbound	-	-	0.668	0.016	0.41	0.400
						1.62	0.031
						2.73	0.011
						4.62	0.012
						6.08	0.011
12	Span 9, Eastbound	-	-			2.77	0.009
13	Span 9, Eastbound	Full	2.5 - at bar	0.703	0.368	0.34	0.604
						1.39	0.516
						2.52	0.471
						4.85	0.033
14	Span 7, Eastbound	3.0	-			3.07	0.143
15	Span 4, Eastbound	2.0	-			2.86	0.020
16	Span 1, Eastbound	-	-	0.777	0.013	0.48	0.391
						1.54	0.031
						2.39	0.007
						4.45	0.005
						5.79	0.005
17	Span 10, Eastbound	Full	-	0.617	0.188	0.47	0.557
						1.38	0.334
						2.55	0.212
						3.45	0.159
18	Span 2, Eastbound	-	-			2.42	0.011

Bridge: US 18

Age: 18 years

Background Chloride (% by wt. conc.): 0.027



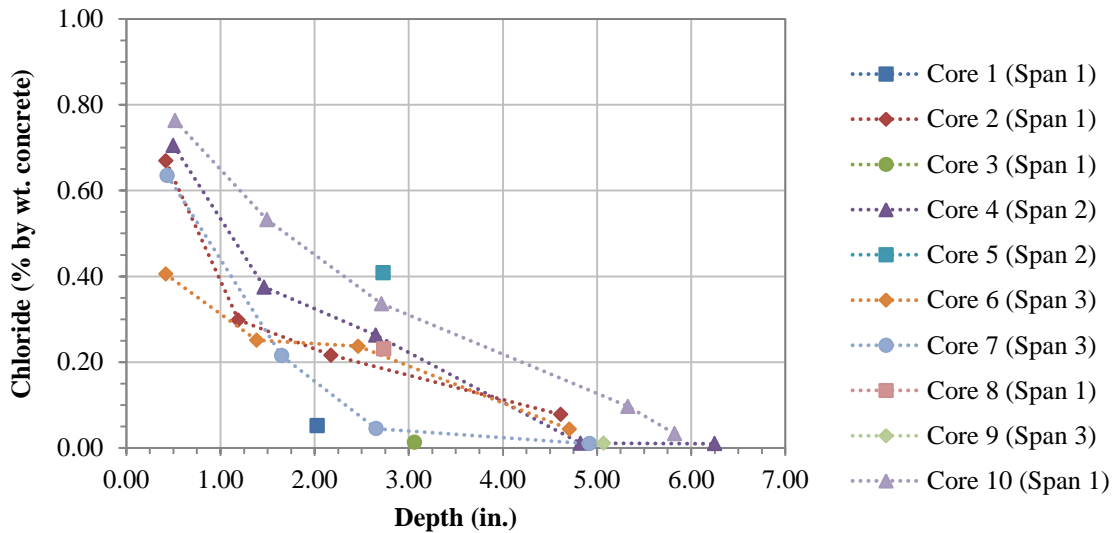
Core Number	Location	Cracking		Diffusion Coefficients		Acid-soluble Chloride Contents	
		Vertical (Depth, In.)	Horizontal (Depth, In.)	C _s (% by wt. conc.)	D (in. ² /yr.)	Average Depth (in.)	Chloride (% by wt. conc.)
1	Span 2	Full	-	0.556	0.140	0.44	0.484
						1.46	0.269
						2.42	0.208
						3.94	0.055
3	Span 1	-	-	0.438	0.099	0.38	0.377
						1.42	0.196
						2.15	0.153
						4.16	0.025
4	Span 1	-	-			5.94	0.026 / 0.002 ^[1]
						2.75	0.080
5	Span 3	Full	-	0.615	0.173	0.47	0.519
						1.19	0.405
						2.44	0.239
						4.41	0.041
6	Span 2	-	-	0.674	0.027	0.47	0.437
						1.57	0.098
						2.86	0.019
						4.51	0.029
7	Span 3	-	-	0.648	0.052	5.71	0.027
						0.35	0.522
						1.50	0.206
						2.49	0.054
8	Span 3	-	3.3 - at bar			4.59	0.026
						2.44	0.062

[1]. Water-soluble chloride measurement

Bridge: US 65 Southbound

Age: 31 years

Background Chloride (% by wt. conc.): 0.010



Core Number	Location	Cracking		Diffusion Coefficients		Acid-soluble Chloride Contents	
		Vertical (Depth, In.)	Horizontal (Depth, In.)	C _s (% by wt. conc.)	D (in. ² /yr.)	Average Depth (in.)	Chloride (% by wt. conc.)
1	Span 1	-	-			2.03	0.052
2	Span 1	-	1.0 - not at bar	0.794	0.044	0.42	0.669
						1.19	0.298
						2.18	0.216
						4.62	0.078
3	Span 1	-	-			3.06	0.013
4	Span 2	2.0	-	0.825	0.083	0.50	0.705
						1.47	0.375
						2.65	0.263
						4.83	0.011
5	Span 2	Full	2.7 - at bar 3.7 - at bar			6.25	0.010
						2.73	0.408
						0.42	0.405
						1.39	0.251
6	Span 3	Full	2.4 - at bar	Patch material in top portion of core - no diffusion coefficients calculated		2.47	0.237
						4.71	0.044
						0.44	0.635
						1.65	0.215
7	Span 3	-	1.0 - not at bar	0.839	0.032	2.66	0.045
						4.92	0.010
						2.74	0.231
						5.07	0.011
8	Span 1	-	-			2.74	0.231
9	Span 3	-	-			5.07	0.011
10	Span 1	Full	2.8 - at bar	0.875	0.146	0.52	0.763
						1.50	0.532
						2.71	0.336
						5.33	0.097
						5.83	0.033

Core Number	Location	Cracking		Diffusion Coefficients		Acid-soluble Chloride Contents	
		Vertical (Depth, In.)	Horizontal (Depth, In.)	C _s (% by wt. conc.)	D (in. ² /yr.)	Average Depth (in.)	Chloride (% by wt. conc.)
1	Span 1	-	-	0.712	0.022	0.34	0.553
						1.34	0.201
						2.48	0.012
						4.66	0.011
						6.13	0.010
2	Span 1	-	-			2.58	0.132
3	Span 2	-	-	0.601	0.086	0.33	0.560
						0.96	0.369
						1.53	0.317
						4.43	0.069
4	Span 3	-	-	0.635	0.032	0.49	0.467
						1.50	0.187
						3.07	0.038
						4.89	0.010
						6.14	0.010
5	Span 3	Full	2.9 - at bar			2.89	0.242
6	Span 3	2.4	2.4 - at bar 3.4 - at bar			2.32	0.398
7	Span 2	Full	2.3 - at bar	0.787	0.158	0.48	0.736
						1.21	0.519
						2.17	0.347
						5.22	0.154
8	Span 1	-	-	0.838	0.019	0.38	0.618
						1.23	0.222
						2.32	0.051
						6.01	0.010